PONTIFICIA UNIVERSIDAD CATÓLICA DE CHILE
ESCUELA DE INGENIERÍA

PHYSICOCHEMICAL STUDY OF DEEP EUTECTIC SOLVENTS MIXED WITH ALCOHOLS: EFFECT OF TEMPERATURE, HYDROGEN BOND DONOR AND ALCOHOL CHAIN LENGTH

VINCENZO PAOLO COTRONEO FIGUEROA

Thesis submitted to the Office of Research and Graduate Studies
in partial fulfillment of the requirements for the degree of
Master of Science in Engineering

Advisor:
ROBERTO CANALES MUÑOZ

Santiago de Chile, March 2020

© MMXX, VINCENZO P. COTRONEO

PONTIFICIA UNIVERSIDAD CATÓLICA DE CHILE
ESCUELA DE INGENIERÍA

PHYSICOCHEMICAL STUDY OF DEEP EUTECTIC SOLVENTS MIXED WITH ALCOHOLS: EFFECT OF TEMPERATURE, HYDROGEN BOND DONOR AND ALCOHOL CHAIN LENGTH

VINCENZO PAOLO COTRONEO FIGUEROA

Members of the Committee:
ROBERTO CANALES MUÑOZ
NESTÓR ESCALONA BURGOS
JUAN DE LA FUENTE BADILLA
FRANCISCO SUÁREZ POCH

Thesis submitted to the Office of Research and Graduate Studies
in partial fulfillment of the requirements for the degree of
Master of Science in Engineering

Santiago de Chile, March 2020

© MMXX, VINCENZO P. COTRONEO

To my friends and family, who have unconditionally supported me along this road. They make every day an incredible adventure.

ACKNOWLEDGEMENTS

First of all I would like to thank my parents and family for giving me the opportunity to do this master's degree, for trusting and believing that this is a challenge that I wanted to accomplish.

To Dr. Roberto Canales, my advisor, for accepting me as his pupil and the trust of a friend, supporting me at all times and giving me incredible opportunities such as traveling to different places representing the research team and meeting experts in the field.

I would also like to express my gratitude to Nicolás Gajardo, for his unconditional support throughout this period, his company, friendship and recommendation to carry out this research, practically a big brother to me.

To my colleagues and laboratory friends, especially Bruno Sepúlveda, Matías Campos and Sebastián Ormazabal, with whom we shared many anecdotes, many learnings and above all many laughs.

To my undergraduate research students: Alejandro Sepúlveda, Colín Poblete, Joaquín Meruane, María Francisca Ríos and Sebastián Faúndez, with whom we learned a lot along the way, thanking them for their willingness to learn and help. I make special mention of Sebastián and Joaquín, who have accompanied me from the beginning and I consider them my little brothers.

To the all staff working at the Department of Chemical and Bioprocess Engineering, specially to Jose Manuel, Daniel, Néstor, Olga, Karina, Gladys, Irma, Jackeline and Rosa for their constant help, trust and conversations.

To the experts who helped write the papers derived from this research: PhD María González Miquel, MSc Pablo López Porfiri, PhD Ángel Leiva and PhD Velisa Vesovic.

I thank my friends at the university, school, projects and congresses who have listened to me and helped me on many occasions, have always supported and motivated me to improve day by day. I make special mention to Alejandra Chaparro who accompanied me and motivated me to work for the School and accompanied me in the last months of writing this thesis, thus becoming an exceptional friend.

I am very grateful to all those who have been part of one or another of my lives on this trip, because without you, this would never have been achieved. This work is especially dedicated to my grandparents Renato and Rubi.

Finally I want to thank the financial support of CONICYT Chile through the project Fondecyt de Iniciación 2016 N°11160882. Also, the support of the Academic Exchange Fund and the financing of the Master's Degree in Student Support, both from the Escuela de Ingeniería of the Pontificia Universidad Católica de Chile.

TABLE OF CONTENTS

LIST OF FIGURES

LIST OF TABLES

ABSTRACT

Deep eutectic solvents are mixtures composed typically by a hydrogen bond donor and a hydrogen bond acceptor. They have appeared as an alternative of ionic liquids in several processes due to their tunability, biodegradability and low cost. Recently, deep eutectic solvents have been studied as potential solvents for different applications. Then, their physicochemical properties need to be characterized for understanding the interaction between its constituents and with other compounds. Deep eutectic solvents prepared for this work were based on choline chloride mixed with ethylene glycol, 1,3-propanediol or 1,4-butanediol at a 1:3 mole ratio. Different families of DESs based on choline chloride and betaine are performed in parallel to generate a database, see the fit and prediction using the hard sphere model. Density and viscosity of the pseudo-pure deep eutectic solvents were measured from 293.15 K to 333.15 K at 101.13 kPa. Also, the same properties at the same temperature and pressure conditions were obtained for the pseudo-binary mixtures of the three deep eutectic solvents with four alcohols: methanol, ethanol, 1-propanol or 1-butanol. The excess volumes were calculated for each system for understanding the effect of the temperature variation, the length of the alcohol chain, and length of the hydrogen bond donor on the configurational aspects of the mixture. Subsequently, a prediction of the excess molar enthalpy was performed with COSMO-RS in order to assess the behavior of the same variables on different type of intermolecular interactions from the energetic point of view. The results suggest that mixing each deep eutectic solvent with an alcohol produce negative molar excess volumes and molar excess enthalpies, observing a higher affinity between unlike species. For viscosity prediction, it is obtained that the hard sphere model correlates with an error under the values for the different families of the DESs, but the model does not predict the behavior of the families.

Keywords: Deep eutectic solvents, choline chloride, excess molar volume, excess molar enthalpy, density, viscosity, predictive model.

RESUMEN

Los solventes eutécticos profundos son mezclas compuestas típicamente por un donador de puentes de hidrógeno y un aceptor de puentes de hidrógeno. Han aparecido como una alternativa de los líquidos iónicos en varios procesos debido a su capacidad de adaptación, biodegradabilidad y bajo costo. Recientemente, los solventes eutécticos profundos se han estudiado como solventes potenciales para diferentes aplicaciones. Entonces, sus propiedades fisicoquímicas deben caracterizarse para comprender la interacción entre sus componentes y con otros compuestos. Los solventes eutécticos profundos preparados para este trabajo se basaron en cloruro de colina mezclado con etilenglicol, 1,3-propanodiol o 1,4-butanodiol en una relación molar de 1:3. Se realizan diferentes familias de DES basadas en cloruro de colina y betaína en paralelo para generar una base de datos, ver el ajuste y la predicción utilizando el modelo de esfera dura. La densidad y la viscosidad de los disolventes eutécticos profundos pseudo puros se midieron de 293,15 K a 333,15 K a 101,13 kPa. Además, se obtuvieron las mismas propiedades a las mismas condiciones de temperatura y presión para las mezclas pseudobinarias de los tres solventes eutécticos profundos con cuatro alcoholes: metanol, etanol, 1-propanol o 1-butanol. Los volúmenes en exceso se calcularon para cada sistema para comprender el efecto de la variación de temperatura, la longitud de la cadena de alcohol y la longitud del donante de enlace de hidrógeno en los aspectos de configuración de la mezcla. Posteriormente, se realizó una predicción del exceso de entalpía molar con COSMO-RS para evaluar el comportamiento de las mismas variables en diferentes tipos de interacciones intermoleculares desde el punto de vista energético. Los resultados sugieren que mezclar cada solvente eutéctico profundo con un alcohol produce volúmenes molares de exceso negativos y entalpías molares de exceso, observando una mayor afinidad entre especies diferentes. Para la predicción de la viscosidad, se obtiene que el modelo de esfera dura se correlaciona con un error bajo los valores para las diferentes familias de los DES, pero el modelo no predice el comportamiento de las familias.

Palabras Claves: *Deep eutectic solvents*, cloruro de colina, volumen molar de exceso, entalpía molar de exceso, densidad, viscosidad, modelo predictivo.

1. INTRODUCTION

Since ancient times the study of chemical reactivity was centered on the employment of water as a solvent. This was a limitation in the investigations, as water is not a global solvent. On 19th century organic solvents emerged, which contributed to the evolution of chemistry and industrial processes. However, a lot of organic solvents have a major disadvantage, which is their high toxicity and volatility. It is for this reason that the discovery of new ecological solvents is one of the fundamental objectives of Green Chemistry.

Green solvents are used extensively in the industry, to minimize the environmental issue identified with the use of traditional solvents in chemical production, as well as to reduce the cost, improve safety and health (Bi, Tian, & Row, 2013). Green solvents can be defined by four ways: (i) substitution of dangerous solvents with ones which are safer, healthier and more environmentally friendlier, (ii) use of bio-solvents, who can be produced with renewable resources, (iii) change organic solvents with supercritical fluids environmentally friendly and (iv) some applied ionic liquids (Capello, Fischer, & Hungerbühler, 2007). An examples of these definitions can be found in Table 1.1.

The potency of green solvents can be quantified through the use of environmental assessment methods, e.g. the EHS method (identification of potential hazards of substances) (Sugiyama, Fischer, & Hungerbühler, 2006) and the LCA (life cycle assessment) method (Rebitzer et al., 2004).

Table 1.1. Examples of green solvents

Type	Definition	Example
i	Substitution dangerous solvent	2,2,2-trifluoroethyl
ii	Bio-solvents	bioethanol
iii	Supercritical fluids	CO_2 supercritical
iv	Ionic liquids	$[C_{14}C_1]Im[PF_6]$

In this field, Ionic Liquids (ILs) and Deep Eutectic Solvents (DES) have been the focus of great attention to replace severe organic solvents and have been applied to many industrial processes such as the synthesis and extraction of high value compounds (Dai, van Spronsen, Witkamp, Verpoorte, & Choi, 2013; Disale, Kale, Kahandal, Srinivasan, & Jayaram, 2012).

The first ionic liquids was produced in 1914, where the researcher synthesized ethyl ammonium nitrate with a melting point of 285K (Walden, 1914). Then over time several ILs were synthesized and their different properties and applications were observed at an industrial level.

This solvents are synthesized by the combination of an organic or inorganic anion with an organic cation. A simple way to define ILs is the formation of a salt whose melting temperature is below 393K. This way we can differentiate it from a molten salt such as NaCl, since its melting point is above 1000K, which makes it impossible for it to be used as a pure solvent in the chemical industry because of its high corrosivity and high viscosity.

The principal properties of ILs are: low volatility, vapor pressure and melting point; high thermal and chemical stability, which makes them a great alternative to ordinary solvents; miscibility and polarity adaptable to the process, distinguished in the solubility of gases (Cammarata, Kazarian, Salter, & Welton, 2001; Quijada-Maldonado, Sanchez, Perez, Tapia, & Romero, 2018). It is important to highlight its disadvantages, the process of synthesis is tedious, which is due to its high cost and toxicity (Romero, Santos, Tojo, & Rodriguez, 2008), which restricts its use in certain processes, such as the food industry.

DESs display imperceptible vapor pressure (which means they're not volatile), great solubility, they are non-flammable, posses a high chemical and thermal stability, they are bio-degradable and also posses a huge ionic conductivity making them exceptionally adequate as absorbents, solvents, and catalysts for diverse operations (Dutta & Nath, 2018).

The study of physicochemical properties are of high importance in process industry as they determine the design of equipment such as pumps, pipes, reactors, etc. Viscosity plays a fundamental role in the calculation of mass transfer and reaction rates (Haghbakhsh, Parvaneh, Raeissi, & Shariati, 2018; Haghbakhsh & Raeissi, 2015).

This work is part of an exhaustive study of density, viscosity and excess volumes of the DES composed by choline chloride + ethylene glycol, choline chloride + 1,3 propanediol, and choline chloride + 1,4 butanediol and their mixtures with methanol, ethanol, 1-propanol or 1-butanol. All the DES were characterized by Fourier-transform infrared spectroscopy (FT-IR) to study potential interactions between the precursors and to determine whether or not there is any chemical reaction that take place between the HBA and HBD.

Densities and viscosities of the pseudo-binary mixtures DES + alcohol were measured between the temperatures of 293.15 K and 333.15 K at a pressure of 101.3 kPa, and the excess volumes were calculated from density data. The density was correlated with a linear equation, viscosity with the Vogel-Fulcher-Tamman (VFT) equation, and the excess molar volume with the Redlich-Kister (RK) correlation.

In order to understand the driving forces behind the observed mixing behavior, excess enthalpies were calculated with the COnductor like Screening MOdel for Real Solvents (COSMO-RS). With this approach, the effect of the alcohol chain length will be elucidated on the basis of the physicochemical properties of DES and the mixtures. Therefore, through experimental data and quantum chemical methods, this work provides a comprehensive analysis of the mixing phenomena and its implication on the macroscopic behavior of DES for separation processes.

In parallel, viscosity and density measurements of different DES based on choline chloride or betaine are performed using ethylene glycol, phenol, 1,2-propanediol, 1,3-propanediol and 1,4-butanediol as HBD at different temperatures and molar ratios to see the effectiveness of the hard sphere predictive model.

1.1. Hypothesis

A correct comprehension of the intermolecular interactions in the formation of DES and its binary mixtures with differents alcohols is high importance in determining the impact of DES as a solvent in the separation industry. The characterization of the complex after the mixture is essential to determine that DES are formed by molecular interactions of hydrogen bond type and not by chemical reaction. Also, the properties such as density, viscosity and decomposition temperature are important for establishing confidence intervals in the performance of DES during industrial processes. Binary mixtures with methanol, ethanol, 1-propanol and 1-butanol can be used to understand the behavior of the effect of the length of the alcohol chain on the physical properties of DES due to the addition of an organic compound. The variation in the length of the HBD chain makes it possible to understand if there is a behaviour in the properties of binary mixtures when modifying the DES. Specifically, a contraction of the physical properties is expected to be observed at the smaller alcohol chain and in the HBD precursor chain employed, due to the creation of larger networks of hydrogen bonds between alcohols and DES or between HBD and choline chloride.

As a result, it is expected that the increase in temperature, the decrease in the length of the chain and the hydrogen bridge donor will allow a decrease in the excess volume of the mixtures formed by the various DES. In predictive models such as COSMO-RS they are able to predict the behaviour of the mixture by explaining intermolecular interactions, while the hard-sphere model allows the behaviour of the viscosities of different DES to be predicted.

1.2. Goals

In accordance with the proposed hypothesis, the general objective of this thesis is to study the physicochemical behaviour of DES by analysing the temperature effect, change effect of the hydrogen bond donor and the length of alcohol chains in binary mixtures.

To achieve this goal, the metrics of this thesis are:

(i) To understand the intermolecular forces in DES formation, different HBD are used to understand the stability generated.
(ii) Characterize the properties of pure DES and binary mixtures with alcohols.
(iii) Understand the phenomena and relationships of the differents binary systems under the influence of temperature, HBD and alcohol.
(iv) Use the COSMO-RS model to predict the behaviour of excess enthalpy and characterize the highest energy agents in intermolecular interactions
(v) Use the hard-sphere model to adjust and/or predict the viscosities of DES.

This investigation is organized as follows: Section 2, state of the art, describes the different edges of the deep eutectic solvents, their physicochemical properties and different models used in the field. Section 3 presents the materials and methods used in the thesis, section 4 presents the results and discussions following a scheme of classical journal articles. Section 6 presents the main conclusions and future work on the topic.

2. STATE OF ART

The next section is designed as below. The subsection 2.1 add the concept of deep eutectic solvents (DES), their preparation on subsubsection 2.1.1, types on subsubsection 2.1.2 and applications on subsubsection 2.1.3. Subsection 2.2 refers to pure eutectic mixtures, which are analysed for their outstanding properties which characterise them. Subsection 2.3 describes the principal properties of binary systems. After that on subsection 2.4 introduce the differents equation of state used to fitted the excess properties. Finally, in subsection 2.5 is documented the importance of predictive viscosity models in the characterization of physical properties of solvents.

2.1. Deep Eutectic Solvents

The first researches on DES are dated in 2001 (Abbott, Capper, Davies, Munro, & Rasheed, 2011), where the potential of eutectic mixtures can be observed due to the ease of mixing them and their properties and characteristics similar to ionic liquids, adding their low (or null) toxicity (M. Hayyan et al., 2013; A. Hayyan et al., 2012; Jhong, Wong, Wan, Wang, & Wei, 2009), biodegradability and low monetary cost (Bi et al., 2013). This solvents in some papers are recognized a specific class of ionic liquids (Dutta & Nath, 2018; Shishov, Bulatov, Locatelli, Carradori, & Andruch, 2017) due to their similar physicochemical characteristics but in others research indicates that DESs can't be considered as such because they can be obtained from non-ionic species and aren't completely composed of ions (Q. Zhang, Vigier, Royer, & Jerome, 2012).

This solvent are mixtures of quaternary salt who can accept a hydrogen bond (HBA) and hydrogen bond donor (HBD), most frequently solid, the mixture produce is liquid at room temperature as its melting point decreases substantially respect to individual compounds (Q. Zhang et al., 2012), on section 2.1.1 shows the different methods for make de DES.

A classic example of this anomaly is the 1:2 molar mixture of choline chloride with urea, where the freezing point of both is 575.15K and 407.15K, respectively, while the mixture is 285.15K (Abbott, Capper, Davies, Rasheed, & Tambyrajah, 2003). In figure 2.1 the phenomena can be understood graphically. Four different types of DES can be classified, which are described in subsection 2.1.2.

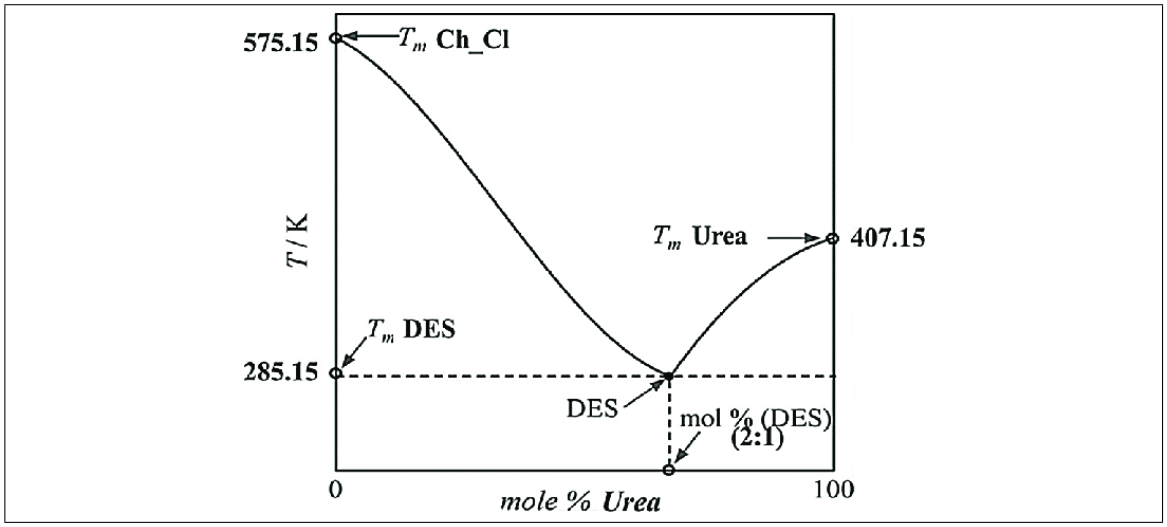

Figure 2.1. Schematic solid liquid phase diagram for ChCl and urea (G. Garcia et al., 2015).

The principal differences with the ILs are: (i) DES is a chemical mixture formed by Bronsted-Lowry or Lewis acids theory, (ii) do the eutectic mixture is much easier than to synthesize the IL, (iii) the raw material and production cost are lower compared to ionic solvents and (iv) the range of applications are appreciably different, irrespective the physical properties are similar (M. Hayyan et al., 2013; B. S. Singh, Lobo, & Shankarling, 2012). The Figure 2.2 shows a different examples of DESs mixtures.

It is important to note that some of these eutectic mixtures have certain disadvantages, such as their high viscosity and volatility which can affect their use in scalability in industry (physical properties will be elaborated with more detail in section 2.2). But given its low price and ecological footprint, is a solvent of great interest to industry, so we have also amplified the studies of this in recent times. Until 2018 there are more than 2000

publications (Kroon, Allen, Brennecke, Savage, & Schatz, 2017; Rodriguez Rodriguez, van den Bruinhorst, Kollau, Kroon, & Binnemans, 2019). In Section 2.1.3 indicates the different applications of eutectic mixtures.

One of the hydrogen bound acceptor chemicals by excellence in DES forming is choline chloride (ChCl). ChCl is a biodegradable, biocompatible, non-toxic and very economical quaternary ammonium salt that can be obtained from biomass or easily synthesized from fossil reserves. Can be found in the vitamin B_4 (Blusztajn, 1998) and one of its major uses is as chicken feed in the aviary industry. (Q. Zhang et al., 2012).

It is important to note that in the literature the concept of "natural deep eutectic solvents" (NaDES) can be found, which exactly refers to the DES described but which are used naturally in processes of solubilization, transport and storage of insoluble metabolites at the cellular level and of living organisms (Dai et al., 2013).

2.1.1. DES Preparation

It is important to note that the formation of DES is an endergonic process, which requires external disturbances to generate the liquid mixture. In the literature there are three main pathways: the first called heating and stirring method, which incorporates the compounds in a closed bottle and increases the temperature to approximately 333.15K under magnetic agitation (Florindo, Oliveira, Rebelo, Fernandes, & Marrucho, 2014). The second called evaporation method consists in the use of a rotatory evaporator where the components are dissolved in water at approximately 323.15K. Lastly and in lesser use in researches, it is the freeze-drying method, in which it is based on the freeze-drying of a mixture of the aqueous solutions of the individual analogue (Ruesgas-Ramon, Figueroa-Espinoza, & Durand, 2017; Gutierrez, Ferrer, Mateo, & del Monte, 2009). On the Table 2.1 we can observed a summary of the three methods.

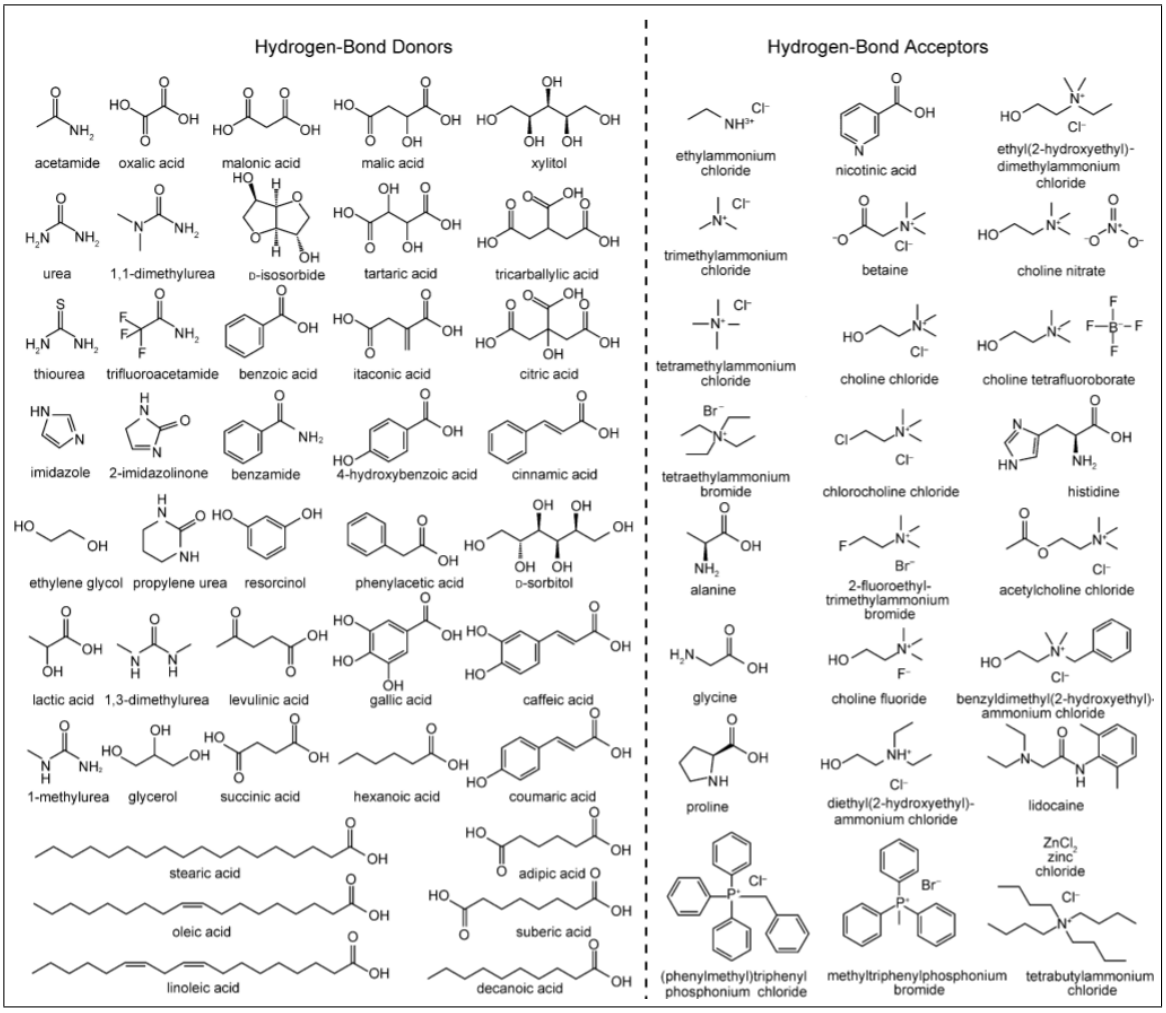

Figure 2.2. Molecular structures of HBDs and HBAs that can be combined to form a DES (Francisco et al., 2013).

Table 2.1. Different ways to prepare DES.

Method of preparation	Parameter variable	Equipment
Heating and stirring method	T, ω	Magnetic shaker
Evaporating method	T, P	Rotatory evaporator
Freeze-drying method	T, P	Lyophilizer

2.1.2. Types of DES

The global formula of DES is:

$$\text{Cat}^{+}X^{-}zY \tag{2.1}$$

Where Cat^+ is a cation, such as phosphonium, ammonium or sulfonium, X represents a Lewis base, Y describes a Brönsted Lowry or Lewis acid and z the number of molecules of that acid that interact with the anion (Smith, Abbott, & Ryder, 2014). Depending on the compounds and organic groups involved, we can classify DES into 4 types, which is described in the Table 2.2.

Table 2.2. General Formula for the Classification of DESs (Smith et al., 2014).

Types	General formula	Terms	Example
Type I	$Cat^+X^- + zMCl_x$	M = Zn, In, Ga, Sn, Al, Fe	$AlCl_4^- + AgCl$
Type II	$Cat^+X^- + zMCl_x \cdot yH_2O$	M=Cr, Co, Cu, Ni, Fe	$ChCl + CoCl_2 \cdot 6H_2O$
Type III	$Cat^+X^- + zRZ$	Z = OH, COOH, $CONH_2$	ChCl + Ethylene glycol
Type IV	$MCl_x + zRZ$	M = Zn, Al ; Z = OH, $CONH_2$	$ZnCl_2$ + Acetamide

In this document DES type III based on choline chloride, ethylene glycol, 1,3-propanediol and 1,4-butanediol will be used. For the study of the viscosity model, the use of betaine, phenol and 1,2-propanediol is incorporated, which also form DES type III.

2.1.3. Applications of DES

The first applications of eutectic compounds are before of recognition of DES by Abbott, such as enzymatic catalysis (Gill & Vulfson, 1994), enzymatic synthesis (Erbeldinger, Ni, & Halling, 1998), separation and purification of molecular mixes (Davey, Garside, Hilton, McEwan, & Morrison, 1995), pharmaceutical procceses (Stott, Williams, & Barry, 1998) .

After the definition of DES for Abbott, have been studied and strengthened applications in biocatalysis (Gutiérrez, Ferrer, Yuste, Rojo, & del Monte, 2010), electrochemistry (Nkuku & LeSuer, 2007), synthesis of materials (Parnham, Drylie, Wheatley, Slawin, & Morris, 2006), extraction of phenolic acids (Peng et al., 2016), extraction of flavonoids (Duan, Dou, Guo, Li, & Liu, 2016a), separation processes, preparation of materials, organic synthesis, catalysis, extract DNA, etc (Khezeli, Daneshfar, & Sahraei, 2016; Handy & Lavender, 2013; Bougouma, Van Elewyck, Steichen, Buess-Herman, & Doneux, 2013; Tang, Zhang, & Row, 2015; Duan, Dou, Guo, Li, & Liu, 2016b; Gage, Ruddy, Pylypenko, & Richards, 2016; Vigier, Chatel, & Jérôme, 2015; Rodriguez Rodriguez et al., 2019).

In Figure 2.3 we can observe in simple terms a chronology of the applications of the eutectic mixture in the last years, in Figure 2.4 we can see a summary diagram of the great applications of DES. The future uses of this solvents depends of the characterization of his crucial properties, the comprehension of phase conduct of the compounds and the interactions set up between the sets that comprise the eutectic blend.

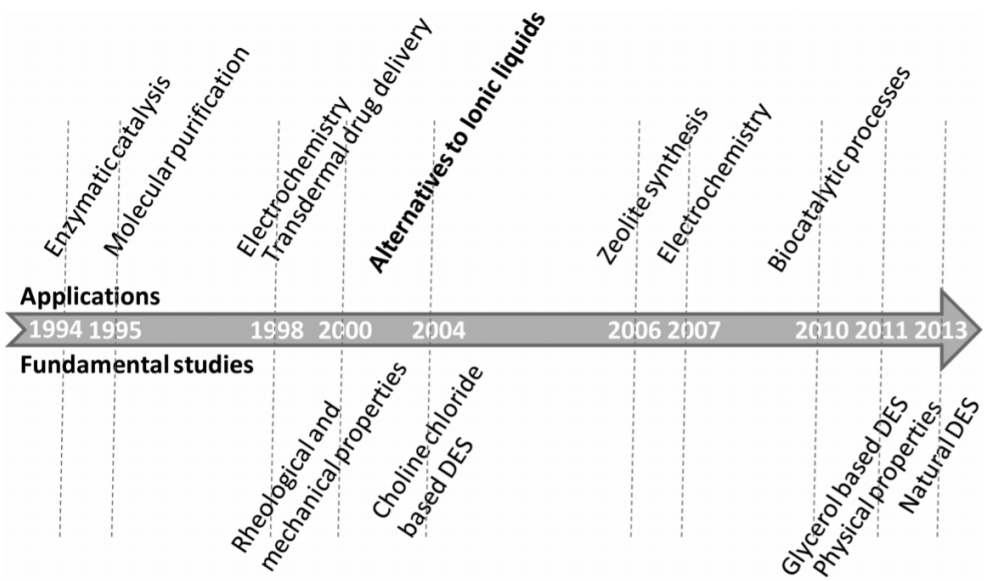

Figure 2.3. Timeline of revealed advancements, both on applications and crucial considers on deep eutectic solvents (Paiva et al., 2014).

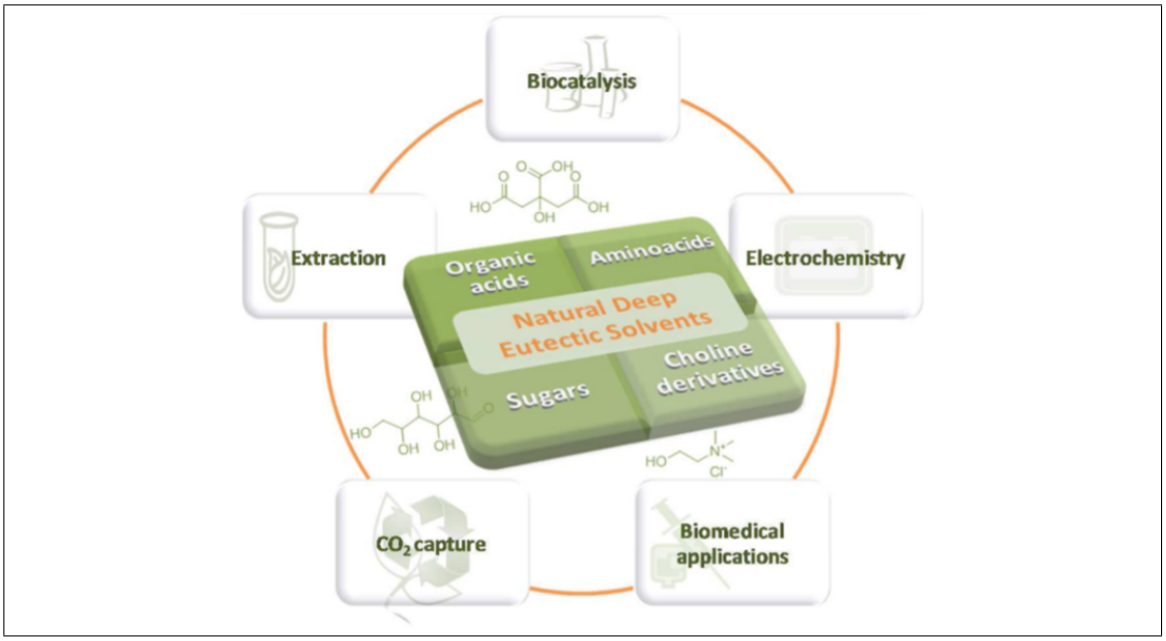

Figure 2.4. Application of DES (Paiva et al., 2014).

2.2. Properties of pure DES

In this section, thermodynamic properties of authentic deep eutectic solvents will be talk about. Thermophysical properties of solvents are significant beginning stage for examining their purity and watching their potential applications as indicated by these qualities. Properties like density, viscosity and warm steadiness are basic for the total portrayal of the DESs.

2.2.1. Thermal decomposition

Thermal decomposition is one of the most important properties to analyze when researching a DES, since it delivers temperature values where the DES can be used in industrial operations without problems. The decomposition temperature is the temperature at which the solvent begins to disintegrate or breakdown into smaller molecules. This temperature is determined by the mass loss of the sample.

There are very few studies of the thermal decomposition of DES. There are only reports of the compounds used traditionally, as well as their curves that are made mainly by thermigravimetric analysis (TGA) (Sánchez, González, Salgado, José Parajó, & Domínguez, 2019; Francisco et al., 2013; Gajardo-Parra et al., 2019; Florindo et al., 2014; Q. Zhang et al., 2012; Ullah et al., 2015), in the Figure 2.5 shows an example of this analysis.

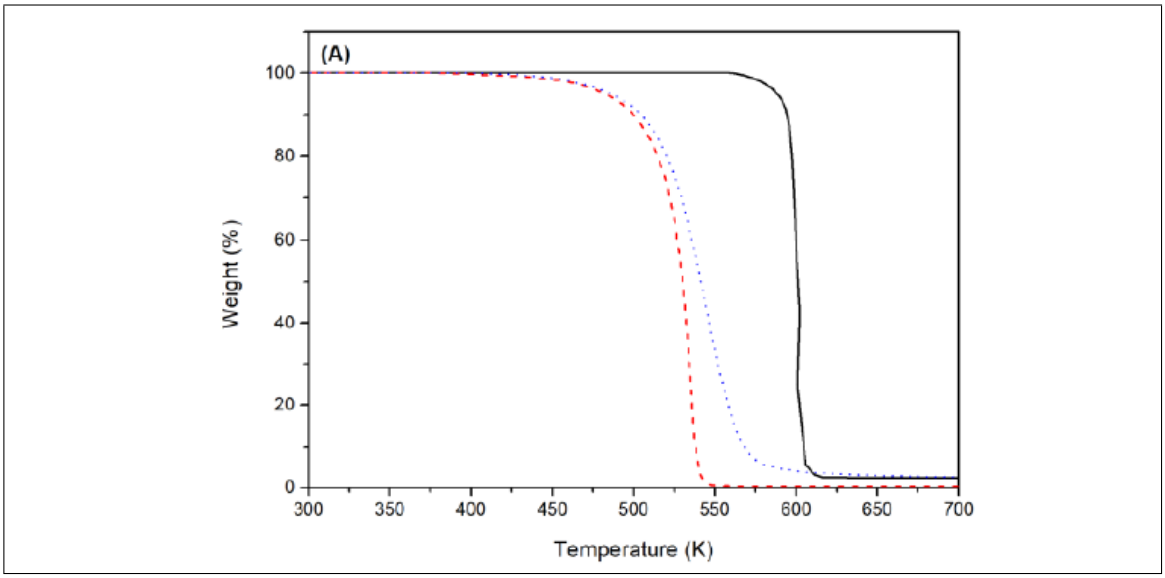

Figure 2.5. Example of TGA analysis for ChCl + ethylene glycol molar ratio 1:2 (Gajardo-Parra et al., 2019).

2.2.2. Density

The density is an important physical property of any material, as this property affects reaction speeds, turbulence, diffusivity, among others. This property varies according to the chain, functional groups and structures of the HBA and HBD used, generally DES are always denser than water, and their miscibility in it depends on the nature of the anion and cation that form it.

In the Table 2.3 some examples of DES measurement can be observed, some of these data are obtained directly from the equipment that is part of the laboratory.

Table 2.3. Density in g·cm^{-3} of common DESs at 298.15K. Data without reference are measured in the laboratory.

HBD	HBA:HBD (molar ratio)	Density g·cm^3	Reference
Urea	1:2	1.25	(Yadav, Trivedi, Rai, & Pandey, 2014a)
Ethylene glycol	1:2	1.12	(Shahbaz, Mjalli, Hashim, & Alnashef, 2011)
Glycerol	1:2	1.18	(Abbott, Capper, et al., 2011)
Glycerol	1:2	1.19	(Rodriguez, Ferre Guell, & Kroon, 2016)
1,2-propanediol	1:3	1.07	-
1,3-propanediol	1:2	1.09	-
1,4-butanediol	1:3	1.05	-
Levulinic acid	1:2	1.12	(Gajardo-Parra et al., 2019)
Malonic acid	1:2	1.25	(D'Agostino, Harris, Abbott, Gladden, & Mantle, 2011)
Phenol	1:2	1.10	(Gajardo-Parra et al., 2019)

There have also been studies of the effects of density with respect to the molar fraction of DES precursors, (Abbott, Harris, et al., 2011) reports a graph exposed in Figure 2.6 and there is a linear trend of this phenomenon, where density decreases to a higher percentage of choline chloride, in general this trend is maintained among several DES generated.

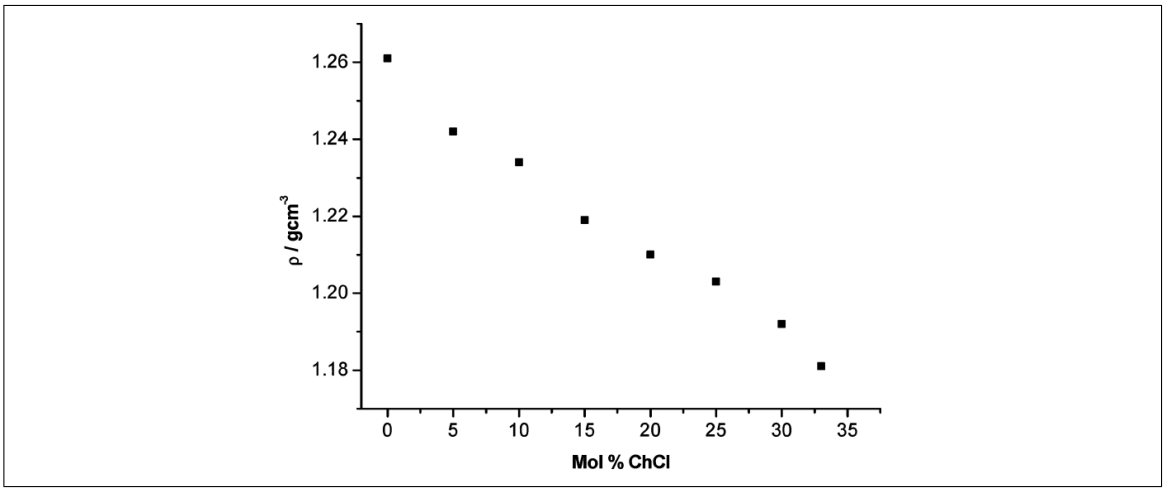

Figure 2.6. Correlation of density and molar % of ChCl in DES with glycerol. Retrieved from (Abbott, Harris, et al., 2011).

2.2.3. Viscosity

In general, deep eutectic solvents have high viscosities, due to the diverse molecular interactions between the compounds that conform it, particularly the network of hydrogen bonds, that reduces the mobility of the molecular compounds (Abbott, Capper, & Gray, 2006; Fukaya, Iizuka, Sekikawa, & Ohno, 2007). Another way of explaining viscosity is through the "hole theory" (Durand, Lecomte, & Villeneuve, 2013) which indicates that solid ionic compounds when fused produce certain cavities that arise from fluctuations generated thermally from local densities, so that if the compound opposite to the cavity generator finds these spaces available, it will modify the magnitude of the viscosity present in the mixture.

There have also been studies of the effects of viscosity with respect to the molar fraction of DES precursors, (Abbott, Harris, et al., 2011) reports a graph exposed in Figure 2.7 and there is a tendency of logarithmic nature of this phenomenon, where viscosity decreases to a higher percentage of choline chloride. As well as density, in general this trend is maintained among several DES generated.

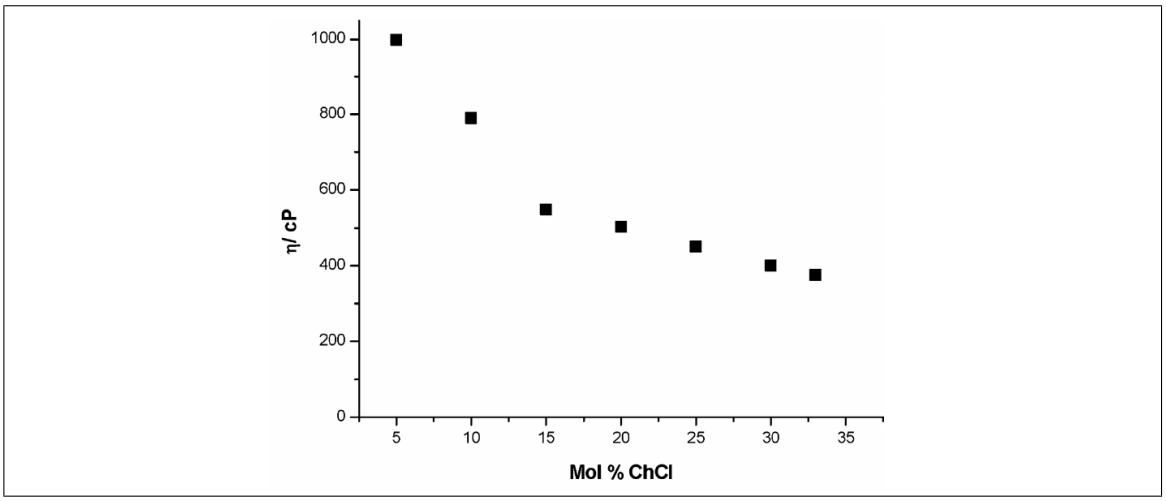

Figure 2.7. Correlation of viscosity and molar % of ChCl in DES with glycerol. Retrieved from (Abbott, Harris, et al., 2011).

2.3. Binary system properties

Mixing systems focused on DES can be found in literature mainly measurements of vapor-liquid equilibrium (VLE), liquid-liquid equilibrium (LLE), values of the coefficient at infinite dilution (γ^{∞}) and the value of different excess properties.

VLE data are obtained through experiments mainly from distillation, where the compounds obtained in the form of vapour and liquid can be quantified. LLE comes mainly in experiments of agitation and presence of several aqueous phases to analyze the effectiveness of miscibility of compounds in various solvents. γ^{∞} provides a vital parameter for system modeling at different conditions.

Excess properties are attributes of mixtures that compute the non-ideal behavior of real mixtures. They are described as the subtraction between the property in a real mixture and the value that would exist in an ideal solution under the same conditions. Given the previous, there exist the excess volume (V^E), enthalpy (H^E), entropy (S^E) and gibbs (G^E).

The binary properties used in this report are described in more detail below.

2.3.1. Excess volume

Understanding that excess properties are the difference between idealism and reality, the formula that describes excess volume is found in the Equation 2.2 (Walas, 2013), where x_i is the mole fraction of a component i, $V_{mixture}$ is the molar volume of the mixture and V_i is the volume of a component i.

$$V^E = V_{mixture} - \sum x_i V_i \tag{2.2}$$

This formula is simplified for a binary system as indicated in Equation 2.3, where x_1 and x_2 indicate the molar fractions of compound 1 and 2, respectively.

$$V^E = V_{mixture} - \left(x_1 V_1^o + x_2 V_2^o\right) \tag{2.3}$$

The value of the excess volume may depend on many factors that will be indicated below (Redhi, 2003):

(i) The formation of interactions between molecules of different compounds, resulting in a decrease in the occupied volume of the initial compounds.

(ii) The rupture of the interactions of molecules of the same compound without binding to the other chemical, generating an increase in the volume of the mixture.

(iii) The packaging effect given the space occupied by the molecules of the mixed compounds, allowing a positive or negative effect depending on the accommodation.

(iv) The formation of new chemical compounds.

DES are not expected to react with binary mixtures, since the potential sought in these is their use as high-value solvent extraction. This thesis seeks to understand the behavior of this property in the face of various manipulable changes in binary mixtures with DES. Also, this data will be calculated by means of the indirect method which is explained together with the equipment used in the section 3.4.

The advancement of high precision vibratory tube densitometers has permitted the determination of V^E with acceptable precision from the density of the mixture using the Equation 2.4 (Oswal & Desai, 2001), where x_1 and x_2 are mole fractions, M_1 and M_2 are molar masses of the compounds, ρ_m is the density of the mixture and ρ_i represent the density to the component 1 and 2.

$$V^E = \frac{x_1 M_1 + x_2 M_2}{\rho_m} - \frac{x_1 M_1}{\rho_1} - \frac{x_2 M_2}{\rho_2} \tag{2.4}$$

This is a field that has been studied very little in the DES with some solvents, where in most cases seeks to reduce the viscosity of the mixture (Leron, Soriano, & Li, 2012;

Siongco, Leron, & Li, 2013; Yadav, Kar, Verma, Naqvi, & Pandey, 2015; Yadav, Trivedi, Rai, & Pandey, 2014b; Leron, Wong, & Li, 2012; Mjalli & Ahmed, 2016; Leron & Li, 2012; Harifi-Mood & Buchner, 2017; Shekaari, Zafarani-Moattar, & Mohammadi, 2017; Kim & Park, 2018; Gajardo-Parra et al., 2019). In most cases the behavior of DES is a contraction in the whole range of molar fraction, as can be seen in Figure 2.8.

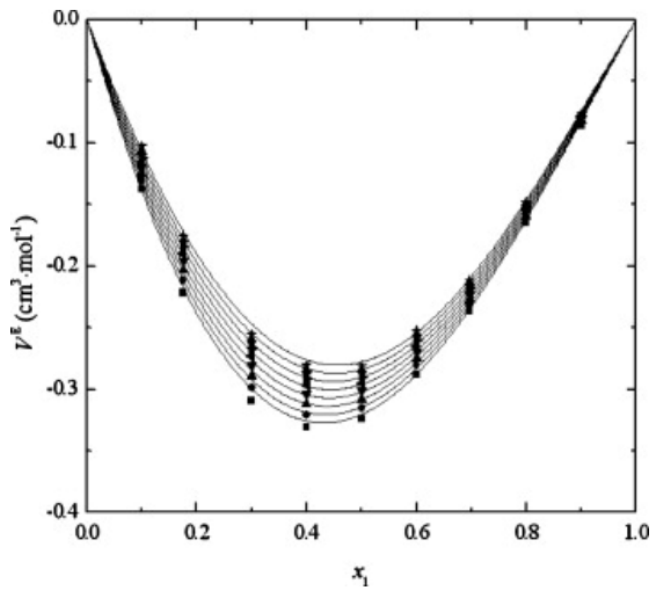

Figure 2.8. Excess molar volume against x_1 for DES (1) of ChCl + ethylene glycol (molar ratio 1:2) + H_2O (2) solutions at different temperatures (Leron, Soriano, & Li, 2012).

2.3.2. Excess entalphy

As mentioned above, the excess enthalpy indicates the difference of the ideal mixture enthalpy with the real mixture, this is quantified from the Equation 2.5, where it can be seen that it depends on the value of molar gibbs. This mathematical statement can be represented in another way, indicated in the Equation 2.6, where R is the universal gas constant, T system temperature, P system pressure, x_i indicates the molar fractions of the compounds in the system, $ln(\gamma_i)$ refers to the natural logarithm of the activity coefficient of the compound εiε.

$$H^E = -RT^2 \left[\frac{\partial G_m^E}{\partial T} \right]_{P,x} \tag{2.5}$$

$$H^E = -RT^2 \sum_i^n x_i \left[\frac{\partial \ln \gamma_1}{\partial T} \right]_{P,x} \tag{2.6}$$

The excess enthalpy data are important for the characterization of the correct temperature dependence of the activity coefficients in accordance with the Gibbs-Helmholtz equation, from this value other relevant thermodynamic parameters can be determined as equilibrium values and also to understand the energetic contributions of intermolecular interactions (Wei, Han, & Wang, 2014). Activity coefficient is a critical parameter considered in the design of chemical processes which involving phase separation.

When the value of H^E is positive, it indicates an endothermic release of energy, while if the value is negative, it indicates an exothermic interaction, an example of both behaviors can be seen in the Figure 2.9.

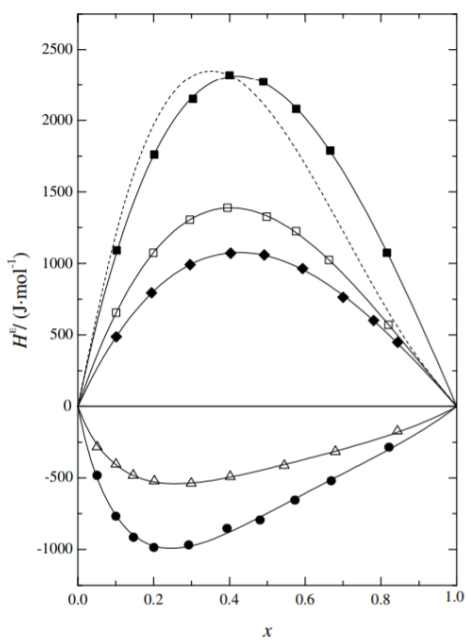

Figure 2.9. Excess molar enthalpy example (García-Miaja et al., 2009).

The heats of the mixture can be measured with different experimental devices but can also be predicted from different complex thermodynamic models, the most typical equipment is the calorimeter. However, in the papers there is no information on excess enthalpies yet, which makes it a fascinating territory to investigate.

2.4. Modeling and equations of adjustment in DES binary mixtures

For many properties and physicochemical parameters there are endless models and correlations that allow to relate the data obtained from different systems with a mathematical equation that allows to quantify the parameters from functions. In this report, two of these models will be used, which are explained in this subsection.

2.4.1. Redlich-Kister

The Redlich-Kister equation of state (EoS) provides a flexible algebraic expression to represent the excess properties of a liquid mixture, this shows in Equation 2.7, where M represents a property of excess previously indicated, x_1 and x_2 indicate the molar fractions of the compounds in study, α represents the parameter of adjustment of the equation and N the quantity of parameters to obtain in the adjustment.

$$M^E = x_1 x_2 \sum_{i=0}^{N} \alpha_i \left(x_1 - x_2\right)^i \tag{2.7}$$

This equation also provides a convenient method of representing the activity coefficients of the liquid phase, and additionally a classification of the different types of liquid solutions. The number of data required in Equation 2.7 to represent the adjustment parameters of a binary mixture is an indication of the apparent complexity of the mixture. If the number of necessary parameters is high (4 or more), the mixture can be called complex, if it is reduced, the mixture is considered simple.

2.4.2. COSMO-RS

The COSMO-RS method is a quantum chemical model for the prediction of thermodynamic properties of pure substances and mixtures in liquid phase using only unimolecular structural information of the fluid. One of the main advantages of this methodology is that, at different from the classical methods traditionally used in engineering Chemistry, allows the prediction of the thermodynamic properties of compounds without the need for experimental data for the definition of their parameters. The COSMO-RS method is therefore particularly suitable for the determination of data in systems where little is available experimental information, as is the case for deep eutectic solvents, as well as for the design of new products and processes based on these solvents. Furthermore, COSMO-RS allows to identify molecular affinities, i.e., repulsive or attractive interactions, in terms of excess enthalpy (H^E) contributions: hydrogen bonding (HB), electrostatics or misfit interactions (MF), and van de Waals forces (vdW), according to Equation 2.8(Palomar, Gonzalez-Miquel, Polo, & Rodriguez, 2011; Palomar, Gonzalez-Miquel, Bedia, Rodriguez, & Rodriguez, 2011; Gonzalez-Miquel, Palomar, Omar, & Rodriguez, 2011).:

$$H^E = H^E_{HB} + H^E_{MF} + H^E_{vdW} \tag{2.8}$$

The most important advantages provided by the COSMO-RS method compared to other models commonly used in Chemical Engineering are a) it predicts thermodynamic properties without the need to resort to experimental data; b) it provides a qualitative and quantitative description of the different chemical-physical interactions between the molecules of the pure components and mixtures and therefore contributes to the interpretation of the behaviour of these fluids; (c) includes in its calculation the effects associated with intramolecular interactions and the proximity effects associated with hydrogen bonds; (d) allows the difference between isomers to be resolved and therefore their contribution to the mixing properties to be estimated; and (e) presents a good description of the temperature dependence of the properties (Gonzalez-Miquel et al., 2012; Gonzalez-Miquel, Bedia,

Abrusci, Palomar, & Rodriguez, 2013; Gonzalez-Miquel, Bedia, Palomar, & Rodriguez, 2014).

COSMO based models calculations were carried out performing the following procedure. Quantum chemical software Turbomole (Schäfer, Klamt, Sattel, Lohrenz, & Eckert, 2000) was used to optimize the molecular geometries of the differents DESs and generate the corresponding COSMO file. For alcohols compounds the COSMO file available in Cosmologic database was used. Thus, COSMO files were used as an input in COSMOthermX (version C3.0 Release 18.0)(Klamt, Eckert, & Arlt, 2010) software, and its implicit parametrization (BP TZVP 18) was used to obtain the σ-profiles and σ-potentials of the compounds. For compounds with more than one conformation available, all were considered for calculations. Then, the σ-profile that contains the main chemical information necessary to predict interactions (Palomar, Gonzalez-Miquel, Bedia, et al., 2011).

In this work, COSMO-RS was employed to compute the mixing properties of pure DES and the detailed excess enthalpies of DES + alcohol mixtures. COSMO-RS calculations were performed considering a multicomponent quaternary mixture as input, fixing the ratio of cation and anion of the HBA and the HBD to represent the stoichiometry of DES along the whole composition range. Afterwards, all compositions and excess enthalpies obtained from COSMO-RS calculations were converted from the COSMO-RS framework (i.e., quaternary mixture) to the laboratory framework (i.e., pseudo-binary mixture) as explained in previous works (Bezold, Weinberger, & Minceva, 2017).

Computational calculations were performed using the COSMOtherm software, version C30, release 18.0.2, at the parametrization BP_TZVP_18.

2.5. The extended hard-sphere model

The hard sphere model was originally proposed by Dymond and Assael(Assael, Dymond, Papadaki, & Patterson, 1992b, 1992a) using a smooth-hard sphere representation of the molecules to express thermodunamic and transport properties such as heat capacity

and viscosity. Subsequently, the model was refined in order to include new capabilities such as working with mixtures(Assael, Dymond, & Papadaki, 1992; Assael, Dymond, & Patterson, 1992). As the transport properties are athermal they can be expressed as a function of the reduced volume $V^* = V_m / V_0$, where Vm is the molar volume, $V_0 = N_A \sigma^3 / \sqrt{2}$ is the molar volume for close-packed hard spheres, N_A is Avogadro's constant and σ is the diameter of the molecules. Also, reduce coefficients are used to transport properties in this scheme, the reduce viscosity was defined as follows:

$$\eta^* = \left(\frac{\eta}{\eta_0}\right)\left(\frac{V_m}{V_0}\right)^{\frac{2}{3}} \tag{2.9}$$

where η_0 is the viscosity of the same system in the dilute gas limit. The full expression for η^* is:

$$\eta^* = \left(\frac{16}{5}\right)\left(2N_A\right)^{\frac{1}{3}}\left(\frac{\pi}{MRT}\right)^{\frac{1}{2}} V_m^{\frac{2}{3}}\eta \tag{2.10}$$

where M is the molar mass and R the gas constant. The first approach to calculate the reduce viscosity η^* was combine the Enskog approximation with simulations from molecular dynamics calculations(Ciotta, Trusler, & Vesovic, 2014). In order to model real spherical molecules, repulsive molecular interactions have to be taken into account. For this purpose, a universal curve of reduced viscosity as a function of V_0 can be obtained for a given temperature. In practical terms, V_0 decreases with temperature and can be correlated as a temperature polynomial if a range of temperatures was considered. Having an simulated value for η^* could help to find the optimal value for V_0 correlating the viscosity of a simple molecular fluid along an isotherm(Huber, Hanley, Millat, Dymond, & de Castro, 1996).

In order to apply the model to non-spherical molecules it is necessary to treat them as rough hard-spheres. For this, it is necessary to incorporate a multiplicative term to the expression of viscosity, independent of temperature. Then, a more generalized expression

of reduced viscosity is:

$$\eta * = \left(\frac{16}{5}\right)\left(2N_A\right)^{\frac{1}{3}}\left(\frac{\pi}{MRT}\right)^{\frac{1}{2}} V_m^{\frac{2}{3}}\left(\frac{\eta}{R_\eta}\right) \tag{2.11}$$

where R_η is the roughness factor(Assael, Dymond, Papadaki, & Patterson, 1992a). To correlate the results of the simulation scheme of Dymond and Assael (Assael, Dymond, Papadaki, & Patterson, 1992b) a function from experimental data for $\Delta\eta^*$ was found to be universal for all liquids is equal to:

$$\log_{10}(\Delta\eta^*) = \sum_{i=1}^{7} a_i \left(\frac{1}{V*}\right)^i \tag{2.12}$$

where a_i are the constants of a polynomial that describes the reduced viscosity as a function of V_0, limited to values below 50 for η^* in the original scheme(Assael, Dymond, Papadaki, & Patterson, 1992b). Ciotta(Ciotta et al., 2014) proposed a new set of parameters for high viscosity hydrocarbons, expanding the range to $\eta^* \geq 2000$. DES have a higher viscosity than hydrocarbons, then the validity of the method is taken into account for $\eta^* \geq 2000$. Gaciño et al.(Gaciño, Comuñas, Fernández, Mylona, & Assael, 2014) had good results for ionic liquids with η^* between 50 and 200000. The parameters reported by Gaciño et al.(Gaciño et al., 2014) were those chosen for this work and are shown in Table 2.4. The original hard-sphere scheme for viscosity is successful within its range of applicability, often representing experimental data within ±5%. It is important to note that the method is very sensitive to the values of molar volume used, with relative errors in V_m typically leading at high densities to relative errors in approximately one order of magnitude greater. Thus, when interpreting experimental data at given temperature and pressure, one requires precise knowledge of the corresponding molar volume.

I	$\alpha_{\eta i}$	$\alpha_{\lambda i}$	$\alpha_{\eta i}$ (Ciotta et al., 2014)
0	1.0945	1.0655	0
1	-9.26324	-3.538	5.14262
2	71.0385	12.121	-35.5878
3	-301.9012	-12.469	192.05015
4	797.6900	4.562	-573.37246
5	-1221.9770	-	957.41955
6	987.5574	-	-833.36825
7	-314.4636	-	299.40932

Table 2.4. Constants obtain by Gaciño and Ciotta (Gaciño et al., 2014).

3. MATERIAL AND METHODS

3.1. Chemicals

The compounds for preparing the DES as choline chloride, ethylene glycol, and 1,4-butanediol were supplied by Acros Organics and 1,3-propanediol by Sigma-Aldrich. The alcohols used for the pseudo-binary systems DES + alcohol as methanol, ethanol, and 1-butanol were purchased in Acros Organics and 1-propanol in Merck KGaA. Table 3.1 shows the specifications of each compound as molar mass, CAS number, purities, and source of the compounds used in this study. Figure 3.1 shows the structures of all the molecules used in this study.

Three types of DES were prepared using choline chloride as the HBA and ethylene glycol (DES-A), 1,3-propanediol (DES-B), and 1,4-butanediol (DES-C) as the HBD. All the DES have a molar ratio of HBA:HBD of approximately 1:3.

For the study of viscosity prediction using the hard sphere model, DES is prepared on the basis of choline chloride or betaine as HBA, while it is used as HBD ethylene glycol, 1,2-propanediol, 1,3-propanediol, 1,4-butanediol and phenol, at molar ratios between 1:2 and 1:6, in some cases not performed due to DES instability.

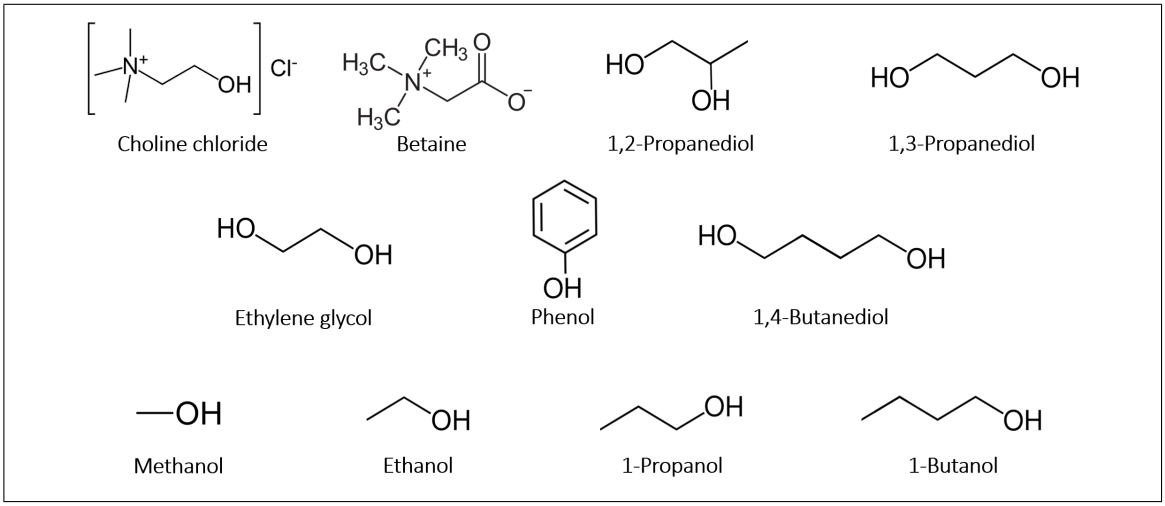

Figure 3.1. Chemicals used in the study.

Table 3.1. Specifications of chemicals used in this work as molar mass (M), CAS number, supplier, type and purity.

Chemical name	***M*** **(g·mol^{-1})**	**CAS**	**Supplier**	**Type**	**Purity**
Choline chloride	139.63	67-48-1	Acros Organics	-	>0.990
Betaine	117.15	107-43-7	Acros organics	Anhydous	>0.980
Ethylene glycol	62.07	107-21-1	Acros Organics	Anhydrous, AcroSeal®	>0.998
1,2-propanediol	76.10	54-55-6	Acros organics	Extra pure	>0.990
1,3-Propanediol	76.09	504-63-2	Sigma Aldrich	-	>0.980
1,4-Butanediol	90.12	110-63-4	Acros Organics	-	>0.990
Phenol	94.11	106-95-2	Sigma aldrich	Aldrich	>0.990
Methanol	32.04	67-56-1	Acros Organics	Anhydrous, AcroSeal®	>0.999
Ethanol	46.07	64-17-5	Acros Organics	Anhydrous, AcroSeal®	>0.995
1-Propanol	60.10	71-23-8	Merck KGaA	LiChrosolv®	>0.998
1-Butanol	74.12	71-36-3	Sigma Aldrich	Anhydrous	>0.998

3.2. Preparation of DES + DES mixtures

Before preparing the DES used in this study, choline chloride was dried in a Schlenk line under a high vacuum (10^{-4} mbar) during 72 hours to remove water absorbed from ambient humidity. Non–anhydrous HBDs and alcohols were placed under molecular sieves for 72 hours, also for decreasing their water content. Anhydrous compounds were used as received. DES were prepared by mass using an analytic balance (Practum 224-1s Sartorius, Germany, uncertainty $\pm$ 0.1 mg) adding the components to a vial. Then, the vial was quickly closed with a septum cap. The mixture was placed in a sonicator (iSonic P4862-IT, Australia) at 323.15 K until a homogeneous liquid was formed. The water content of all the DES was measured using a Karl Fischer Coulometer (831KF Metrohm, Switzerland). The DES were approximately mixed in a mole ratio of 1:3. Four batches of each DES were prepared and each one was mixed with a specific alcohol. All the properties

were measured shortly after the DES preparation for avoiding the absorption of water in the DES and its mixtures with the alcohols. All the DES with their respective molar ratios, molas mass and water content are shown in Table 3.2, where it is also specified the alcohol which is mixed with each batch of DES. DES + alcohol mixtures were also prepared by mass and mixed with a magnetic stir bar.

Figure 3.2. Schlenk line under high vacuum.

Figure 3.3. DES Mixing Stages.

Figure 3.4. Karl Fisher Coulometer.

Table 3.2. Components, mole ratio, composition, molar mass (M) and water content (wt.) of deep eutectic solvents and alcohols + deep eutectic solvent liquid mixture used in the excess properties study.

Abbreviation	**Salt**	**HBD**	**Mole ratio**	**M_{DES} (g·mol^{-1})**	**wt. %**	**Alcohol**
DES-A1	ChCl	Ethylene glycol	1:3.000	81.449	0.032	Methanol
DES-A2	ChCl	Ethylene glycol	1:3.002	81.441	0.078	Ethanol
DES-A3	ChCl	Ethylene glycol	1:2.999	81.447	0.061	1-Propanol
DES-A4	ChCl	Ethylene glycol	1:3.000	81.451	0.018	1-Butanol
DES-B1	ChCl	1,3 Propanediol	1:3.037	91.974	0.092	Methanol
DES-B2	ChCl	1,3 Propanediol	1:3.002	91.962	0.091	Ethanol
DES-B3	ChCl	1,3 Propanediol	1:3.000	91.971	0.053	1-Propanol
DES-B4	ChCl	1,3 Propanediol	1:3.001	91.969	0.060	1-Butanol
DES-C1	ChCl	1,4 Butanediol	1:3.000	102.494	0.049	Methanol
DES-C2	ChCl	1,4 Butanediol	1:2.999	102.496	0.019	Ethanol
DES-C3	ChCl	1,4 Butanediol	1:3.000	102.495	0.021	1-Propanol
DES-C4	ChCl	1,4 Butanediol	1:3.000	102.495	0.092	1-Butanol

Table 3.3. Abbreviation, components, mole ratio, and water content of deep eutectic solvents used in the viscosity prediction study.

Abbreviation	**Salt**	**HBD**	**Molar ratio**	**Water content (wt %)**
DES-VA1	ChCl	1,2-propanediol	1:3	0.0642
DES-VA2	ChCl	1,2-propanediol	1:4	0.0613
DES-VA3	ChCl	1,2-propanediol	1:5	0.0503
DES-VA4	ChCl	1,2-propanediol	1:6	0.0608
DES-VB1	ChCl	1,3-propanediol	1:3	0.0355
DES-VB2	ChCl	1,3-propanediol	1:4	0.0340
DES-VB3	ChCl	1,3-propanediol	1:5	0.0581
DES-VB4	ChCl	1,3-propanediol	1:6	0.0446
DES-VC1	ChCl	1,4-butanediol	1:3	0.0402
DES-VC2	ChCl	1,4-butanediol	1:4	0.0287
DES-VC3	ChCl	1,4-butanediol	1:5	0.0383
DES-VC4	ChCl	1,4-butanediol	1:6	0.0505
DES-VD1	ChCl	ethylene glycol	1:2	0.0790
DES-VD2	ChCl	ethylene glycol	1:3	0.0651
DES-VD3	ChCl	ethylene glycol	1:4	0.0389
DES-VD4	ChCl	ethylene glycol	1:5	0.0579
DES-VD5	ChCl	ethylene glycol	1:6	0.0465
DES-VE1	ChCl	phenol	1:2	0.0251
DES-VE2	ChCl	phenol	1:3	0.0209
DES-VE3	ChCl	phenol	1:4	0.0228
DES-VE4	ChCl	phenol	1:5	0.0196
DES-VE5	ChCl	phenol	1:6	0.0102
DES-VF1	betaine	1,2-propanediol	1:4	0.0603
DES-VF2	betaine	1,2-propanediol	1:5	0.0557
DES-VF3	betaine	1,2-propanediol	1:6	0.0376
DES-VG1	betaine	1,3-propanediol	1:5	0.0195
DES-VG2	betaine	1,3-propanediol	1:6	0.0249
DES-VH1	betaine	1,4-butanediol	1:6	0.0450
DES-VI1	betaine	ethylene glycol	1:4	0.0217
DES-VI2	betaine	ethylene glycol	1:5	0.0319
DES-VI3	betaine	ethylene glycol	1:6	0.0160
DES-VJ1	betaine	phenol	1:5	0.0220
DES-VJ2	betaine	phenol	1:6	0.0249

3.3. Fourier transform infrared spectroscopy

A Fourier transform infrared spectroscopy (FT-IR) analysis was performed to characterize choline chloride, the HBDs and the three types of DES. Measurements were made on a Shimadzu IRTracer-100 (Kyoto, Japan) between 400 and 4,000 cm^{-1}. The liquid samples were supported by transparent KBr films, while the solid samples were prepared in KBr pellets.

3.4. Equipment and instrumentation

Density (ρ) and dynamic viscosity (η) were measured for all the DES, the alcohols and their mixtures. These properties were obtained in an integrated system composed of an Anton Paar DMA4500M Densitometer (Graz, Austria) and an Anton Paar Lovis 2000ME microviscometer (Graz, Austria). The densitometer uses a vibrating U-tube technology to measure density with an accuracy of 0.00005 $g{\cdot}cm^{-3}$. The temperature inside the tube has an accuracy of 0.01 K using Pt-100 thermometer. These values are reported by the manufacturer. The densitometer was calibrated with double-distilled deionized and degassed water and dry air at 293.15 K and 101.3 kPa. The dynamic viscosity measurements are based on the falling ball principle using calibrated glass capillaries of 1.59 mm, 1.80 mm and 2.50 mm of internal diameter and steel balls. The calibration of the capillaries was done with the viscosity standards provided by Anton Paar. Viscosity measurements, as reported by the manufacturer, have repeatabilities of 0.1% and measurement accuracies between 0.17% and 0.50%, depending on the type of capillary used.

Figure 3.5 and 3.6 show the density and visibility equipment, respectively.

Figure 3.5. Anton Paar DMA4500M Densitometer.

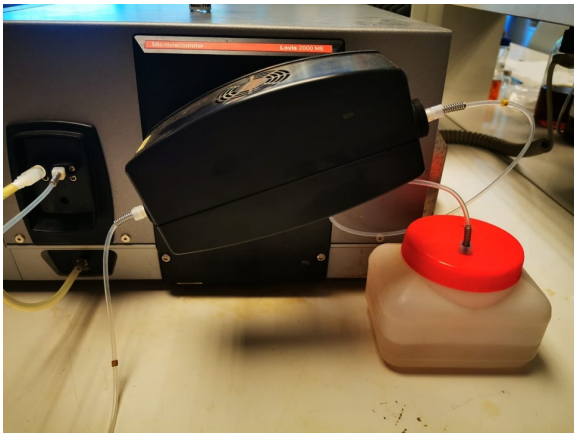

Figure 3.6. Anton Paar Lovis 2000ME microviscometer.

4. RESULTS AND DISCUSSION

4.1. FT-IR analysis of DES

FT-IR analysis was performed for choline chloride, ethylene glycol, 1,3-propanediol, 1,4-butanediol and all the DES formed by the mixtures of choline chloride with a diol, i.e., DES-A, DES-B and DES-C. The spectra for all the components and the DES are shown in Figure 4.1. The spectra agree with the expected structures and show the typical signals for the precursors and the DES.

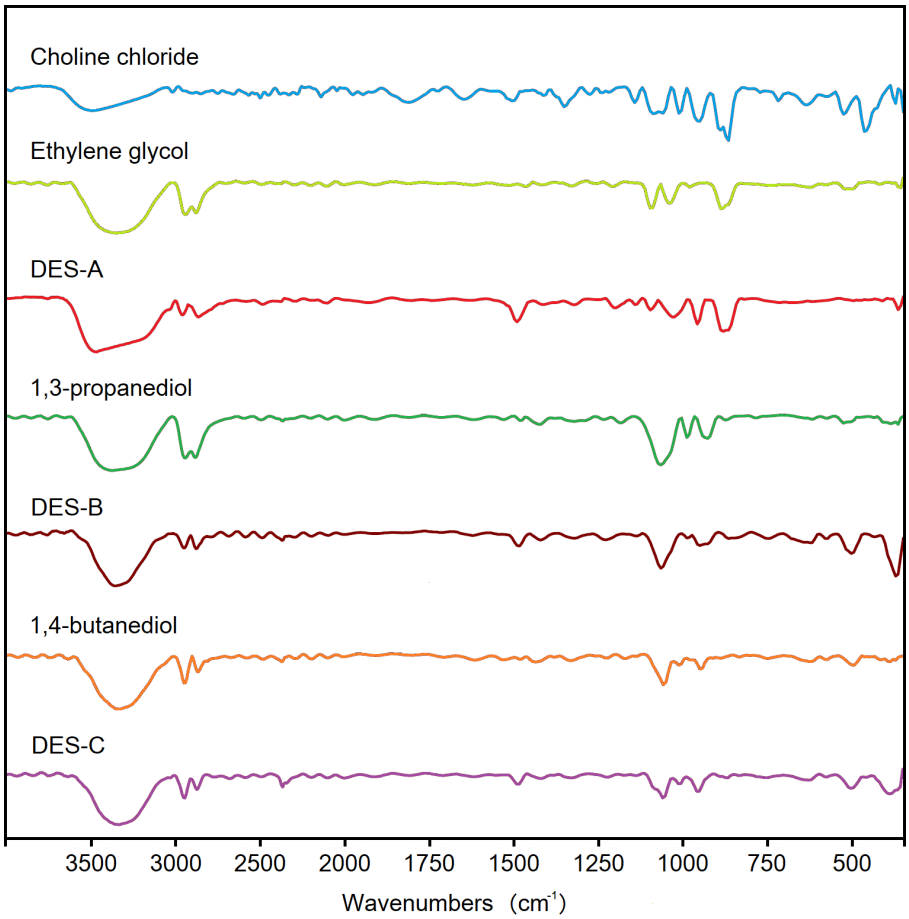

Figure 4.1. FT-IR analysis for DES and their precursors.

The IR spectrum of choline chloride shows the typical hydroxyl (OH) groups signal in the 3200-3700 cm^{-1} range. In the case of the alcohols spectra more defined and wider signals of the hydroxyl groups are observed together with the carbon-hydrogen (CH) sp3 group in the 2700 to 2950 cm^{-1} range.

From the respective IR spectra molecular interactions can be inferred in the formation of the DESs because of the displacements in the wavenumbers of the DES compared with their corresponding precursors as shown in Figure 4.1.(Gajardo-Parra et al., 2019) A shift from the original position of the -OH groups can be observed between 3500 - 2800 cm^{-1} due to the interaction of the -OH groups of the diols with the one of choline chloride, generating a stretch of the protons in the hydroxyl groups. Furthermore, it is observed that the interaction of hydroxyl groups becomes less important as the carbon chain of the diols is longer. For instance, it is observed a shift in the DES-A spectrum (2-carbons diol) while in DES-C (4-carbon diol) the change is almost undetectable. At the same time, a signal around 956 - 949 cm^{-1} presents a peak associated with the ammonium part of choline chloride in the DES, consistent with Aissaoui (Aissaoui, 2015), Zullaikah et al.(Zullaikah, Rachmaniah, Utomo, Niawanti, & Ju, 2017) and Gajardo et al.(Gajardo-Parra et al., 2019) Therefore, the FT-IR study proves that intermolecular interactions form the eutectic mixtures and there is no sign of a chemical reaction between the precursors.

4.2. Density and dynamic viscosities of DES and alcohols

Density and viscosity measurements were carried out for pure methanol, ethanol, 1-propanol, and 1-butanol at temperatures between 293.15 K and 333.15 K at a pressure of 101.3 kPa. These results were compared with literature data reported different authors for density(Sahin, Erkan, & Ayranci, 2016; Long & Ding, 2015; Gonfa, Bustam, Muhammad, & Ullah, 2015; Z. Zhang, Zhou, Lu, Qiao, & Zhang, 2014; Varfolomeev, Zaitseva, Rakipov, Solomonov, & Marczak, 2014; Smyth & Stoops, 1929; Khimenko, 1973; Tashima, 1981; Mikhail & Kimel, 1963; J. Singh & Benson, 1968; Westmeier, 1976; Fukuchi, 1980; Boruń & Bald, 2016; Safarov, Ahmadov, Mirzayev, Shahverdiyev,

& Hassel, 2015; Iglesias-Silva, Bravo-Sanchez, Estrada-Baltazar, Bouchot, & Hall, 2015; Zhu, Han, Liu, & Ma, 2014) and viscosity.(Khalilov, 1939; Ledneva, 1956; Mikhail & Kimel, 1961; Rauf & Stewart, 1983; Saha, Das, & Hazra, 1995; Misra & Varshni, 1961; Tommila, 1969; Phillips & Murphy, 1970; B. Garcia, Herrera, & Leal, 1991; Nikam, Shirsat, & Hasan, 1998; Pal & Dass, 1999; Chen et al., 2014; Knezeć-Stevanović, Radović, Serbanović, & Kijevcanin, 2014; N. Živković, Šerbanović, Kijevčanin, & Živković, 2013; Estrada-Baltazar, 2013) The comparison is shown in Figure 4.2(a) and in Figure 4.2(b) for density and viscosity, respectively, as an average relative deviation (ARD(%)). It is observed that all the ARD(%) values for density are below 0.15 % and for viscosity below 10 %. ARD(%) calculations are done according to Equation 4.1:

$$ARD(\%) = 100 \cdot \left(\frac{N_{\text{exp}} - N_{\text{lit}}}{N_{\text{exp}}} \right) \tag{4.1}$$

where N_{exp} and N_{lit} are the density or viscosity of the pure alcohol at a specific temperature of data from this work and from literature, respectively.

Density and viscosity results for the DES studied in this work are reported in Figure 4.3(a) and Figure 4.3(b), respectively, for all the pseudo-pure DES batches listed on Table 3.2. These results are also compared with literature observing a good agreement for the density of DES with the same molar ratio(Shahbaz, Baroutian, Mjalli, Hashim, & Al-Nashef, 2012; Ozturk, Parkinson, & Gonzalez-Miquel, 2018; Abbott, Harris, & Ryder, 2007; Chen et al., 2014; Rogošić & Kučan, 2019). Viscosity data follows a trend with the other authors, the difference in magnitude lies in the amount of water each sample has, where the more water the viscosity decreases to a greater extent. (Ozturk, Parkinson, & Gonzalez-Miquel, 2018; Abbott et al., 2007; Rogošić & Kučan, 2019; ?, ?) The density of the DES decrease with temperature and there is a clear dependence on the chain length of the HBD. The densities, in terms of the HBD, are ethylene glycol > 1,3-propanediol > 1,4-butanediol. This is consistent with the results reported by Garcia *et al.*(G. Garcia et al.,

2015) about the density decay due to a longer alkyl chain in organics acids(Gajardo-Parra et al., 2019).

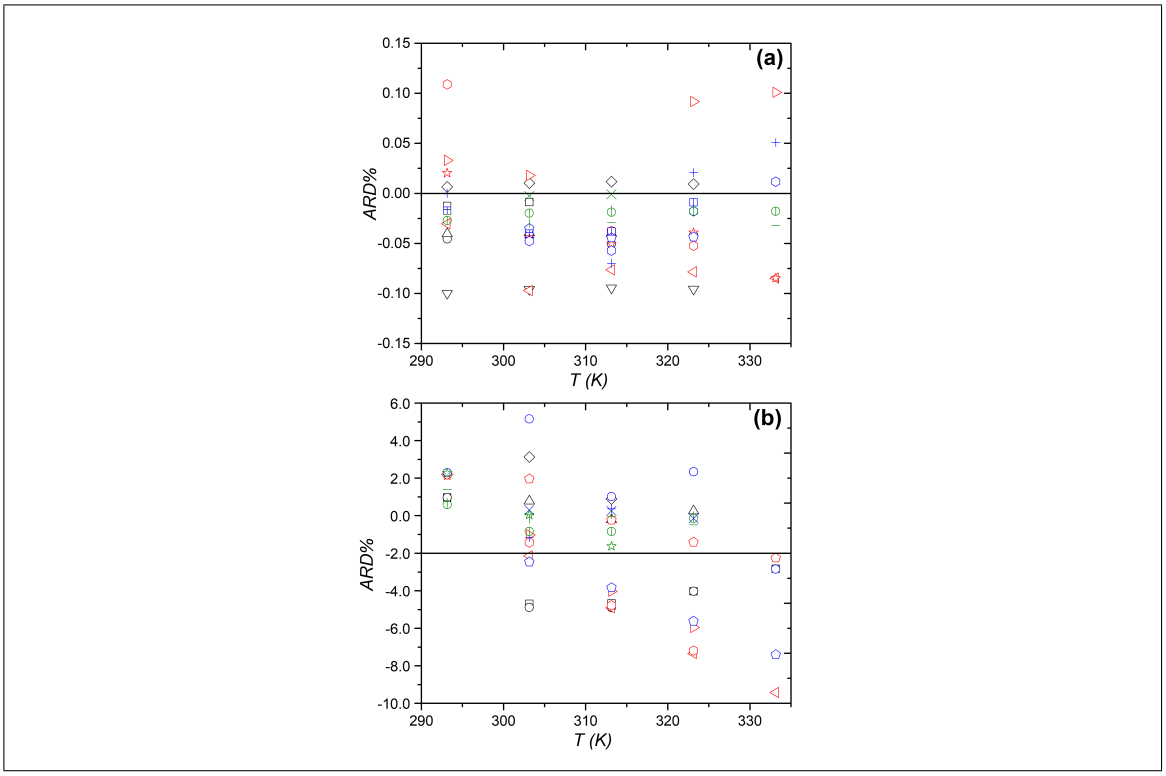

Figure 4.2. $ARD(\%)$ of the literature date for compared with this work: **(a)** Density comparison with data reported from Sahin et al. (Sahin et al., 2016) (□), Long et al.(Long & Ding, 2015)(○), Gonfa et al.(Gonfa et al., 2015)(△), Zhang et al.(Z. Zhang et al., 2014)(▽), Varfolomeev et al. (Varfolomeev et al., 2014)(◇), Smyth et al.(Smyth & Stoops, 1929)(◁), Khimenko et al.(Khimenko, 1973)(▷), Fukuchi et al.(Fukuchi, 1980)(⬡), Tashima et al. (Tashima, 1981)(☆), Mikhail et al.(Mikhail & Kimel, 1963)(⬠),Singh al.(J. Singh & Benson, 1968)(◫), Westmeier et al.(Westmeier, 1976)(+), Fukuchi et al.(Fukuchi, 1980)(⬡), Borun et al.(Boruń & Bald, 2016)(×), Safarov et al.(Safarov et al., 2015)(−), Iglesias et al.(Iglesias-Silva et al., 2015)(|), Zhu et al.(Zhu et al., 2014)(⦶). **(b)** Viscosity comparison with data reported from Khalilov et al. (Khalilov, 1939) (□), Ledneva et al.(Ledneva, 1956)(○), Mikhail et al.(Mikhail & Kimel, 1961)(△), Rauf et al.(Rauf & Stewart, 1983)(▽), Saha et al. (Saha et al., 1995)(◇), Misra et al.(Misra & Varshni, 1961)(◁), Tommila et al.(Tommila, 1969)(▷), Phillips et al.(Phillips & Murphy, 1970)(⬡), García et al.(B. Garcia et al., 1991)(⬠), Ledneva et al.(Ledneva, 1956)(○), García et al.(B. Garcia et al., 1991)(⬠), Nikam et al.(Nikam et al., 1998)(+), Pal et al.(Pal & Dass, 1999)(×), Chen et al. (Chen et al., 2014)(☆), Knezevic-Stevanonic et al.(Knezeć-Stevanović et al., 2014)(−), Vzivkovic et al.(E. M. Živković et al., 2014)(|), Estrada-Baltazar et al.(Estrada-Baltazar, 2013)(⦶).

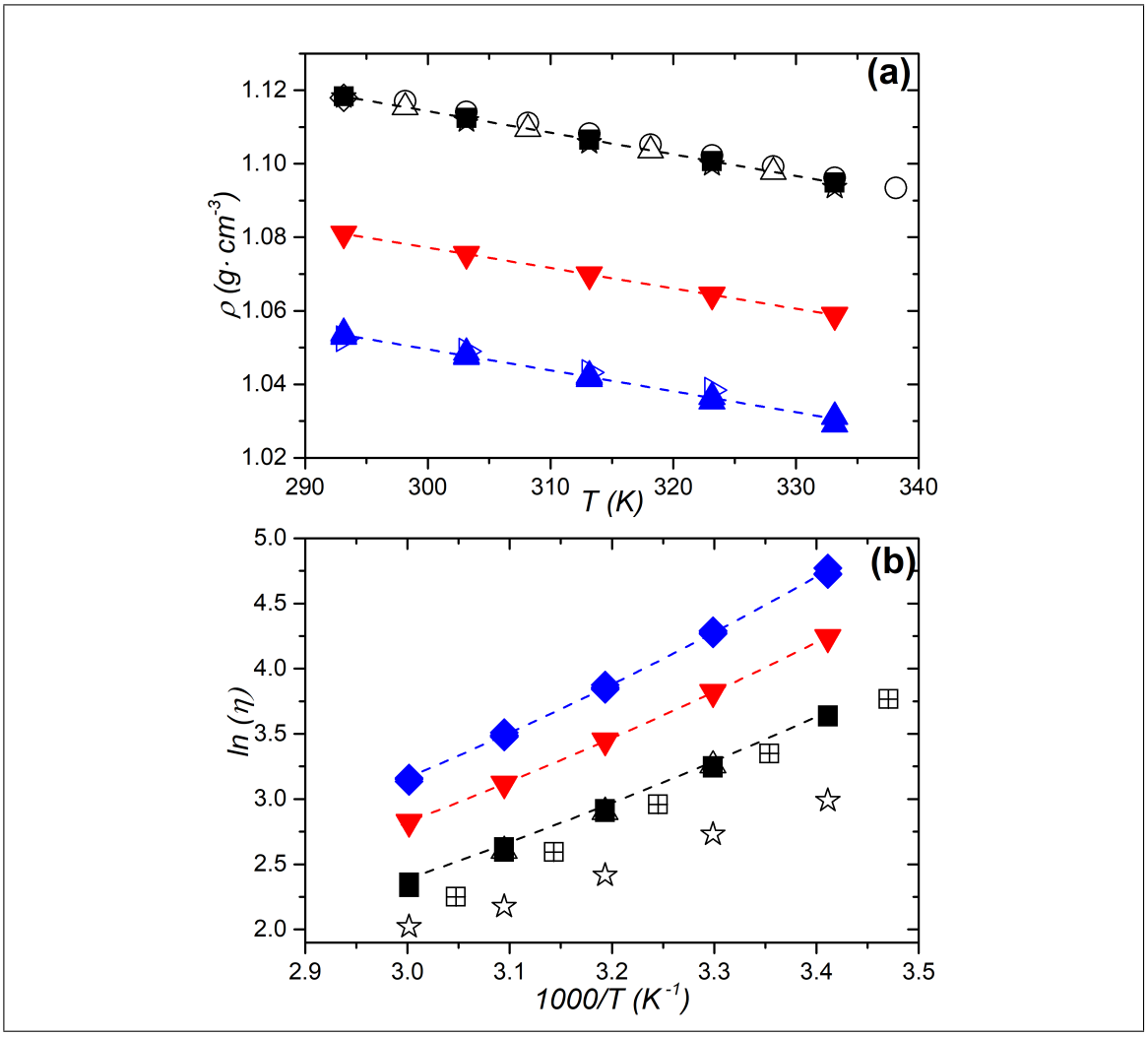

Figure 4.3. **(a)** Density (g·cm^{-3}) and **(b)** dynamic viscosity (mPa·s) of DES-A (■), DES-B (●), DES-C (▲) measured in this work as a function of temperature at a pressure of 101.3 kPa. Comparision data with **(a)** Shahbaz et al.(Shahbaz et al., 2012)(○), Ozturk et al. (Ozturk, Parkinson, & Gonzalez-Miquel, 2018)(☆), Abbott et al. (Abbott et al., 2007)(◇), Chen et al.(Chen et al., 2014)(▷). Dashed line (- - -) represents the fitting with linear equation with parameters in **(a)** and fitting with VFT equation with parameters in **(b)**, both reported in Table 4.1.

Also, the trend shows the same behaviour of pure HBDs, for example, at 298.15 K ethylene glycol has a density of 1.2201 g·cm^{-3}(Esteban & Gonzalez-Miquel, 2018), 1.0501 g·cm^{-3}(Canosa, Rodriguez, Iglesias, Orge, & Tojo, 1998) for 1,3-propanediol and

1.0126 g·cm^{-3} (Hawrylak, Gracie, & Palepu, 1998) for 1,4-butanediol. Thus, the addition of choline chloride generates an increase in density of the eutectic mixture. The amount of water does not seem to be a variable that greatly affects density, probably due to the similarity of the density of DES with that of water. Density this work and literature date were fitted with a linear fit showed in Equation 4.2. In this equation, a and b represents the intercept and the slope, respectively. The obtained parameters are presented in Table 4.1 obtaining and average absolute deviation (AAD) beetwen 0.002 and 0.016%. AAD is showed in Equation 4.3, where θ its the property and n the number of date considered in the calculation.

$$\rho(T) = a + b \cdot T \tag{4.2}$$

$$AAD(\%) = \frac{100}{n} \cdot \sum_{i=1}^{n} \left| \frac{\theta_{\text{exp}} - \theta_{\text{cal}}}{\theta_{\text{cal}}} \right| \tag{4.3}$$

Table 4.1. Linear fitting coefficients from equation 4.2 (a intercept and b slope) for correlating the densities of deep eutectic solvents used in this work as specified in Table 3.2, and the respective coefficient of determination (R^2) and the average absolute deviation (AAD) of the correlation.

Linear fitting				
System	a	$10^{-4}\cdot$ b	R^2	AAD /(%)
DES-A	1.290	-5.9	1.000	0.002
DES-B	1.243	-5.5	1.000	0.002
DES-C	1.221	-5.7	1.000	0.007

Viscosities decrease greatly with the temperature. In terms of the HBD, the observed viscosity trend is 1,4-butanediol > 1,3-propanediol > ethylene glycol. This is same behaviour to the pure HBD, where at 298.15 K the viscosity of pure ethylene glycol is 13.108 mPa·s (Esteban & Gonzalez-Miquel, 2018), 41.507 mPa·s for 1,3-propanediol(E. M. Živković

et al., 2014) and 72.326 mPa·s for 1,4-butanediol(Moosavi, Motahari, Omrani, & Rostami, 2013). When choline chloride is added in DES preparation viscosity increase due to stronger molecular interactions, i.e. hydrogen bonds and electrostatic interactions affecting the molecular movement. Also, the longer alkyl chain in 1,4-butanediol influence the molecular mobility increasing the viscosity.

Viscosity data were correlated with the temperature (T) in the Vogel-Fulcher-Tamman correlation(Vogel, 1921) (VFT, with parameter adjustment A, B and T_0) shown in Equation 4.4:

$$\eta_{VFT}(T) = A \cdot \exp\left(\frac{B}{T - T_0}\right) \tag{4.4}$$

Fitting parameters for all the systems measured in this work are shown in Table 4.1, along with their respective AAD. VFT equation provides an average absolute deviation for the DES between 0.459 % and 0.228 % . Therefore, viscosity data from this work are correlated with VFT equation in Figure 4.3(b).

Table 4.2. Viscosity fitting coefficients from VFT equations 4.4 of deep eutectic solvents used in this work as specified in Table 3.2, and the respective coefficient of determination (R^2) and the average absolute deviation (AAD) of the correlation.

Vogel-Fulcher-Tamman				
System	A	B	T_0	AAD /(%)
DES-A	0.141	795.084	152.501	1.363
DES-B	0.148	821.819	159.692	0.305
DES-C	0.151	846.415	165.801	0.820

4.3. Mixture Densities and Molar Excess Volumes

Density measurements of binary mixtures composed by alcohol + DES were obtained at temperatures between 293.15 K – 333.15 K and 101.3 kPa in the full range of compositions. The four alcohols used in the study are completely miscible with the three DES at all the measurement conditions. Density data for mixtures of the alcohols with DES-A, DES-B and DES-C are shown in Tables 4.3, 4.4 and 4.5, respectively. Considering that the four alcohols have a lower density compared with the three DES, the density of the mixtures decrease by adding alcohol to the mixture. Also, the density decreases by increasing the temperature at a constant alcohol composition in the DES, as expected.

From this study different phenomena could be analyzed: the effect of temperature, effect of alcohol chain length and the effect of HBD chain length on choline chloride deep eutectic solvents, which are discussed below.

4.3.1. V^E Temperature effect

In order to assess the non-ideality, structural adjustment and molecular interactions of the pseudo-binary mixtures alcohol + DES, data from Tables 4.3, 4.4 and 4.5 are also shown in the form of molar excess volume (V^E) which is determined using equation 4.5:

$$V^{\mathrm{E}} = \frac{x_1 \cdot M_1 + x_2 \cdot M_2}{\rho} - \left(\frac{x_1 \cdot M_1}{\rho_1}\right) - \left(\frac{x_2 \cdot M_2}{\rho_2}\right) \tag{4.5}$$

where x_i, ρ_i and M_i are the composition, density and molar mass of the compound i, respectively and ρ is the density of the mixture.

V^E for all the binary systems was fit to the Redlich - Kister (RK) correlation shown in equation 4.6, where V^E_{RK} is the V^E calculated with RK, x_1 is the molar fraction of the alcohols, x_2 molar fraction of the DES and α_i are the adjustable parameters of the polynomial of $k + 1$ terms. All the RK fitting parameters are reported in Table 4.6.

$$V_{RK}^{\mathrm{E}} = x_1 \cdot x_2 \cdot \sum_{i=0}^{k} \alpha_i \cdot \left(x_1 - x_2\right)^i \tag{4.6}$$

V^E of the binary mixtures have negative values for all the binary systems alcohol + DES at all the temperatures and compositions, as observed in Figure 4.4 for the DES-A in mixtures with (a) methanol, (b) ethanol, (c) 1-propanol and (d) 1-butanol. That is, the volume of the mixture is lower than in the ideal mixture of DES-A and the four alcohols used in this work. The Figures A.1 and A.2 show the same behavior for all the alcohols in DES-B and DES-C. It is also observed that the V^E becomes increasingly negative at higher temperatures for all the mixtures. This is typically explained as stronger interactions of alcohol - DES molecules compared with alcohol - alcohol or DES - DES interactions. Then, by increasing the temperature, the interaction between the same molecules decrease and the interaction of unlike molecules become more important, allowing a better interstitial accommodation. In addition, the specific interactions are weaker at higher temperatures producing an increase in the size of interstitial molecular space. That suggest that packing effects dominate the volumetric behavior of the binary mixtures alcohol + DES. This behavior is different for aqueous mixtures of DES where at higher temperatures V^E is less negative as discussed elsewhere.(Gajardo-Parra et al., 2019)

Table 4.3. Densities (g·cm^{-3}) and excess molar volume (cm^3·mol^{-1}) of alcohols(1) + DES(2) (choline chloride + ethylene glycol) liquid mixture at different temperatures (K), molar compositions of alcohols (x_1) and a pressure of 101.3 kPa. Deep eutectic solvents binary system used for these measurements are detailed in Table 3.2.

DES-A1										
	Density (g·cm^{-3})					Excess Volume (cm^3·mol^{-1})				
x_1	293.15K	303.15 K	313.15 K	323.15 K	333.15 K	293.15K	303.15 K	313.15 K	323.15 K	333.15 K
0.0000	1.1183	1.1124	1.1065	1.1007	1.0949	0.0000	0.0000	0.0000	0.0000	0.0000
0.1398	1.0967	1.0906	1.0846	1.0785	1.0725	-0.3403	-0.3629	-0.3869	-0.4121	-0.4379
0.2802	1.0707	1.0644	1.0578	1.0514	1.0448	-0.6279	-0.6662	-0.6949	-0.7343	-0.8014
0.4187	1.0396	1.0331	1.0265	1.0199	1.0133	-0.8406	-0.9001	-0.9622	-1.0291	-1.0981
0.5597	1.0004	0.9935	0.9866	0.9797	0.9727	-0.9571	-1.0267	-1.1001	-1.1804	-1.2671
0.7007	0.9515	0.9441	0.9367	0.9291	0.9217	-0.9533	-1.0252	-1.1018	-1.1827	-1.2763
0.8402	0.8892	0.8810	0.8729	0.8646	0.8563	-0.7442	-0.7978	-0.8606	-0.9300	-1.0054
1.0000	0.7913	0.7819	0.7724	0.7627	0.7529	0.0000	0.0000	0.0000	0.0000	0.0000
DES-A2										
	Density (g·cm^{-3})					Excess Volume (cm^3·mol^{-1})				
x_1	293.15K	303.15 K	313.15 K	323.15 K	333.15 K	293.15K	303.15 K	313.15 K	323.15 K	333.15 K
0.0000	1.1184	1.1125	1.1066	1.1007	1.0949	0.0000	0.0000	0.0000	0.0000	0.0000
0.1397	1.0862	1.0802	1.0741	1.0680	1.0619	-0.3706	-0.4019	-0.4300	-0.4590	-0.4881
0.2800	1.0500	1.0437	1.0374	1.0311	1.0247	-0.6346	-0.6901	-0.7404	-0.7937	-0.8537
0.4197	1.0097	1.0032	0.9965	0.9899	0.9832	-0.7851	-0.8593	-0.9242	-0.9952	-1.0746
0.5601	0.9648	0.9579	0.9509	0.9438	0.9368	-0.8229	-0.9087	-0.9811	-1.0612	-1.1508
0.6999	0.9153	0.9080	0.9006	0.8931	0.8855	-0.7502	-0.8377	-0.9075	-0.9838	-1.0716
0.8401	0.8605	0.8527	0.8448	0.8367	0.8285	-0.5522	-0.6219	-0.6741	-0.7285	-0.7989
1.0000	0.7899	0.7808	0.7721	0.7632	0.7541	0.0000	0.0000	0.0000	0.0000	0.0000
DES-A3										
	Density (g·cm^{-3})					Excess Volume (cm^3·mol^{-1})				
x_1	293.15K	303.15 K	313.15 K	323.15 K	333.15 K	293.15K	303.15 K	313.15 K	323.15 K	333.15 K
0.0000	1.1184	1.1125	1.1066	1.1007	1.0949	0.0000	0.0000	0.0000	0.0000	0.0000
0.1285	1.0808	1.0750	1.0692	1.0634	1.0576	-0.2623	-0.3056	-0.3496	-0.3934	-0.4345
0.2798	1.0353	1.0289	1.0225	1.0160	1.0098	-0.4735	-0.5186	-0.5619	-0.6008	-0.6615
0.4195	0.9918	0.9852	0.9785	0.9718	0.9651	-0.5588	-0.6193	-0.6782	-0.7382	-0.7963
0.5597	0.9474	0.9405	0.9336	0.9265	0.9194	-0.5749	-0.6421	-0.7054	-0.7682	-0.8273
0.7362	0.8907	0.8835	0.8762	0.8686	0.8610	-0.4807	-0.5491	-0.6208	-0.664	-0.7098
0.8404	0.8566	0.8491	0.8414	0.8335	0.8256	-0.3457	-0.4015	-0.4474	-0.4851	-0.5089
1.0000	0.8035	0.7952	0.7870	0.7787	0.7704	0.0000	0.0000	0.0000	0.0000	0.0000
DES-A4										
	Density (g·cm^{-3})					Excess Volume (cm^3·mol^{-1})				
x_1	293.15K	303.15 K	313.15 K	323.15 K	333.15 K	293.15K	303.15 K	313.15 K	323.15 K	333.15 K
0.0000	1.1184	1.1125	1.1066	1.1007	1.0949	0.0000	0.0000	0.0000	0.0000	0.0000
0.1405	1.0697	1.0637	1.0576	1.0515	1.0455	-0.2835	-0.3097	-0.3368	-0.3679	-0.3988
0.2796	1.0220	1.0156	1.0093	1.0029	0.9965	-0.3740	-0.4057	-0.4507	-0.4964	-0.5489
0.4204	0.9758	0.9692	0.9625	0.9559	0.9492	-0.3944	-0.4349	-0.4831	-0.5372	-0.6009
0.5595	0.9327	0.9258	0.9189	0.9119	0.9049	-0.3810	-0.4234	-0.4707	-0.5261	-0.5934
0.6998	0.8913	0.8842	0.8770	0.8698	0.8624	-0.3168	-0.3527	-0.3934	-0.4432	-0.5031
0.8385	0.8525	0.8452	0.8377	0.8302	0.8225	-0.2056	-0.2296	-0.2576	-0.2915	-0.3347
1.0000	0.8095	0.8019	0.7941	0.7862	0.7780	0.0000	0.0000	0.0000	0.0000	0.0000

Standard uncertainties μ are $\mu(x_1) = 0.005$, μ(T) = 0.01 K, μ(P) = 1 kPa and $\mu(\rho) = 0.004$ g·cm^{-3}

Table 4.4. Densities (g·cm^{-3}) and excess molar volume (cm^3·mol^{-1}) of alcohols(1) + DES(2) (choline chloride + 1,3 propanediol) liquid mixture at different temperatures (K), molar compositions of alcohols (x_1) and a pressure of 101.3 kPa. Deep eutectic solvents binary system used for these measurements are detailed in Table 3.2.

DES-B1										
	Density (g·cm^{-3})					Excess Volume (cm^3·mol^{-1})				
x_1	293.15K	303.15 K	313.15 K	323.15 K	333.15 K	293.15K	303.15 K	313.15 K	323.15 K	333.15 K
0.0000	1.0810	1.0754	1.0699	1.0644	1.0589	0.0000	0.0000	0.0000	0.0000	0.0000
0.1394	1.0643	1.0586	1.0529	1.0472	1.0415	-0.3005	-0.3231	-0.3469	-0.3724	-0.3990
0.2796	1.0439	1.0379	1.0320	1.0260	1.0197	-0.5579	-0.5999	-0.6442	-0.6877	-0.7116
0.4209	1.0184	1.0122	1.0060	0.9994	0.9928	-0.7727	-0.8315	-0.8946	-0.9333	-0.9769
0.5587	0.9867	0.9802	0.9736	0.9668	0.9600	-0.8927	-0.9632	-1.0392	-1.1060	-1.1816
0.7013	0.9438	0.9367	0.9296	0.9225	0.9154	-0.8930	-0.9664	-1.0459	-1.1326	-1.2276
0.8388	0.8878	0.8800	0.8721	0.8642	0.8562	-0.7072	-0.7690	-0.8354	-0.9091	-0.9899
1.0000	0.7913	0.7819	0.7724	0.7627	0.7529	0.0000	0.0000	0.0000	0.0000	0.0000
DES-B2										
	Density (g·cm^{-3})					Excess Volume (cm^3·mol^{-1})				
x_1	293.15K	303.15 K	313.15 K	323.15 K	333.15 K	293.15K	303.15 K	313.15 K	323.15 K	333.15 K
0.0000	1.0809	1.0754	1.0698	1.0643	1.0588	0.0000	0.0000	0.0000	0.0000	0.0000
0.1401	1.0563	1.0506	1.0448	1.0391	1.0334	-0.3549	-0.3859	-0.4143	-0.4461	-0.4796
0.2805	1.0282	1.0222	1.0162	1.0103	1.0043	-0.6511	-0.7080	-0.7604	-0.8165	-0.8783
0.4201	0.9951	0.9889	0.9826	0.9763	0.9700	-0.8020	-0.8785	-0.9468	-1.0227	-1.1059
0.5687	0.9545	0.9478	0.9412	0.9345	0.9277	-0.8600	-0.9495	-1.0274	-1.1136	-1.2101
0.6996	0.9127	0.9057	0.8985	0.8914	0.8841	-0.7828	-0.8751	-0.9508	-1.0350	-1.1305
0.8399	0.8610	0.8534	0.8456	0.8378	0.8298	-0.5673	-0.6489	-0.7074	-0.7736	-0.8485
1.0000	0.7899	0.7808	0.7721	0.7632	0.7541	0.0000	0.0000	0.0000	0.0000	0.0000
DES-B3										
	Density (g·cm^{-3})					Excess Volume (cm^3·mol^{-1})				
x_1	293.15K	303.15 K	313.15 K	323.15 K	333.15 K	293.15K	303.15 K	313.15 K	323.15 K	333.15 K
0.0000	1.0810	1.0754	1.0699	1.0643	1.0588	0.0000	0.0000	0.0000	0.0000	0.0000
0.1400	1.0504	1.0446	1.0388	1.0329	1.0270	-0.3293	-0.3547	-0.3792	-0.4006	-0.4151
0.2802	1.0167	1.0107	1.0048	0.9986	0.9923	-0.5242	-0.5739	-0.6291	-0.6665	-0.6937
0.4196	0.9808	0.9746	0.9683	0.9617	0.9553	-0.6291	-0.7027	-0.7690	-0.8149	-0.8756
0.5606	0.9422	0.9356	0.9289	0.9222	0.9154	-0.6636	-0.7373	-0.8093	-0.8789	-0.9472
0.7004	0.9018	0.8948	0.8877	0.8806	0.8733	-0.6409	-0.7150	-0.7852	-0.8536	-0.9109
0.8436	0.8574	0.8499	0.8424	0.8348	0.8270	-0.4924	-0.5556	-0.6110	-0.6599	-0.6946
1.0000	0.8035	0.7952	0.7870	0.7787	0.7704	0.0000	0.0000	0.0000	0.0000	0.0000
DES-B4										
	Density (g·cm^{-3})					Excess Volume (cm^3·mol^{-1})				
x_1	293.15K	303.15 K	313.15 K	323.15 K	333.15 K	293.15K	303.15 K	313.15 K	323.15 K	333.15 K
0.0000	1.0810	1.0755	1.0699	1.0644	1.0589	0.0000	0.0000	0.0000	0.0000	0.0000
0.1399	1.0441	1.0384	1.0327	1.0269	1.0212	-0.2945	-0.3182	-0.3473	-0.3802	-0.4167
0.2851	1.0048	0.9988	0.9927	0.9867	0.9806	-0.4610	-0.5003	-0.5442	-0.5935	-0.6506
0.4199	0.9678	0.9615	0.9552	0.9489	0.9425	-0.5189	-0.5661	-0.6191	-0.6812	-0.7517
0.5599	0.9293	0.9227	0.9160	0.9093	0.9026	-0.4962	-0.5443	-0.5990	-0.6623	-0.7378
0.7105	0.8884	0.8815	0.8745	0.8674	0.8602	-0.4370	-0.4800	-0.5289	-0.5873	-0.6566
0.8397	0.8531	0.8459	0.8386	0.8312	0.8236	-0.2909	-0.3209	-0.3559	-0.3982	-0.4491
1.0000	0.8095	0.8019	0.7941	0.7862	0.7780	0.0000	0.0000	0.0000	0.0000	0.0000

Standard uncertainties μ are $\mu(x_1) = 0.005$, μ(T) = 0.01 K, μ(P) = 1 kPa and $\mu(\rho) = 0.004$ g·cm^{-3}

Table 4.5. Densities (g·cm^{-3}) and excess molar volume (cm^3·mol^{-1}) of alcohols(1) + DES(2) (choline chloride + 1,4 butanediol) liquid mixture at different temperatures (K), molar compositions of alcohols (x_1) and a pressure of 101.3 kPa. Deep eutectic solvents binary system used for these measurements are detailed in Table 3.2.

DES-C1										
	Density (g·cm^{-3})					Excess Volume (cm^3·mol^{-1})				
x_1	293.15K	303.15 K	313.15 K	323.15 K	333.15 K	293.15K	303.15 K	313.15 K	323.15 K	333.15 K
0.0000	1.0536	1.0478	1.0415	1.0353	1.0291	0.0000	0.0000	0.0000	0.0000	0.0000
0.1403	1.0395	1.0339	1.0283	1.0228	1.0172	-0.2231	-0.2758	-0.3685	-0.4535	-0.5473
0.2801	1.0229	1.0171	1.0112	1.0052	0.9996	-0.4629	-0.5265	-0.6199	-0.7053	-0.8211
0.4197	1.0022	0.9962	0.9901	0.9835	0.9773	-0.6810	-0.7578	-0.8636	-0.9316	-1.0388
0.5597	0.9749	0.9685	0.9621	0.9556	0.9491	-0.8087	-0.8915	-0.9995	-1.1108	-1.2268
0.7001	0.9382	0.9313	0.9244	0.9174	0.9104	-0.8500	-0.9325	-1.0349	-1.1426	-1.2614
0.8399	0.8860	0.8783	0.8706	0.8628	0.8549	-0.6871	-0.7548	-0.8346	-0.9200	-1.0153
1.0000	0.7913	0.7819	0.7724	0.7627	0.7529	0.0000	0.0000	0.0000	0.0000	0.0000
DES-C2										
	Density (g·cm^{-3})					Excess Volume (cm^3·mol^{-1})				
x_1	293.15K	303.15 K	313.15 K	323.15 K	333.15 K	293.15K	303.15 K	313.15 K	323.15 K	333.15 K
0.0000	1.0540	1.0486	1.0424	1.0367	1.0312	0.0000	0.0000	0.0000	0.0000	0.0000
0.1400	1.0331	1.0278	1.0219	1.0162	1.0106	-0.2359	-0.2855	-0.3402	-0.3947	-0.4297
0.2791	1.0100	1.0043	0.9982	0.9923	0.9864	-0.4941	-0.5571	-0.6354	-0.7035	-0.7622
0.4201	0.9822	0.9762	0.9699	0.9637	0.9575	-0.6780	-0.7607	-0.8462	-0.9336	-1.0141
0.5598	0.9495	0.9431	0.9366	0.9301	0.9235	-0.7796	-0.8660	-0.9752	-1.0765	-1.1700
0.7000	0.9096	0.9027	0.8959	0.8889	0.8818	-0.7449	-0.8374	-0.9475	-1.0485	-1.1455
0.8400	0.8610	0.8535	0.8459	0.8382	0.8304	-0.5573	-0.6413	-0.7154	-0.7911	-0.8728
1.0000	0.7899	0.7808	0.7721	0.7632	0.7541	0.0000	0.0000	0.0000	0.0000	0.0000
DES-C3										
	Density (g·cm^{-3})					Excess Volume (cm^3·mol^{-1})				
x_1	293.15K	303.15 K	313.15 K	323.15 K	333.15 K	293.15K	303.15 K	313.15 K	323.15 K	333.15 K
0.0000	1.0530	1.0475	1.0420	1.0366	1.0311	0.0000	0.0000	0.0000	0.0000	0.0000
0.1404	1.0288	1.0232	1.0177	1.0121	1.0065	-0.3315	-0.3676	-0.4097	-0.4473	-0.4824
0.2796	1.0014	0.9955	0.9897	0.9838	0.9780	-0.5206	-0.5731	-0.6286	-0.6830	-0.7387
0.4198	0.9708	0.9647	0.9585	0.9524	0.9462	-0.6286	-0.6971	-0.7666	-0.8364	-0.9055
0.5617	0.9365	0.9301	0.9236	0.9171	0.9105	-0.6630	-0.7415	-0.8187	-0.8973	-0.9709
0.6997	0.8996	0.8927	0.8859	0.8790	0.8720	-0.6036	-0.6823	-0.7673	-0.8397	-0.9116
0.8400	0.8577	0.8504	0.8430	0.8355	0.8278	-0.4231	-0.4904	-0.5486	-0.6011	-0.6406
1.0000	0.8035	0.7952	0.7870	0.7787	0.7704	0.0000	0.0000	0.0000	0.0000	0.0000
DES-C4										
	Density (g·cm^{-3})					Excess Volume (cm^3·mol^{-1})				
x_1	293.15K	303.15 K	313.15 K	323.15 K	333.15 K	293.15K	303.15 K	313.15 K	323.15 K	333.15 K
0.0000	1.0530	1.0475	1.0420	1.0365	1.0311	0.0000	0.0000	0.0000	0.0000	0.0000
0.1515	0.8511	0.8440	0.8368	0.8294	0.8219	-0.3129	-0.3509	-0.3978	-0.4502	-0.5108
0.2983	0.8896	0.8829	0.8761	0.8692	0.8622	-0.4763	-0.5341	-0.6039	-0.6828	-0.7703
0.4504	0.9281	0.9217	0.9152	0.9087	0.9019	-0.5533	-0.6199	-0.6998	-0.7847	-0.8630
0.5993	0.9640	0.9579	0.9517	0.9455	0.9391	-0.5299	-0.5953	-0.6724	-0.7513	-0.8179
0.6754	0.9817	0.9759	0.9701	0.9640	0.9577	-0.4743	-0.5516	-0.6519	-0.7248	-0.7721
0.8991	1.0312	1.0256	1.0197	1.0139	1.0084	-0.1882	-0.2303	-0.2523	-0.2920	-0.3430
1.0000	0.8095	0.8019	0.7941	0.7862	0.7780	0.0000	0.0000	0.0000	0.0000	0.0000

Standard uncertainties μ are $\mu(x_1) = 0.005$, μ(T) = 0.01 K, μ(P) = 1 kPa and $\mu(\rho) = 0.004$ g·cm^{-3}

Table 4.6. Redlich-Kister polynomial fitting coefficients (a_0, a_1, a_2 and a_3) from equation 4.6 for the excess volume of alcohol + deep eutectic solvent with their respective absolute average deviation (AAD) at different temperatures (K) and a pressure of 101.3 kPa. Deep eutectic solvents used are detailed in Table 3.2.

DES-A1						DES-A2					
T/(K)	a_0	a_1	a_2	a_3	AAD/(%)	T/(K)	a_0	a_1	a_2	a_3	AAD/(%)
293.15	-3.6779	-1.5731	-1.1481	-0.8335	0.1422	293.15	-3.2759	-0.4242	-0.7137	-0.6853	0.2318
303.15	-4.0063	-1.9707	-0.9852	-0.3191	0.8880	303.15	-3.5966	-0.6488	-0.8586	-0.6163	0.2355
313.15	-4.2156	-1.9075	-1.3444	-0.8626	0.5517	313.15	-3.8837	-0.6827	-0.9188	-0.7760	0.2031
323.15	-4.4971	-2.2628	-1.5110	-0.6031	0.7330	323.15	-4.1895	-0.8536	-0.9559	-0.6697	0.1897
333.15	-4.7675	-2.0471	-1.8001	-1.5691	1.0344	333.15	-4.5286	-0.8701	-1.0694	-1.0559	0.1938
DES-A3						DES-A4					
T/(K)	a0	a1	a2	a3	AAD/(%)	T/(K)	a0	a1	a2	a3	AAD/(%)
293.15	-2.3204	-0.0649	-0.2997	-0.2345	0.4442	293.15	-1.5622	0.2252	-0.7072	0.6962	0.3428
303.15	-2.5700	-0.2631	-0.5823	0.0797	0.0818	303.15	-1.7315	0.1930	-0.7577	0.8148	0.5180
313.15	-2.8062	-0.5149	-0.8059	0.6159	0.4174	313.15	-1.9060	0.3330	-0.8524	0.5452	0.4290
323.15	-3.0258	-0.6594	-1.0061	1.0267	0.6542	323.15	-2.1455	0.2137	-0.8663	0.7917	0.3771
333.15	-3.2790	-0.5439	-1.0329	1.0575	0.4142	333.15	-2.4144	0.1590	-0.9115	0.8149	0.3317
DES-B1						DES-B2					
T/(K)	a_0	a_1	a_2	a_3	AAD/(%)	T/(K)	a_0	a_1	a_2	a_3	AAD/(%)
293.15	-3.4095	-1.6648	-1.0532	-0.6737	0.3790	293.15	-3.4250	-0.4368	-0.3992	-0.9946	0.3533
303.15	-3.6571	-1.7218	-1.2287	-0.9644	0.4725	303.15	-3.7542	-0.6070	-0.6223	-1.1719	0.3515
313.15	-3.9531	-1.9755	-1.3327	-0.8864	0.4258	313.15	-4.0686	-0.7584	-0.6745	-1.1610	0.3631
323.15	-4.1612	-2.2919	-1.6889	-0.7542	0.1305	323.15	-4.3951	-0.9240	-0.7868	-1.1647	0.3473
333.15	-4.4229	-2.8560	-1.9782	-0.1782	0.1711	333.15	-4.7510	-1.0659	-0.9266	-1.2923	0.3051
DES-B3						DES-B4					
T/(K)	a_0	a_1	a_2	a_3	AAD/(%)	T/(K)	a_0	a_1	a_2	a_3	AAD/(%)
293.15	-2.6138	-0.4992	-1.2931	-0.5064	0.1145	293.15	-2.0501	0.3394	-0.5239	-0.3186	0.1745
303.15	-2.9028	-0.5666	-1.4209	-0.7627	0.2912	303.15	-2.2504	0.3860	-0.5325	-0.4684	0.3660
313.15	-3.1827	-0.6527	-1.4949	-0.9041	0.2597	313.15	-2.4622	0.4139	-0.6348	-0.5451	0.4601
323.15	-3.4403	-0.8587	-1.5286	-0.7673	0.1230	323.15	-2.7697	0.0591	-0.5803	0.1225	0.8960
333.15	-3.6923	-1.0851	-1.4017	-0.5073	0.3333	333.15	-3.0433	0.1450	-0.7313	-0.1733	0.6649
DES-C1						DES-C2					
T/(K)	a_0	a_1	a_2	a_3	AAD/(%)	T/(K)	a_0	a_1	a_2	a_3	AAD/(%)
293.15	-3.0375	-1.9880	-1.0305	-0.7792	0.3720	293.15	-3.0263	-1.1148	-0.1509	-0.9182	0.3205
303.15	-3.3415	-2.1446	-1.3632	-0.5820	0.5032	303.15	-3.3372	-1.4035	-0.5742	-0.6790	0.6539
313.15	-3.7473	-2.3575	-1.8966	0.0617	0.8524	313.15	-3.7917	-1.6727	-0.6597	-0.2773	0.6138
323.15	-4.1685	-2.5832	-2.2489	0.7702	0.7212	323.15	-4.1615	-1.6079	-0.9582	-0.5950	0.4615
333.15	-4.6140	-2.7078	-2.9769	0.8911	0.3351	333.15	-4.4843	-2.0587	-1.2084	-0.1587	0.5740
DES-C3						DES-C4					
T/(K)	a_0	a_1	a_2	a_3	AAD/(%)	T/(K)	a_0	a_1	a_2	a_3	AAD/(%)
293.15	-2.6260	-0.3949	-0.6620	0.1670	0.9161	293.15	-2.2197	0.0772	-0.1149	0.3082	0.3264
303.15	-2.9294	-0.5644	-0.8639	0.2024	0.9857	303.15	-2.4881	-0.0103	-0.3029	-0.2967	0.2093
313.15	-3.2195	-0.7301	-1.0767	0.3841	1.2150	313.15	-2.2826	-0.0474	-0.2658	0.5007	0.7922
323.15	-3.5127	-0.8744	-1.2287	0.5009	1.4576	323.15	-3.1628	0.0215	-0.4100	0.3698	0.7085
333.15	-3.8000	-1.0323	-1.1762	0.8893	1.2070	333.15	-3.4487	0.3820	-0.7496	-0.3142	0.5417

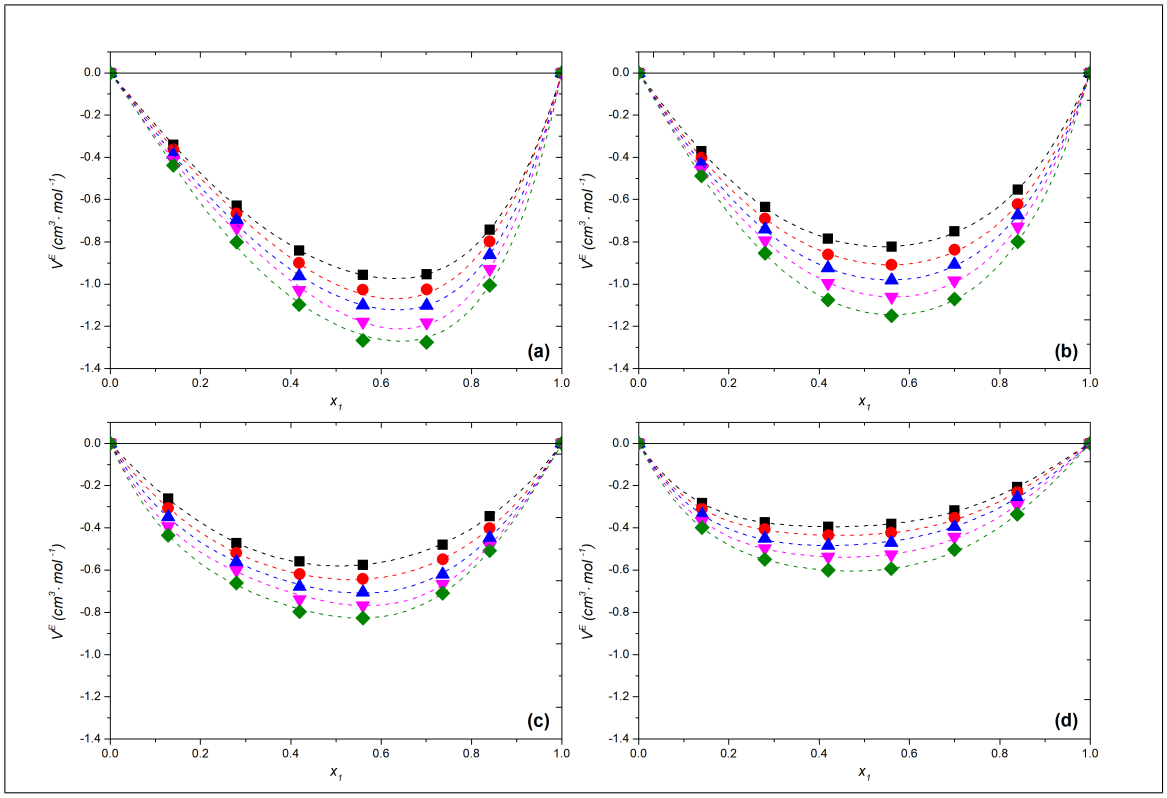

Figure 4.4. Excess molar volume (cm^3·mol^{-1}) in terms of the mole fraction of alcohol for the binary mixtures **(a)** methanol + DES-A, **(b)** ethanol + DES-A, **(c)** 1-propanol + DES-A, **(d)** 1-butanol + DES-A at a pressure of 101.3 kPa and temperatures between 298.15 K and 333.15 K. Temperatures of 293.15 K (■), 303.15 K (●), 313.15 K (▲), 323.15 K (▼) and 333.15 K (◆). The dashed line represents the Redlich-Kister polynomial fitting with parameters reported in Table 4.6.

4.3.2. V^E Alcohol chain effect

Additionally, an alcohol chain effect is observed on the behavior of the V^E. Figure 4.5 shows the V^E for (a) DES-A, (b) DES-B and (c) DES-C mixed with the different alcohols at 293.15 K as a function of mole fraction of alcohol. Figures A.3 to A.6 show the behavior of the remaining temperatures. A lower V^E (most negative value) is observed, in general, by mixing any DES with methanol, followed by ethanol, 1-propanol and 1-butanol. It is also noted that the minimum V^E value shifts to a lower molar fraction of alcohol as the alcohol chain increases.

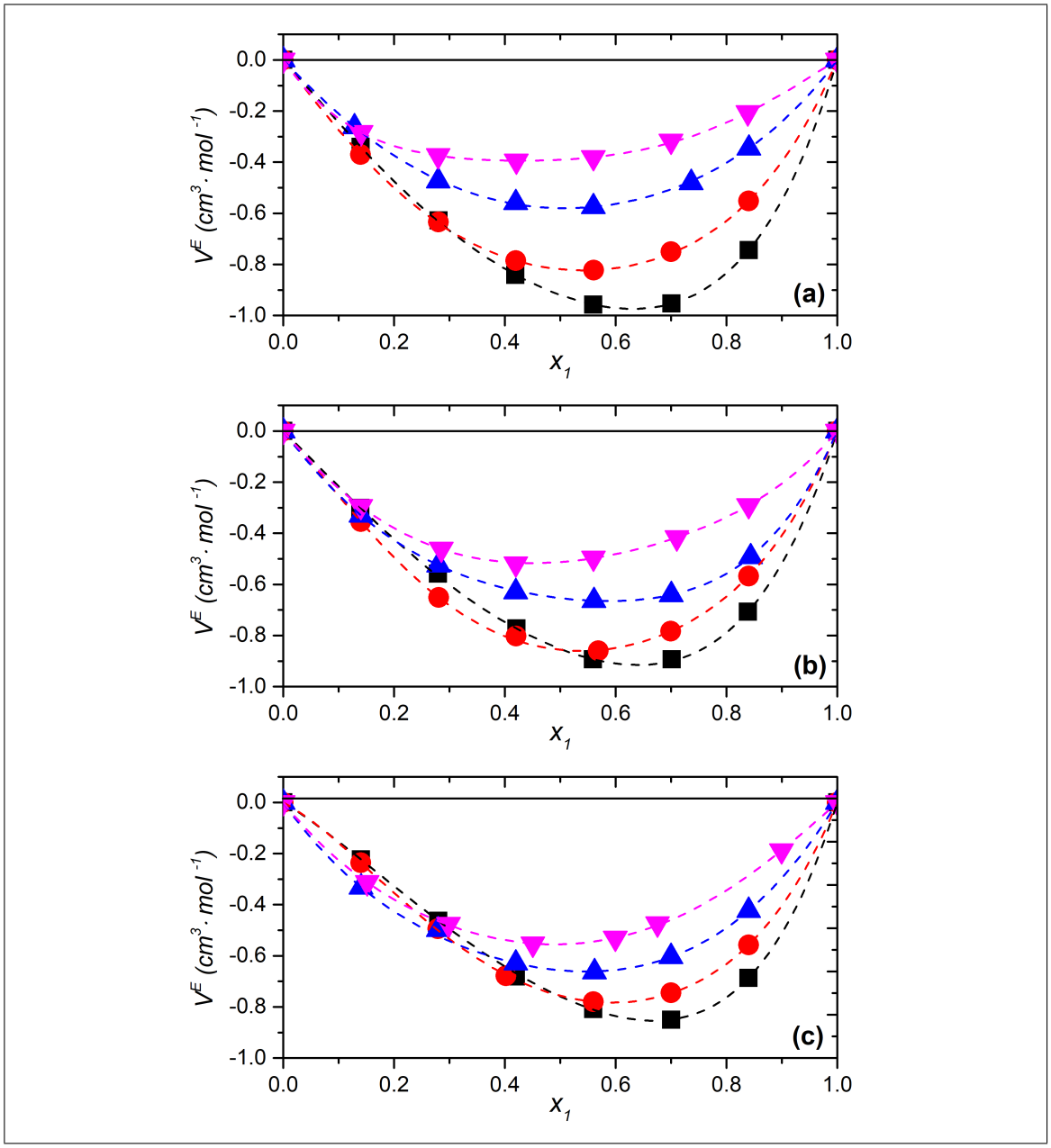

Figure 4.5. Excess molar volume ($cm^3 \cdot mol^{-1}$) in terms of the mole fraction of alcohol for the binary mixtures of **(a)** DES-A, **(b)** DES-B , **(c)** DES-C, at a pressure of 101.3 kPa, temperature of 293.15 K and DES binary system with methanol (■), ethanol (●), 1-propanol (▲), 1-butanol (▼). The dashed line represents the Redlich-Kister polynomial fitting with parameters reported in Table 9.

For instance, taking the DES-A which is shown in Figure 4.5(a) and using the correlation of Redlich-Kister, the minimum values of x_1 are 0.63 for the mixture with methanol, 0.54 for ethanol, 0.50 for 1-propanol, and 0.43 for 1-butanol, obtaining values of V^{E}_{RK} of -0.974 $cm^3 \cdot mol^{-1}$, -0.823 $cm^3 \cdot mol^{-1}$, -0.580 $cm^3 \cdot mol^{-1}$ and -0.394 $cm^3 \cdot mol^{-1}$, respectively. These results suggest that a longer carbon chain of the alcohol obstruct the intermolecular interactions between DES and alcohols, since the larger molecule restricts interstitial accommodation within the DES.

4.3.3. V^E HBD effect

Figure 4.6 compares the behavior of the V^E of different DES using the same alcohol at 293.15 K. Figures A.7 to A.10 show the behavior of the remaining temperatures. In this case, the effect of the HBD does not have a clear tendency and, in general, V^E is very similar for all the cases. From this comparison, it is observed that in the studied systems there is a small effect of the HBD, suggesting that these compounds interact mainly with choline chloride and leave very few empty vacancies for the interaction with another compound, in this case, alcohols.

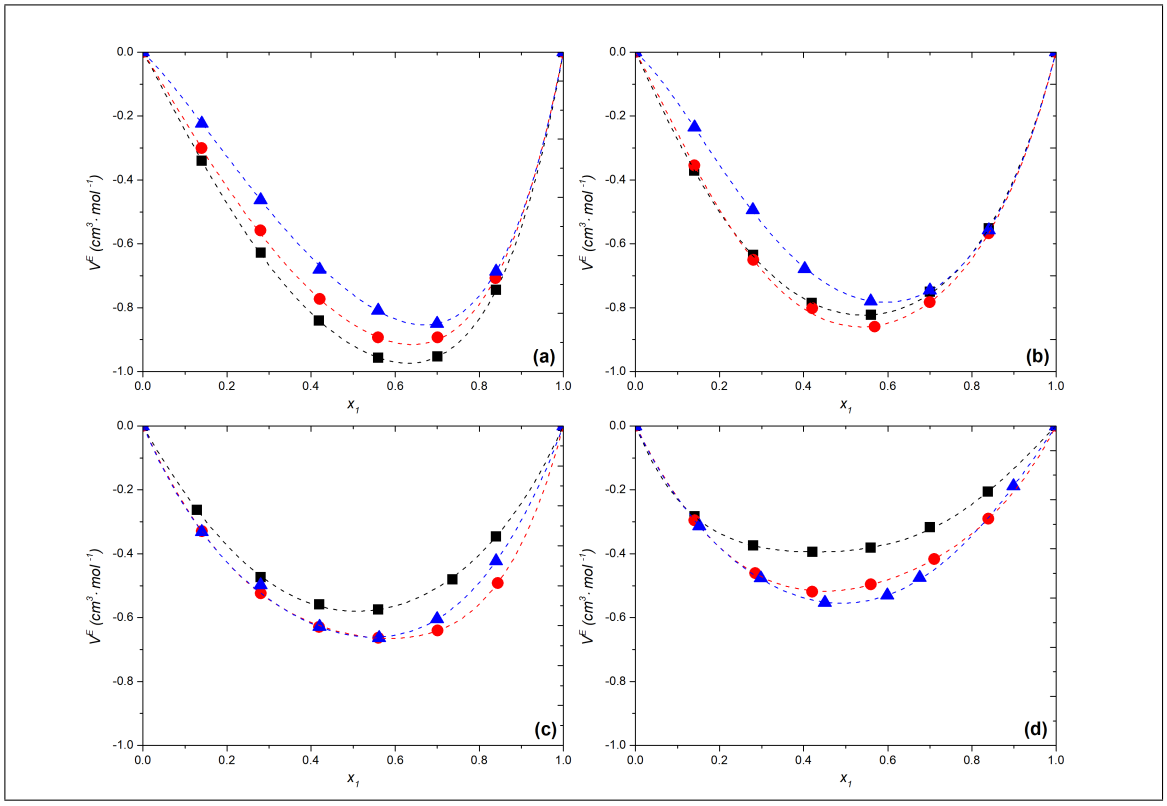

Figure 4.6. HBD effect on excess molar volume (cm^3·mol^{-1}) in terms of the mole fraction of alcohol for the binary mixtures of DES with **(a)** methanol, **(b)** ethanol , **(c)** 1-propanol, **(d)** 1-butanol at a pressure of 101.3 kPa, temperature of 293.15 K and binary system with DES-A (■), DES-B (●), DES-C (▲). The dashed line represents the Redlich-Kister polynomial fitting with parameters reported in Table 9.

4.4. Molar Excess Enthalpy using COSMO-RS

The mixing behavior of systems containing DES can be described through the thermodynamic interactions occurring within the system. In particular, the H^E is a key thermodynamic property which illustrates the strength of interactions between the like and unlike species within a mixture, allowing to better understand the solvent behaviour upon mixing (Gonzalez-Miquel, Massel, et al., 2014; López-Porfiri, Brennecke, & Gonzalez-Miquel, 2016). Therefore, to further evaluate the thermodynamic equilibria and molecular interactions of mixtures containing alcohols + DES, the H^E of these systems will be evaluated

Table 4.7. Mixing enthalpies of pseudo-pure choline chloride-based DES at molar ratio 1:3 predicted with COSMO-RS.

	DES-A	DES-B	DES-C
T / K	ΔH_{mix} / kJ·mol^{-1}		
293.15	-9.61	-8.25	-5.07
303.15	-9.48	-7.96	-5.01
313.15	-9.33	-7.68	-4.96
323.15	-9.15	-7.43	-4.92
333.15	-8.95	-7.19	-4.89

using COSMO-RS method. Previous studies have proved the suitability of COSMO-RS to estimate H^E of complex mixtures containing ionic liquids (Gonzalez-Miquel, Massel, et al., 2014) and to support the volumetric properties of binary mixtures containing alcohols (Esteban & Gonzalez-Miquel, 2018), while qualitatively explaining the main molecular interactions occurring during the mixing process. Moreover, recent studies have successfully employed COSMO-RS to determine the thermodynamic equilibria (Bezold et al., 2017; Jeliński & Cysewski, 2018) and explain the molecular affinities (Ozturk, Esteban, & Gonzalez-Miquel, 2018; Ozturk & Gonzalez-Miquel, 2019; Wongsirichot, Gonzalez-Miquel, & Winterburn, 2019) of systems containing DES.

H^E of pure choline chloride-based DES were calculated computing the solid-liquid equilibria of salt + HBD components and subtracting the energy associated with the salt melting involved in the solvent formation, as proposed before (López-Porfiri et al., 2016). The results corresponding to the mixing enthalpies of pure choline chloride-based DES at the different temperatures are collected in Table 4.7. Subsequently, the H^E of alcohol + DES mixtures were normalized by subtracting the H^E of pure DES as a function of the composition and temperature for each system, as shown in Figure 4.7, A.11 and A.12. This procedure allows to describe solely the alcohol + DES mixing phenomena without the other energy effects.

H^E of all alcohol + DES systems are negative, denoting the exothermic nature of the mixing process. Additionally, as expected by DES nature, the H^E contributions are

distributed mainly as negative (favorable) hydrogen bonding (HB), as well as negative (attractive) electrostatic (MF) interactions, while positive (unfavorable) van der Waals (vdW) forces are almost negligible as observed in Figure 4.8. H^E of DES mixtures with alcohols show a maximum negative value (i.e., highest exothermicity) at alcohol molar fractions between 0.6 and 0.8 as shown in Figures 4.7, A.11 and A.12. H^E results and their deviation with respect to the equimolar composition support the stronger affinities observed on the experimental V^E at higher alcoholic fraction in the mixture. DES display a high affinity towards the alcohol component, forming new interactions between unlike species up to high alcohol fractions, before the alcohol like-like interaction become predominant. Considering the overall H^E results for each system and the energetic contributions at their maximum value, three main effects will be further analyzed as follows: temperature, alcohol chain length, and HBD component.

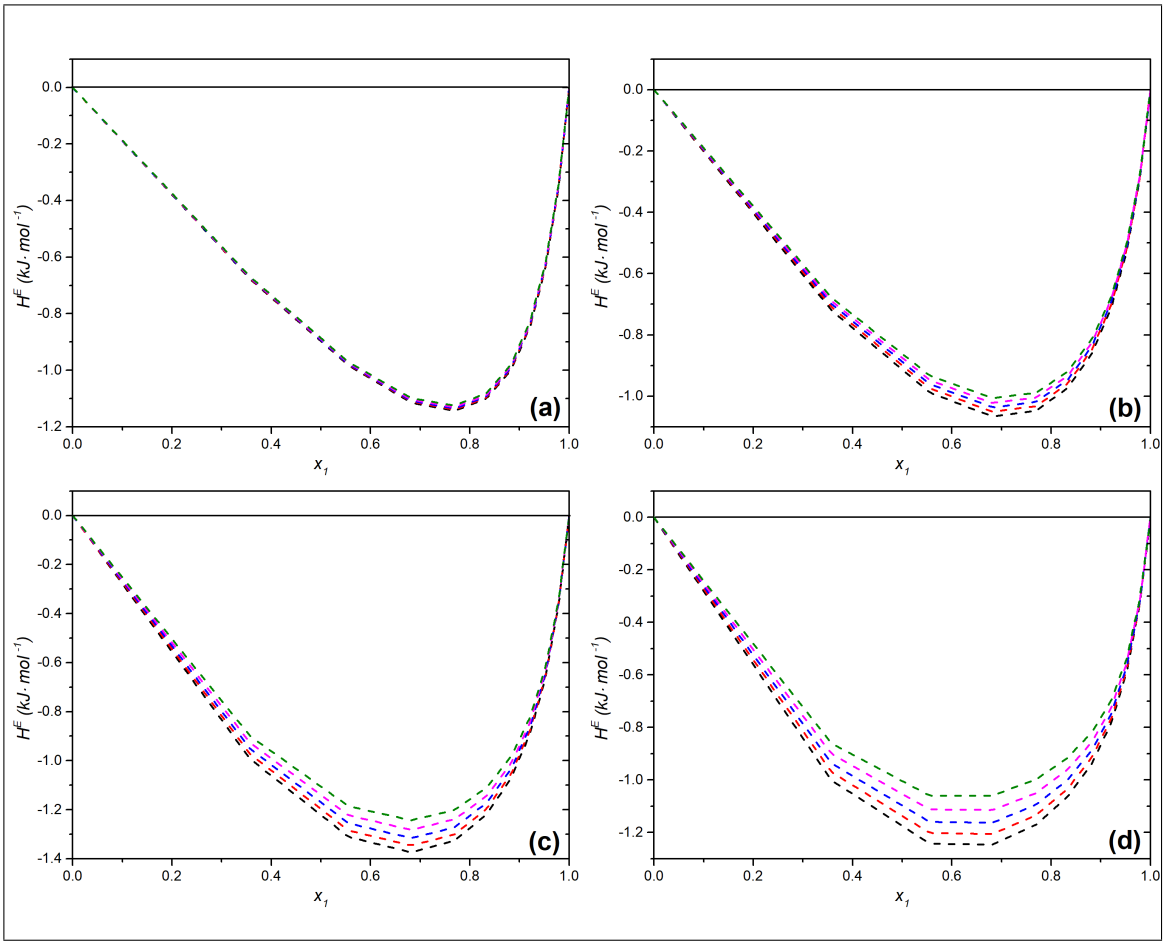

Figure 4.7. Temperature effect on the molar excess enthalpy of alcohol + DES-A mixtures predicted with COSMO-RS.]Temperature effect on the molar excess enthalpy of alcohol + DES-A mixtures predicted with COSMO-RS. The molar excess enthalpies (kJ·mol^{-1}) are in terms of the mole fraction of alcohol for the binary mixtures of **(a)** methanol + DES-A, **(b)** ethanol + DES-A, **(c)** 1-propanol + DES-A, **(d)** 1-butanol + DES-A at a pressure of 101.3 kPa and temperatures between 293.15 K and 333.15 K. The dashed line represents the temperatures of 293.15 K (−), 303.15 K (−), 313.15 K (−), 323.15 K (−), 333.15 K (−).

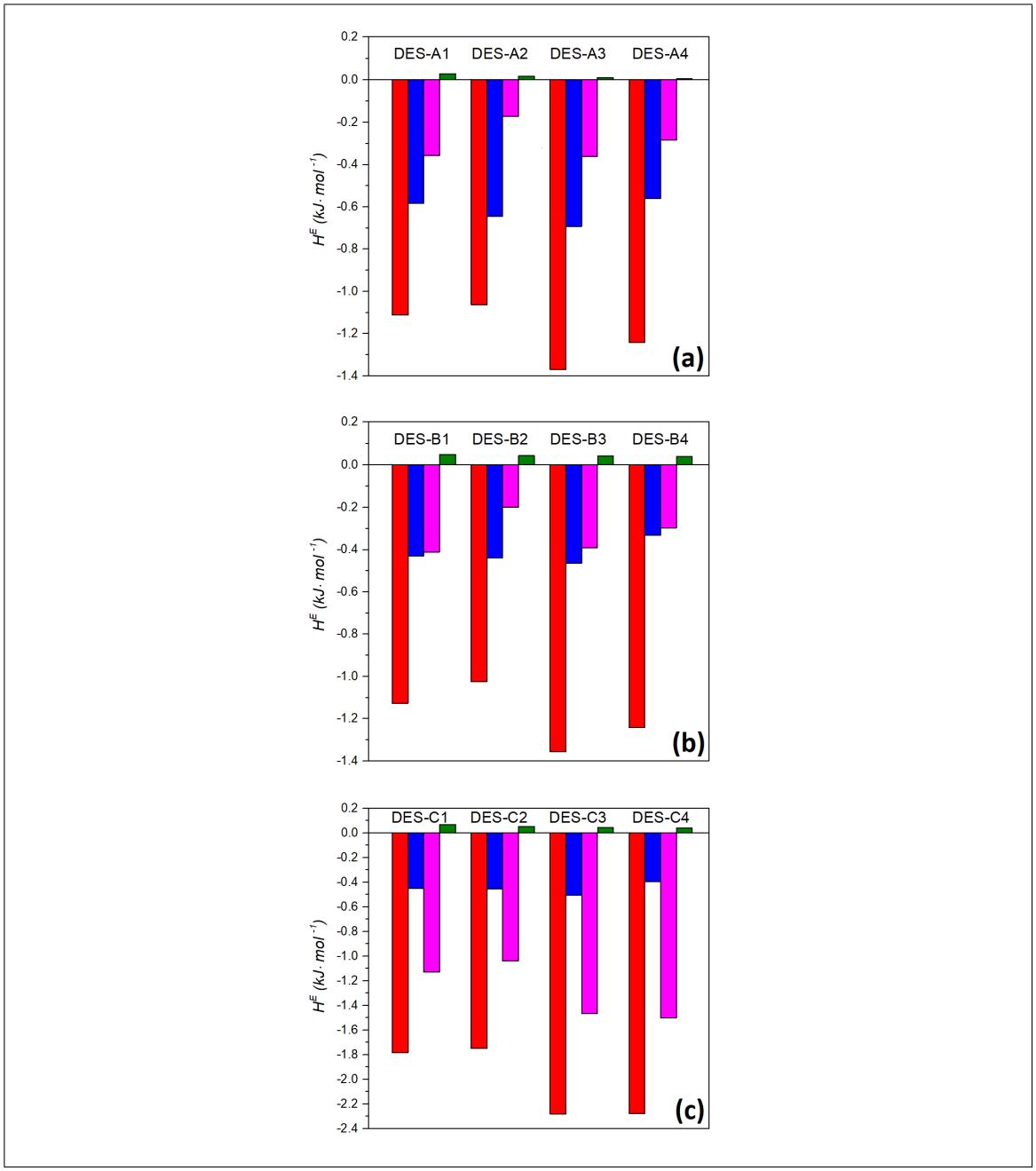

Figure 4.8. Molar excess entalphy (kJ·mol^{-1}) contributions(■) for the alcohol + DES mixtures of **(a)** alcohol + DES-A, **(b)** alcohol + DES-B and **(c)** alcohol + DES-C distributed in hydrogen bonding (■), electrostatic (■) and van der Walls (■) interactions at a concentration of alcohol of x_1=0.68, pressure of 101.3 kPa and temperature of 293.15 K.

4.4.1. H^E Temperature effect

Regarding the effect of the temperature, despite the strong temperature dependence of experimental V^E, no significant changes along the temperature range were observed for the computed H^E of alcohol + DES mixtures in Figures 4.7, A.11 and A.12. Nevertheless, two different trends can be observed: On the one hand, for ethylene glycol-based and 1,4-butanediol-based DES, the H^E magnitude decrease slightly with temperature. This behavior agrees with that reported in literature for solvent mixtures, where higher temperatures weaken the molecular interactions within the mixture. On the other hand, for 1,3-propanediol-based DES, higher temperatures increase the exothermicity of the mixture (i.e., increasingly negative H^E) due to stronger molecular interactions, supporting the lower experimental V^E. H^E contribution analysis shows minimal changes with respect to temperature, yet shows a clear trend: as temperature increases, attractive HB energy decreases, attractive MF energy increases, and for all systems, slightly repulsive vdW forces were found, with no change with temperature. The rise of favorable MF interactions comes from an interstitial accommodation of DES-alcohol molecules, which increases the magnitude of the V^E for the three diol-based DES. For the case of 1,3-propanediol-based DES, attractive electrostatic interactions increase faster than HB decreases, explaining its particular behavior found on the H^E analysis.

4.4.2. H^E Alcohol chain effect

H^E for DES-A and DES-B present small changes with the alcohol chain length, observed in Figure 4.9, where H^E increase in magnitude following ethanol < methanol < 1-butanol < 1-propanol. Meanwhile, DES-C shows two levels of H^E with an important magnitude increment, following ethanol ≈ methanol < 1-butanol ≈ 1-propanol. On the other hand, experimental V^E results exhibit the same overall trend for the three diol-based DES: methanol > ethanol > 1-propanol > 1-butanol, indicating an impediment in the DES – alcohol interaction by the carbon chain length. According to the σ-profiles of the four alcohols, their molecular interactions differ not on their hydrogen bond donor and acceptor

capacity, given by the hydroxyl group, but on their non-polar charge surface area, which increases with the chain length.

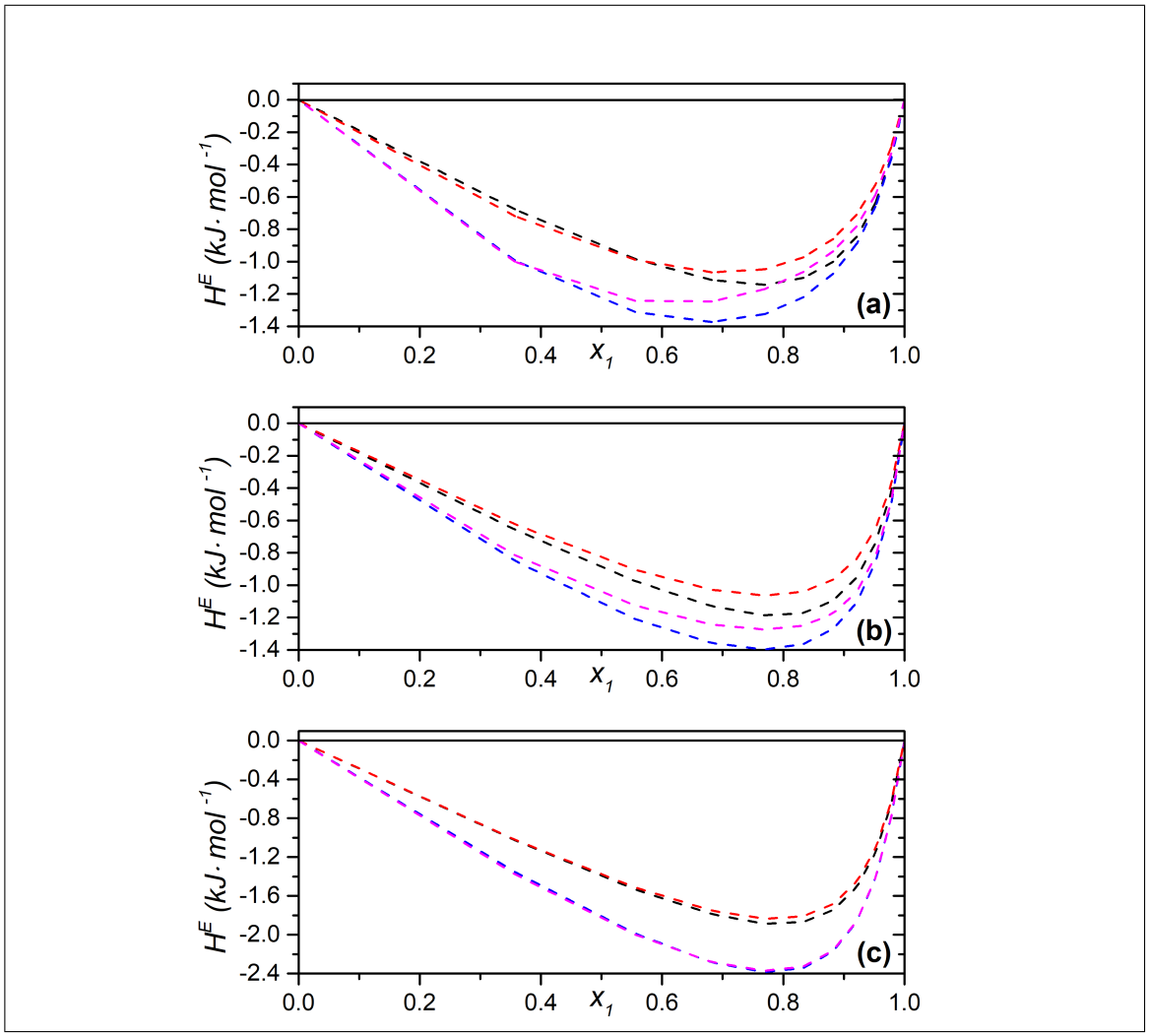

Figure 4.9. Alcohol chain effect on the molar excess enthalpy of alcohol + DES mixtures predicted with COSMO-RS. The molar excess enthalpies (kJ·mol^{-1}) are in terms of the mole fraction of alcohol for the binary mixtures of **(a)** DES-A, **(b)** DES-B, **(c)** DES-C, at a pressure of 101.3 kPa and temperature of 293.15 K. The dashed line represents the binary system with methanol (−), ethanol (−), 1-propanol (−) and 1-butanol (−).

4.4.3. H^E HBD effect

The effect of HBD length in binary mixtures was studied in Figure 4.10. Although the overall behavior of each system is due to the combined interaction effects, hydrogen bond donor shows to have a major effect on the H^E, where its minimum value shifts to a higher alcohol molar fraction as the HBD chain length increases. DES-A and DES-B based mixtures show similar magnitudes, while 1,4-butanediol-based DES present the larger H^E, growing significantly more than the ethylene glycol or 1,3-propanediol based DESs with increasing alcohol concentrations. The four-carbon chain of 1,4-butanediol enable the molecule to adopt different stable configurations, improving the steric accommodation within the system. Such trend is observed regardless the alcohol component. However, the increment is mainly due to increasing MF contributions, whereas HB energies and vdW forces remain relativity constants for the three diols.

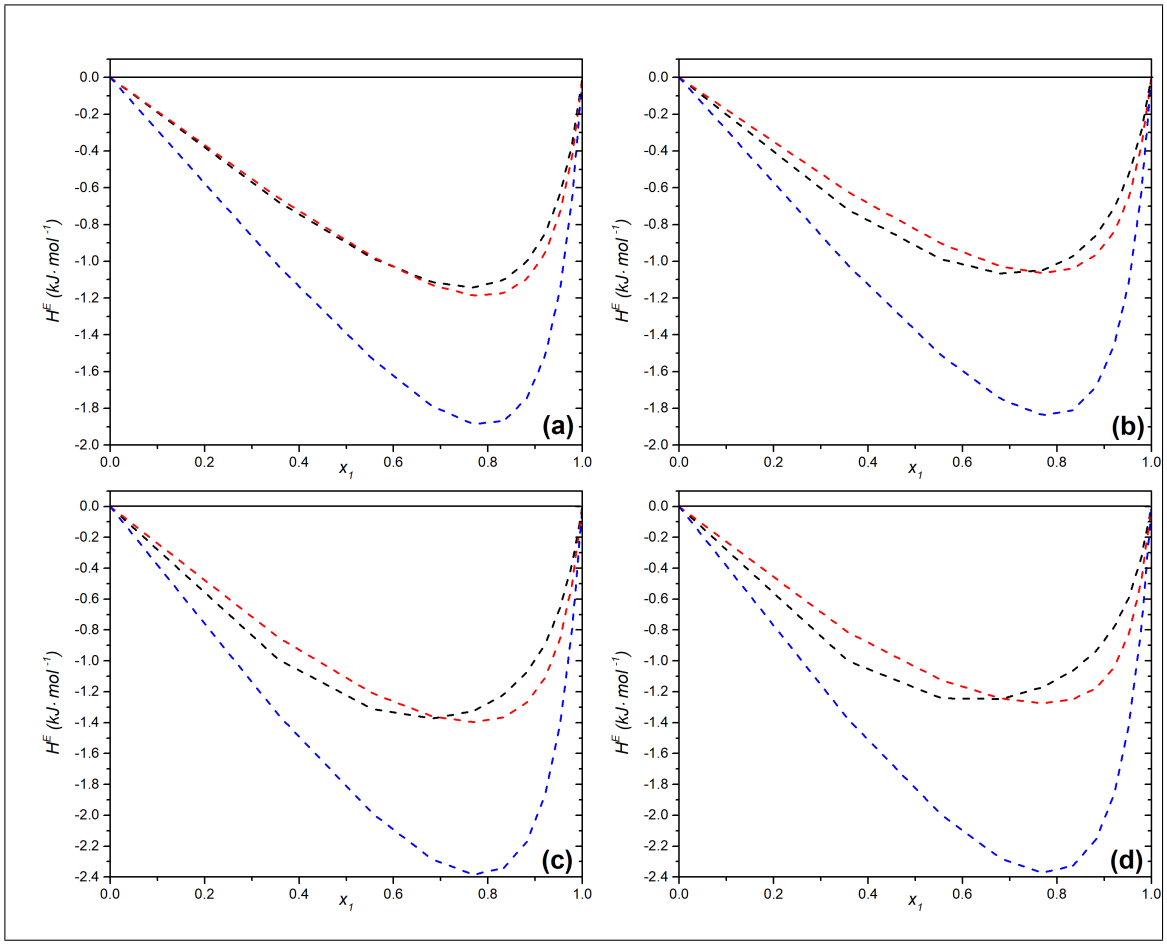

Figure 4.10. HBD effect on the molar excess enthalpy of alcohol + DES mixtures predicted with COSMO-RS. The molar excess enthalpies (kJ·mol^{-1}) are in terms of the mole fraction of alcohol for the binary mixtures of DES with **(a)** methanol, **(b)** ethanol, **(c)** 1-propanol, **(d)** 1-butanol at a pressure of 101.3 kPa and temperature of 293.15 K. The dashed line represents the binary system with DES-A (–), DES-B (–) and DES-C (–).

4.5. Mixture viscosity on DESs binary system

Dynamic viscosity measurements of mixtures are shown in Figure 4.11 composed of (alcohol + DES) as a function of composition of alcohol, were obtained at 101.3 kPa and temperatures between 293.15 K – 333.15 K in the full range of compositions. Viscosities decreases with temperature and adding the differents alcohols, since pure alcohols have

much lower viscosities than DES, it is observed that in the vast majority of molar fractions the viscosities of binary mixtures follow the following trend: DES + methanol < DES + ethanol < DES + 1-propanol < DES + 1-butanol, this because the viscosity of pure alcohol follows the same trend.

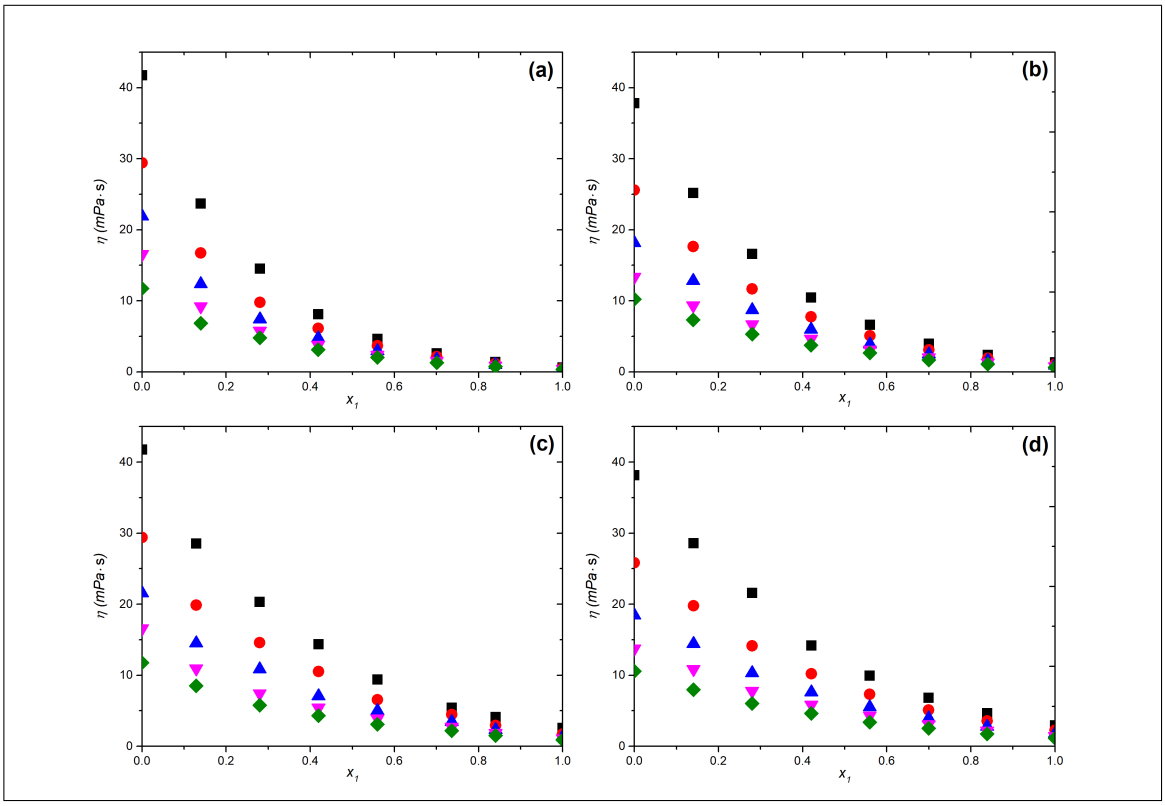

Figure 4.11. Dynamic viscosity (mPa·s) in terms of the mole fraction of alcohol for the binary mixtures of **(a)** DES-A1, **(b)** DES-A2, **(c)** DES-A3, **(d)** DES-A4 at a pressure of 101.3 kPa and temperatures between 298.15 K and 333.15 K. Temperatures of 293.15 K (■), 303.15 K (●), 313.15 K (▲), 323.15 K (▼) and 333.15 K (◆).

4.6. Hard-sphere model viscosity prediction

As noted, viscosity had been correlated for a large number of DES for which data at atmospheric pressure were available. The parameters of V_0 (Equation 2.12) by adjusting the viscosity data for each set of DESs and R were obtained by adjusting the experimental

Table 4.8. Dynamic viscosity (mPa·s) of alcohols + DES (choline chloride + ethylene glycol) liquid mixture at different temperatures (K), compositions of alcohols (x_1) and a pressure of 101.3 kPa. Deep eutectic solvents binary system used for these measurements are detailed in Table 3.2.

DES-A1					
	Viscosity (mPa·s)				
x_1	293.15K	303.15 K	313.15 K	323.15 K	333.15 K
0.0000	41.76	29.41	21.88	16.58	11.76
0.1398	23.70	16.73	12.36	9.23	6.84
0.2802	14.50	9.79	7.42	5.78	4.81
0.4187	8.10	6.12	4.77	3.81	3.11
0.5597	4.66	3.67	2.95	2.43	2.02
0.7007	2.62	2.14	1.78	1.55	1.32
0.8402	1.39	1.18	1.01	0.87	0.76
1.0000	0.59	0.51	0.45	0.40	0.36
DES-A2					
	Viscosity (mPa·s)				
x_1	293.15K	303.15 K	313.15 K	323.15 K	333.15 K
0.0000	37.80	25.57	18.16	13.39	10.22
0.1397	25.18	17.62	12.85	9.34	7.33
0.2800	16.59	11.70	8.73	6.71	5.30
0.4197	10.47	7.77	5.95	4.68	3.75
0.5601	6.61	5.08	3.91	3.14	2.65
0.6999	3.97	3.12	2.51	2.05	1.70
0.8401	2.39	1.94	1.59	1.32	1.10
1.0000	1.23	0.98	0.80	0.65	0.54
DES-A3					
	Viscosity (mPa·s)				
x_1	293.15K	303.15 K	313.15 K	323.15 K	333.15 K
0.0000	41.76	29.41	21.58	16.58	11.76
0.1285	28.52	19.89	14.50	10.95	8.52
0.2798	20.33	14.57	10.85	7.45	5.78
0.4195	14.35	10.54	7.08	5.45	4.30
0.5597	9.42	6.55	5.00	3.91	3.12
0.7362	5.42	4.48	3.48	2.75	2.22
0.8404	4.12	2.95	2.33	1.86	1.51
1.0000	2.19	1.73	1.38	1.11	0.91
DES-A4					
	Viscosity (mPa·s)				
x_1	293.15K	303.15 K	313.15 K	323.15 K	333.15 K
0.0000	38.15	25.83	18.45	13.75	10.59
0.1405	28.56	19.78	14.42	10.87	7.97
0.2796	21.59	14.13	10.33	7.80	6.05
0.4204	14.18	10.22	7.61	5.83	4.65
0.5595	9.96	7.33	5.55	4.31	3.41
0.6998	6.84	5.13	3.95	3.10	2.52
0.8385	4.68	3.57	2.78	2.20	1.77
1.0000	2.94	2.27	1.78	1.41	1.14

Standard uncertainties u are $u(x_1)$=0.005, $u(T)$=0.01 K, $u(P)$= 1 kPa. Relative standard uncertainties $u_r(\eta)$=0.06

Table 4.9. Dynamic viscosity (mPa·s) of alcohols + DES (choline chloride + 1,3 propanediol) liquid mixture at different temperatures (K), compositions of alcohols (x_1) and a pressure of 101.3 kPa. Deep eutectic solvents binary system used for these measurements are detailed in Table 3.2.

DES-B1					
	Viscosity (mPa·s)				
x_1	293.15K	303.15 K	313.15 K	323.15 K	333.15 K
0.0000	69.24	45.52	31.39	22.59	16.83
0.1394	41.84	28.56	20.41	15.15	11.61
0.2796	24.53	17.48	12.96	9.92	6.97
0.4209	13.96	10.40	7.13	5.56	4.44
0.5587	7.53	5.31	4.18	3.36	2.75
0.7013	3.47	2.78	2.27	1.88	1.59
0.8388	1.66	1.39	1.17	1.01	0.87
1.0000	0.59	0.51	0.45	0.40	0.36
DES-B2					
	Viscosity (mPa·s)				
x_1	293.15K	303.15 K	313.15 K	323.15 K	333.15 K
0.0000	69.51	45.64	31.46	22.57	16.87
0.1401	45.31	30.83	21.84	16.03	12.17
0.2805	28.95	20.28	14.81	11.21	8.81
0.4201	17.45	12.62	8.78	6.74	5.41
0.5687	9.39	7.02	5.39	4.23	3.39
0.6996	5.44	4.25	3.34	2.68	2.18
0.8399	2.85	2.29	1.86	1.53	1.27
1.0000	1.23	0.98	0.80	0.65	0.54
DES-B3					
	Viscosity (mPa·s)				
x_1	293.15K	303.15 K	313.15 K	323.15 K	333.15 K
0.0000	69.29	45.58	31.37	22.57	16.85
0.1400	49.21	33.12	23.34	17.07	12.87
0.2802	33.60	23.22	16.75	12.50	9.72
0.4196	22.51	15.95	11.78	9.04	6.47
0.5606	14.48	10.62	7.17	5.47	4.34
0.7004	8.11	6.02	4.58	3.57	2.83
0.8436	4.63	3.54	2.76	2.18	1.75
1.0000	2.19	1.73	1.38	1.11	0.91
DES-B4					
	Viscosity (mPa·s)				
x_1	293.15K	303.15 K	313.15 K	323.15 K	333.15 K
0.0000	69.19	45.42	31.39	22.56	16.80
0.1399	49.87	33.44	23.50	17.18	12.96
0.2851	34.44	23.69	17.06	12.70	9.84
0.4199	23.20	16.49	12.11	8.46	7.04
0.5599	14.53	10.43	7.72	5.85	4.56
0.7105	8.92	6.57	4.97	3.84	3.02
0.8397	5.61	4.22	3.24	2.54	2.02
1.0000	2.94	2.27	1.78	1.41	1.14

Standard uncertainties u are $u(x_1)$=0.005, $u(T)$=0.01 K, $u(P)$= 1 kPa. Relative standard uncertainties $u_r(\eta)$=0.06

Table 4.10. Dynamic viscosity (mPa·s) of alcohols + DES (choline chloride + 1,4 butanediol) liquid mixture at different temperatures (K), compositions of alcohols (x_1) and a pressure of 101.3 kPa. Deep eutectic solvents binary system used for these measurements are detailed in Table 3.2.

DES-C1					
	Viscosity (mPa·s)				
x_1	293.15K	303.15 K	313.15 K	323.15 K	333.15 K
0.0000	118.08	71.29	47.29	32.78	23.63
0.1403	65.29	42.87	29.60	21.24	15.77
0.2801	36.87	25.36	18.22	13.56	10.34
0.4197	19.94	14.40	10.76	7.54	6.38
0.5597	10.34	7.02	5.49	4.30	3.54
0.7001	4.45	3.59	2.84	2.34	1.96
0.8399	1.91	1.58	1.33	1.13	0.99
1.0000	0.59	0.51	0.45	0.40	0.36
DES-C2					
	Viscosity (mPa·s)				
x_1	293.15K	303.15 K	313.15 K	323.15 K	333.15 K
0.0000	117.95	72.10	47.02	32.54	23.50
0.1400	69.57	45.52	31.29	22.41	16.60
0.2791	41.93	28.65	20.34	15.02	11.35
0.4020	24.63	17.49	12.88	9.81	7.57
0.5598	13.96	10.30	7.16	5.55	4.39
0.7000	6.74	5.23	4.10	3.33	2.72
0.8400	3.26	2.61	2.11	1.73	1.43
1.0000	1.23	0.98	0.80	0.65	0.54
DES-C3					
	Viscosity (mPa·s)				
x_1	293.15K	303.15 K	313.15 K	323.15 K	333.15 K
0.0000	112.36	72.22	48.19	33.47	22.97
0.1404	76.39	48.23	33.12	23.54	16.96
0.2796	48.79	32.67	22.91	16.67	12.52
0.4198	30.67	21.34	15.35	11.42	8.89
0.5617	18.42	13.34	10.02	6.86	5.29
0.6997	10.00	7.34	5.53	4.26	3.34
0.8400	5.27	4.00	3.09	2.43	1.94
1.0000	2.19	1.73	1.38	1.11	0.91
DES-C4					
	Viscosity (mPa·s)				
x_1	293.15K	303.15 K	313.15 K	323.15 K	333.15 K
0.0000	113.17	73.02	46.60	32.35	23.35
0.1515	74.69	48.67	33.16	23.55	17.31
0.2983	49.85	33.41	23.39	16.99	12.73
0.4504	32.05	22.23	15.98	11.86	9.19
0.5993	21.12	14.60	10.23	7.29	5.61
0.6754	11.27	8.21	6.13	4.69	3.66
0.8991	6.30	4.72	3.61	2.82	2.23
1.0000	2.94	2.27	1.78	1.41	1.14

Standard uncertainties u are $u(x_1)$=0.005, $u(T)$=0.01 K, $u(P)$= 1 kPa. Relative standard uncertainties $u_r(\eta)$=0.06

viscosity data using the value of V_0 obtained previously. The adjusted values of d_i, as well as the parameter R_η for the data at 0.1 MPa are shown in the Table 4.11, in addition to the data references and the values of the Average Absolute Deviations (AADs) between the computed and experimental data. In total, 330 viscosity data points were correlated for 33 DESs data points. The overall AAD for the viscosity data was 2.49 %, the BIAS was 1.44 % and the maximum deviation (MD) was 6.64 %.

Values of V_0 and R_η for DESs with a common anion were found to follow regular trends with the molecular weight (M_W) of the DES for atmospheric pressure systems. The predictive capability of the scheme was demonstrated in all the cases of DESs using calculated values of V_0 and R_η and the experimental density at one specific temperature. This is shown in the Figure 4.11 where for almost all the systems the scheme retains an error of less than 6% . This work can be compared with Gaciño et al. (Gaciño et al., 2014) where the hard-sphere scheme was used to predict ionic liquids viscosity and thermal conductivity, in general it is observed that the orders of magnitude of the parameters V_0 and R_η are aligned with this work for DES. In addition, similar values were obtained for the AAD and points below the 5% of error, that is, the use of the scheme for viscosity prediction from experimental DESs density data could be validated.

Through only the data of V_0 of the different families of DESs we tried to predict the viscosity values of the DESs measured experimentally in this study, the results show that only for the VA family the prediction is fulfilled, but in the other families of DESs the prediction is out of range of the obtained data, therefore it is indicated that the hard sphere model allows to correlate well the viscosity data, but there is no evidence that allows to predict the viscosity of the DESs.

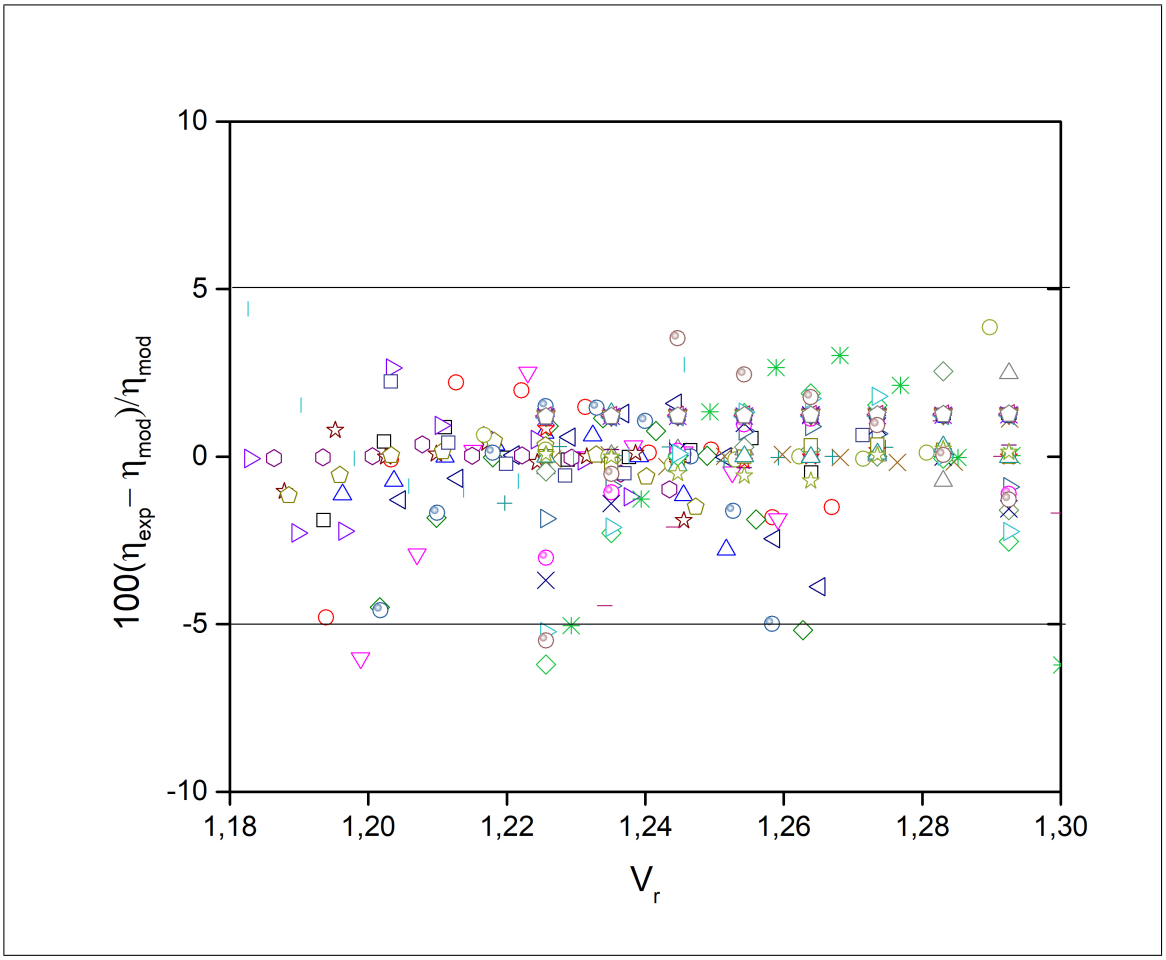

Figure 4.12. Percentage deviations of the viscosity measurements, from the values calculated by the hard sphere scheme, as function of the reduced volume for each system..

Table 4.11. V_0 Polynomial constants, R_η and stadistical analysis for each DESs system

Abbreviaton	d_0	d_1	d_2	d_3	Viscosity				
					R_η	Dev>5%	AAD (%)	BIAS (%)	MD (%)
DES-VA1	3.72E-05	4.6536E-07	-1.8E-09	1.99E-12	1.75	0	0.24	-0.02	0.83
DES-VA2	4.3E-05	4.4062E-07	-1.9E-09	2.26E-12	1.75	0	0.96	-0.44	2.68
DES-VA3	3.49E-05	4.6128E-07	-1.8E-09	2.03E-12	1.75	0	0.51	-0.05	1.90
DES-VA4	4.06E-05	4.3945E-07	-1.8E-09	2.23E-12	1.75	0	1.58	-0.25	4.80
DES-VB1	4.15E-05	4.4809E-07	-1.8E-09	2.26E-12	1.80	0	0.83	-0.45	2.78
DES-VB2	4.52E-05	4.1126E-07	-1.8E-09	2.23E-12	1.80	1	1.60	-0.90	6.01
DES-VB3	4.18E-05	4.25E-07	-1.8E-09	2.27E-12	1.80	1	1.80	-1.17	5.18
DES-VB4	4.36E-05	4.0078E-07	-1.8E-09	2.23E-12	1.80	0	1.31	-0.53	3.89
DES-VC1	4.13E-05	5.0561E-07	-1.9E-09	2.06E-12	1.89	0	1.18	-0.13	2.64
DES-VC2	4.28E-05	4.8367E-07	-1.8E-09	2.01E-12	1.89	0	0.23	-0.13	0.98
DES-VC3	4.27E-05	4.9023E-07	-1.9E-09	2.15E-12	1.89	0	0.50	-0.19	1.90
DES-VC4	4.21E-05	4.8539E-07	-1.8E-09	2.1E-12	1.89	0	0.54	-0.31	1.50
DES-VD1	5.21E-05	3.3753E-07	-1.6E-09	2.22E-12	1.85	0	1.89	-0.97	5.00
DES-VD2	4.04E-05	2.99E-07	-1.20E-09	1.40E-12	1.85	0	0.27	-0.97	5.00
DES-VD3	1.2E-05	5.3454E-07	-1.9E-09	2.16E-12	1.85	0	0.22	0.06	1.12
DES-VD4	3.76E-05	3.7791E-07	-1.8E-09	2.34E-12	1.85	2	2.41	-0.38	6.21
DES-VD5	3.01E-05	4.1626E-07	-1.8E-09	2.34E-12	1.85	0	1.78	-0.96	4.44
DES-VE1	4.21E-05	5.1705E-07	-1.9E-09	1.98E-12	1.98	0	1.27	0.67	4.41
DES-VE2	4.03E-05	5.1113E-07	-1.9E-09	2.06E-12	1.98	0	0.52	0.23	2.24
DES-VE3	4.06E-05	5.0148E-07	-1.9E-09	2.12E-12	1.98	0	0.58	0.49	3.85
DES-VE4	4.57E-05	4.5831E-07	-1.8E-09	2.1E-12	1.98	0	0.54	0.13	2.49
DES-VE5	4.15E-05	4.7938E-07	-1.9E-09	2.1E-12	1.98	1	1.18	-0.50	5.45
DES-VF1	3.43E-05	4.8134E-07	-1.9E-09	2.29E-12	1.84	0	0.93	-0.39	2.31
DES-VF2	1.82E-05	5.7333E-07	-2.1E-09	2.23E-12	1.84	0	0.23	0.00	0.84
DES-VF3	5.79E-05	2.5564E-07	-1.3E-09	1.63E-12	1.84	0	1.26	-0.55	3.02
DES-VG1	4E-05	4.3732E-07	-1.8E-09	2.26E-12	1.92	0	1.53	-0.79	3.79
DES-VG2	1.1E-05	6.3681E-07	-2.3E-09	2.49E-12	1.92	0	0.24	-0.07	0.52
DES-VH1	3.73E-05	5.0084E-07	-1.8E-09	1.94E-12	1.20	0	0.21	0.00	0.60
DES-VI1	9.8E-06	5.4905E-07	-2E-09	2.16E-12	1.93	0	0.28	0.09	1.29
DES-VI2	3.54E-05	3.9126E-07	-1.8E-09	2.35E-12	1.93	2	2.49	-1.44	6.64
DES-VI3	3.35E-05	3.9472E-07	-1.8E-09	2.34E-12	1.93	1	2.17	-1.06	5.23
DES-VJ1	4.17E-05	5.0493E-07	-1.9E-09	2.05E-12	1.99	0	0.26	-0.15	0.72
DES-VJ2	4.27E-05	4.8488E-07	-1.9E-09	2.04E-12	1.99	1	2.07	-0.13	5.49

5. CONCLUSIONS AND PERSPECTIVES

Density and viscosity of the pure compounds ethylene glycol, 1,3-propanediol, 1,4-butanediol and DES formed by choline chloride with these precursors, in a molar ratio of 1:3, were measured in the range of temperatures from 293.15 to 333.15 K at a pressure of 101.3 kPa. Pseudo-binary mixtures formed by the differents DES and four different alcohols (methanol, ethanol, 1-propanol and 1-butanol) were also characterized by density and viscosity at the same conditions of temperature and pressure of the pure components.

All the binary mixtures were completely miscible in the full range of compositions between 293.15 to 333.15 K and 101.3 kPa. Molar excess volumes were calculated from the density of the binary mixtures obtaining negative values for all the systems, suggesting a better interaction of the molecules of the different type and a favorable accommodation of molecules in their interstitial space. This behavior produces a lower volume compared with the one expected for an ideal mixture. Density and excess volumes of the binary mixtures were correlated with Redlich-Kister. All the molar excess volumes were correlated with an AAD(%) below 1.458%. About the effect of the alcohol chain length on excess properties, it is suggested that the greater the alcohol chain, the greater the capacity to make a strong molecular interaction given the decrease in the steric effect, together with the accommodation of the DES polar site.

Experimental excess volumes were supported by an enthalpic study based on COSMO-RS method to provide insights into the molecular interactions occurring within the system. Overall results indicate that mixing of DES and alcohols involves an exothermic process and support the stronger affinities observed on the experimental excess volumes at higher alcohol concentrations. Energetic analysis suggests a competition between the interstitial accommodation of unlike species and the molecular affinity between like species, reflected as attractive electrostatic interactions and favorable hydrogen bonding HB contributions, respectively. Therefore, alcohol + DES mixing entails a complex phenomenon driven by competitive hydrogen bonding and electrostatics affinities between the species within the

mixture, which determines the solvent mixing behavior and their macroscopic properties for practical applications.

With respect to the hard sphere model, it is obtained that it correlates well with the data obtained, but from this study it is concluded that this model cannot effectively predict the DESs

As future work is recommended to obtain the values of the decomposition temperature of the different DESs studied, together to analyze the different balances that can generate the various systems, this can have a clear picture of the application of these solvents in the separation industry.

REFERENCES

Abbott, A. P., Capper, G., Davies, D. L., Munro, H. L., & Rasheed, R. K. (2011). Preparation of novel, moisture-stable, Lewis-acidic ionic liquids containing quaternary ammonium salts with functional side chains. , 2010–2011. doi: 10.1039/b106357j

Abbott, A. P., Capper, G., Davies, D. L., Rasheed, R. K., & Tambyrajah, V. (2003). Novel solvent properties of choline chloride/urea mixtures. *Chemical Communications*, 9 (1), 70–71. doi: 10.1039/b210714g

Abbott, A. P., Capper, G., & Gray, S. (2006). Design of improved deep eutectic solvents using hole theory. Chemphyschem*: a European journal of chemical physics and physical chemistry* , 7 (4), 803–806.

Abbott, A. P., Harris, R. C., & Ryder, K. S. (2007). Application of hole theory to define ionic liquids by their transport properties. *The Journal of Physical Chemistry B*, 111 (18), 4910–4913.

Abbott, A. P., Harris, R. C., Ryder, K. S., D'Agostino, C., Gladden, L. F., & Mantle, M. D. (2011). Glycerol eutectics as sustainable solvent systems. *Green Chemistr*y, 13 (1), 82–90.

Aissaoui, T. (2015). Novel contribution to the chemical structure of choline chloride based deep eutectic solvents. Pharm Anal Acta, 6, 11.

Assael, M., Dymond, J., & Papadaki, M. (1992). Viscosity coefficients of binary n-heptane+ n-alkane mixtures. *Fluid phase equilibria*, 75, 287–297.

Assael, M., Dymond, J., Papadaki, M., & Patterson, P. (1992a). Correlation and prediction of dense fluid transport coefficients. iii. n-alkane mixtures. *International journal of thermophysics*, 13 (4), 659–669

thermophysics, *13*(4), 659–669.

Assael, M., Dymond, J., Papadaki, M., & Patterson, P. (1992b). Correlation and prediction of dense fluid transport coefficients. i. n-alkanes. *International Journal of Thermophysics*, *13*(2), 269–281.

Assael, M., Dymond, J., & Patterson, P. (1992). Correlation and prediction of dense fluid transport coefficients. iv. a note on diffusion. *International journal of thermophysics*, *13*(4), 729–733.

Bezold, F., Weinberger, M. E., & Minceva, M. (2017). Assessing solute partitioning in deep eutectic solvent-based biphasic systems using the predictive thermodynamic model cosmo-rs. *Fluid Phase Equilib.*, *437*, 23–33.

Bi, W., Tian, M., & Row, K. H. (2013). Evaluation of alcohol-based deep eutectic solvent in extraction and determination of flavonoids with response surface methodology optimization. *Journal of Chromatography A*, *1285*, 22–30. Retrieved from `http://dx.doi.org/10.1016/j.chroma.2013.02.041` doi: 10.1016/j.chroma.2013.02.041

Blusztajn, J. K. (1998). Choline, a vital amine. *Science*, *281*(5378), 794–795.

Boruń, A., & Bald, A. (2016). Ionic association and conductance of [emim][bf4] and [bmim][bf4] in 1-butanol in a wide range of temperature. *The Journal of Chemical Thermodynamics*, *96*, 175–180.

Bougouma, M., Van Elewyck, A., Steichen, M., Buess-Herman, C., & Doneux, T. (2013). Selenium electrochemistry in choline chloride-urea deep eutectic electrolyte. *Journal of Solid State Electrochemistry*, *17*(2), 527–536. doi: 10.1007/s10008-012-1955-5

Cammarata, L., Kazarian, S., Salter, P., & Welton, T. (2001). Molecular states of water in room temperature ionic liquids. *Physical Chemistry Chemical Physics*, *3*(23), 5192–5200.

Canosa, J., Rodriguez, A., Iglesias, M., Orge, B., & Tojo, J. (1998). Thermodynamic properties of alkanediols+ acetates at 298.15 k. *Journal of thermal analysis and calorimetry*,

52(3), 915–932.

Capello, C., Fischer, U., & Hungerbühler, K. (2007). What is a green solvent? A comprehensive framework for the environmental assessment of solvents. *Green Chemistry*, *9*(9), 927–934. doi: 10.1039/b617536h

Chen, Y., Ai, N., Li, G., Shan, H., Cui, Y., & Deng, D. (2014). Solubilities of carbon dioxide in eutectic mixtures of choline chloride and dihydric alcohols. *Journal of Chemical and Engineering Data*, *59*(4), 1247–1253. doi: 10.1021/je400884v

Ciotta, F., Trusler, J. M., & Vesovic, V. (2014). Extended hard-sphere model for the viscosity of dense fluids. *Fluid Phase Equilibria*, *363*, 239–247.

D'Agostino, C., Harris, R. C., Abbott, A. P., Gladden, L. F., & Mantle, M. D. (2011). Molecular motion and ion diffusion in choline chloride based deep eutectic solvents studied by 1H pulsed field gradient NMR spectroscopy. *Physical Chemistry Chemical Physics*, *13*(48), 21383–21391. doi: 10.1039/c1cp22554e

Dai, Y., van Spronsen, J., Witkamp, G.-J., Verpoorte, R., & Choi, Y. H. (2013). Natural deep eutectic solvents as new potential media for green technology. *Analytica chimica acta*, *766*, 61–68.

Davey, R., Garside, J., Hilton, A., McEwan, D., & Morrison, J. (1995). Purification of molecular mixtures below the eutectic by emulsion crystallization. *Nature*, *375*(6533), 664.

Disale, S. T., Kale, S. R., Kahandal, S. S., Srinivasan, T. G., & Jayaram, R. V. (2012). Choline chloride· 2zncl2 ionic liquid: an efficient and reusable catalyst for the solvent free kabachnik–fields reaction. *Tetrahedron Letters*, *53*(18), 2277–2279.

Duan, L., Dou, L.-L., Guo, L., Li, P., & Liu, E.-H. (2016a). Comprehensive evaluation of deep eutectic solvents in extraction of bioactive natural products. *ACS Sustainable Chemistry & Engineering*, *4*(4), 2405–2411.

Duan, L., Dou, L. L., Guo, L., Li, P., & Liu, E. H. (2016b). Comprehensive Evaluation of Deep Eutectic Solvents in Extraction of Bioactive Natural Products. *ACS Sustainable Chemistry and Engineering*, *4*(4), 2405–2411. doi: 10.1021/acssuschemeng.6b00091

Durand, E., Lecomte, J., & Villeneuve, P. (2013). Deep eutectic solvents: Synthesis, application, and focus on lipase-catalyzed reactions. *European journal of lipid science and technology*, *115*(4), 379–385.

Dutta, S., & Nath, K. (2018). Prospect of ionic liquids and deep eutectic solvents as new generation draw solution in forward osmosis process. *Journal of Water Process Engineering*, *21*, 163–176.

Erbeldinger, M., Ni, X., & Halling, P. J. (1998). Enzymatic synthesis with mainly undissolved substrates at very high concentrations. *Enzyme and Microbial Technology*, *23*(1-2), 141–148.

Esteban, J., & Gonzalez-Miquel, M. (2018). Thermodynamic insights on the viscometric and volumetric properties of binary mixtures of ketals and polyols. *Journal of Molecular Liquids*, *263*, 125–138.

Estrada-Baltazar, A. (2013). Iglesias-silva, caballero-ceron, c. *J. Chem. Eng. Data*, *58*, 3351.

Florindo, C., Oliveira, F. S., Rebelo, L. P., Fernandes, A. M., & Marrucho, I. M. (2014). Insights into the synthesis and properties of deep eutectic solvents based on cholinium chloride and carboxylic acids. *ACS Sustainable Chemistry and Engineering*, *2*(10), 2416–2425. doi: 10.1021/sc500439w

Francisco, M., Van Den Bruinhorst, A., & Kroon, M. C. (2013). Low-transition-temperature mixtures (LTTMs): A new generation of designer solvents. *Angewandte Chemie - International Edition*, *52*(11), 3074–3085. doi: 10.1002/anie.201207548

Fukaya, Y., Iizuka, Y., Sekikawa, K., & Ohno, H. (2007). Bio ionic liquids: room temperature ionic liquids composed wholly of biomaterials. *Green Chemistry*, *9*(11), 1155–1157.

Fukuchi, K. Y. S. A. Y. K. S. K. D., K.; Ogiwara. (1980). Densities of alcohols and their mixtures. , *53*, 187.

Gaciño, F. M., Comuñas, M. J., Fernández, J., Mylona, S. K., & Assael, M. J. (2014). Correlation and prediction of dense fluid transport coefficients. ix. ionic liquids. *International Journal of Thermophysics*, *35*(5), 812–829.

Gage, S. H., Ruddy, D. A., Pylypenko, S., & Richards, R. M. (2016). Deep Eutectic Solvent Approach Towards Nickel/Nickel Nitride Nanocomposites. *Catalysis Today*, 1–7. Retrieved from `http://dx.doi.org/10.1016/j.cattod.2016.12.016` doi: 10.1016/j.cattod.2016.12.016

Gajardo-Parra, N. F., Lubben, M. J., Winnert, J. M., Leiva, , Brennecke, J. F., & Canales, R. I. (2019). Physicochemical properties of choline chloride-based deep eutectic solvents and excess properties of their pseudo-binary mixtures with 1-butanol. *Journal of Chemical Thermodynamics*, 272–284. Retrieved from `https://doi.org/10.1016/j.jct.2019.02.010` doi: 10.1016/j.jct.2019.02.010

Garcia, B., Herrera, C., & Leal, J. M. (1991). Shear viscosities of binary liquid mixtures: 2-pyrrolidinone with 1-alkanols. *Journal of Chemical and Engineering Data*, *36*(3), 269–274.

Garcia, G., Aparicio, S., Ullah, R., & Atilhan, M. (2015). Deep eutectic solvents: physicochemical properties and gas separation applications. *Energy & Fuels*, *29*(4), 2616–2644.

García-Miaja, G., Troncoso, J., & Romaní, L. (2009). Excess enthalpy, density, and heat capacity for binary systems of alkylimidazolium-based ionic liquids+ water. *The Journal of Chemical Thermodynamics*, *41*(2), 161–166.

Gill, I., & Vulfson, E. (1994). Enzymic catalysis in heterogeneous eutectic mixtures of

substrates. *Trends in biotechnology*, *12*(4), 118–122.

Gonfa, G., Bustam, M. A., Muhammad, N., & Ullah, S. (2015). Density and excess molar volume of binary mixture of thiocyanate-based ionic liquids and methanol at temperatures 293.15–323.15 k. *Journal of Molecular Liquids*, *211*, 734–741.

Gonzalez-Miquel, M., Bedia, J., Abrusci, C., Palomar, J., & Rodriguez, F. (2013). Anion effects on kinetics and thermodynamics of co2 absorption in ionic liquids. *The Journal of Physical Chemistry B*, *117*(12), 3398–3406.

Gonzalez-Miquel, M., Bedia, J., Palomar, J., & Rodriguez, F. (2014). Solubility and diffusivity of co2 in [hxmim][ntf2],[omim][ntf2], and [dcmim][ntf2] at t=(298.15, 308.15, and 323.15) k and pressures up to 20 bar. *Journal of Chemical & Engineering Data*, *59*(2), 212–217.

Gonzalez-Miquel, M., Massel, M., DeSilva, A., Palomar, J., Rodriguez, F., & Brennecke, J. F. (2014). Excess enthalpy of monoethanolamine+ ionic liquid mixtures: how good are cosmo-rs predictions? *J. Phys. Chem. B*, *118*(39), 11512–11522.

Gonzalez-Miquel, M., Palomar, J., Omar, S., & Rodriguez, F. (2011). Co2/n2 selectivity prediction in supported ionic liquid membranes (silms) by cosmo-rs. *Industrial & Engineering Chemistry Research*, *50*(9), 5739–5748.

Gonzalez-Miquel, M., Talreja, M., Ethier, A. L., Flack, K., Switzer, J. R., Biddinger, E. J., … others (2012). Cosmo-rs studies: structure–property relationships for co2 capture by reversible ionic liquids. *Industrial & Engineering Chemistry Research*, *51*(49), 16066–16073.

Gutiérrez, M. C., Ferrer, M. L., Yuste, L., Rojo, F., & del Monte, F. (2010). Bacteria incorporation in deep-eutectic solvents through freeze-drying. *Angewandte Chemie International Edition*, *49*(12), 2158–2162.

Gutierrez, M. C., Ferrer, M. L., Mateo, C. R., & del Monte, F. (2009). Freeze-drying of

aqueous solutions of deep eutectic solvents: a suitable approach to deep eutectic suspensions of self-assembled structures. *Langmuir*, *25*(10), 5509–5515.

Haghbakhsh, R., Parvaneh, K., Raeissi, S., & Shariati, A. (2018). A general viscosity model for deep eutectic solvents: The free volume theory coupled with association equations of state. *Fluid Phase Equilibria*, *470*, 193–202. Retrieved from `http://dx.doi.org/10.1016/j.fluid.2017.08.024` doi: 10.1016/j.fluid.2017.08.024

Haghbakhsh, R., & Raeissi, S. (2015). Two simple correlations to predict viscosities of pure and aqueous solutions of ionic liquids. *Journal of Molecular Liquids*, *211*, 948–956. Retrieved from `http://dx.doi.org/10.1016/j.molliq.2015.08.036` doi: 10.1016/j.molliq.2015.08.036

Handy, S., & Lavender, K. (2013). Organic synthesis in deep eutectic solvents: Paal-Knorr reactions. *Tetrahedron Letters*, *54*(33), 4377–4379. Retrieved from `http://dx.doi.org/10.1016/j.tetlet.2013.05.122` doi: 10.1016/j.tetlet.2013.05.122

Harifi-Mood, A. R., & Buchner, R. (2017). Density, viscosity, and conductivity of choline chloride+ ethylene glycol as a deep eutectic solvent and its binary mixtures with dimethyl sulfoxide. *Journal of Molecular Liquids*, *225*, 689–695.

Hawrylak, B., Gracie, K., & Palepu, R. (1998). Thermodynamic properties of binary mixtures of butanediols with water. *Journal of solution chemistry*, *27*(1), 17–31.

Hayyan, A., Mjalli, F. S., AlNashef, I. M., Al-Wahaibi, T., Al-Wahaibi, Y. M., & Hashim, M. A. (2012). Fruit sugar-based deep eutectic solvents and their physical properties. *Thermochimica acta*, *541*, 70–75.

Hayyan, M., Hashim, M. A., Hayyan, A., Al-Saadi, M. A., AlNashef, I. M., Mirghani, M. E., & Saheed, O. K. (2013). Are deep eutectic solvents benign or toxic? *Chemosphere*, *90*(7), 2193–2195.

Huber, M., Hanley, H., Millat, J., Dymond, J., & de Castro, C. N. (1996). Transport

properties of fluids: Their correlation, prediction and estimation. In *Iupac*. Cambridge Univ. Press Cambridge.

Iglesias-Silva, G. A., Bravo-Sanchez, M., Estrada-Baltazar, A., Bouchot, C., & Hall, K. R. (2015). P–ρ–t data for 1-butanol and isobutyl alcohol from (283.15 to 363.15) k at pressures up to 66 mpa. *Journal of Chemical & Engineering Data*, *60*(4), 1076–1090.

Jeliński, T., & Cysewski, P. (2018). Application of a computational model of natural deep eutectic solvents utilizing the cosmo-rs approach for screening of solvents with high solubility of rutin. *J. Mol. Model.*, *24*(7), 180.

Jhong, H.-R., Wong, D. S.-H., Wan, C.-C., Wang, Y.-Y., & Wei, T.-C. (2009). A novel deep eutectic solvent-based ionic liquid used as electrolyte for dye-sensitized solar cells. *Electrochemistry Communications*, *11*(1), 209–211.

Khalilov, K. M. Z. E. T. F. (1939). Viscosity of liquids and saturated vapors at high temperatures & pressures. , *9*, 335-345.

Khezeli, T., Daneshfar, A., & Sahraei, R. (2016). A green ultrasonic-assisted liquid-liquid microextraction based on deep eutectic solvent for the HPLC-UV determination of ferulic, caffeic and cinnamic acid from olive, almond, sesame and cinnamon oil. *Talanta*, *150*, 577–585. Retrieved from `http://dx.doi.org/10.1016/j.talanta.2015.12.077` doi: 10.1016/j.talanta.2015.12.077

Khimenko, V. V. G. N. N. Z. F. K., M. T.; Aleksandrov. (1973). Polarizabilities and molecular radii of some pure liquids. , *47*, 2914.

Kim, K.-S., & Park, B. H. (2018). Volumetric properties of solutions of choline chloride+ glycerol deep eutectic solvent with water, methanol, ethanol, or iso-propanol. *Journal of Molecular Liquids*, *254*, 272–279.

Klamt, A., Eckert, F., & Arlt, W. (2010). Cosmo-rs: an alternative to simulation for calculating thermodynamic properties of liquid mixtures. *Annual review of chemical and*

biomolecular engineering, *1*, 101–122.

Knezeć-Stevanović, A. B., Radović, I. R., Serbanović, S. P., & Kijevcanin, M. L. (2014). Densities, viscosities, and refractive indices of the ternary mixture dimethyladipate+ 2-butanone+ 1-butanol at t=(288.15 to 323.15) k. *Journal of Chemical & Engineering Data*, *59*(12), 4133–4150.

Kroon, M. C., Allen, D. T., Brennecke, J. F., Savage, P. E., & Schatz, G. C. (2017). ACS Virtual Issue on Deep Eutectic Solvents. *Journal of Chemical and Engineering Data*, *62*(7), 1927–1928. doi: 10.1021/acs.jced.7b00545

Ledneva, T. M. V. M. U. (1956). Bulk viscosity and its temperature dependence for some organc liquids. , *2*, 49-60.

Leron, R. B., & Li, M. H. (2012). High-pressure volumetric properties of choline chloride-ethylene glycol based deep eutectic solvent and its mixtures with water. *Thermochimica Acta*, *546*, 54–60. Retrieved from `http://dx.doi.org/10.1016/j.tca.2012.07.024` doi: 10.1016/j.tca.2012.07.024

Leron, R. B., Soriano, A. N., & Li, M.-H. (2012). Densities and refractive indices of the deep eutectic solvents (choline chloride+ ethylene glycol or glycerol) and their aqueous mixtures at the temperature ranging from 298.15 to 333.15 k. *Journal of the Taiwan Institute of Chemical Engineers*, *43*(4), 551–557.

Leron, R. B., Wong, D. S. H., & Li, M.-H. (2012). Densities of a deep eutectic solvent based on choline chloride and glycerol and its aqueous mixtures at elevated pressures. *Fluid Phase Equilibria*, *335*, 32–38.

Long, B., & Ding, Y. (2015). Probing the intermolecular attractive interactions of binary mixtures of formic acid+ methanol or water via volumetric studies. *Journal of Molecular Liquids*, *206*, 137–144.

López-Porfiri, P., Brennecke, J. F., & Gonzalez-Miquel, M. (2016). Excess molar enthalpies of deep eutectic solvents (dess) composed of quaternary ammonium salts and glycerol or ethylene glycol. *J. Chem. Eng. Data*, *61*(12), 4245–4251.

Mikhail, S., & Kimel, W. (1961). Densities and viscosities of methanol-water mixtures. *Journal of Chemical and Engineering Data*, *6*(4), 533–537.

Mikhail, S., & Kimel, W. (1963). Densities and viscosities of 1-propanol-water mixtures. *Journal of Chemical and Engineering Data*, *8*(3), 323–328.

Misra, B. N., & Varshni, Y. (1961). Viscosity-temperature relation for solutions. *Journal of Chemical and Engineering Data*, *6*(2), 194–196.

Mjalli, F. S., & Ahmed, O. U. (2016). Physical properties and intermolecular interaction of eutectic solvents binary mixtures: reline and ethaline. *Asia-Pacific Journal of Chemical Engineering*, *11*(4), 549–557.

Moosavi, M., Motahari, A., Omrani, A., & Rostami, A. A. (2013). Investigation on some thermophysical properties of poly (ethylene glycol) binary mixtures at different temperatures. *The Journal of Chemical Thermodynamics*, *58*, 340–350.

Nikam, P. S., Shirsat, L. N., & Hasan, M. (1998). Density and viscosity studies of binary mixtures of acetonitrile with methanol, ethanol, propan-1-ol, propan-2-ol, butan-1-ol, 2-methylpropan-1-ol, and 2-methylpropan-2-ol at (298.15, 303.15, 308.15, and 313.15) k. *Journal of Chemical & Engineering Data*, *43*(5), 732–737.

Nkuku, C. A., & LeSuer, R. J. (2007). Electrochemistry in deep eutectic solvents. *The Journal of Physical Chemistry B*, *111*(46), 13271–13277.

Oswal, S., & Desai, H. (2001). Studies of viscosity and excess molar volume of binary mixtures: 3. 1-alkanol+ di-n-propylamine, and+ di-n-butylamine mixtures at 303.15 and 313.15 k. *Fluid Phase Equilibria*, *186*(1-2), 81–102.

Ozturk, B., Esteban, J., & Gonzalez-Miquel, M. (2018). Deterpenation of citrus essential

oils using glycerol-based deep eutectic solvents. *J. Chem. Eng. Data*, *63*(7), 2384–2393.

Ozturk, B., & Gonzalez-Miquel, M. (2019). Alkanediol-based deep eutectic solvents for isolation of terpenoids from citrus essential oil: Experimental evaluation and cosmo-rs studies. *Sep. Purif. Technol.*, *227*, 115707.

Ozturk, B., Parkinson, C., & Gonzalez-Miquel, M. (2018). Extraction of polyphenolic antioxidants from orange peel waste using deep eutectic solvents. *Separation and Purification Technology*, *206*, 1–13.

Paiva, A., Craveiro, R., Aroso, I., Martins, M., Reis, R. L., & Duarte, A. R. C. (2014). Natural deep eutectic solvents–solvents for the 21st century. *ACS Sustainable Chemistry & Engineering*, *2*(5), 1063–1071.

Pal, A., & Dass, G. (1999). Excess molar volumes and viscosities for binary liquid mixtures of methyl tert-butyl ether and of tert-amyl methyl ether with methanol, 1-propanol, and 1-pentanol at 298.15 k. *Journal of Chemical & Engineering Data*, *44*(6), 1325–1329.

Palomar, J., Gonzalez-Miquel, M., Bedia, J., Rodriguez, F., & Rodriguez, J. J. (2011). Task-specific ionic liquids for efficient ammonia absorption. *Separation and purification technology*, *82*, 43–52.

Palomar, J., Gonzalez-Miquel, M., Polo, A., & Rodriguez, F. (2011). Understanding the physical absorption of co2 in ionic liquids using the cosmo-rs method. *Industrial & Engineering Chemistry Research*, *50*(6), 3452–3463.

Parnham, E. R., Drylie, E. A., Wheatley, P. S., Slawin, A. M., & Morris, R. E. (2006). Ionothermal materials synthesis using unstable deep-eutectic solvents as template-delivery agents. *Angewandte Chemie International Edition*, *45*(30), 4962–4966.

Peng, X., Duan, M.-H., Yao, X.-H., Zhang, Y.-H., Zhao, C.-J., Zu, Y.-G., & Fu, Y.-J. (2016). Green extraction of five target phenolic acids from lonicerae japonicae flos with deep eutectic solvent. *Separation and Purification Technology*, *157*, 249–257.

Phillips, T. W., & Murphy, K. P. (1970). Liquid viscosity of halocarbons. *Journal of Chemical and Engineering Data*, *15*(2), 304–307.

Quijada-Maldonado, E., Sanchez, F., Perez, B., Tapia, R., & Romero, J. (2018). Task-specific ionic liquids as extractants for the solvent extraction of molybdenum (vi) from aqueous solution using different commercial ionic liquids as diluents. *Industrial & Engineering Chemistry Research*, *57*(5), 1621–1629.

Rauf, M. A., & Stewart, G. H. (1983). Viscosities and densities of binary mixtures of 1-alkanols from 15 to 55. degree. c. *Journal of Chemical and Engineering Data*, *28*(3), 324–328.

Rebitzer, G., Ekvall, T., Frischknecht, R., Hunkeler, D., Norris, G., Rydberg, T., ... Pennington, D. W. (2004). Life cycle assessment: Part 1: Framework, goal and scope definition, inventory analysis, and applications. *Environment international*, *30*(5), 701–720.

Redhi, G. G. (2003). *Thermodynamics of liquid mixtures containing carboxylic acids* (Unpublished doctoral dissertation). University of Natal, Durban.

Rodriguez, N. R., Ferre Guell, J., & Kroon, M. C. (2016). Glycerol-Based Deep Eutectic Solvents as Extractants for the Separation of MEK and Ethanol via Liquid-Liquid Extraction. *Journal of Chemical and Engineering Data*, *61*(2), 865–872. doi: 10.1021/acs.jced.5b00717

Rodriguez Rodriguez, N., van den Bruinhorst, A., Kollau, L. J. B. M., Kroon, M. C., & Binnemans, K. (2019). Degradation of Deep-Eutectic Solvents Based on Choline Chloride and Carboxylic Acids. *ACS Sustainable Chemistry & Engineering*, *7*(13), 11521–11528. doi: 10.1021/acssuschemeng.9b01378

Rogošić, M., & Kučan, K. Z. (2019). Deep eutectic solvents based on choline chloride and ethylene glycol as media for extractive denitrification/desulfurization/dearomatization of motor fuels. *Journal of Industrial and Engineering Chemistry*, *72*, 87–99.

Romero, A., Santos, A., Tojo, J., & Rodriguez, A. (2008). Toxicity and biodegradability of imidazolium ionic liquids. *Journal of Hazardous Materials*, *151*(1), 268–273.

Ruesgas-Ramon, M., Figueroa-Espinoza, M. C., & Durand, E. (2017). Application of deep eutectic solvents (des) for phenolic compounds extraction: overview, challenges, and opportunities. *Journal of agricultural and food chemistry*, *65*(18), 3591–3601.

Safarov, J., Ahmadov, B., Mirzayev, S., Shahverdiyev, A., & Hassel, E. P. (2015). Thermophysical properties of 1-butanol over a wide range of temperatures and pressures up to 200 mpa. *Journal of Molecular Liquids*, *209*, 465–479.

Saha, N., Das, B., & Hazra, D. K. (1995). Viscosities and excess molar volumes for acetonitrile+ methanol at 298.15, 308.15, and 318.15 k. *Journal of Chemical and Engineering Data*, *40*(6), 1264–1266.

Sahin, M., Erkan, N., & Ayranci, E. (2016). Solution behavior of p-coumaric, caffeic and ferulic acids in methanol as determined from volumetric properties: attempts to explore a correlation with antioxidant activities. *Journal of Solution Chemistry*, *45*(1), 52–66.

Sánchez, P. B., González, B., Salgado, J., José Parajó, J., & Domínguez, (2019). Physical properties of seven deep eutectic solvents based on L-proline or betaine. *Journal of Chemical Thermodynamics*, *131*, 517–523. doi: 10.1016/j.jct.2018.12.017

Schäfer, A., Klamt, A., Sattel, D., Lohrenz, J. C., & Eckert, F. (2000). Cosmo implementation in turbomole: Extension of an efficient quantum chemical code towards liquid systems. *Physical Chemistry Chemical Physics*, *2*(10), 2187–2193.

Shahbaz, K., Baroutian, S., Mjalli, F., Hashim, M., & AlNashef, I. (2012). Densities of ammonium and phosphonium based deep eutectic solvents: Prediction using artificial intelligence and group contribution techniques. *Thermochimica Acta*, *527*, 59–66.

Shahbaz, K., Mjalli, F. S., Hashim, M. A., & Alnashef, I. M. (2011). Prediction of deep

eutectic solvents densities at different temperatures. *Thermochimica Acta*, *515*(1-2), 67–72. Retrieved from http://dx.doi.org/10.1016/j.tca.2010.12.022 doi: 10.1016/j.tca.2010.12.022

Shekaari, H., Zafarani-Moattar, M. T., & Mohammadi, B. (2017). Thermophysical characterization of aqueous deep eutectic solvent (choline chloride/urea) solutions in full ranges of concentration at t=(293.15–323.15) k. *Journal of Molecular Liquids*, *243*, 451–461.

Shishov, A., Bulatov, A., Locatelli, M., Carradori, S., & Andruch, V. (2017). Application of deep eutectic solvents in analytical chemistry. a review. *Microchemical Journal*, *135*, 33–38.

Singh, B. S., Lobo, H. R., & Shankarling, G. S. (2012). Choline chloride based eutectic solvents: Magical catalytic system for carbon–carbon bond formation in the rapid synthesis of β-hydroxy functionalized derivatives. *Catalysis Communications*, *24*, 70–74.

Singh, J., & Benson, G. (1968). Vapor–liquid equilibrium studies of n-propanol–n-decanol mixtures. *Canadian Journal of Chemistry*, *46*(12), 2065–2069.

Siongco, K. R., Leron, R. B., & Li, M.-H. (2013). Densities, refractive indices, and viscosities of n, n-diethylethanol ammonium chloride–glycerol or–ethylene glycol deep eutectic solvents and their aqueous solutions. *The Journal of Chemical Thermodynamics*, *65*, 65–72.

Smith, E. L., Abbott, A. P., & Ryder, K. S. (2014). Deep Eutectic Solvents (DESs) and Their Applications. *Chemical Reviews*, *114*(21), 11060–11082. doi: 10.1021/cr300162p

Smyth, C., & Stoops, W. (1929). The dielectric polarization of liquids. vi. ethyl iodide, ethanol, normal-butanol and normal-octanol. *Journal of the American Chemical Society*, *51*(11), 3312–3329.

Stott, P. W., Williams, A. C., & Barry, B. W. (1998). Transdermal delivery from eutectic systems: enhanced permeation of a model drug, ibuprofen. *Journal of controlled release*,

50(1-3), 297–308.

Sugiyama, H., Fischer, U., & Hungerbühler, K. (2006). *The ehs tool, eth zurich, safety & environmental technology group, zurich, 2006.*

Tang, B., Zhang, H., & Row, K. H. (2015). Application of deep eutectic solvents in the extraction and separation of target compounds from various samples. *Journal of Separation Science*, *38*(6), 1053–1064. doi: 10.1002/jssc.201401347

Tashima, Y. M. F. E. K. U., Y.; Arai. (1981).

, *41*, 217.

Tommila, E. V. M. L. L. R. S. K. B., E.; Lindell. (1969). Densities, viscosities, surface tensions, dielectric constants, vapor pressures, activities, and heats of mixing of sulpholane + water, sulpholane + methanol, and sulpholane + ethanol mixtures. *Journal of Chemical and Engineering Data*, *42*, 95–104.

Ullah, R., Atilhan, M., Anaya, B., Khraisheh, M., García, G., ElKhattat, A., . . . Aparicio, S. (2015). A detailed study of cholinium chloride and levulinic acid deep eutectic solvent system for co 2 capture via experimental and molecular simulation approaches. *Physical Chemistry Chemical Physics*, *17*(32), 20941–20960.

Varfolomeev, M. A., Zaitseva, K. V., Rakipov, I. T., Solomonov, B. N., & Marczak, W. (2014). Speed of sound, density, and related thermodynamic excess properties of binary mixtures of butan-2-one with c1–c4 n-alkanols and chloroform. *Journal of Chemical & Engineering Data*, *59*(12), 4118–4132.

Vigier, K. D. O., Chatel, G., & Jérôme, F. (2015). Contribution of deep eutectic solvents for biomass processing: Opportunities, challenges, and limitations. *ChemCatChem*, *7*(8), 1250–1260. doi: 10.1002/cctc.201500134

Vogel, H. (1921). The law of the relation between the viscosity of liquids and the temperature. *Phys. Z*, *22*, 645–646.

Walas, S. M. (2013). *Phase equilibria in chemical engineering*. Butterworth-Heinemann.

Walden, P. (1914). Molecular weights and electrical conductivity of several fused salts. *Bull. Acad. Imper. Sci.(St. Petersburg)*, *1800*.

Wei, D., Han, S., & Wang, B. (2014). Excess molar enthalpies for binary mixtures of cyclopentanone, cyclohexanone, or cycloheptanone with n-nonane at t= 298.15 k and atmospheric pressure. *The Journal of Chemical Thermodynamics*, *76*, 87–92.

Westmeier, S. (1976). Excess enthalpy, free excess enthalpy, excess volume and viscosity of selected binary liquid mixtures. part iii: The water-n-propanol and water- isopropanol systems. *Canadian Journal of Chemistry*, *28*, 480–3.

Wongsirichot, P., Gonzalez-Miquel, M., & Winterburn, J. (2019). Holistic valorization of rapeseed meal utilizing green solvents extraction and biopolymer production with pseudomonas putida. *J. Cleaner Prod.*, *230*, 420–429.

Yadav, A., Kar, J. R., Verma, M., Naqvi, S., & Pandey, S. (2015). Densities of aqueous mixtures of (choline chloride+ ethylene glycol) and (choline chloride+ malonic acid) deep eutectic solvents in temperature range 283.15–363.15 k. *Thermochimica acta*, *600*, 95–101.

Yadav, A., Trivedi, S., Rai, R., & Pandey, S. (2014a). Densities and dynamic viscosities of (choline chloride+glycerol) deep eutectic solvent and its aqueous mixtures in the temperature range (283.15-363.15)K. *Fluid Phase Equilibria*, *367*, 135–142. Retrieved from `http://dx.doi.org/10.1016/j.fluid.2014.01.028` doi: 10.1016/j.fluid.2014.01.028

Yadav, A., Trivedi, S., Rai, R., & Pandey, S. (2014b). Densities and dynamic viscosities of (choline chloride+ glycerol) deep eutectic solvent and its aqueous mixtures in the temperature range (283.15–363.15) k. *Fluid Phase Equilibria*, *367*, 135–142.

Zhang, Q., Vigier, K. D. O., Royer, S., & Jerome, F. (2012). Deep eutectic solvents: syntheses, properties and applications. *Chemical Society Reviews*, *41*(21), 7108–7146.

Zhang, Z., Zhou, Q., Lu, X., Qiao, C., & Zhang, S. (2014). Densities and viscosities of binary mixtures containing 1, 3-dimethylimidazolium dimethylphosphate and alcohols. *Journal of Chemical & Engineering Data*, *59*(8), 2377–2388.

Zhu, C., Han, S., Liu, J., & Ma, Y. (2014). Densities and viscosities of diaminotoluene with water, ethanol, propan-1-ol, and butan-1-ol from (293.15 to 333.15) k. *Journal of Chemical & Engineering Data*, *59*(3), 880–889.

Živković, E. M., Bajić, D. M., Radović, I. R., Šerbanović, S. P., & Kijevčanin, M. L. (2014). Volumetric and viscometric behavior of the binary systems ethyl lactate+ 1, 2-propanediol,+ 1, 3-propanediol,+ tetrahydrofuran and+ tetraethylene glycol dimethyl ether. new unifac–visco and asog–visco parameters determination. *Fluid Phase Equilibria*, *373*, 1–19.

Živković, N., Šerbanović, S., Kijevčanin, M., & Živković, E. (2013). Volumetric properties, viscosities, and refractive indices of the binary systems 1-butanol+ peg 200,+ peg 400, and+ tegdme. *International Journal of Thermophysics*, *34*(6), 1002–1020.

Zullaikah, S., Rachmaniah, O., Utomo, A. T., Niawanti, H., & Ju, Y. H. (2017). Green separation of bioactive natural products using liquefied mixture of solids. *Green Chemistry*, 17–38.

APPENDIX

A. SUPPORTING INFORMATION

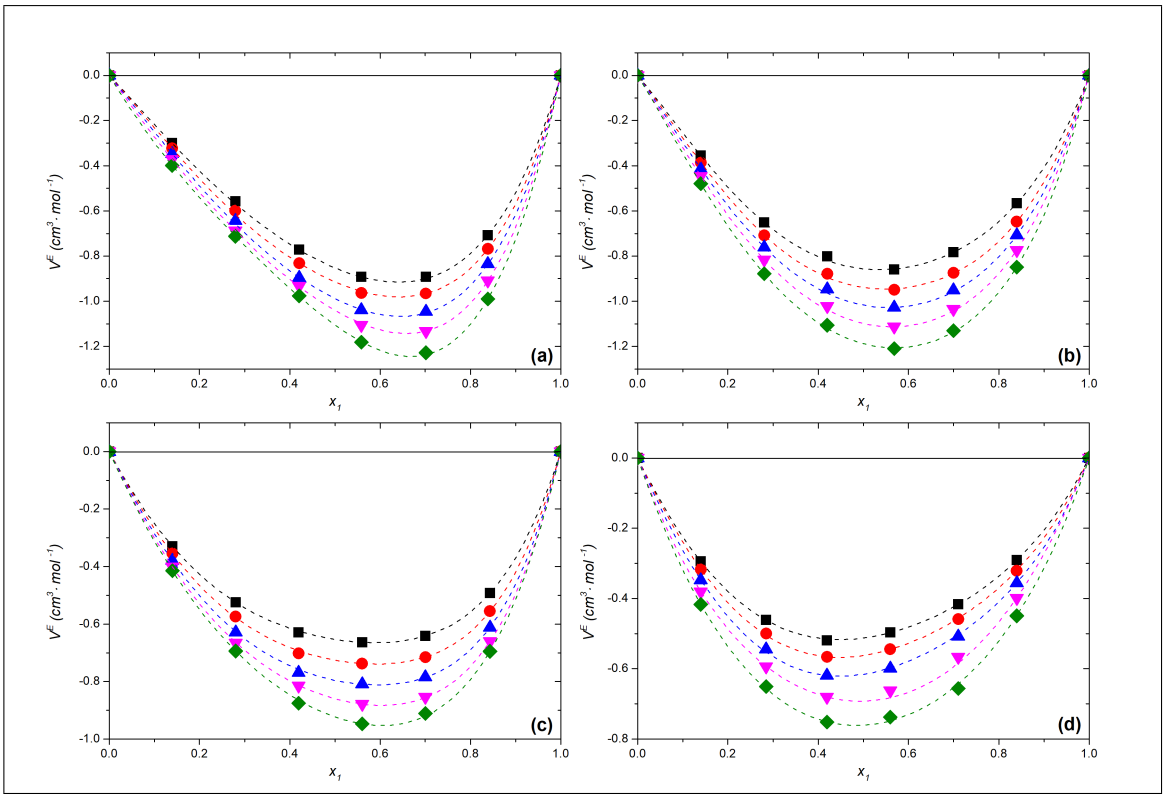

Figure A.1. Excess molar volume (cm^3·mol^{-1}) in terms of the mole fraction of alcohol for the binary mixtures **(a)** methanol + DES-B, **(b)** ethanol + DES-B, **(c)** 1-propanol + DES-B, **(d)** 1-butanol + DES-B at a pressure of 101.3 kPa and temperatures between 298.15 K and 333.15 K. Temperatures of 293.15 K (■), 303.15 K (●), 313.15 K (▲), 323.15 K (▼), 333.15 K (◆). The dashed line represents the Redlich-Kister polynomial fitting with parameters reported in Table 9.

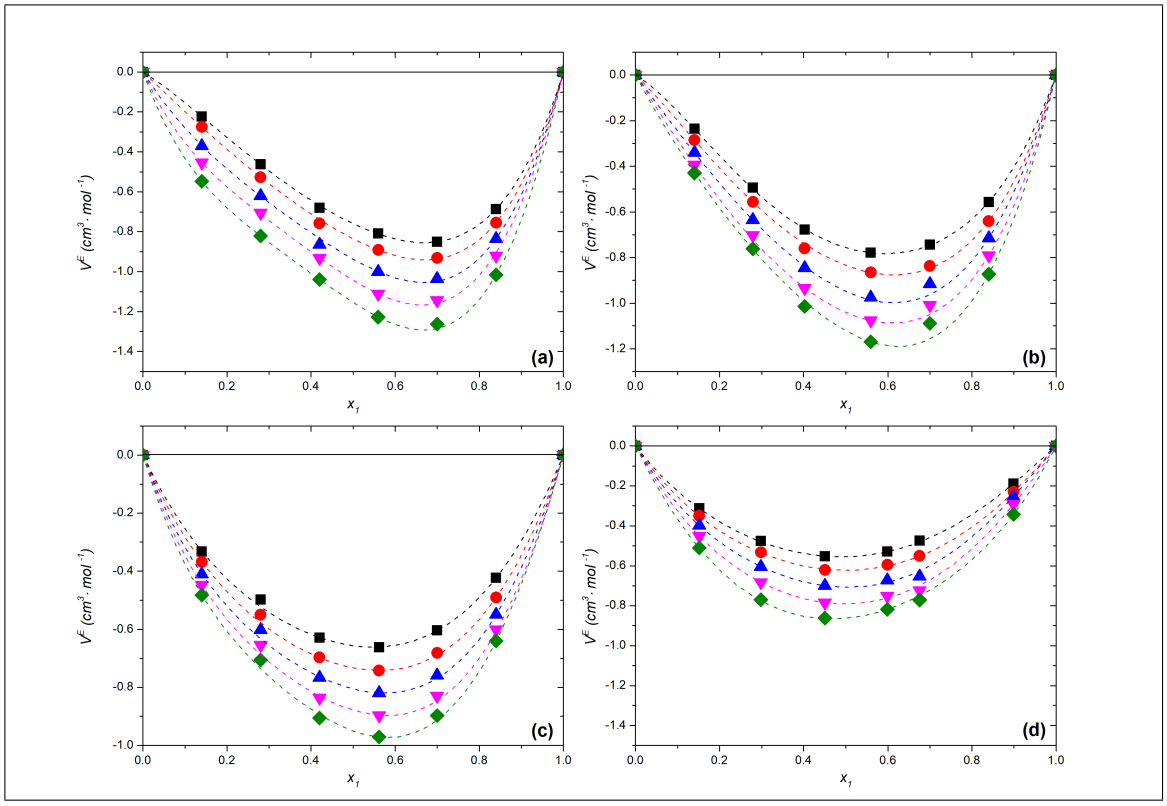

Figure A.2. Excess molar volume (cm^3·mol^{-1}) in terms of the mole fraction of alcohol for the binary mixtures **(a)** methanol + DES-C, **(b)** ethanol + DES-C, **(c)** 1-propanol + DES-C, **(d)** 1-butanol + DES-C at a pressure of 101.3 kPa and temperatures between 298.15 K and 333.15 K. Temperatures of 293.15 K (■), 303.15 K (●), 313.15 K (▲), 323.15 K (▼), 333.15 K (◆). The dashed line represents the Redlich-Kister polynomial fitting with parameters reported in Table 9.

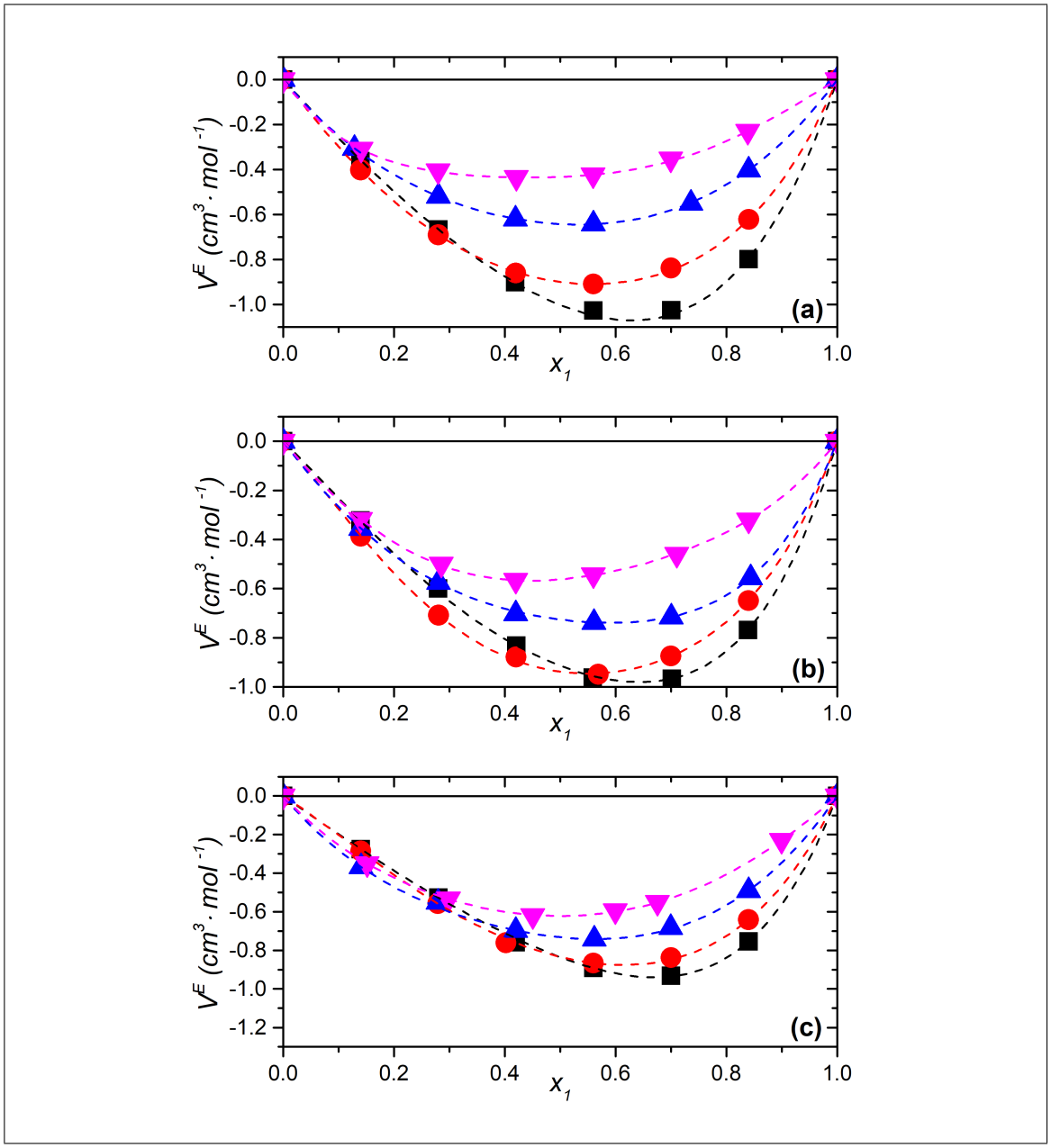

Figure A.3. Excess molar volume ($cm^3 \cdot mol^{-1}$) in terms of the mole fraction of alcohol for the binary mixtures of **(a)** DES-A, **(b)** DES-B , **(c)** DES-C, at a pressure of 101.3 kPa, temperature of 303.15 K and DES binary system with methanol (■), ethanol (●), 1-propanol (▲), 1-butanol (▼). The dashed line represents the Redlich-Kister polynomial fitting with parameters reported in Table 9.

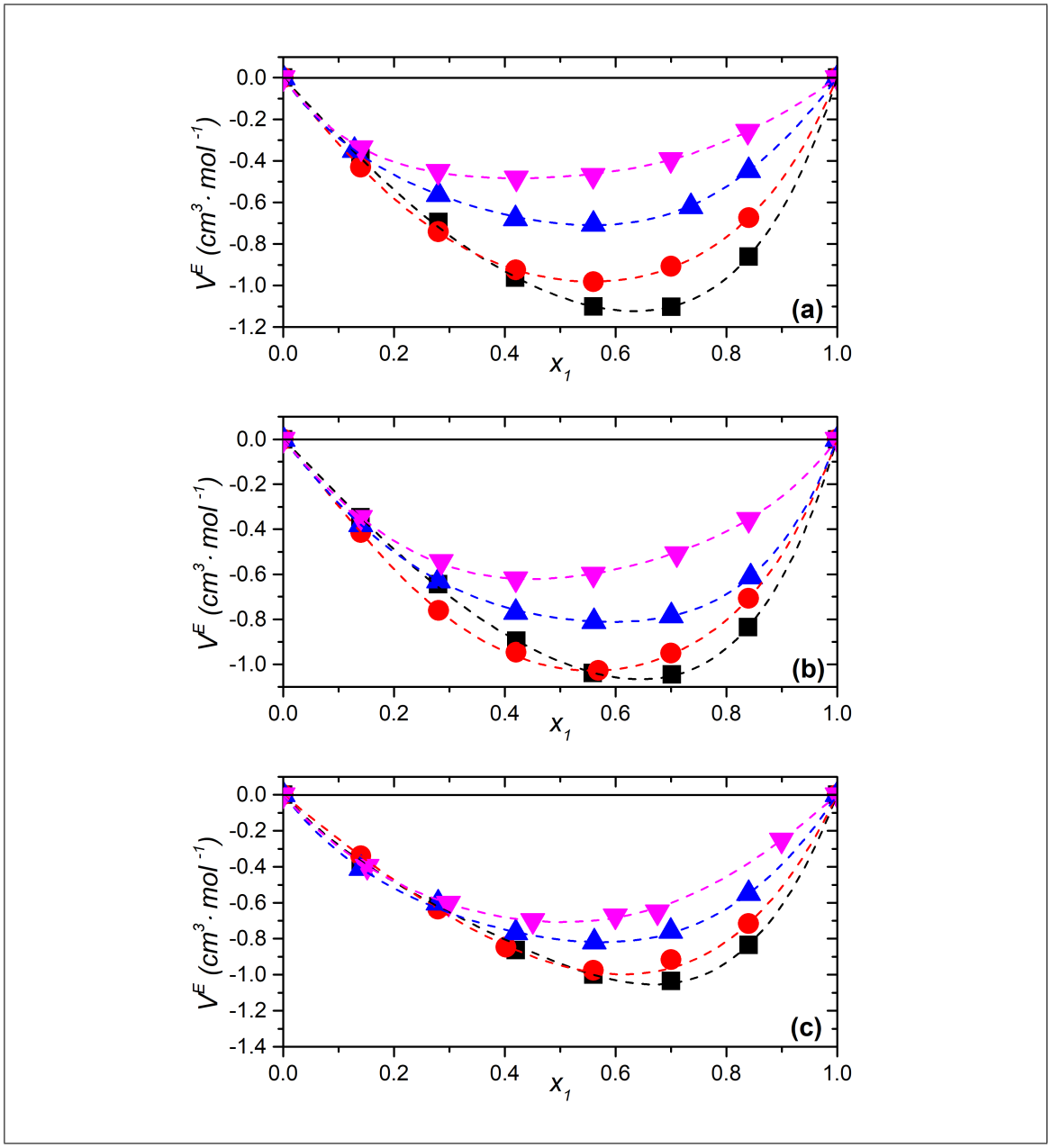

Figure A.4. Excess molar volume ($cm^3 \cdot mol^{-1}$) in terms of the mole fraction of alcohol for the binary mixtures of **(a)** DES-A, **(b)** DES-B , **(c)** DES-C, at a pressure of 101.3 kPa, temperature of 313.15 K and DES binary system with methanol (■), ethanol (●), 1-propanol (▲), 1-butanol (▼). The dashed line represents the Redlich-Kister polynomial fitting with parameters reported in Table 9.

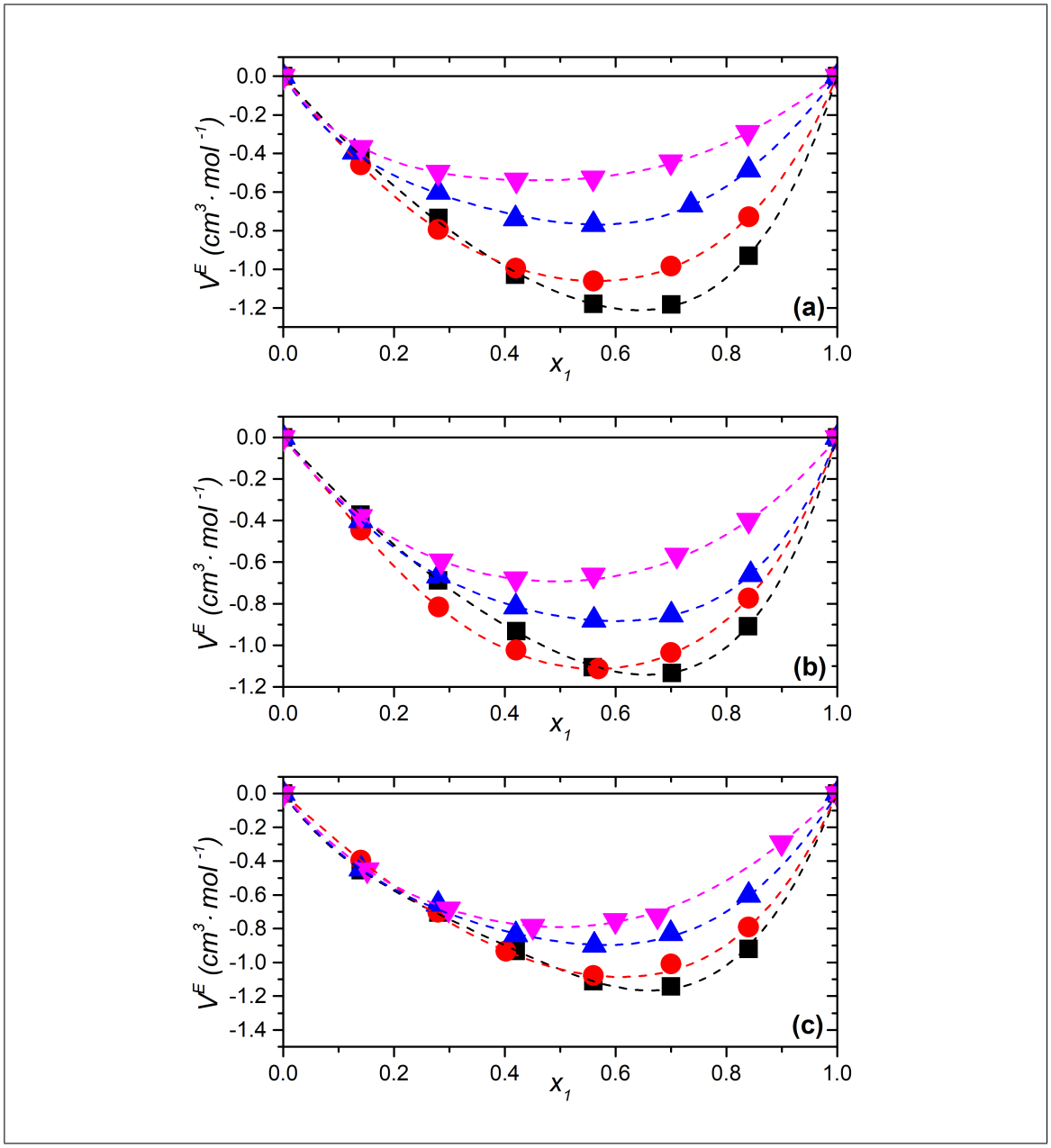

Figure A.5. Excess molar volume ($cm^3 \cdot mol^{-1}$) in terms of the mole fraction of alcohol for the binary mixtures of **(a)** DES-A, **(b)** DES-B , **(c)** DES-C, at a pressure of 101.3 kPa, temperature of 323.15 K and DES binary system with methanol (■), ethanol (●), 1-propanol (▲), 1-butanol (▼). The dashed line represents the Redlich-Kister polynomial fitting with parameters reported in Table 9.

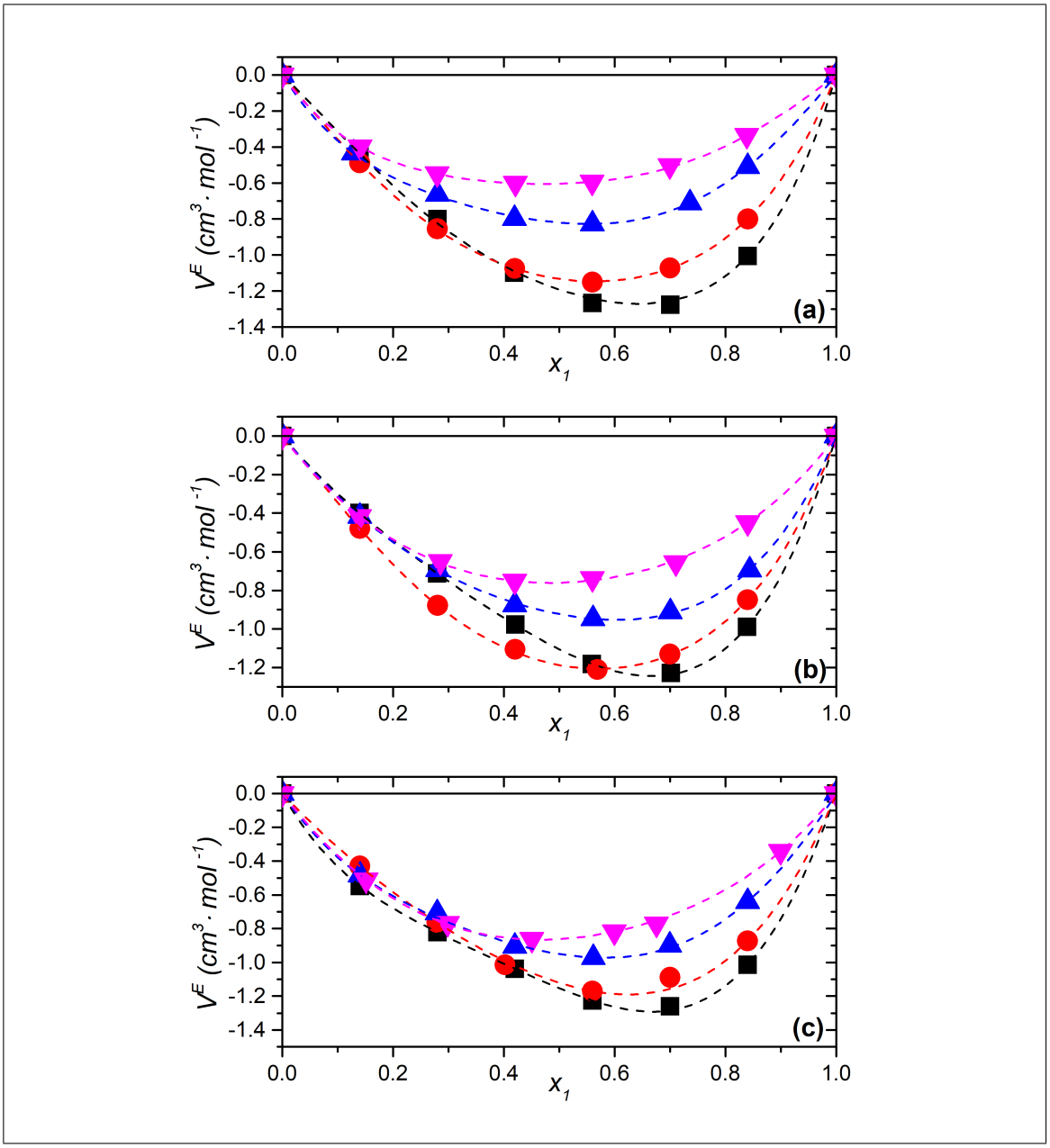

Figure A.6. Excess molar volume ($cm^3 \cdot mol^{-1}$) in terms of the mole fraction of alcohol for the binary mixtures of **(a)** DES-A, **(b)** DES-B , **(c)** DES-C, at a pressure of 101.3 kPa, temperature of 333.15 K and DES binary system with methanol (■), ethanol (●), 1-propanol (▲), 1-butanol (▼). The dashed line represents the Redlich-Kister polynomial fitting with parameters reported in Table 9.

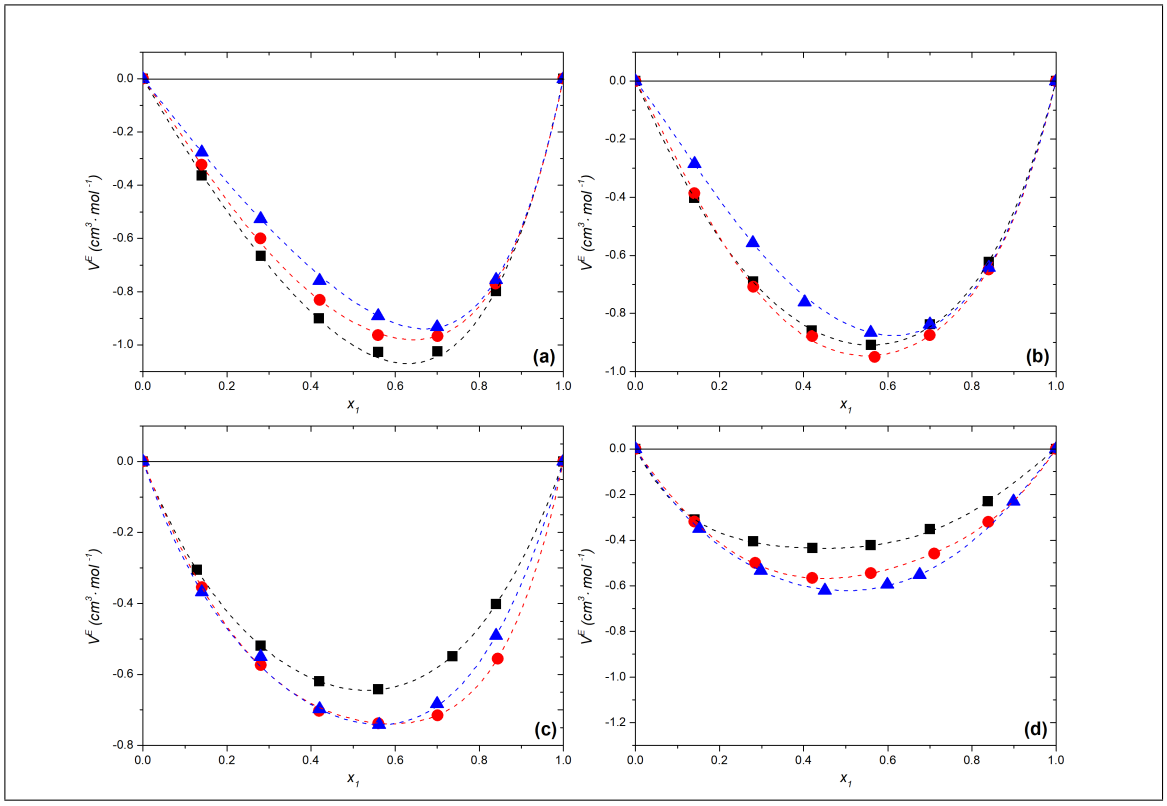

Figure A.7. HBD effect on excess molar volume ($cm^3 \cdot mol^{-1}$) in terms of the mole fraction of alcohol for the binary mixtures of DES with **(a)** methanol, **(b)** ethanol , **(c)** 1-propanol, **(d)** 1-butanol at a pressure of 101.3 kPa, temperature of 303.15 K and binary system with DES-A (■), DES-B (●), DES-C (▲). The dashed line represents the Redlich-Kister polynomial fitting with parameters reported in Table 9.

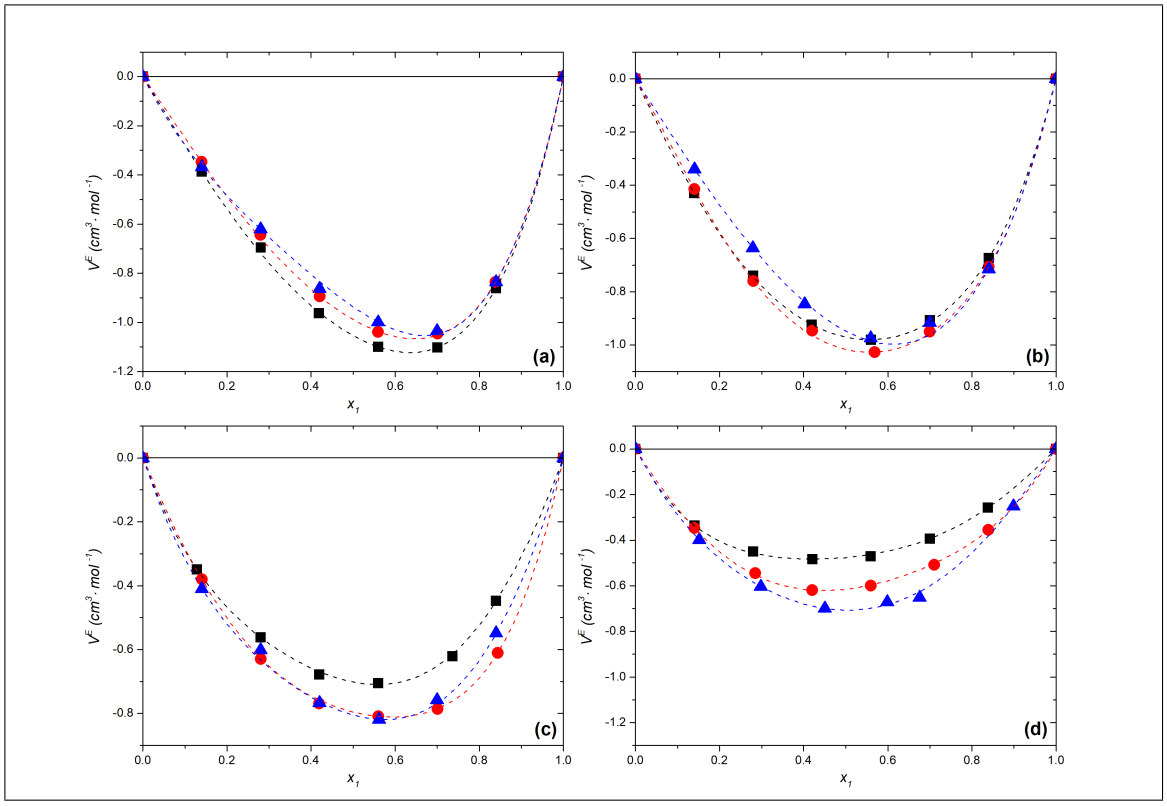

Figure A.8. HBD effect on excess molar volume (cm^3·mol^{-1}) in terms of the mole fraction of alcohol for the binary mixtures of DES with **(a)** methanol, **(b)** ethanol , **(c)** 1-propanol, **(d)** 1-butanol at a pressure of 101.3 kPa, temperature of 313.15 K and binary system with DES-A (■), DES-B (●), DES-C (▲). The dashed line represents the Redlich-Kister polynomial fitting with parameters reported in Table 9.

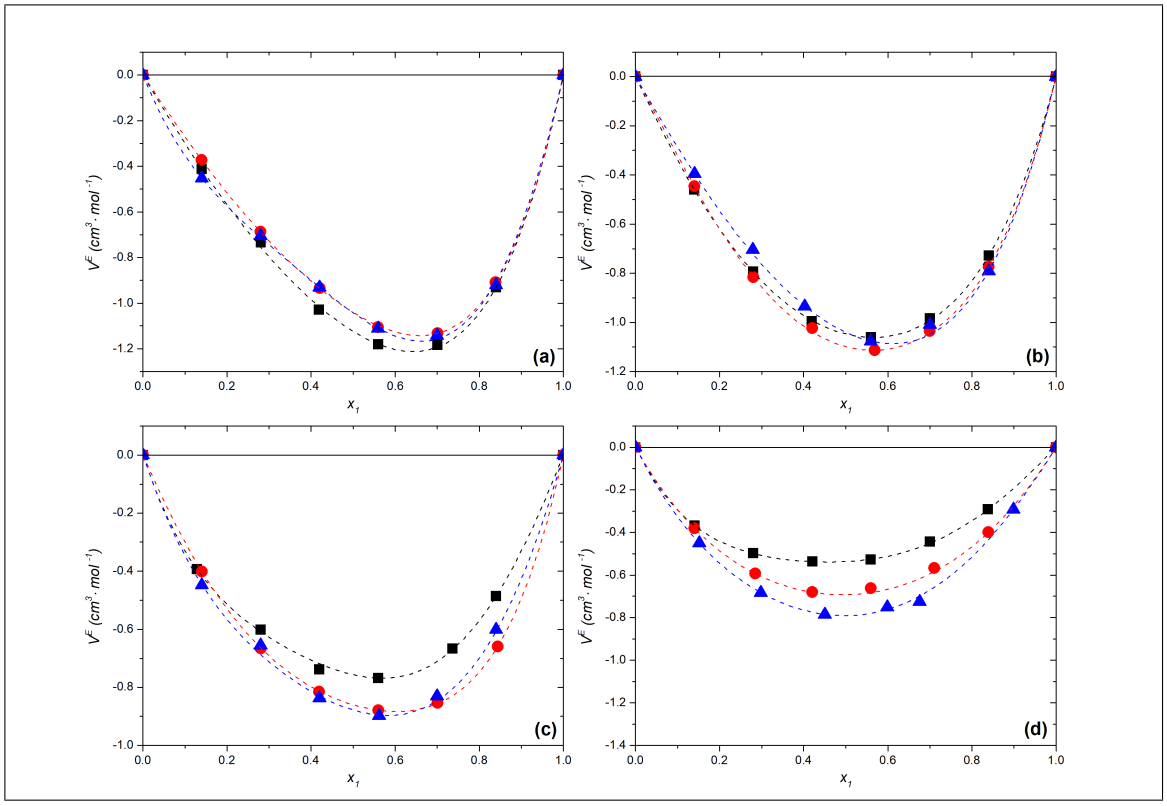

Figure A.9. HBD effect on excess molar volume ($cm^3 \cdot mol^{-1}$) in terms of the mole fraction of alcohol for the binary mixtures of DES with **(a)** methanol, **(b)** ethanol , **(c)** 1-propanol, **(d)** 1-butanol at a pressure of 101.3 kPa, temperature of 323.15 K and binary system with DES-A (■), DES-B (●), DES-C (▲). The dashed line represents the Redlich-Kister polynomial fitting with parameters reported in Table 9.

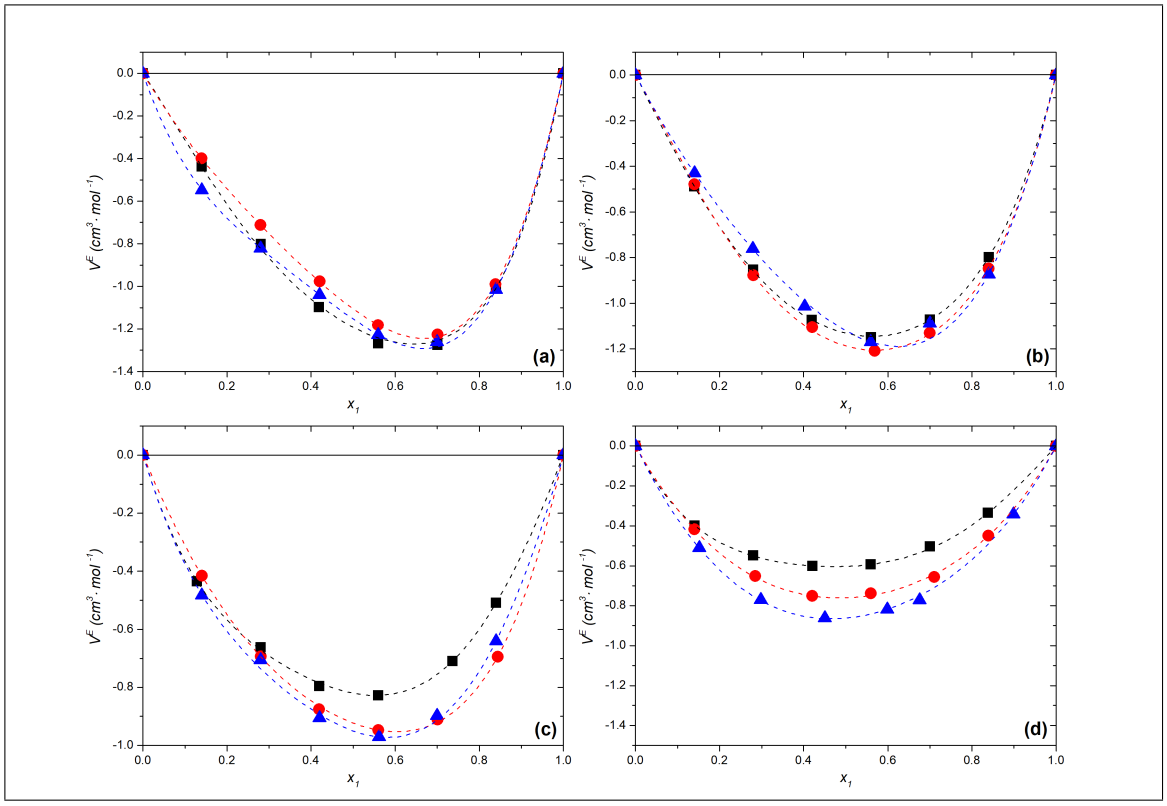

Figure A.10. HBD effect on excess molar volume (cm^3·mol^{-1}) in terms of the mole fraction of alcohol for the binary mixtures of DES with **(a)** methanol, **(b)** ethanol , **(c)** 1-propanol, **(d)** 1-butanol at a pressure of 101.3 kPa, temperature of 333.15 K and binary system with DES-A (■), DES-B (●), DES-C (▲). The dashed line represents the Redlich-Kister polynomial fitting with parameters reported in Table 9.

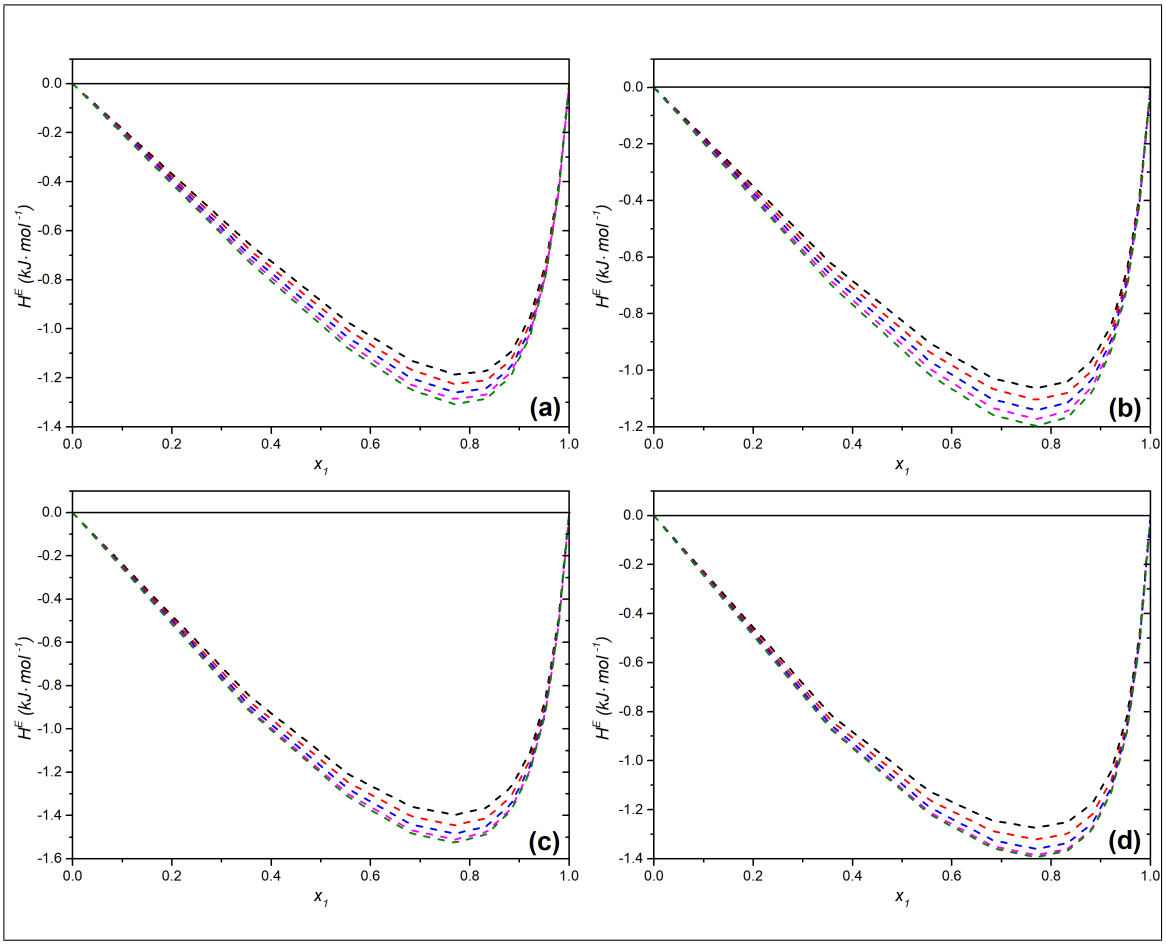

Figure A.11. Temperature effect on the molar excess enthalpy of alcohol + DES-B mixtures predicted with COSMO-RS.]Temperature effect on the molar excess enthalpy of alcohol + DES-A mixtures predicted with COSMO-RS. The molar excess enthalpies (kJ·mol^{-1}) are in terms of the mole fraction of alcohol for the binary mixtures of **(a)** methanol + DES-B, **(b)** ethanol + DES-B, **(c)** 1-propanol + DES-B, **(d)** 1-butanol + DES-B at a pressure of 101.3 kPa and temperatures between 293.15 K and 333.15 K. The dashed line represents the temperatures of 293.15 K (−), 303.15 K (−), 313.15 K (−), 323.15 K (−), 333.15 K (−).

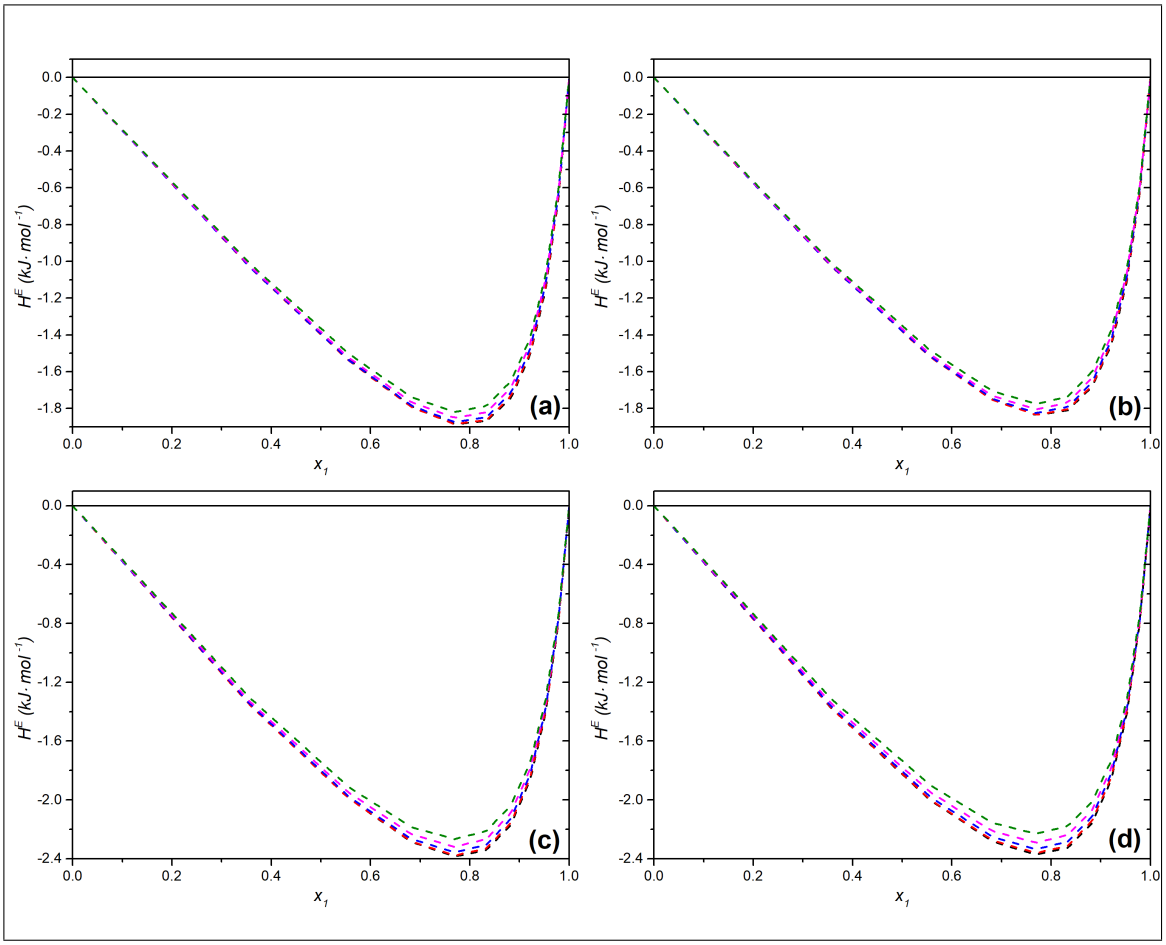

Figure A.12. Temperature effect on the molar excess enthalpy of alcohol + DES-C mixtures predicted with COSMO-RS.]Temperature effect on the molar excess enthalpy of alcohol + DES-A mixtures predicted with COSMO-RS. The molar excess enthalpies (kJ·mol^{-1}) are in terms of the mole fraction of alcohol for the binary mixtures of **(a)** methanol + DES-C, **(b)** ethanol + DES-C, **(c)** 1-propanol + DES-C, **(d)** 1-butanol + DES-C at a pressure of 101.3 kPa and temperatures between 293.15 K and 333.15 K. The dashed line represents the temperatures of 293.15 K (−), 303.15 K (−), 313.15 K (−), 323.15 K (−), 333.15 K (−)..

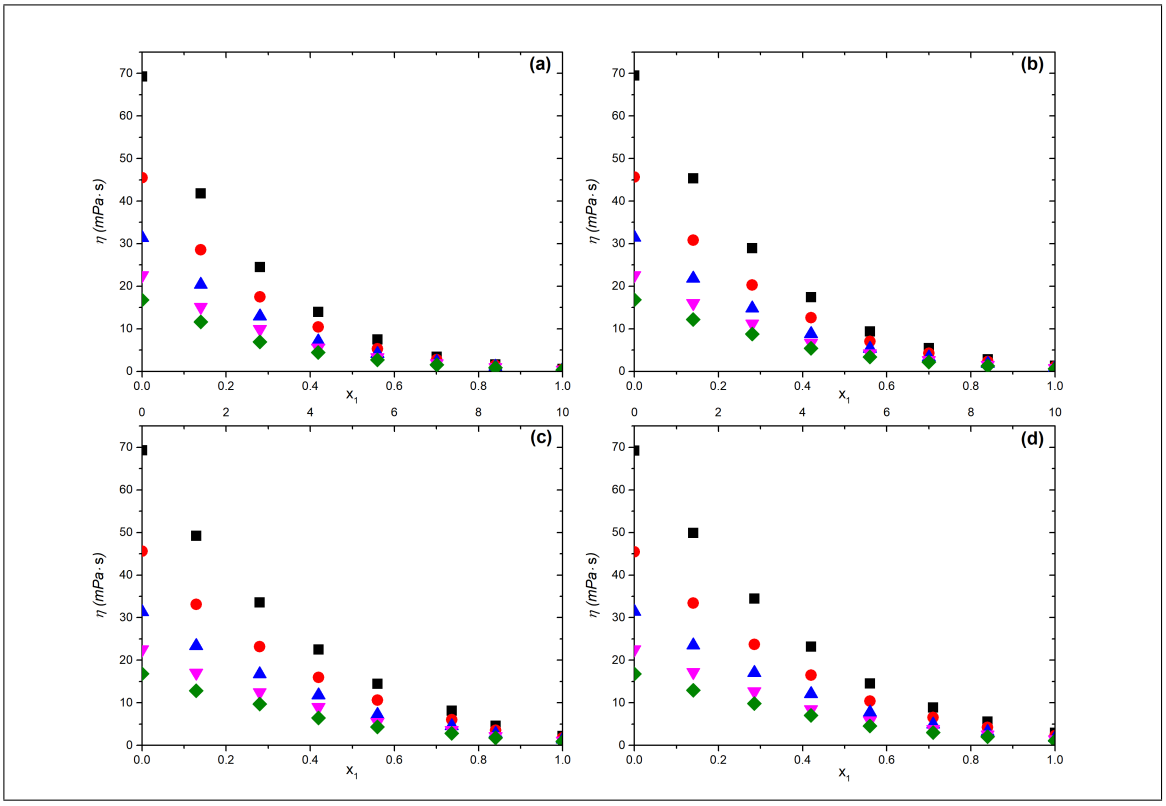

Figure A.13. Dynamic viscosity (mPa·s) in terms of the mole fraction of alcohol for the binary mixtures of **(a)** DES-B1, **(b)** DES-B2, **(c)** DES-B3, **(d)** DES-B4 at a pressure of 101.3 kPa and temperatures between 298.15 K and 333.15 K. Temperatures of 293.15 K (■), 303.15 K (●), 313.15 K (▲), 323.15 K (▼) and 333.15 K (◆).

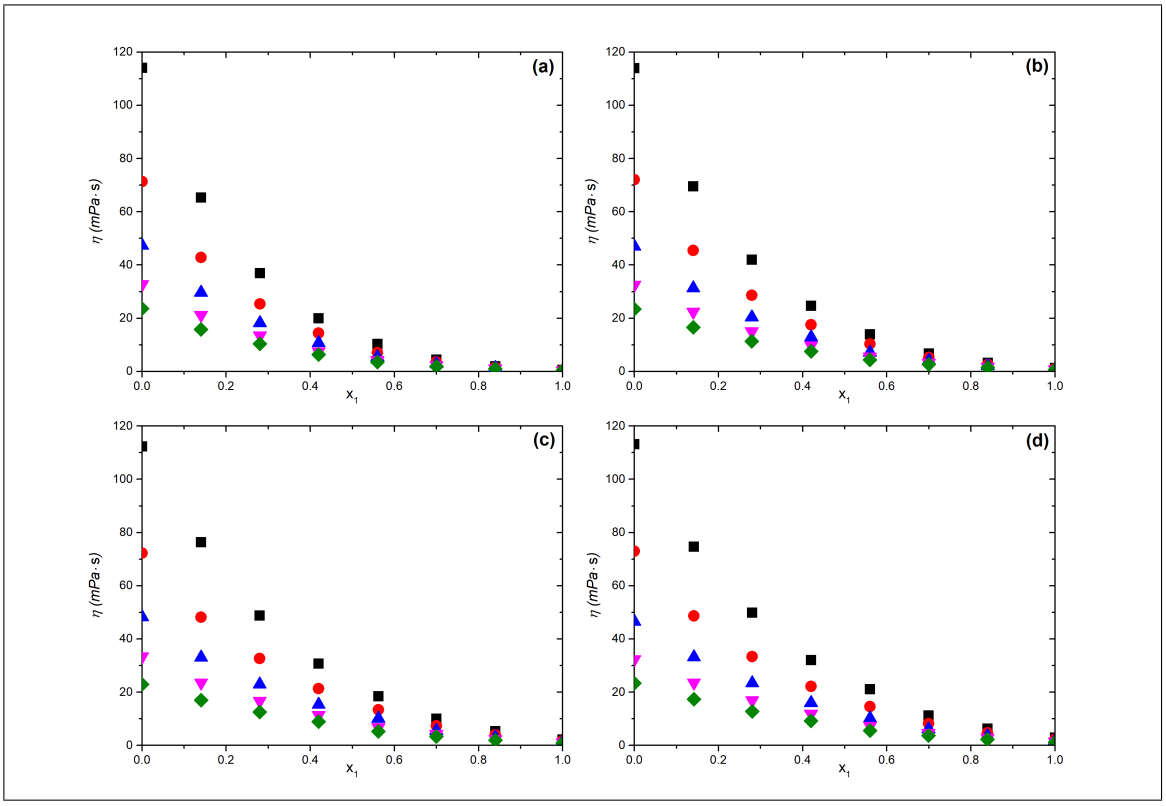

Figure A.14. Dynamic viscosity (mPa·s) in terms of the mole fraction of alcohol for the binary mixtures of **(a)** DES-C1, **(b)** DES-C2, **(c)** DES-C3, **(d)** DES-C4 at a pressure of 101.3 kPa and temperatures between 298.15 K and 333.15 K. Temperatures of 293.15 K (■), 303.15 K (●), 313.15 K (▲), 323.15 K (▼) and 333.15 K (◆).

B. HYDROGEN BOND DONOR AND ALCOHOL CHAIN LENGTH EFFECT ON THE PHYSICOCHEMICAL PROPERTIES OF CHOLINE CHLORIDE BASED DEEP EUTECTIC SOLVENTS MIXED WITH ALCOHOLS

Graphical Abstract

Hydrogen bond donor and alcohol chain length effect on the physicochemical properties of choline chloride based deep eutectic solvents mixed with alcohols

Vincenzo P. Cotroneo-Figueroa, Nicolás F. Gajardo-Parra, Pablo López-Porfiri, Ángel Leiva, Maria Gonzalez-Miquel, Roberto I. Canales

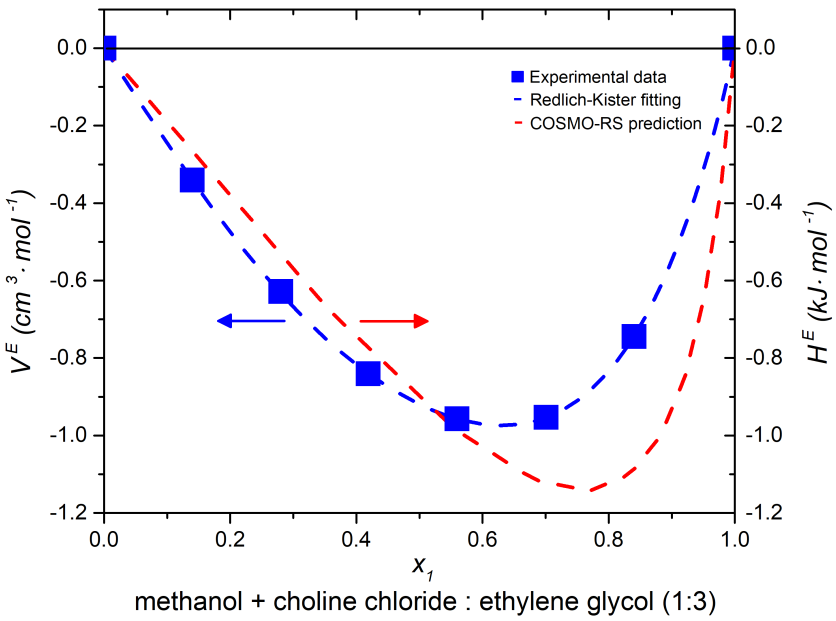

Highlights

Hydrogen bond donor and alcohol chain length effect on the physicochemical properties of choline chloride based deep eutectic solvents mixed with alcohols

Vincenzo P. Cotroneo-Figueroa, Nicolás F. Gajardo-Parra, Pablo López-Porfiri, Ángel Leiva, Maria Gonzalez-Miquel, Roberto I. Canales

- Density, viscosity, and FT-IR spectra for choline chloride and glycol-based deep eutectic solvents are obtained.
- Density and viscosity of the pseudo-binary mixtures of choline chloride:ethylene glycol, choline chloride:1,3-propanediol, or choline chloride:1,4-butanediol mixed with metanol, ethanol, 1-propanol or 1-butanol are measured.
- Excess volumes calculated from the density of the mixtures are negative and excess enthalpies predicted with COSMO-RS are exothermic for all the pseudo-binary mixtures.
- Effect of temperature, hydrogen bond donor and alcohol chain length on the excess properties are analyzed.

Hydrogen bond donor and alcohol chain length effect on the physicochemical properties of choline chloride based deep eutectic solvents mixed with alcohols

Vincenzo P. Cotroneo-Figueroa[a], Nicolás F. Gajardo-Parra[a], Pablo López-Porfiri[b], Ángel Leiva[c], Maria Gonzalez-Miquel[d], Roberto I. Canales[a,*]

[a]*Departamento de Ingeniería Química y Bioprocesos, Pontificia Universidad Católica de Chile, Avenida Vicuña Mackenna 4860, Macul, Santiago, Chile*
[b]*School of Chemical Engineering and Analytical Sciences, Faculty of Science and Engineering, The University of Manchester, Manchester M13 9PL, United Kingdom*
[c]*Departamento de Química Física, Facultad de Química, Pontificia Universidad Católica de Chile, Avenida Vicuña Mackenna 4860, Macul, Santiago, Chile*
[d]*Departamento de Ingeniería Química Industrial y del Medioambiente, Universidad Politécnica de Madrid, E-28006 Madrid, Spain*

Abstract

Deep eutectic solvents are mixtures composed typically by a hydrogen bond donor and a hydrogen bond acceptor. They have appeared as an alternative of ionic liquids in several processes due to their tunability, biodegradability and low cost. Recently, deep eutectic solvents have been studied as potential solvents for different applications. Then, their physicochemical properties need to be characterized for understanding the interaction between its constituents and with other compounds. Deep eutectic solvents prepared for this work were based on choline chloride mixed with ethylene glycol, 1,3-propanediol or 1,4-butanediol at a 1:3 mole ratio. Density and viscosity of the pseudo-pure deep eutectic solvents were measured from 293.15 K to 333.15 K at 101.13 kPa. Also, the same properties at the same temperature and pressure conditions were obtained for the pseudo-binary mixtures of the three deep eutectic solvents with four alcohols: methanol, ethanol, 1-propanol or 1-butanol. The excess volumes were calculated for each system for understanding the effect of the temperature variation, the length of the alcohol chain, and length of the hydrogen bond donor on the configurational aspects of the mixture. Subsequently, a prediction of the excess molar enthalpy was performed with COSMO-RS in order to assess the behavior of the same variables on different type of intermolecular interactions from the energetic point of view. The results suggest that mixing each deep eutectic solvent with an alcohol produce negative molar excess volumes and molar excess enthalpies, observing a higher affinity between unlike species.

*Corresponding author
Email address: rocanalesm@ing.puc.cl (Roberto I. Canales)

Keywords: Deep eutectic solvents, molar excess volume, molar excess entalphy, COSMO-RS, density, viscosity

1. Introduction

The separation processes have an essential role in the chemical industry. A few examples are the recuperation of biological solutes, the purification of relevant chemicals from residues, and the separation of synthesized high-value compounds.[1, 2] Many of these applications require large amounts of energy, costly components, expensive operations, and environmentally unfriendly procedures due to the nature of the solvents involved in the process. In this context, deep eutectic solvents (DES) have appeared as a green alternative for typical toxic solvents used in industrial processes because of their interesting properties as low toxicity, high biodegradability, and relatively low vapor pressure.[3–5] DES used in separation processes are prepared by mixing a hydrogen bond acceptor (HBA), e.g., choline chloride, betaine, etc., with a hydrogen bond donor (HBD), e.g., sugars, glycols, organic acids, etc. In general, HBDs and HBAs are selected among natural compounds or primary metabolites. The idea, after mixing the HBA and the HBD, is to produce a homogeneous liquid DES with similar characteristics as the industrial solvents that need to be replaced. It is important to note that some of these eutectic mixtures have certain disadvantages, such as their high viscosity, non-negligible vapor pressure, and instability, which can affect their use in a large scale chemical process.[6]

Until 2019, DES have appeared in more than 3000 publications[7, 8] on diverse applications as pharmaceutical, electrochemistry, separation processes, preparation of materials, organic synthesis, catalysis, DNA extraction, etc. [4, 8–14] Thus, the study of the physicochemical properties of DES have a high importance for all the mentioned applications because they determine the design parameters for process equipment such as pumps, pipes, reactors, heat exchangers, separators, etc. Then, density, viscosity, and liquid range of DES are relevant for understanding their applicability in those specific processes. For improving the transport properties of DES, their mixtures with alcohols generate a significant decrease in viscosity, allowing a better mass transfer if these mixtures are used for separations or improving the reaction rates if they are used as a reaction media. [3, 15] Alcohols are commonly used as co-solvents in separation processes, so it is necessary to study their interactions with DES as a way of validating them as a mixture for these kind of applications.

This work is part of an exhaustive study of density, viscosity and excess volumes of the DES composed by choline chloride + ethylene glycol, choline chloride + 1,3 propanediol, and choline chloride + 1,4 butanediol and their mixtures with methanol, ethanol, 1-propanol or 1-butanol. All the DES were characterized by Fourier-transform infrared spectroscopy (FT-IR) to study potential interactions between the precursors and to determine whether or not there is any chemical reaction that take place between the HBA

and HBD. Densities and viscosities of the pseudo-binary mixtures DES + alcohol were measured between the temperatures of 293.15 K and 333.15 K at a pressure of 101.3 kPa, and the excess volumes were calculated from density data. The density was correlated with a linear equation, viscosity with the Vogel-Fulcher-Tamman (VFT) equation, and the excess molar volume with the Redlich-Kister (RK) correlation. In order to understand the driving forces behind the observed mixing behavior, excess enthalpies were calculated with the COnductor like Screening MOdel for Real Solvents (COSMO-RS). With this approach, the effect of the alcohol chain length will be elucidated on the basis of the physicochemical properties of DES and the mixtures. Therefore, through experimental data and quantum chemical methods, this work provides a comprehensive analysis of the mixing phenomena and its implication on the macroscopic behavior of DES for separation processes.

2. Materials and methods

2.1. Chemicals

The compounds for preparing the DES as choline chloride, ethylene glycol, and 1,4-butanediol were supplied by Acros Organics and 1,3-propanediol by Sigma-Aldrich. The alcohols used for the pseudo-binary systems DES + alcohol as methanol, ethanol, and 1-butanol were purchased in Acros Organics and 1-propanol in Merck KGaA. Table 1 shows the specifications of each compound as molar mass, CAS number, purities, and source of the compounds used in this study. Figure 1 shows the structures of all the molecules used in the mixtures prepared for this work. Three types of DES were prepared using choline chloride as the HBA and ethylene glycol (DES-A), 1,3-propanediol (DES-B), and 1,4-butanediol (DES-C) as the HBD. All the DES have a molar ratio of HBA:HBD of approximately 1:3.

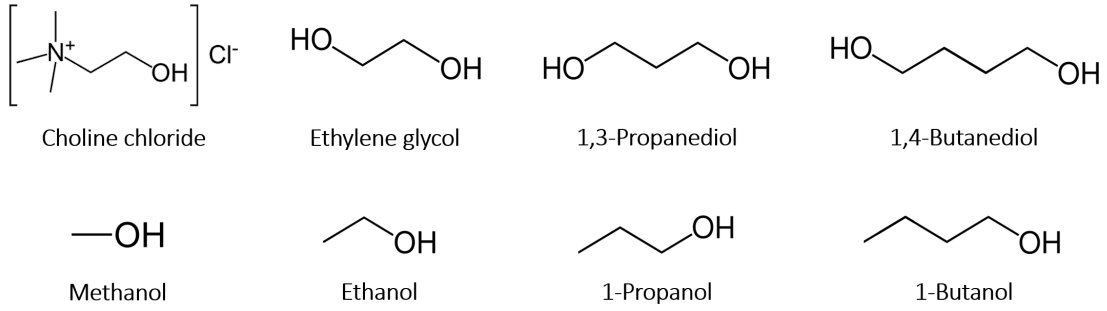

Figure 1: Chemicals used in this study.

Table 1: Specifications of chemicals used in this work as molar mass (M), CAS number, supplier, type and purity

Chemical name	M **(g·mol^{-1})**	**CAS**	**Supplier**	**Type**	**Purity**
Choline chloride	139.63	67-48-1	Acros Organics	-	>0.990
Ethylene glycol	62.07	107-21-1	Acros Organics	Anhydrous, AcroSeal®	>0.998
1,3-propanediol	76.09	504-63-2	Sigma Aldrich	-	>0.980
1,4-butanediol	90.12	110-63-4	Acros Organics	-	>0.990
Methanol	32.04	67-56-1	Acros Organics	Extra Dry, AcroSeal®	>0.999
Ethanol	46.07	64-17-5	Acros Organics	Extra Dry, absolute, AcroSeal®	>0.995
1-propanol	60.10	71-23-8	Merck KGaA	LiChrosolv®	>0.998
1-butanol	74.12	71-36-3	Sigma Aldrich	Anhydrous	>0.998

2.2. Preparation of DES and alcohol + DES mixtures

Before preparing the DES used in this study, choline chloride was dried in a Schlenk line under a high vacuum (10^{-4} mbar) during 72 hours to remove water absorbed from ambient humidity. Non–anhydrous HBDs and alcohols were placed under molecular sieves for 72 hours, also for decreasing their water content. Anhydrous compounds were used as received. DES were prepared by mass using an analytic balance (Practum 224-1s Sartorius, Germany, uncertainty ± 0.1 mg) adding the components to a vial. Then, the vial was quickly closed with a septum cap. The mixture was placed in a sonicator (iSonic P4862-IT, Australia) at 323.15 K until a homogeneous liquid was formed. The water content of all the DES was measured using a Karl Fischer Coulometer (831KF Metrohm, Switzerland). The DES were approximately mixed in a mole ratio of 1:3. Four batches of each DES were prepared and each one was mixed with a specific alcohol. All the properties were measured shortly after the DES preparation for avoiding the absorption of water in the DES and its mixtures with the alcohols. All the DES with their respective molar ratios, molas mass and water content are shown in Table 2, where it is also specified the alcohol which is mixed with each batch of DES. DES + alcohol mixtures were also prepared by mass and mixed with a magnetic stir bar.

Table 2: Abbreviation, components, mole ratio, molar mass (M) and water content (wt.%) of deep eutectic solvents used in this work.

Abbreviation	**Salt**	**HBD**	**Mole ratio**	**M_{DES} (g·mol^{-1})**	**Water content (wt. %)**	**Mixed with**
DES-A1	ChCl	Ethylene glycol	1:3.000	81.449	0.032	Methanol
DES-A2	ChCl	Ethylene glycol	1:3.002	81.441	0.078	Ethanol
DES-A3	ChCl	Ethylene glycol	1:2.999	81.447	0.061	1-Propanol
DES-A4	ChCl	Ethylene glycol	1:3.000	81.451	0.018	1-Butanol
DES-B1	ChCl	1,3 Propanediol	1:3.037	91.974	0.092	Methanol
DES-B2	ChCl	1,3 Propanediol	1:3.002	91.962	0.091	Ethanol
DES-B3	ChCl	1,3 Propanediol	1:3.000	91.971	0.053	1-Propanol
DES-B4	ChCl	1,3 Propanediol	1:3.001	91.969	0.060	1-Butanol
DES-C1	ChCl	1,4 Butanediol	1:3.000	102.494	0.049	Methanol
DES-C2	ChCl	1,4 Butanediol	1:2.999	102.496	0.019	Ethanol
DES-C3	ChCl	1,4 Butanediol	1:3.000	102.495	0.021	1-Propanol
DES-C4	ChCl	1,4 Butanediol	1:3.000	102.495	0.092	1-Butanol

2.3. Fourier transform infrared spectroscopy

A Fourier transform infrared spectroscopy (FT-IR) analysis was performed to characterize choline chloride, the HBDs and the three types of DES. Measurements were made on a Shimadzu IRTracer-100 (Kyoto, Japan) between 400 and 4,000 cm^{-1}. The liquid samples were supported in transparent KBr films, while the solid samples were prepared in KBr pellets.

2.4. Density and viscosity measurements

Density (ρ) and dynamic viscosity (η) were measured for all the DES, the alcohols and their mixtures. These properties were obtained in an integrated system composed of an Anton Paar DMA4500M Densitometer (Graz, Austria) and an Anton Paar Lovis 2000ME microviscometer (Graz, Austria). The densitometer uses a vibrating U-tube technology to measure density with an accuracy of 0.00005 g·cm^{-3}. The temperature inside the tube has an accuracy of 0.01 K using Pt-100 thermometer. These values are reported by the manufacturer. The densitometer was calibrated with double-distilled deionized and degassed water and dry air at 293.15 K and 101.3 kPa. The dynamic viscosity measurements are based on the falling ball principle using calibrated glass capillaries of 1.59 mm, 1.80 mm and 2.50 mm of internal diameter and steel balls. The calibration of the capillaries was done with the viscosity standards provided by Anton Paar. Viscosity measurements, as reported by the manufacturer, have repeatabilities of 0.1% and measurement accuracies between 0.17% and 0.50%, depending on the type of capillary used.

3. Thermodynamic modeling

The COnductor-like Screening Model for Real Solvents (COSMO-RS) [16] is a quantum chemical method to predict thermophysical data of fluids from the chemical structure

of the compounds. The thermophysical fluid properties can be computed based on the screening charge density, σ, on the molecular surface of each compound, from which chemical potentials and equilibrium properties can be estimated via statistical thermodynamics [17]. Furthermore, COSMO-RS allows to identify molecular affinities, i.e., repulsive or attractive interactions, in terms of excess enthalpy (H^E) contributions: hydrogen bonding (HB), electrostatics or misfit interactions (MF), and van de Waals forces (vdW), according to Equation 1:

$$H^E = H^E_{HB} + H^E_{MF} + H^E_{vdW} \tag{1}$$

In this work, COSMO-RS was employed to compute the mixing properties of pure DES and the detailed excess enthalpies of DES + alcohol mixtures. COSMO-RS calculations were performed considering a multicomponent quaternary mixture as input, fixing the ratio of cation and anion of the HBA and the HBD to represent the stoichiometry of DES along the whole composition range. Afterwards, all compositions and excess enthalpies obtained from COSMO-RS calculations were converted from the COSMO-RS framework (i.e., quaternary mixture) to the laboratory framework (i.e., pseudo-binary mixture) as explained in previous works [18].

Computational calculations were performed using the COSMOtherm software, version C30, release 18.0.2, at the parametrization BP_TZVP_18.

4. Results

4.1. FT-IR analysis of DES and precursors

FT-IR analysis was performed for choline chloride, ethylene glycol, 1,3-propanediol, 1,4-butanediol and all the DES formed by the mixtures of choline chloride with a diol, i.e., DES-A, DES-B and DES-C. The spectra for all the components and the DES are shown in Figure 2. The spectra agree with the expected structures and show the typical signals for the precursors and the DES.

The IR spectrum of choline chloride shows the typical hydroxyl (OH) groups signal in the 3200-3700 cm^{-1} range. In the case of the alcohols, more defined spectra and wider signals of the hydroxyl groups are observed together with the carbon-hydrogen (CH) sp3 group in the 2700 to 2950 cm^{-1} range. From the respective IR spectra, molecular interactions can be inferred in the formation of the DES because of the displacements in the wavenumbers of the DES compared with their corresponding precursors as shown in Figure 2.[6] A shift from the original position of the -OH groups can be observed between 3500 - 2800 cm^{-1} due to the interaction of the -OH groups of the diols with the one of choline chloride, generating a stretch of the protons in the hydroxyl groups. Furthermore, it is observed that the interaction of hydroxyl groups becomes less important as the carbon chain of the diols is longer. For instance, it is observed a shift in the DES-A spectrum (2-carbons diol) while in DES-C (4-carbon diol) the change is almost undetectable. At the

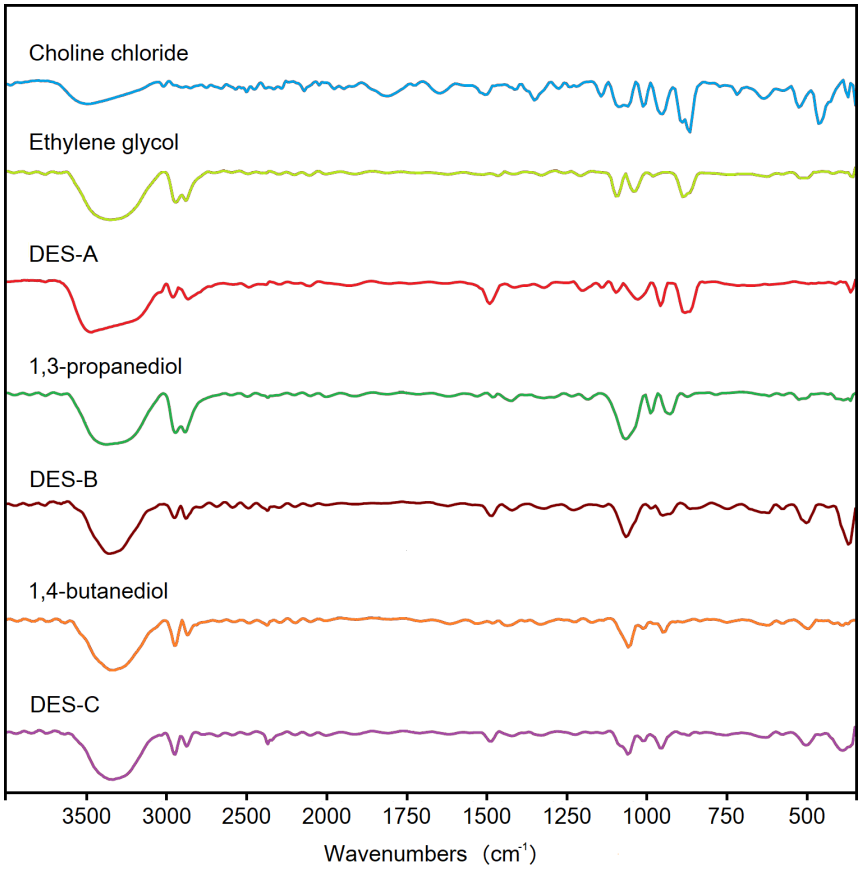

Figure 2: FT-IR analysis for DES and their precursors.

same time, a signal around 956 - 949 cm^{-1} presents a peak associated with the ammonium part of choline chloride in the DES, consistent with Aissaoui [19], Zullaikah et al.[20] and Gajardo et al.[6] Therefore, the FT-IR study proves that intermolecular interactions form the eutectic mixtures and there is no sign of a chemical reaction between the precursors.

4.2. Density and dynamic viscosity

Density and viscosity measurements were carried out for pure methanol, ethanol, 1-propanol, and 1-butanol at temperatures between 293.15 K and 333.15 K at a pressure of 101.3 kPa. These results were compared with literature data from different authors for density[21–36] and viscosity[37–51] with values collected at the same conditions of temperature and pressure as those reported in this work. The comparison is shown in Figure A.1(a) and in Figure A.1(b) for density and viscosity, respectively, as an average relative deviation (ARD(%)). It is observed that all the ARD(%) values for density are

below 0.15 % and for viscosity below 10 %. ARD(%) calculations are done according to Equation 2:

$$ARD(\%) = 100 \cdot \left(\frac{N_{\text{exp}} - N_{\text{lit}}}{N_{\text{exp}}} \right) \tag{2}$$

where N_{exp} and N_{lit} are the density or viscosity of the pure alcohol at a specific temperature of data from this work and from literature, respectively.

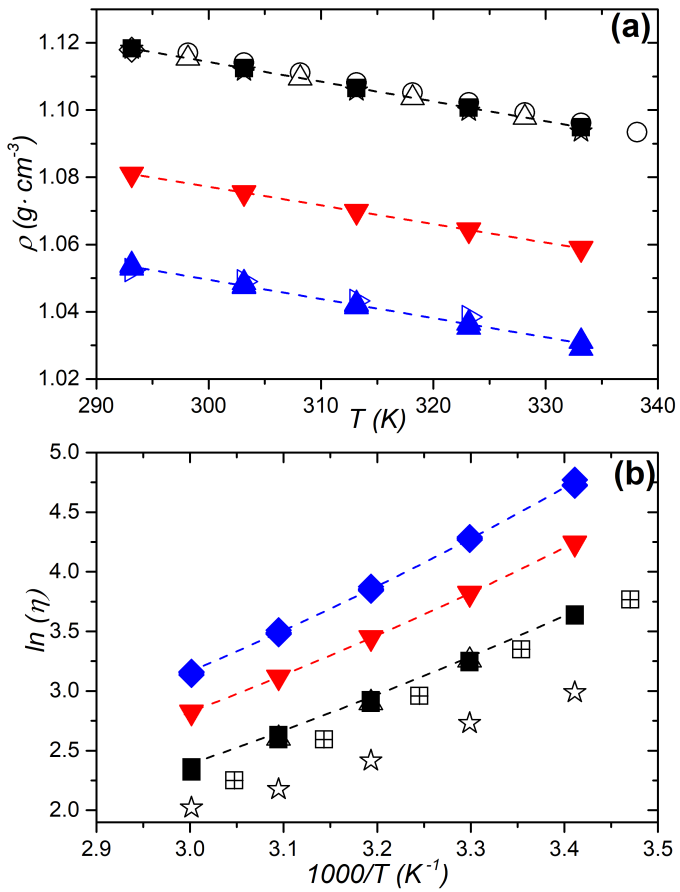

Figure 3: **(a)** Density (g·cm^{-3}) and **(b)** dynamic viscosity (mPa·s) of DES-A (■), DES-B (●), DES-C (▲) measured in this work as a function of temperature at a pressure of 101.3 kPa. Data from literature were obtained from Shahbaz et al.*[52](○), Abbott et al. [53](◇), Rogošić et al. [54](△), Shen et al.[55](⊞), Otzurk et al.[56](☆) and Chen et al.[48](▷). Dashed line (- - -) represents the fit using parameters from Table 3 with the linear equation for density in Figure **(a)** and VFT equation for viscosity in Figure **(b)**.* In Shahbaz *et al.* the molar ratio of DES-A is 1:2.5.

Density and viscosity results for the DES studied in this work are reported in Figure

3(a) and Figure 3(b), respectively, for all the pseudo-pure DES batches listed on Table 2. Each DES have a very small difference of density and viscosity when comparing all their batches. Then, all the measured values shown in Figure 3(a) and Figure 3(b) have values falling in almost the same point. These results are also compared with literature, observing a good agreement for the density of DES with the same molar ratio[48, 52–54, 56]. Viscosity data was found in literature only for DES based on ethylene glycol at a similar mole ratio. Our data is in agreement with the work of Rogošić et al. [54], there is some deviation with data reported by Shen et al.[55], and lower values of viscosity compared with the other works are reported by Otzurk et al.[56] . These differences in the measured viscosities are also observed elsewhere for several DES[6] and the discrepancies are typically attributed to variable amounts of water contents in the initial samples. Water markedly decreases the viscosity of the DES at lower temperatures because its viscosity is much lower than pseudo-pure DES at temperatures close to ambient conditions.

The density of the DES decrease with temperature and there is a clear dependence on the chain length of the HBD. The densities, in terms of the HBD, are ethylene glycol > 1,3-propanediol > 1,4-butanediol. This is consistent with the results reported by Garcia *et al.*[57] about the density decay due to a longer alkyl chain for organics acids.[6] Also, the trend shows the same behaviour of pure HBDs, for example, at 298.15 K and 101.3 kPa, ethylene glycol has a density of 1.2201 g·cm^{-3}[58], 1,3-propanediol of 1.0501 g·cm^{-3},[59] and 1,4-butanediol of 1.0126 g·cm^{-3}.[60] Thus, the addition of choline chloride generates an increase in density of the eutectic mixture because the addition of electrostatic forces and hydrogen bonding. This produces a decrease in the free volume available in the mixture. The amount of water does not seem to be a variable that greatly affects density, probably due to the similarity of the density of the DES compared with water. Density from this work was fit with linear Equation 3. In this equation, a and b represents the intercept and the slope, respectively. The obtained parameters are presented in Table 3 obtaining and average absolute deviation (AAD(%)) beetwen 0.002% and 0.016%. AAD(%) is showed in Equation 4, where θ is the the property (density or viscosity) and n the number of data considered in the calculation.

$$\rho(T) = a + b \cdot T \tag{3}$$

$$AAD(\%) = \frac{100}{n} \cdot \sum_{i=1}^{n} \left| \frac{\theta_{\text{exp}} - \theta_{\text{cal}}}{\theta_{\text{cal}}} \right| \tag{4}$$

Table 3: Linear fitting coefficients from Equation 3 (a intercept and b slope) for correlating the densities and viscosity fitting coefficients from VFT Equation 5 of deep eutectic solvents used in this work as specified in Table 2, and the respective coefficient of determination (R^2) and the average absolute deviation (AAD(%)) of the correlation

Linear fitting				
System	a	$10^{-4} \cdot b$	R^2	AAD(%)
DES-A	1.290	-5.9	1.000	0.002
DES-B	1.243	-5.5	1.000	0.002
DES-C	1.221	-5.7	1.000	0.007
Vogel-Fulcher-Tamman				
System	A	B	T_0	AAD(%)
DES-A	0.141	795.084	152.501	1.363
DES-B	0.148	821.819	159.692	0.305
DES-C	0.151	846.415	165.801	0.820

Viscosities decrease greatly with the temperature. In terms of the HBD, the observed viscosity trend is 1,4-butanediol > 1,3-propanediol > ethylene glycol. This is the same behaviour as the pure HBDs, where at 298.15 K the viscosity of pure ethylene glycol is 13.108 mPa·s [58], 41.507 mPa·s for 1,3-propanediol[61] and 72.326 mPa·s for 1,4-butanediol[62]. When choline chloride is added to the DES, the viscosity increases due to stronger molecular interactions, i.e. more hydrogen bonds and electrostatic interactions added to the mixture affecting the molecular movement. Also, the longer alkyl chain in 1,4-butanediol influence the molecular mobility by increasing the viscosity. Viscosity data were correlated as a function of the temperature (T) with the Vogel-Fulcher-Tamman correlation[63] (VFT) with fitting parameters A, B and T_0 shown in Equation 5:

$$\eta_{VFT}(T) = A \cdot \exp\left(\frac{B}{T - T_0}\right) \tag{5}$$

AAD(%) using the VFT equation are between 0.305 % and 1.363 %, as shown in Table 3 where also all the VFT fitting parameters are reported.

Table 4: Densities (g·cm^{-3}) and molar excess volumes (cm^3·mol^{-1}) of alcohol(1) + DES-A(2) (choline chloride + ethylene glycol) liquid mixture at different temperatures (K), molar compositions of alcohols (x_1) and a pressure of 101.3 kPa. Deep eutectic solvents pseudo-binary systems used for these measurements are detailed in Table 2.

methanol + DES-A1										
	Density (g·cm^{-3})					Molar Excess Volume (cm^3·mol^{-1})				
x_1	293.15K	303.15 K	313.15 K	323.15 K	333.15 K	293.15K	303.15 K	313.15 K	323.15 K	333.15 K
0.0000	1.1183	1.1124	1.1065	1.1007	1.0949	0.000	0.000	0.000	0.000	0.000
0.1398	1.0967	1.0906	1.0846	1.0785	1.0725	-0.340	-0.363	-0.387	-0.412	-0.438
0.2802	1.0707	1.0644	1.0578	1.0514	1.0448	-0.628	-0.666	-0.695	-0.734	-0.801
0.4187	1.0396	1.0331	1.0265	1.0199	1.0133	-0.841	-0.900	-0.962	-1.029	-1.098
0.5597	1.0004	0.9935	0.9866	0.9797	0.9727	-0.957	-1.027	-1.100	-1.180	-1.267
0.7007	0.9515	0.9441	0.9367	0.9291	0.9217	-0.953	-1.025	-1.102	-1.183	-1.276
0.8402	0.8892	0.8810	0.8729	0.8646	0.8563	-0.744	-0.798	-0.861	-0.930	-1.005
1.0000	0.7913	0.7819	0.7724	0.7627	0.7529	0.000	0.000	0.000	0.000	0.000
ethanol + DES-A2										
	Density (g·cm^{-3})					Molar Excess Volume (cm^3·mol^{-1})				
x_1	293.15K	303.15 K	313.15 K	323.15 K	333.15 K	293.15K	303.15 K	313.15 K	323.15 K	333.15 K
0.0000	1.1184	1.1125	1.1066	1.1007	1.0949	0.000	0.000	0.000	0.000	0.000
0.1397	1.0862	1.0802	1.0741	1.0680	1.0619	-0.371	-0.402	-0.430	-0.459	-0.488
0.2800	1.0500	1.0437	1.0374	1.0311	1.0247	-0.635	-0.690	-0.740	-0.794	-0.854
0.4197	1.0097	1.0032	0.9965	0.9899	0.9832	-0.785	-0.859	-0.924	-0.995	-1.075
0.5601	0.9648	0.9579	0.9509	0.9438	0.9368	-0.823	-0.909	-0.981	-1.061	-1.151
0.6999	0.9153	0.9080	0.9006	0.8931	0.8855	-0.750	-0.838	-0.908	-0.984	-1.072
0.8401	0.8605	0.8527	0.8448	0.8367	0.8285	-0.552	-0.622	-0.674	-0.729	-0.799
1.0000	0.7899	0.7808	0.7721	0.7632	0.7541	0.000	0.000	0.000	0.000	0.000
1-propanol + DES-A3										
	Density (g·cm^{-3})					Molar Excess Volume (cm^3·mol^{-1})				
x_1	293.15K	303.15 K	313.15 K	323.15 K	333.15 K	293.15K	303.15 K	313.15 K	323.15 K	333.15 K
0.0000	1.1184	1.1125	1.1066	1.1007	1.0949	0.000	0.000	0.000	0.000	0.000
0.1285	1.0808	1.0750	1.0692	1.0634	1.0576	-0.262	-0.306	-0.350	-0.393	-0.435
0.2798	1.0353	1.0289	1.0225	1.0160	1.0098	-0.474	-0.519	-0.562	-0.601	-0.662
0.4195	0.9918	0.9852	0.9785	0.9718	0.9651	-0.559	-0.619	-0.678	-0.738	-0.796
0.5597	0.9474	0.9405	0.9336	0.9265	0.9194	-0.575	-0.642	-0.705	-0.768	-0.827
0.7362	0.8907	0.8835	0.8762	0.8686	0.8610	-0.481	-0.549	-0.621	-0.664	-0.710
0.8404	0.8566	0.8491	0.8414	0.8335	0.8256	-0.346	-0.402	-0.447	-0.485	-0.510
1.0000	0.8035	0.7952	0.7870	0.7787	0.7704	0.000	0.000	0.000	0.000	0.000
1-butanol + DES-A4										
	Density (g·cm^{-3})					Molar Excess Volume (cm^3·mol^{-1})				
x_1	293.15K	303.15 K	313.15 K	323.15 K	333.15 K	293.15K	303.15 K	313.15 K	323.15 K	333.15 K
0.0000	1.1184	1.1125	1.1066	1.1007	1.0949	0.000	0.000	0.000	0.000	0.000
0.1405	1.0697	1.0637	1.0576	1.0515	1.0455	-0.284	-0.310	-0.337	-0.368	-0.399
0.2796	1.0220	1.0156	1.0093	1.0029	0.9965	-0.374	-0.406	-0.451	-0.496	-0.549
0.4204	0.9758	0.9692	0.9625	0.9559	0.9492	-0.394	-0.435	-0.483	-0.537	-0.601
0.5595	0.9327	0.9258	0.9189	0.9119	0.9049	-0.381	-0.423	-0.471	-0.526	-0.593
0.6998	0.8913	0.8842	0.8770	0.8698	0.8624	-0.317	-0.353	-0.393	-0.443	-0.503
0.8385	0.8525	0.8452	0.8377	0.8302	0.8225	-0.206	-0.230	-0.258	-0.292	-0.335
1.0000	0.8095	0.8019	0.7941	0.7862	0.7780	0.000	0.000	0.000	0.000	0.000

Standard uncertainties u are $u(T)$=0.01 K, $u(P)$= 1 kPa and $u(\rho)$=0.0005 g·cm^{-3}.

Combined expanded uncertainties $U_c(x_1)$=0.002 and $U_c(V^E)$=0.08 cm^{-3}·mol^{-1} with a 0.95 level of confidence.

Table 5: Densities (g·cm^{-3}) and molar excess volumes (cm^3·mol^{-1}) of alcohol(1) + DES-B(2) (choline chloride + 1,3 propanediol) liquid mixture at different temperatures (K), molar compositions of alcohols (x_1) and a pressure of 101.3 kPa. Deep eutectic solvents pseudo-binary system used for these measurements are detailed in Table 2.

methanol + DES-B1										
	Density (g·cm^{-3})					Molar Excess Volume (cm^3·mol^{-1})				
x_1	293.15K	303.15 K	313.15 K	323.15 K	333.15 K	293.15K	303.15 K	313.15 K	323.15 K	333.15 K
0.0000	1.0810	1.0754	1.0699	1.0644	1.0589	0.000	0.000	0.000	0.000	0.000
0.1394	1.0643	1.0586	1.0529	1.0472	1.0415	-0.301	-0.323	-0.347	-0.372	-0.399
0.2796	1.0439	1.0379	1.0320	1.0260	1.0197	-0.558	-0.600	-0.644	-0.688	-0.712
0.4209	1.0184	1.0122	1.0060	0.9994	0.9928	-0.773	-0.832	-0.895	-0.933	-0.977
0.5587	0.9867	0.9802	0.9736	0.9668	0.9600	-0.893	-0.963	-1.039	-1.106	-1.182
0.7013	0.9438	0.9367	0.9296	0.9225	0.9154	-0.893	-0.966	-1.046	-1.133	-1.228
0.8388	0.8878	0.8800	0.8721	0.8642	0.8562	-0.707	-0.769	-0.835	-0.909	-0.990
1.0000	0.7913	0.7819	0.7724	0.7627	0.7529	0.000	0.000	0.000	0.000	0.000

ethanol + DES-B2										
	Density (g·cm^{-3})					Molar Excess Volume (cm^3·mol^{-1})				
x_1	293.15K	303.15 K	313.15 K	323.15 K	333.15 K	293.15K	303.15 K	313.15 K	323.15 K	333.15 K
0.0000	1.0809	1.0754	1.0698	1.0643	1.0588	0.000	0.000	0.000	0.000	0.000
0.1401	1.0563	1.0506	1.0448	1.0391	1.0334	-0.355	-0.386	-0.414	-0.446	-0.480
0.2805	1.0282	1.0222	1.0162	1.0103	1.0043	-0.651	-0.708	-0.760	-0.817	-0.878
0.4201	0.9951	0.9889	0.9826	0.9763	0.9700	-0.802	-0.879	-0.947	-1.023	-1.106
0.5687	0.9545	0.9478	0.9412	0.9345	0.9277	-0.860	-0.950	-1.027	-1.114	-1.210
0.6996	0.9127	0.9057	0.8985	0.8914	0.8841	-0.783	-0.875	-0.951	-1.035	-1.131
0.8399	0.8610	0.8534	0.8456	0.8378	0.8298	-0.567	-0.649	-0.707	-0.774	-0.849
1.0000	0.7899	0.7808	0.7721	0.7632	0.7541	0.000	0.000	0.000	0.000	0.000

1-propanol + DES-B3										
	Density (g·cm^{-3})					Molar Excess Volume (cm^3·mol^{-1})				
x_1	293.15K	303.15 K	313.15 K	323.15 K	333.15 K	293.15K	303.15 K	313.15 K	323.15 K	333.15 K
0.0000	1.0810	1.0754	1.0699	1.0643	1.0588	0.000	0.000	0.000	0.000	0.000
0.1400	1.0504	1.0446	1.0388	1.0329	1.0270	-0.329	-0.355	-0.379	-0.401	-0.415
0.2802	1.0167	1.0107	1.0048	0.9986	0.9923	-0.524	-0.574	-0.629	-0.667	-0.694
0.4196	0.9808	0.9746	0.9683	0.9617	0.9553	-0.629	-0.703	-0.769	-0.815	-0.876
0.5606	0.9422	0.9356	0.9289	0.9222	0.9154	-0.664	-0.737	-0.809	-0.879	-0.947
0.7004	0.9018	0.8948	0.8877	0.8806	0.8733	-0.641	-0.715	-0.785	-0.854	-0.911
0.8436	0.8574	0.8499	0.8424	0.8348	0.8270	-0.492	-0.556	-0.611	-0.660	-0.695
1.0000	0.8035	0.7952	0.7870	0.7787	0.7704	0.000	0.000	0.000	0.000	0.000

1-butanol + DES-B4										
	Density (g·cm^{-3})					Molar Excess Volume (cm^3·mol^{-1})				
x_1	293.15K	303.15 K	313.15 K	323.15 K	333.15 K	293.15K	303.15 K	313.15 K	323.15 K	333.15 K
0.0000	1.0810	1.0755	1.0699	1.0644	1.0589	0.000	0.000	0.000	0.000	0.000
0.1399	1.0441	1.0384	1.0327	1.0269	1.0212	-0.295	-0.318	-0.347	-0.380	-0.417
0.2851	1.0048	0.9988	0.9927	0.9867	0.9806	-0.461	-0.500	-0.544	-0.594	-0.651
0.4199	0.9678	0.9615	0.9552	0.9489	0.9425	-0.519	-0.566	-0.619	-0.681	-0.752
0.5599	0.9293	0.9227	0.9160	0.9093	0.9026	-0.496	-0.544	-0.599	-0.662	-0.738
0.7105	0.8884	0.8815	0.8745	0.8674	0.8602	-0.437	-0.480	-0.529	-0.587	-0.657
0.8397	0.8531	0.8459	0.8386	0.8312	0.8236	-0.291	-0.321	-0.356	-0.398	-0.449
1.0000	0.8095	0.8019	0.7941	0.7862	0.7780	0.000	0.000	0.000	0.000	0.000

Standard uncertainties u are $u(T)$=0.01 K, $u(P)$= 1 kPa and $u(\rho)$=0.0005 g·cm^{-3}.

Combined expanded uncertainties $U_c(x_1)$=0.002 and $U_c(V^E)$=0.08 cm^{-3}·mol^{-1} with a 0.95 level of confidence.

Table 6: Densities (g·cm^{-3}) and molar excess volumes (cm^3·mol^{-1}) of alcohol(1) + DES-C(2) (choline chloride + 1,4 butanediol) liquid mixture at different temperatures (K), molar compositions of alcohols (x_1) and a pressure of 101.3 kPa. Deep eutectic solvents pseudo-binary system used for these measurements are detailed in Table 2.

methanol + DES-C1										
	Density (g·cm^{-3})					Molar Excess Volume (cm^3·mol^{-1})				
x_1	293.15K	303.15 K	313.15 K	323.15 K	333.15 K	293.15K	303.15 K	313.15 K	323.15 K	333.15 K
0.0000	1.0536	1.0478	1.0415	1.0353	1.0291	0.000	0.000	0.000	0.000	0.000
0.1403	1.0395	1.0339	1.0283	1.0228	1.0172	-0.223	-0.276	-0.369	-0.454	-0.547
0.2801	1.0229	1.0171	1.0112	1.0052	0.9996	-0.463	-0.527	-0.620	-0.705	-0.821
0.4197	1.0022	0.9962	0.9901	0.9835	0.9773	-0.681	-0.758	-0.864	-0.932	-1.039
0.5597	0.9749	0.9685	0.9621	0.9556	0.9491	-0.809	-0.892	-0.999	-1.111	-1.227
0.7001	0.9382	0.9313	0.9244	0.9174	0.9104	-0.850	-0.933	-1.035	-1.143	-1.261
0.8399	0.8860	0.8783	0.8706	0.8628	0.8549	-0.687	-0.755	-0.835	-0.920	-1.015
1.0000	0.7913	0.7819	0.7724	0.7627	0.7529	0.000	0.000	0.000	0.000	0.000

ethanol + DES-C2										
	Density (g·cm^{-3})					Molar Excess Volume (cm^3·mol^{-1})				
x_1	293.15K	303.15 K	313.15 K	323.15 K	333.15 K	293.15K	303.15 K	313.15 K	323.15 K	333.15 K
0.0000	1.0540	1.0486	1.0424	1.0367	1.0312	0.000	0.000	0.000	0.000	0.000
0.1400	1.0331	1.0278	1.0219	1.0162	1.0106	-0.236	-0.286	-0.340	-0.395	-0.430
0.2791	1.0100	1.0043	0.9982	0.9923	0.9864	-0.494	-0.557	-0.635	-0.704	-0.762
0.4201	0.9822	0.9762	0.9699	0.9637	0.9575	-0.678	-0.761	-0.846	-0.934	-1.014
0.5598	0.9495	0.9431	0.9366	0.9301	0.9235	-0.780	-0.866	-0.975	-1.077	-1.170
0.7000	0.9096	0.9027	0.8959	0.8889	0.8818	-0.745	-0.837	-0.948	-1.049	-1.146
0.8400	0.8610	0.8535	0.8459	0.8382	0.8304	-0.557	-0.641	-0.715	-0.791	-0.873
1.0000	0.7899	0.7808	0.7721	0.7632	0.7541	0.000	0.000	0.000	0.000	0.000

1-propanol + DES-C3										
	Density (g·cm^{-3})					Molar Excess Volume (cm^3·mol^{-1})				
x_1	293.15K	303.15 K	313.15 K	323.15 K	333.15 K	293.15K	303.15 K	313.15 K	323.15 K	333.15 K
0.0000	1.0530	1.0475	1.0420	1.0366	1.0311	0.000	0.000	0.000	0.000	0.000
0.1404	1.0288	1.0232	1.0177	1.0121	1.0065	-0.332	-0.368	-0.410	-0.447	-0.482
0.2796	1.0014	0.9955	0.9897	0.9838	0.9780	-0.521	-0.573	-0.629	-0.683	-0.739
0.4198	0.9708	0.9647	0.9585	0.9524	0.9462	-0.629	-0.697	-0.767	-0.836	-0.906
0.5617	0.9365	0.9301	0.9236	0.9171	0.9105	-0.663	-0.742	-0.819	-0.897	-0.971
0.6997	0.8996	0.8927	0.8859	0.8790	0.8720	-0.604	-0.682	-0.767	-0.840	-0.912
0.8400	0.8577	0.8504	0.8430	0.8355	0.8278	-0.423	-0.490	-0.549	-0.601	-0.641
1.0000	0.8035	0.7952	0.7870	0.7787	0.7704	0.000	0.000	0.000	0.000	0.000

1-butanol + DES-C4										
	Density (g·cm^{-3})					Molar Excess Volume (cm^3·mol^{-1})				
x_1	293.15K	303.15 K	313.15 K	323.15 K	333.15 K	293.15K	303.15 K	313.15 K	323.15 K	333.15 K
0.0000	1.0530	1.0475	1.0420	1.0365	1.0311	0.000	0.000	0.000	0.000	0.000
0.1515	0.8511	0.8440	0.8368	0.8294	0.8219	-0.313	-0.351	-0.398	-0.450	-0.511
0.2983	0.8896	0.8829	0.8761	0.8692	0.8622	-0.476	-0.534	-0.604	-0.683	-0.770
0.4504	0.9281	0.9217	0.9152	0.9087	0.9019	-0.553	-0.620	-0.700	-0.785	-0.863
0.5993	0.9640	0.9579	0.9517	0.9455	0.9391	-0.530	-0.595	-0.672	-0.751	-0.818
0.6754	0.9817	0.9759	0.9701	0.9640	0.9577	-0.474	-0.552	-0.652	-0.725	-0.772
0.8991	1.0312	1.0256	1.0197	1.0139	1.0084	-0.188	-0.230	-0.252	-0.292	-0.343
1.0000	0.8095	0.8019	0.7941	0.7862	0.7780	0.000	0.000	0.000	0.000	0.000

Standard uncertainties u are $u(T)$=0.01 K, $u(P)$= 1 kPa and $u(\rho)$=0.0005 g·cm^{-3}.

Combined expanded uncertainties $U_c(x_1)$=0.002 and $U_c(V^E)$=0.08 cm^{-3}·mol^{-1} with a 0.95 level of confidence.

4.3. Mixture Densities and Molar Excess Volumes

Density measurements of binary mixtures composed by alcohol + DES were obtained at temperatures between 293.15 K – 333.15 K and 101.3 kPa in the full range of compositions. The four alcohols used in the study are completely miscible with the three DES at all the measurement conditions. Density data for mixtures of the alcohols with DES-A, DES-B and DES-C are shown in Tables 4, 5 and 6, respectively. Considering that the four alcohols have a lower density compared with the three DES, the density of the mixtures decrease by adding alcohol to the mixture. Also, the density decreases by increasing the temperature at a constant alcohol composition in the DES, as expected.

In order to assess the non-ideality, structural adjustment and molecular interactions of the pseudo-binary mixtures alcohol + DES, data from Tables 4, 5 and 6 are also shown in the form of molar excess volume (V^E) which is determined using equation 6:

$$V^{\mathrm{E}} = \frac{x_1 \cdot M_1 + x_2 \cdot M_2}{\rho} - \left(\frac{x_1 \cdot M_1}{\rho_1}\right) - \left(\frac{x_2 \cdot M_2}{\rho_2}\right) \tag{6}$$

where x_i, ρ_i and M_i are the composition, density and molar mass of the compound i, respectively and ρ is the density of the mixture.

V^E for all the binary systems was fit to the Redlich - Kister (RK) correlation shown in equation 7, where V^E_{RK} is the V^E calculated with RK, x_1 is the molar fraction of the alcohols, x_2 molar fraction of the DES and α_i are the adjustable parameters of the polynomial of k + 1 terms. All the RK fitting parameters are reported in Table 7.

$$V^{\mathrm{E}}_{RK} = x_1 \cdot x_2 \cdot \sum_{i=0}^{k} \alpha_i \cdot \left(x_1 - x_2\right)^i \tag{7}$$

Table 7: Redlich-Kister polynomial fitting coefficients (a_0, a_1, a_2 and a_3) from equation 7 for the excess volume of alcohol + deep eutectic solvent with their respective absolute average deviation (AAD(%)) at different temperatures (K) and a pressure of 101.3 kPa. Deep eutectic solvents used are detailed in Table 2.

methanol + DES-A1						ethanol + DES-A2					
T/(K)	a_0	a_1	a_2	a_3	AAD(%)	T/(K)	a_0	a_1	a_2	a_3	AAD(%)
293.15	-3.6779	-1.5731	-1.1481	-0.8335	0.1422	293.15	-3.2759	-0.4242	-0.7137	-0.6853	0.2318
303.15	-4.0063	-1.9707	-0.9852	-0.3191	0.8880	303.15	-3.5966	-0.6488	-0.8586	-0.6163	0.2355
313.15	-4.2156	-1.9075	-1.3444	-0.8626	0.5517	313.15	-3.8837	-0.6827	-0.9188	-0.7760	0.2031
323.15	-4.4971	-2.2628	-1.5110	-0.6031	0.7330	323.15	-4.1895	-0.8536	-0.9559	-0.6697	0.1897
333.15	-4.7675	-2.0471	-1.8001	-1.5691	1.0344	333.15	-4.5286	-0.8701	-1.0694	-1.0559	0.1938
1-propanol + DES-A3						1-butanol + DES-A4					
T/(K)	a_0	a_1	a_2	a_3	AAD(%)	T/(K)	a_0	a_1	a_2	a_3	AAD(%)
293.15	-2.3204	-0.0649	-0.2997	-0.2345	0.4442	293.15	-1.5622	0.2252	-0.7072	0.6962	0.3428
303.15	-2.5700	-0.2631	-0.5823	0.0797	0.0818	303.15	-1.7315	0.1930	-0.7577	0.8148	0.5180
313.15	-2.8062	-0.5149	-0.8059	0.6159	0.4174	313.15	-1.9060	0.3330	-0.8524	0.5452	0.4290
323.15	-3.0258	-0.6594	-1.0061	1.0267	0.6542	323.15	-2.1455	0.2137	-0.8663	0.7917	0.3771
333.15	-3.2790	-0.5439	-1.0329	1.0575	0.4142	333.15	-2.4144	0.1590	-0.9115	0.8149	0.3317
methanol + DES-B1						ethanol + DES-B2					
T/(K)	a_0	a_1	a_2	a_3	AAD(%)	T/(K)	a_0	a_1	a_2	a_3	AAD(%)
293.15	-3.4095	-1.6648	-1.0532	-0.6737	0.3790	293.15	-3.4250	-0.4368	-0.3992	-0.9946	0.3533
303.15	-3.6571	-1.7218	-1.2287	-0.9644	0.4725	303.15	-3.7542	-0.6070	-0.6223	-1.1719	0.3515
313.15	-3.9531	-1.9755	-1.3327	-0.8864	0.4258	313.15	-4.0686	-0.7584	-0.6745	-1.1610	0.3631
323.15	-4.1612	-2.2919	-1.6889	-0.7542	0.1305	323.15	-4.3951	-0.9240	-0.7868	-1.1647	0.3473
333.15	-4.4229	-2.8560	-1.9782	-0.1782	0.1711	333.15	-4.7510	-1.0659	-0.9266	-1.2923	0.3051
1-propanol + DES-B3						1-butanol + DES-B4					
T/(K)	a_0	a_1	a_2	a_3	AAD(%)	T/(K)	a_0	a_1	a_2	a_3	AAD(%)
293.15	-2.6138	-0.4992	-1.2931	-0.5064	0.1145	293.15	-2.0501	0.3394	-0.5239	-0.3186	0.1745
303.15	-2.9028	-0.5666	-1.4209	-0.7627	0.2912	303.15	-2.2504	0.3860	-0.5325	-0.4684	0.3660
313.15	-3.1827	-0.6527	-1.4949	-0.9041	0.2597	313.15	-2.4622	0.4139	-0.6348	-0.5451	0.4601
323.15	-3.4403	-0.8587	-1.5286	-0.7673	0.1230	323.15	-2.7697	0.0591	-0.5803	0.1225	0.8960
333.15	-3.6923	-1.0851	-1.4017	-0.5073	0.3333	333.15	-3.0433	0.1450	-0.7313	-0.1733	0.6649
methanol + DES-C1						ethanol + DES-C2					
T/(K)	a_0	a_1	a_2	a_3	AAD(%)	T/(K)	a_0	a_1	a_2	a_3	AAD(%)
293.15	-3.0375	-1.9880	-1.0305	-0.7792	0.3720	293.15	-3.0263	-1.1148	-0.1509	-0.9182	0.3205
303.15	-3.3415	-2.1446	-1.3632	-0.5820	0.5032	303.15	-3.3372	-1.4035	-0.5742	-0.6790	0.6539
313.15	-3.7473	-2.3575	-1.8966	0.0617	0.8524	313.15	-3.7917	-1.6727	-0.6597	-0.2773	0.6138
323.15	-4.1685	-2.5832	-2.2489	0.7702	0.7212	323.15	-4.1615	-1.6079	-0.9582	-0.5950	0.4615
333.15	-4.6140	-2.7078	-2.9769	0.8911	0.3351	333.15	-4.4843	-2.0587	-1.2084	-0.1587	0.5740
1-propanol + DES-C3						1-butanol + DES-C4					
T/(K)	a_0	a_1	a_2	a_3	AAD(%)	T/(K)	a_0	a_1	a_2	a_3	AAD(%)
293.15	-2.6260	-0.3949	-0.6620	0.1670	0.9161	293.15	-2.2197	0.0772	-0.1149	0.3082	0.3264
303.15	-2.9294	-0.5644	-0.8639	0.2024	0.9857	303.15	-2.4881	-0.0103	-0.3029	-0.2967	0.2093
313.15	-3.2195	-0.7301	-1.0767	0.3841	1.2150	313.15	-2.2826	-0.0474	-0.2658	0.5007	0.7922
323.15	-3.5127	-0.8744	-1.2287	0.5009	1.4576	323.15	-3.1628	0.0215	-0.4100	0.3698	0.7085
333.15	-3.8000	-1.0323	-1.1762	0.8893	1.2070	333.15	-3.4487	0.3820	-0.7496	-0.3142	0.5417

V^E of the binary mixtures have negative values for all the binary systems alcohol + DES at all the temperatures and compositions, as observed in Figure 4 for the DES-A in mixtures with (a) methanol, (b) ethanol, (c) 1-propanol and (d) 1-butanol. That is, the

volume of the mixture is lower than in the ideal mixture of DES-A and the four alcohols used in this work. The Figures A.2 and A.3 show the same behavior for all the alcohols in DES-B and DES-C. It is also observed that the V^E becomes increasingly negative at higher temperatures for all the mixtures. This is typically explained as stronger interactions of alcohol - DES molecules compared with alcohol - alcohol or DES - DES interactions. Then, by increasing the temperature, the interaction between the same molecules decrease and the interaction of unlike molecules become more important, allowing a better interstitial accommodation. In addition, the specific interactions are weaker at higher temperatures producing an increase in the size of interstitial molecular space. That suggest that packing effects dominate the volumetric behavior of the binary mixtures alcohol + DES. This behavior is different for aqueous mixtures of DES where at higher temperatures V^E is less negative as discussed elsewhere.[6]

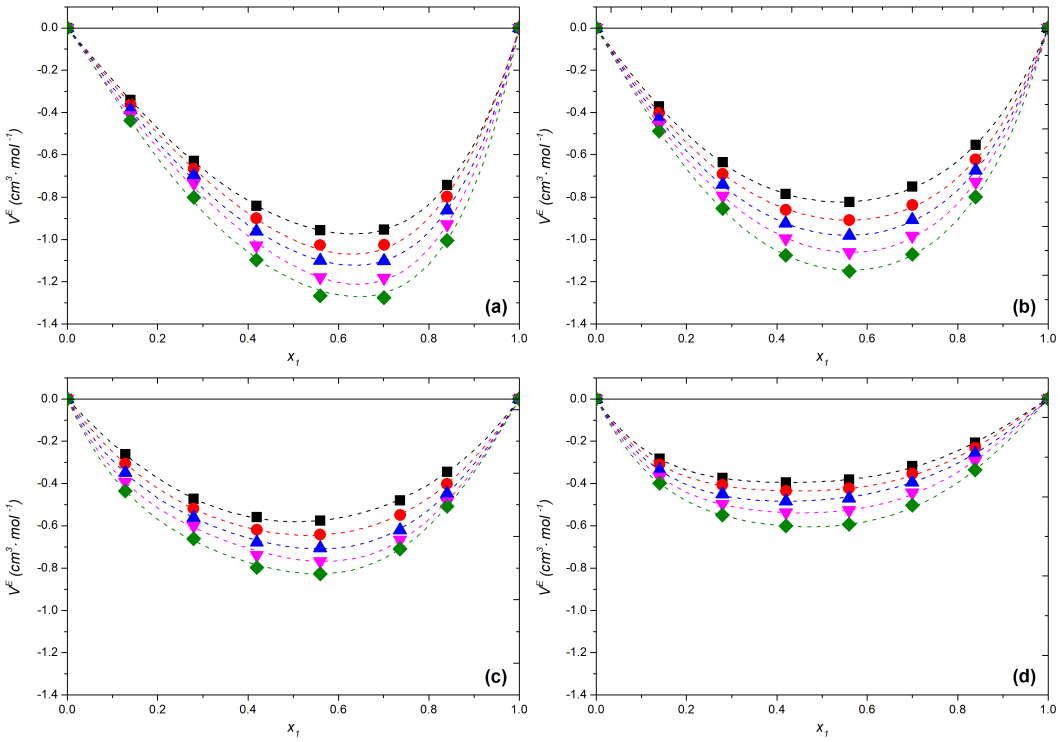

Figure 4: Temperature effect on the molar excess volume of alcohol + DES-A mixtures. The molar excess volumes (cm^3·mol^{-1}) are in terms of the mole fraction of alcohol for the binary mixtures **(a)** methanol + DES-A, **(b)** ethanol + DES-A, **(c)** 1-propanol + DES-A, **(d)** 1-butanol + DES-A at a pressure of 101.3 kPa and temperatures between 298.15 K and 333.15 K. Temperatures of 293.15 K (■), 303.15 K (●), 313.15 K (▲), 323.15 K (▼) and 333.15 K (◆). The dashed line represents the Redlich-Kister polynomial fitting with parameters reported in Table 7.

Additionally, an alcohol chain effect is observed on the behavior of the V^E. Figure 5 shows the V^E for (a) DES-A, (b) DES-B and (c) DES-C mixed with the different alcohols at 293.15 K as a function of mole fraction of alcohol. Figures A.4 to A.7 show the behavior of the remaining temperatures. A lower V^E (most negative value) is observed, in general, by mixing any DES with methanol, followed by ethanol, 1-propanol and 1-butanol. It is also noted that the minimum V^E value shifts to a lower molar fraction of alcohol as the alcohol chain increases. For instance, taking the DES-A which is shown in Figure 5(a) and using the correlation of Redlich-Kister, the minimum values of x_1 are 0.63 for the mixture with methanol, 0.54 for ethanol, 0.50 for 1-propanol, and 0.43 for 1-butanol, obtaining values of V^{E}_{RK} of -0.974 $\mathrm{cm^3 \cdot mol^{-1}}$, -0.823 $\mathrm{cm^3 \cdot mol^{-1}}$, -0.580 $\mathrm{cm^3 \cdot mol^{-1}}$ and -0.394 $\mathrm{cm^3 \cdot mol^{-1}}$, respectively. These results suggest that a longer carbon chain of the alcohol obstruct the intermolecular interactions between DES and alcohols, since the larger molecule restricts interstitial accommodation within the DES.

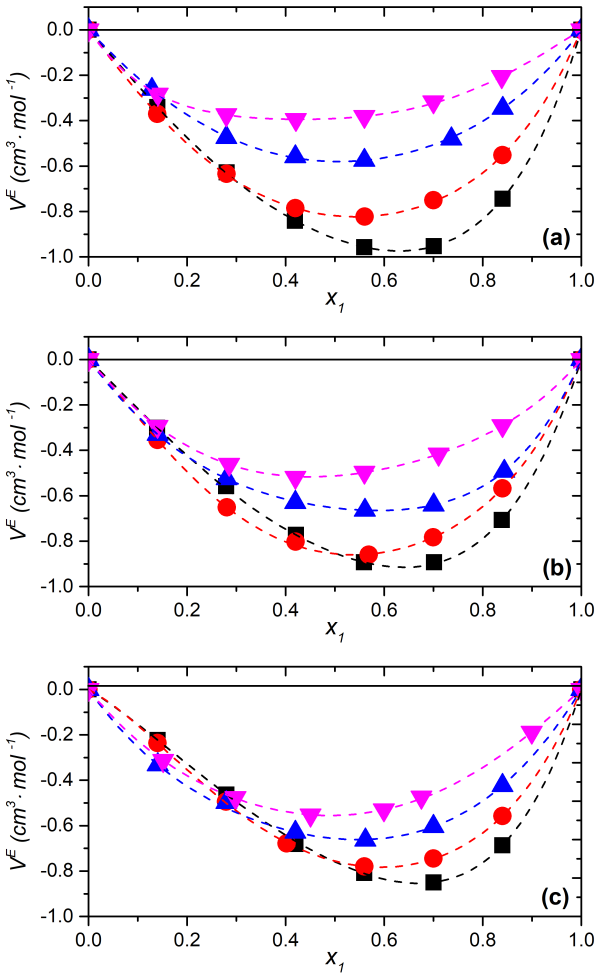

Figure 5: Alcohol chain effect on the molar excess volume of alcohol + DES. The molar excess volumes ($cm^3 \cdot mol^{-1}$) are in terms of the mole fraction of alcohol for the binary mixtures of **(a)** DES-A, **(b)** DES-B , **(c)** DES-C, at a pressure of 101.3 kPa, temperature of 293.15 K and DES binary system with methanol (■), ethanol (●), 1-propanol (▲), 1-butanol (▼). The dashed line represents the Redlich-Kister polynomial fitting with parameters reported in Table 7.

Figure 6 compares the behavior of the V^E of different DES using the same alcohol at 293.15 K. Figures A.8 to A.11 show the behavior of the remaining temperatures. In this case, the effect of the HBD does not have a clear tendency and, in general, V^E is very similar for all the cases. From this comparison, it is observed that in the studied systems there is a small effect of the HBD, suggesting that these compounds interact mainly with choline chloride and leave very few empty vacancies for the interaction with another compound, in this case, alcohols.

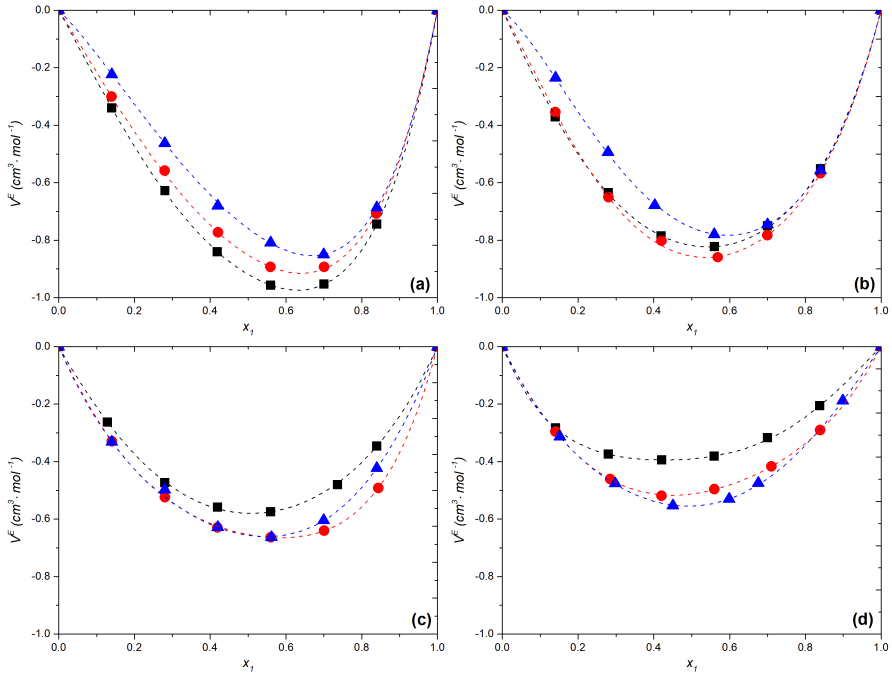

Figure 6: HBD effect on the molar excess volume of alcohol + DES mixtures. The molar excess volumes ($cm^3 \cdot mol^{-1}$) are in terms of the mole fraction of alcohol for the binary mixtures of DES with **(a)** methanol, **(b)** ethanol , **(c)** 1-propanol, **(d)** 1-butanol at a pressure of 101.3 kPa, temperature of 293.15 K and binary system with DES-A (■), DES-B (●), DES-C (▲). The dashed line represents the Redlich-Kister polynomial fitting with parameters reported in Table 7.

4.4. Molar Excess Enthalpy using COSMO-RS

The mixing behavior of systems containing DES can be described through the thermodynamic interactions occurring within the system. In particular, the $\boldsymbol{H}^E$ is a key thermodynamic property which illustrates the strength of interactions between the like and unlike species within a mixture, allowing to better understand the solvent behaviour upon mixing [64, 65]. Therefore, to further evaluate the thermodynamic equilibria and molecular interactions of mixtures containing alcohols + DES, the $\boldsymbol{H}^E$ of these systems will be evaluated using COSMO-RS method. Previous studies have proved the suitability of COSMO-RS to estimate $\boldsymbol{H}^E$ of complex mixtures containing ionic liquids [64] and to support the volumetric properties of binary mixtures containing alcohols [58], while qualitatively explaining the main molecular interactions occurring during the mixing process. Moreover, recent studies have successfully employed COSMO-RS to determine the thermodynamic equilibria [18, 66] and explain the molecular affinities [67–69] of systems containing DES.

$\boldsymbol{H}^E$ of pure choline chloride-based DES were calculated computing the solid-liquid equilibria of salt + HBD components and subtracting the energy associated with the salt melt-

Table 8: Mixing enthalpies of pseudo-pure choline chloride-based DES at molar ratio 1:3 predicted with COSMO-RS.

	DES-A	DES-B	DES-C
T / K	ΔH_{mix} / kJ·mol^{-1}		
293.15	-9.61	-8.25	-5.07
303.15	-9.48	-7.96	-5.01
313.15	-9.33	-7.68	-4.96
323.15	-9.15	-7.43	-4.92
333.15	-8.95	-7.19	-4.89

ing involved in the solvent formation, as proposed before [65]. The results corresponding to the mixing enthalpies of pure choline chloride-based DES at the different temperatures are collected in Table 8. Subsequently, the H^E of alcohol + DES mixtures were normalized by subtracting the H^E of pure DES as a function of the composition and temperature for each system, as shown in Figure 7, A.12 and A.13. This procedure allows to describe solely the alcohol + DES mixing phenomena without the other energy effects.

H^E of all alcohol + DES systems are negative, denoting the exothermic nature of the mixing process. Additionally, as expected by DES nature, the H^E contributions are distributed mainly as negative (favorable) hydrogen bonding (HB), as well as negative (attractive) electrostatic (MF) interactions, while positive (unfavorable) van der Waals (vdW) forces are almost negligible as observed in Figure 8. H^E of DES mixtures with alcohols show a maximum negative value (i.e., highest exothermicity) at alcohol molar fractions between 0.6 and 0.8 as shown in Figures 7, A.12 and A.13. H^E results and their deviation with respect to the equimolar composition support the stronger affinities observed on the experimental V^E at higher alcoholic fraction in the mixture. DES display a high affinity towards the alcohol component, forming new interactions between unlike species up to high alcohol fractions, before the alcohol like-like interaction become predominant. Considering the overall H^E results for each system and the energetic contributions at their maximum value, three main effects will be further analyzed as follows: temperature, alcohol chain length, and HBD component.

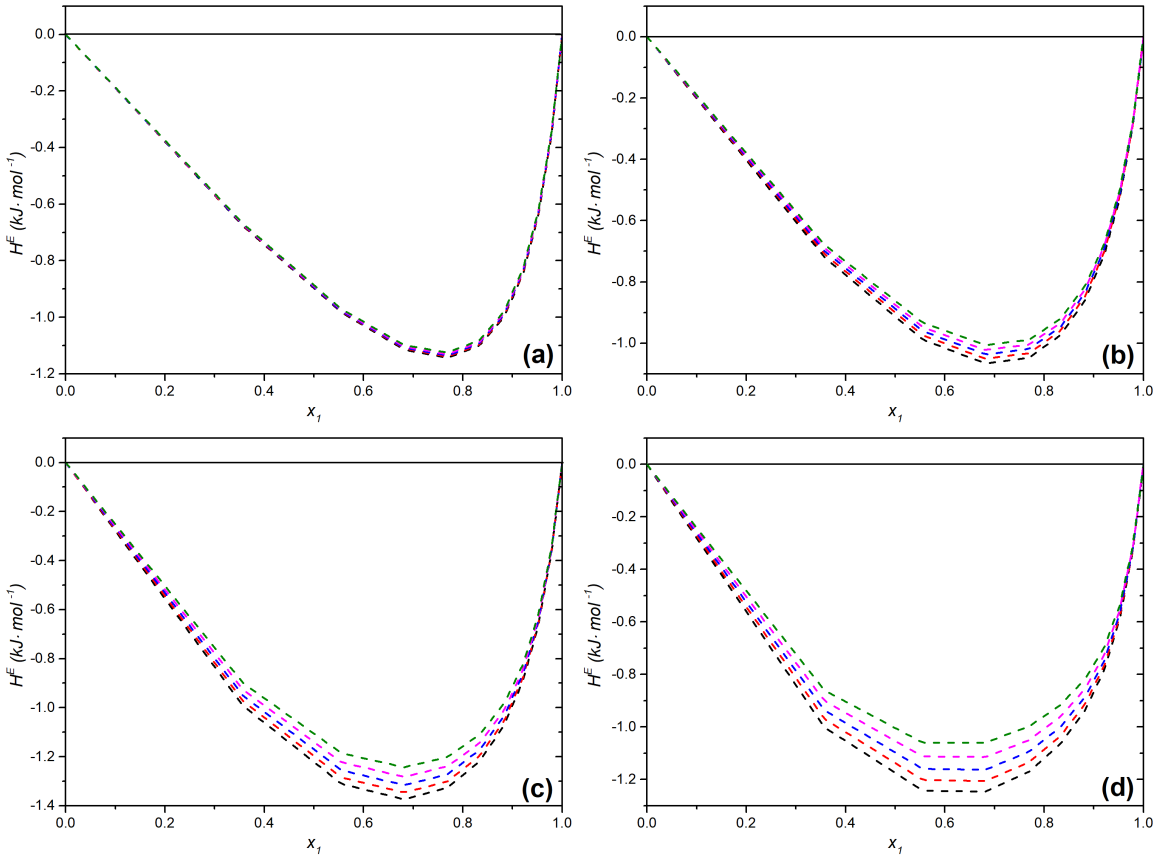

Figure 7: Temperature effect on the molar excess enthalpy of alcohol + DES-A mixtures predicted with COSMO-RS. The molar excess enthalpies (kJ·mol^{-1}) are in terms of the mole fraction of alcohol for the binary mixtures of **(a)** methanol + DES-A, **(b)** ethanol + DES-A, **(c)** 1-propanol + DES-A, **(d)** 1-butanol + DES-A at a pressure of 101.3 kPa and temperatures between 293.15 K and 333.15 K. The dashed line represents the temperatures of 293.15 K (–), 303.15 K (–), 313.15 K (–), 323.15 K (–), 333.15 K (–).

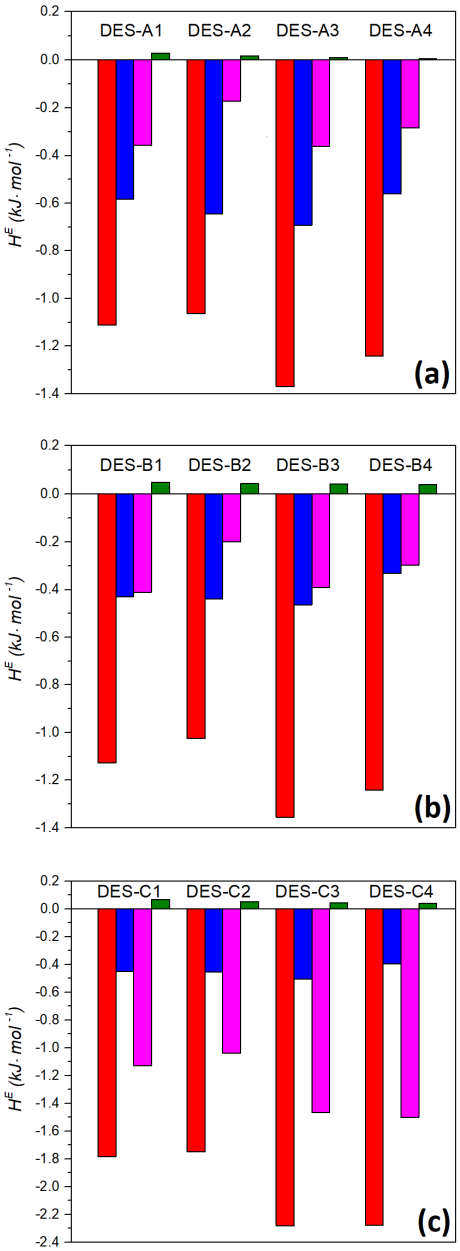

Figure 8: Molar excess entalphy (kJ·mol^{-1}) contributions(■) for the alcohol + DES mixtures of **(a)** alcohol + DES-A, **(b)** alcohol + DES-B and **(c)** alcohol + DES-C distributed in hydrogen bonding (■), electrostatic (■) and van der Walls (■) interactions at a concentration of alcohol of x_1=0.68, pressure of 101.3 kPa and temperature of 293.15 K.

Regarding the effect of the temperature, despite the strong temperature dependence of experimental V^E, no significant changes along the temperature range were observed for the computed H^E of alcohol + DES mixtures in Figures 7, A.12 and A.13. Nevertheless, two different trends can be observed: On the one hand, for ethylene glycol-based and 1,4-butanediol-based DES, the H^E magnitude decrease slightly with temperature. This behavior agrees with that reported in literature for solvent mixtures, where higher temperatures weaken the molecular interactions within the mixture. On the other hand, for 1,3-propanediol-based DES, higher temperatures increase the exothermicity of the mixture (i.e., increasingly negative H^E) due to stronger molecular interactions, supporting the lower experimental V^E. H^E contribution analysis shows minimal changes with respect to temperature, yet shows a clear trend: as temperature increases, attractive HB energy decreases, attractive MF energy increases, and for all systems, slightly repulsive vdW forces were found, with no change with temperature. The rise of favorable MF interactions comes from an interstitial accommodation of DES-alcohol molecules, which increases the magnitude of the V^E for the three diol-based DES. For the case of 1,3-propanediol-based DES, attractive electrostatic interactions increase faster than HB decreases, explaining its particular behavior found on the H^E analysis. H^E for DES-A and DES-B present small changes with the alcohol chain length, observed in Figure 9, where H^E increase in magnitude following ethanol < methanol < 1-butanol < 1-propanol. Meanwhile, DES-C shows two levels of H^E with an important magnitude increment, following ethanol ≈ methanol < 1-butanol ≈ 1-propanol. On the other hand, experimental V^E results exhibit the same overall trend for the three diol-based DES: methanol > ethanol > 1-propanol > 1-butanol, indicating an impediment in the DES – alcohol interaction by the carbon chain length. According to the σ-profiles of the four alcohols, their molecular interactions differ not on their hydrogen bond donor and acceptor capacity, given by the hydroxyl group, but on their non-polar charge surface area, which increases with the chain length.

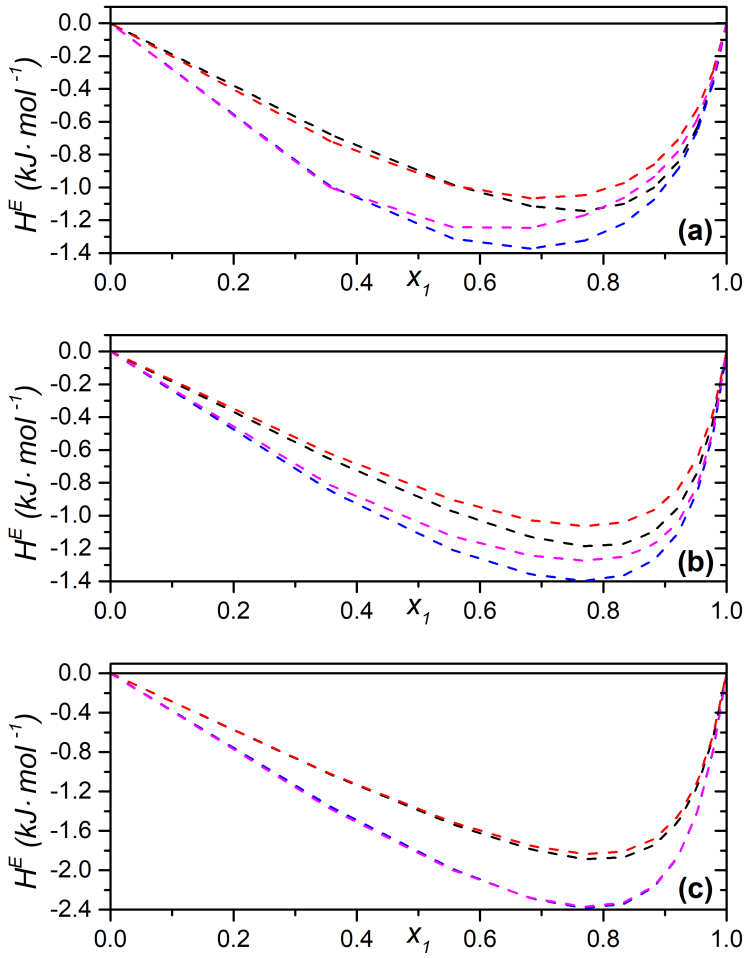

Figure 9: Alcohol chain effect on the molar excess enthalpy of alcohol + DES mixtures predicted with COSMO-RS. The molar excess enthalpies (kJ·mol^{-1}) are in terms of the mole fraction of alcohol for the binary mixtures of **(a)** DES-A, **(b)** DES-B, **(c)** DES-C, at a pressure of 101.3 kPa and temperature of 293.15 K. The dashed line represents the binary system with methanol (–), ethanol (–), 1-propanol (–) and 1-butanol (–).

The effect of HBD length in binary mixtures was studied in Figure 10. Although the overall behavior of each system is due to the combined interaction effects, hydrogen bond donor shows to have a major effect on the $\boldsymbol{H}^E$, where its minimum value shifts to a higher alcohol molar fraction as the HBD chain length increases. DES-A and DES-B based mixtures show similar magnitudes, while 1,4-butanediol-based DES present the larger $\boldsymbol{H}^E$, growing significantly more than the ethylene glycol or 1,3-propanediol based DESs

with increasing alcohol concentrations. The four-carbon chain of 1,4-butanediol enable the molecule to adopt different stable configurations, improving the steric accommodation within the system. Such trend is observed regardless the alcohol component. However, the increment is mainly due to increasing MF contributions, whereas HB energies and vdW forces remain relativity constants for the three diols.

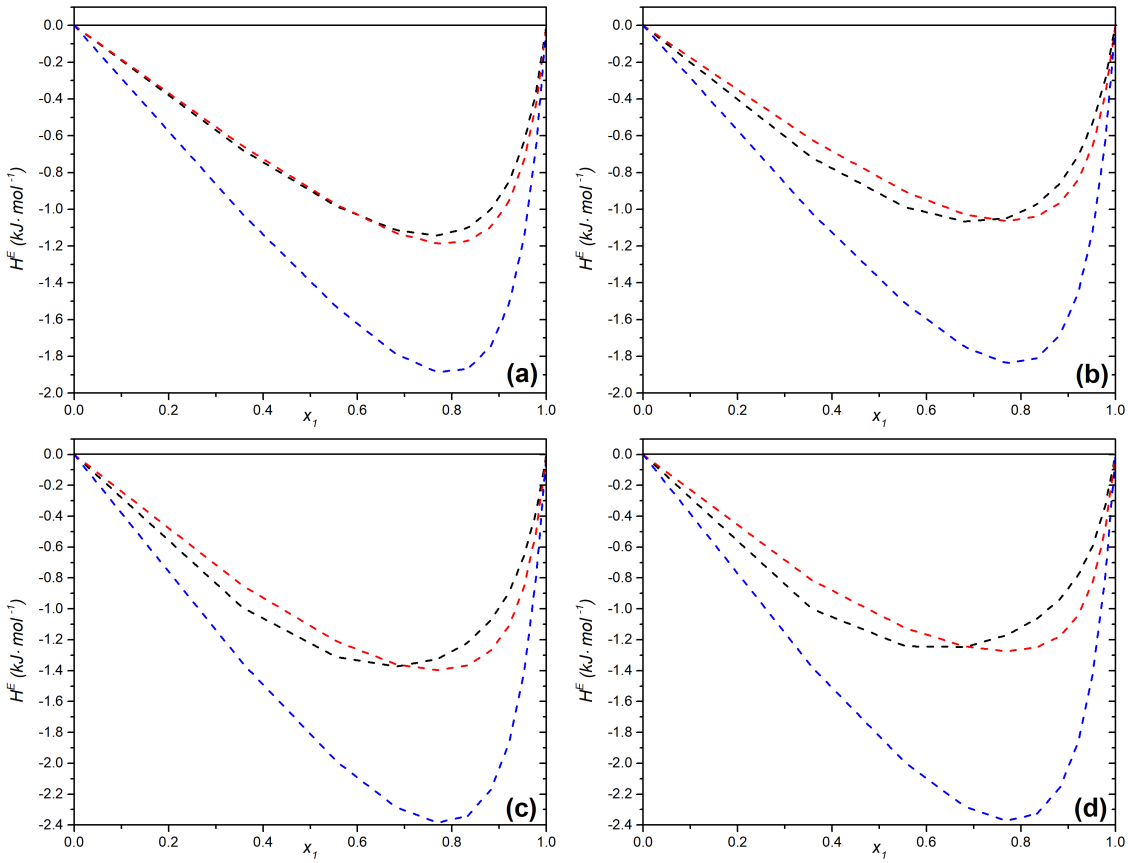

Figure 10: HBD effect on the molar excess enthalpy of alcohol + DES mixtures predicted with COSMO-RS. The molar excess enthalpies (kJ·mol^{-1}) are in terms of the mole fraction of alcohol for the binary mixtures of DES with **(a)** methanol, **(b)** ethanol, **(c)** 1-propanol, **(d)** 1-butanol at a pressure of 101.3 kPa and temperature of 293.15 K. The dashed line represents the binary system with DES-A (–), DES-B (–) and DES-C (–).

4.5. Viscosity mixture

Dynamic viscosity measurements of mixtures are shown in Figure 11 composed of alcohol + DES as a function of composition of alcohol, were obtained at 101.3 kPa and

temperatures between 293.15 K – 333.15 K in the full range of compositions for DES-A. Figures A.14 and A.15 shows the behavior of the DES-B and DES-C respectively. Viscosity decreases with temperature and by adding the differents alcohols, since pure alcohols have much lower viscosities than DES, it is observed that in the vast majority of molar fractions the viscosities of binary mixtures follow the following trend: DES + methanol < DES + ethanol < DES + 1-propanol < DES + 1-butanol. This is because the viscosity of pure alcohol follows the same trend. Viscosity results are shown in Tables 9, 10, and 11.

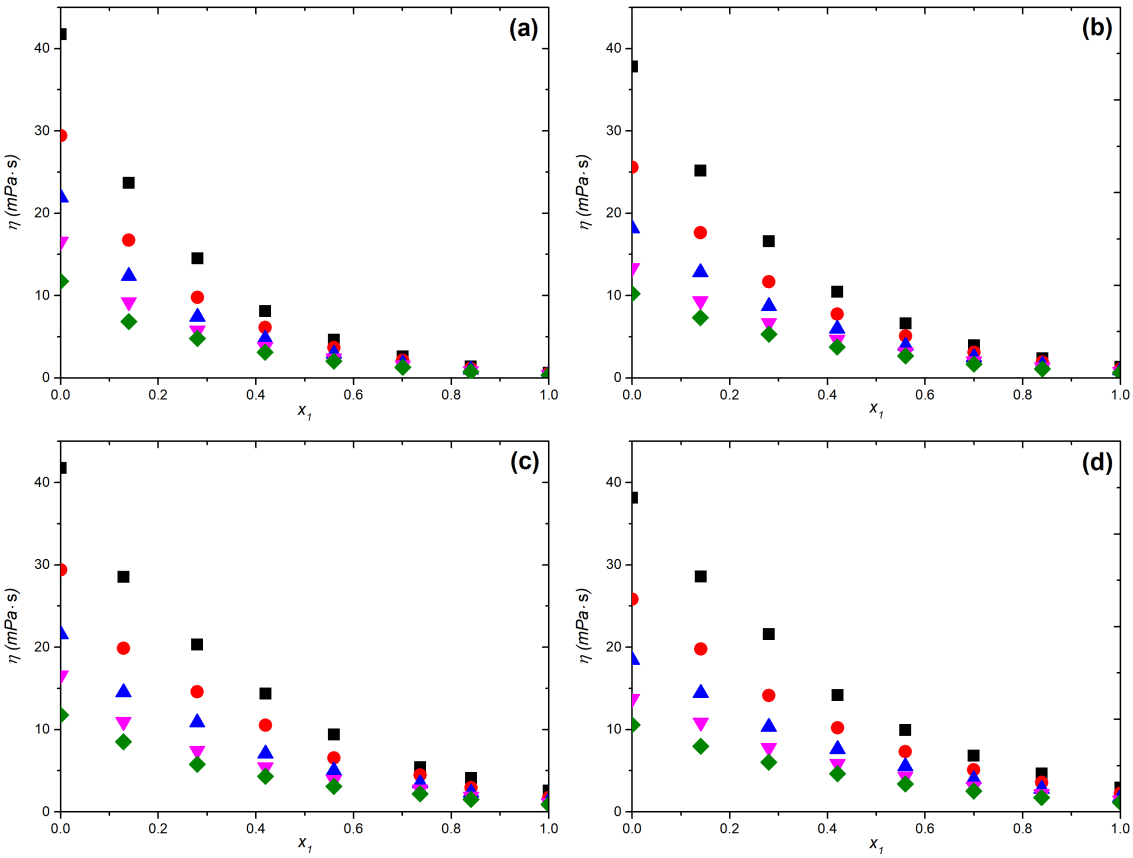

Figure 11: Dynamic viscosity (mPa·s) in terms of the mole fraction of alcohol for the binary mixtures of **(a)** DES-A1, **(b)** DES-A2, **(c)** DES-A3, **(d)** DES-A4 at a pressure of 101.3 kPa and temperatures between 298.15 K and 333.15 K. Temperatures of 293.15 K (■), 303.15 K (●), 313.15 K (▲), 323.15 K (▼) and 333.15 K (◆).

Table 9: Dynamic viscosity (mPa·s) of alcohols + DES (choline chloride + ethylene glycol) liquid mixture at different temperatures (K), compositions of alcohols (x_1) and a pressure of 101.3 kPa. Deep eutectic solvents binary system used for these measurements are detailed in Table 2.

methanol + DES-A1					
	Viscosity (mPa·s)				
x_1	293.15K	303.15 K	313.15 K	323.15 K	333.15 K
0.0000	41.762	29.410	21.880	16.581	11.759
0.1398	23.700	16.730	12.360	9.231	6.835
0.2802	14.500	9.789	7.422	5.778	4.809
0.4187	8.098	6.118	4.765	3.810	3.107
0.5597	4.659	3.668	2.948	2.426	2.020
0.7007	2.624	2.138	1.775	1.547	1.319
0.8402	1.392	1.176	1.005	0.870	0.757
1.0000	0.620	0.511	0.449	0.397	0.353
ethanol + DES-A2					
	Viscosity (mPa·s)				
x_1	293.15K	303.15 K	313.15 K	323.15 K	333.15 K
0.0000	37.800	25.572	18.160	13.391	10.224
0.1397	25.180	17.620	12.850	9.336	7.329
0.2800	16.590	11.700	8.731	6.708	5.299
0.4197	10.470	7.774	5.947	4.675	3.747
0.5601	6.610	5.084	3.905	3.135	2.653
0.6999	3.972	3.121	2.509	2.048	1.702
0.8401	2.394	1.935	1.585	1.316	1.103
1.0000	1.326	1.098	0.905	0.758	0.636
1-propanol + DES-A3					
	Viscosity (mPa·s)				
x_1	293.15K	303.15 K	313.15 K	323.15 K	333.15 K
0.0000	41.761	29.412	21.579	16.580	11.759
0.1285	28.520	19.890	14.500	10.950	8.522
0.2798	20.330	14.570	10.850	7.450	5.783
0.4195	14.350	10.540	7.084	5.452	4.301
0.5597	9.422	6.550	4.995	3.908	3.120
0.7362	5.419	4.484	3.476	2.751	2.217
0.8404	4.121	2.954	2.325	1.862	1.512
1.0000	2.587	1.725	1.377	1.114	0.913
1-butanol + DES-A4					
	Viscosity (mPa·s)				
x_1	293.15K	303.15 K	313.15 K	323.15 K	333.15 K
0.0000	38.150	25.832	18.451	13.750	10.593
0.1405	28.560	19.780	14.421	10.871	7.966
0.2796	21.590	14.130	10.330	7.799	6.054
0.4204	14.180	10.220	7.610	5.834	4.653
0.5595	9.958	7.330	5.550	4.307	3.414
0.6998	6.839	5.132	3.948	3.099	2.518
0.8385	4.681	3.574	2.781	2.202	1.771
1.0000	2.936	2.269	1.779	1.414	1.140

Standard uncertainties u are $u(x_1)$=0.005, $u(T)$=0.01 K, $u(P)$= 1 kPa. Relative standard uncertainties $u_r(\eta)$=0.06

Table 10: Dynamic viscosity (mPa·s) of alcohols + DES (choline chloride + 1,3 propanediol) liquid mixture at different temperatures (K), compositions of alcohols (x_1) and a pressure of 101.3 kPa. Deep eutectic solvents binary system used for these measurements are detailed in Table 2.

methanol + DES-B1					
	Viscosity (mPa·s)				
x_1	293.15K	303.15 K	313.15 K	323.15 K	333.15 K
0.0000	69.236	45.519	31.387	22.586	16.828
0.1394	41.840	28.564	20.411	15.148	11.608
0.2796	24.531	17.481	12.955	9.924	6.974
0.4209	13.962	10.403	7.125	5.560	4.443
0.5587	7.529	5.307	4.179	3.364	2.755
0.7013	3.473	2.782	2.271	1.885	1.589
0.8388	1.661	1.387	1.174	1.005	0.870
1.0000	0.590	0.511	0.449	0.397	0.353
ethanol + DES-B2					
	Viscosity (mPa·s)				
x_1	293.15K	303.15 K	313.15 K	323.15 K	333.15 K
0.0000	69.506	45.642	31.455	22.574	16.868
0.1401	45.305	30.831	21.842	16.027	12.168
0.2805	28.950	20.277	14.806	11.208	8.808
0.4201	17.453	12.617	8.783	6.736	5.413
0.5687	9.387	7.020	5.389	4.234	3.394
0.6996	5.444	4.248	3.336	2.676	2.179
0.8399	2.848	2.288	1.857	1.531	1.271
1.0000	1.326	1.090	0.905	0.758	0.636
1-propanol + DES-B3					
	Viscosity (mPa·s)				
x_1	293.15K	303.15 K	313.15 K	323.15 K	333.15 K
0.0000	69.290	45.578	31.368	22.568	16.848
0.1400	49.209	33.121	23.339	17.067	12.871
0.2802	33.596	23.222	16.753	12.496	9.722
0.4196	22.505	15.954	11.784	9.040	6.468
0.5606	14.482	10.620	7.171	5.472	4.341
0.7004	8.106	6.021	4.585	3.567	2.826
0.8436	4.629	3.542	2.755	2.182	1.753
1.0000	2.187	1.725	1.377	1.114	0.913
1-butanol + DES-B4					
	Viscosity (mPa·s)				
x_1	293.15K	303.15 K	313.15 K	323.15 K	333.15 K
0.0000	69.190	45.421	31.389	22.559	16.800
0.1399	49.865	33.435	23.501	17.181	12.956
0.2851	34.438	23.694	17.061	12.700	9.836
0.4199	23.204	16.490	12.109	8.457	7.040
0.5599	14.528	10.431	7.717	5.851	4.557
0.7105	8.920	6.569	4.971	3.836	3.019
0.8397	5.606	4.215	3.244	2.538	2.021
1.0000	2.936	2.269	1.779	1.414	1.140

Standard uncertainties u are $u(x_1)$=0.005, $u(T)$=0.01 K, $u(P)$= 1 kPa. Relative standard uncertainties $u_r(\eta)$=0.06

Table 11: Dynamic viscosity (mPa·s) of alcohols + DES (choline chloride + 1,4 butanediol) liquid mixture at different temperatures (K), compositions of alcohols (x_1) and a pressure of 101.3 kPa. Deep eutectic solvents binary system used for these measurements are detailed in Table 2.

methanol + DES-C1					
	Viscosity (mPa·s)				
x_1	293.15K	303.15 K	313.15 K	323.15 K	333.15 K
0.0000	118.080	71.290	47.292	32.776	23.629
0.1403	65.293	42.865	29.696	21.237	15.767
0.2801	36.868	25.357	18.218	13.555	10.344
0.4197	19.937	14.399	10.755	7.543	6.384
0.5597	10.335	7.018	5.492	4.300	3.539
0.7001	4.450	3.594	2.843	2.343	1.956
0.8399	1.905	1.579	1.328	1.132	0.995
1.0000	0.620	0.511	0.449	0.397	0.353
ethanol + DES-C2					
	Viscosity (mPa·s)				
x_1	293.15K	303.15 K	313.15 K	323.15 K	333.15 K
0.0000	117.950	72.100	47.016	32.535	23.500
0.1400	69.568	45.518	31.288	22.406	16.604
0.2791	41.931	28.654	20.344	15.016	11.351
0.4020	24.630	17.490	12.880	9.808	7.569
0.5598	13.963	10.303	7.164	5.546	4.395
0.7000	6.744	5.226	4.099	3.326	2.716
0.8400	3.264	2.612	2.109	1.726	1.430
1.0000	1.326	1.090	0.905	0.758	0.636
1-propanol + DES-C3					
	Viscosity (mPa·s)				
x_1	293.15K	303.15 K	313.15 K	323.15 K	333.15 K
0.0000	112.360	72.220	48.185	33.468	22.968
0.1404	76.387	48.230	33.123	23.541	16.964
0.2796	48.789	32.667	22.914	16.672	12.521
0.4198	30.671	21.339	15.351	11.416	8.891
0.5617	18.423	13.343	10.023	6.863	5.286
0.6997	9.999	7.335	5.528	4.258	3.336
0.8400	5.267	3.997	3.090	2.431	1.942
1.0000	2.187	1.725	1.377	1.114	0.913
1-butanol + DES-C4					
	Viscosity (mPa·s)				
x_1	293.15K	303.15 K	313.15 K	323.15 K	333.15 K
0.0000	113.170	73.020	46.597	32.347	23.354
0.1515	74.689	48.673	33.161	23.554	17.305
0.2983	49.854	33.410	23.393	16.991	12.729
0.4504	32.045	22.227	15.984	11.862	9.187
0.5993	21.120	14.600	10.230	7.292	5.607
0.6754	11.267	8.206	6.129	4.688	3.656
0.8991	6.304	4.718	3.612	2.816	2.231
1.0000	2.936	2.269	1.779	1.414	1.140

Standard uncertainties u are $u(x_1)$=0.005, $u(T)$=0.01 K, $u(P)$= 1 kPa. Relative standard uncertainties $u_r(\eta)$=0.06

5. Conclusions

Density and viscosity of the pure compounds ethylene glycol, 1,3-propanediol, 1,4-butanediol and DES formed by choline chloride with these precursors, in a molar ratio of 1:3, were measured in the range of temperatures from 293.15 to 333.15 K at a pressure of 101.3 kPa. Pseudo-binary mixtures formed by the differents DES and four different alcohols (methanol, ethanol, 1-propanol and 1-butanol) were also characterized by density and viscosity at the same conditions of temperature and pressure of the pure components. All the binary mixtures were completely miscible in the full range of compositions between 293.15 to 333.15 K and 101.3 kPa. Molar excess volumes were calculated from the density of the binary mixtures obtaining negative values for all the systems, suggesting a better interaction of the molecules of the different type and a favorable accommodation of molecules in their interstitial space. This behavior produces a lower volume compared with the one expected for an ideal mixture. Density and excess volumes of the binary mixtures were correlated with Redlich-Kister. All the molar excess volumes were correlated with an AAD(%) below 1.458%. About the effect of the alcohol chain length on excess properties, it is suggested that the greater the alcohol chain, the greater the capacity to make a strong molecular interaction given the decrease in the steric effect, together with the accommodation of the DES polar site. Experimental excess volumes were supported by an enthalpic study based on COSMO-RS method to provide insights into the molecular interactions occurring within the system. Overall results indicate that mixing of DES and alcohols involves an exothermic process and support the stronger affinities observed on the experimental excess volumes at higher alcohol concentrations. Energetic analysis suggests a competition between the interstitial accommodation of unlike species and the molecular affinity between like species, reflected as attractive electrostatic interactions and favorable hydrogen bonding HB contributions, respectively. Therefore, alcohol + DES mixing entails a complex phenomenon driven by competitive hydrogen bonding and electrostatics affinities between the species within the mixture, which determines the solvent mixing behavior and their macroscopic properties for practical applications.

6. Acknowledgments

We acknowledge the financial support from CONICYT Chile through the project Fondecyt de Iniciación 2016 N° 11160882.

References

[1] W. Peter, T. Welton, Ionic liquids in synthesis, John Wiley & Sons, 2008.

[2] V. Pârvulescu, C. Hardacre, Catalysis in Ionic Liquids, Mar. Pollut. Bull. 5 (2007) 2615–2665. doi:10.1038/202649b0.

[3] R. Haghbakhsh, K. Parvaneh, S. Raeissi, A. Shariati, A general viscosity model for deep eutectic solvents: The free volume theory coupled with association equations of state, Fluid Phase Equilib. 470 (2018) 193–202. URL: http://dx.doi.org/10.1016/j.fluid.2017.08.024. doi:10.1016/j.fluid.2017.08.024.

[4] L. Duan, L. L. Dou, L. Guo, P. Li, E. H. Liu, Comprehensive Evaluation of Deep Eutectic Solvents in Extraction of Bioactive Natural Products, ACS Sustain. Chem. Eng 4 (2016) 2405–2411. doi:10.1021/acssuschemeng.6b00091.

[5] A. P. Abbott, D. Boothby, G. Capper, D. L. Davies, R. K. Rasheed, Deep Eutectic Solvents formed between choline chloride and carboxylic acids: Versatile alternatives to ionic liquids, J. Am. Chem. Soc. 126 (2004) 9142–9147. doi:10.1021/ja048266j.

[6] N. F. Gajardo-Parra, M. J. Lubben, J. M. Winnert, Á. Leiva, J. F. Brennecke, R. I. Canales, Physicochemical properties of choline chloride-based deep eutectic solvents and excess properties of their pseudo-binary mixtures with 1-butanol, J. Chem. Thermodyn. 133 (2019) 272–284.

[7] M. C. Kroon, D. T. Allen, J. F. Brennecke, P. E. Savage, G. C. Schatz, ACS Virtual Issue on Deep Eutectic Solvents, J. Chem. Eng. Data 62 (2017) 1927–1928. doi:10.1021/acs.jced.7b00545.

[8] N. Rodriguez Rodriguez, A. van den Bruinhorst, L. J. B. M. Kollau, M. C. Kroon, K. Binnemans, Degradation of Deep-Eutectic Solvents Based on Choline Chloride and Carboxylic Acids, ACS Sustain. Chem. Eng 7 (2019) 11521–11528. doi:10.1021/acssuschemeng.9b01378.

[9] T. Khezeli, A. Daneshfar, R. Sahraei, A green ultrasonic-assisted liquid-liquid microextraction based on deep eutectic solvent for the HPLC-UV determination of ferulic, caffeic and cinnamic acid from olive, almond, sesame and cinnamon oil, Talanta 150 (2016) 577–585. URL: http://dx.doi.org/10.1016/j.talanta.2015.12.077. doi:10.1016/j.talanta.2015.12.077.

[10] S. Handy, K. Lavender, Organic synthesis in deep eutectic solvents: Paal-Knorr reactions, Tetrahedron Lett. 54 (2013) 4377–4379. URL: http://dx.doi.org/10.1016/j.tetlet.2013.05.122. doi:10.1016/j.tetlet.2013.05.122.

[11] M. Bougouma, A. Van Elewyck, M. Steichen, C. Buess-Herman, T. Doneux, Selenium electrochemistry in choline chloride-urea deep eutectic electrolyte, J. Solid State Electrochem. 17 (2013) 527–536. doi:10.1007/s10008-012-1955-5.

[12] B. Tang, H. Zhang, K. H. Row, Application of deep eutectic solvents in the extraction and separation of target compounds from various samples, J. Sep. Sci. 38 (2015) 1053–1064. doi:10.1002/jssc.201401347.

[13] S. H. Gage, D. A. Ruddy, S. Pylypenko, R. M. Richards, Deep Eutectic Solvent Approach Towards Nickel/Nickel Nitride Nanocomposites, Catal. Today (2016) 1–7. URL: http://dx.doi.org/10.1016/j.cattod.2016.12.016. doi:10.1016/j.cattod.2016.12.016.

[14] K. D. O. Vigier, G. Chatel, F. Jérôme, Contribution of deep eutectic solvents for biomass processing: Opportunities, challenges, and limitations, ChemCatChem 7 (2015) 1250–1260. doi:10.1002/cctc.201500134.

[15] R. Haghbakhsh, S. Raeissi, Two simple correlations to predict viscosities of pure and aqueous solutions of ionic liquids, J. Mol. Liq. 211 (2015) 948–956. URL: http://dx.doi.org/10.1016/j.molliq.2015.08.036. doi:10.1016/j.molliq.2015.08.036.

[16] F. Eckert, A. Klamt, Fast solvent screening via quantum chemistry: Cosmo-rs approach, AIChE J. 48 (2002) 369–385.

[17] A. Klamt, F. Eckert, Cosmo-rs: a novel and efficient method for the a priori prediction of thermophysical data of liquids, Fluid Phase Equilib. 172 (2000) 43–72.

[18] F. Bezold, M. E. Weinberger, M. Minceva, Assessing solute partitioning in deep eutectic solvent-based biphasic systems using the predictive thermodynamic model cosmo-rs, Fluid Phase Equilib. 437 (2017) 23–33.

[19] T. Aissaoui, Novel contribution to the chemical structure of choline chloride based deep eutectic solvents, Pharm Anal Acta 6 (2015) 11.

[20] S. Zullaikah, O. Rachmaniah, A. T. Utomo, H. Niawanti, Y. H. Ju, Green separation of bioactive natural products using liquefied mixture of solids, Green Chem. (2017) 17–38.

[21] M. Sahin, N. Erkan, E. Ayranci, Solution behavior of p-coumaric, caffeic and ferulic acids in methanol as determined from volumetric properties: attempts to explore a correlation with antioxidant activities, J. Solution Chem. 45 (2016) 52–66.

[22] B. Long, Y. Ding, Probing the intermolecular attractive interactions of binary mixtures of formic acid+ methanol or water via volumetric studies, J. Mol. Liq. 206 (2015) 137–144.

[23] G. Gonfa, M. A. Bustam, N. Muhammad, S. Ullah, Density and excess molar volume of binary mixture of thiocyanate-based ionic liquids and methanol at temperatures 293.15–323.15 k, J. Mol. Liq. 211 (2015) 734–741.

[24] Z. Zhang, Q. Zhou, X. Lu, C. Qiao, S. Zhang, Densities and viscosities of binary mixtures containing 1, 3-dimethylimidazolium dimethylphosphate and alcohols, J. Chem. Eng. Data 59 (2014) 2377–2388.

[25] M. A. Varfolomeev, K. V. Zaitseva, I. T. Rakipov, B. N. Solomonov, W. Marczak, Speed of sound, density, and related thermodynamic excess properties of binary mixtures of butan-2-one with c1–c4 n-alkanols and chloroform, J. Chem. Eng. Data 59 (2014) 4118–4132.

[26] C. Smyth, W. Stoops, The dielectric polarization of liquids. vi. ethyl iodide, ethanol, normal-butanol and normal-octanol, J. Am. Chem. Soc. 51 (1929) 3312–3329.

[27] M. Khimenko, V. Aleksandrov, N. Gritsenko, Polarizabilities and Molecular Radii of Some Pure Liquids, volume 47, 1973.

[28] Y. Tashima, Y. Arai, Data report Mem. Fac. Eng. Kyushu University, volume 41, 1981.

[29] S. Mikhail, W. Kimel, Densities and viscosities of 1-propanol-water mixtures., J. Chem. Eng. Data 8 (1963) 323–328.

[30] J. Singh, G. Benson, Vapor–liquid equilibrium studies of n-propanol–n-decanol mixtures, Can. J. Chem. 46 (1968) 2065–2069.

[31] S. Westmeier, Excess enthalpy, free excess enthalpy, excess volume and viscosity of selected binary liquid mixtures. part iii: The water-n-propanol and water- isopropanol systems, Can. J. Chem. 28 (1976) 480–3.

[32] K. Fukuchi, K. Ogiwara, S. Yonezawa, Y. Arai, S. Kogaku, D. Kyushu, Densities of Alcohols and Their Mixtures, volume 53, 1980.

[33] A. Boruń, A. Bald, Ionic association and conductance of [emim][bf4] and [bmim][bf4] in 1-butanol in a wide range of temperature, J. Chem. Thermodyn. 96 (2016) 175–180.

[34] J. Safarov, B. Ahmadov, S. Mirzayev, A. Shahverdiyev, E. P. Hassel, Thermophysical properties of 1-butanol over a wide range of temperatures and pressures up to 200 mpa, J. Mol. Liq. 209 (2015) 465–479.

[35] G. A. Iglesias-Silva, M. Bravo-Sanchez, A. Estrada-Baltazar, C. Bouchot, K. R. Hall, P–ρ–t data for 1-butanol and isobutyl alcohol from (283.15 to 363.15) k at pressures up to 66 mpa, J. Chem. Eng. Data 60 (2015) 1076–1090.

[36] C. Zhu, S. Han, J. Liu, Y. Ma, Densities and viscosities of diaminotoluene with water, ethanol, propan-1-ol, and butan-1-ol from (293.15 to 333.15) k, J. Chem. Eng. Data 59 (2014) 880–889.

[37] M. Khalilov, Viscosity of Liquids and Saturated Vapors at High Temperatures & Pressures, volume 9, 1939.

[38] T. Ledneva, Bulk viscosity and its temperature dependence for some organic liquids, volume 2, 1956.

[39] S. Mikhail, W. Kimel, Densities and viscosities of methanol-water mixtures., J. Chem. Eng. Data 6 (1961) 533–537.

[40] M. A. Rauf, G. H. Stewart, Viscosities and densities of binary mixtures of 1-alkanols from 15 to 55. degree. c, J. Chem. Eng. Data 28 (1983) 324–328.

[41] N. Saha, B. Das, D. K. Hazra, Viscosities and excess molar volumes for acetonitrile+ methanol at 298.15, 308.15, and 318.15 k, J. Chem. Eng. Data 40 (1995) 1264–1266.

[42] B. N. Misra, Y. Varshni, Viscosity-temperature relation for solutions., J. Chem. Eng. Data 6 (1961) 194–196.

[43] E. Tommila, E. Lindell, M. Virtalaine, R. Laakso, B. Kemistil, Densities, viscosities, surface tensions, dielectric constants, vapor pressures, activities, and heats of mixing of sulpholane + water, sulpholane + methanol, and sulpholane + ethanol mixtures., J. Chem. Eng. Data 42 (1969) 95–104.

[44] T. W. Phillips, K. P. Murphy, Liquid viscosity of halocarbons, J. Chem. Eng. Data 15 (1970) 304–307.

[45] B. Garcia, C. Herrera, J. M. Leal, Shear viscosities of binary liquid mixtures: 2-pyrrolidinone with 1-alkanols, J. Chem. Eng. Data 36 (1991) 269–274.

[46] P. S. Nikam, L. N. Shirsat, M. Hasan, Density and viscosity studies of binary mixtures of acetonitrile with methanol, ethanol, propan-1-ol, propan-2-ol, butan-1-ol, 2-methylpropan-1-ol, and 2-methylpropan-2-ol at (298.15, 303.15, 308.15, and 313.15) k, J. Chem. Eng. Data 43 (1998) 732–737.

[47] A. Pal, G. Dass, Excess molar volumes and viscosities for binary liquid mixtures of methyl tert-butyl ether and of tert-amyl methyl ether with methanol, 1-propanol, and 1-pentanol at 298.15 k, J. Chem. Eng. Data 44 (1999) 1325–1329.

[48] Y. Chen, N. Ai, G. Li, H. Shan, Y. Cui, D. Deng, Solubilities of carbon dioxide in eutectic mixtures of choline chloride and dihydric alcohols, J. Chem. Eng. Data 59 (2014) 1247–1253. doi:10.1021/je400884v.

[49] A. B. Knezeć-Stevanović, I. R. Radović, S. P. Serbanović, M. L. Kijevcanin, Densities, viscosities, and refractive indices of the ternary mixture dimethyladipate+ 2-butanone+ 1-butanol at t=(288.15 to 323.15) k, J. Chem. Eng. Data 59 (2014) 4133–4150.

[50] N. Živković, S. Šerbanović, M. Kijevčanin, E. Živković, Volumetric properties, viscosities, and refractive indices of the binary systems 1-butanol+ peg 200,+ peg 400, and+ tegdme, Int. J. Thermophys. 34 (2013) 1002–1020.

[51] A. Estrada-Baltazar, G. Iglesias-Silva, C. Caballero-Ceron, Volumetric and transport properties of binary mixtures of n-octane+ ethanol,+ 1-propanol,+ 1-butanol, and+ 1-pentanol from (293.15 to 323.15) k at atmospheric pressure, J. Chem. Eng. Data 58 (2013) 3351.

[52] K. Shahbaz, S. Baroutian, F. Mjalli, M. Hashim, I. AlNashef, Densities of ammonium and phosphonium based deep eutectic solvents: Prediction using artificial intelligence and group contribution techniques, Thermochim. Acta 527 (2012) 59–66.

[53] A. P. Abbott, R. C. Harris, K. S. Ryder, Application of hole theory to define ionic liquids by their transport properties, J. Phys. Chem. B 111 (2007) 4910–4913.

[54] M. Rogošić, K. Z. Kučan, Deep eutectic solvents based on choline chloride and ethylene glycol as media for extractive denitrification/desulfurization/dearomatization of motor fuels, J. Ind. Eng. Chem. 72 (2019) 87–99.

[55] D. Shen, M. B. Vukmirovic, R. Akolkar, Understanding the role of complexation in the charge-transfer kinetics of the cu2++ e cu1+ redox reaction in ethaline deep eutectic solvent, J. Electrochem. Soc. 166 (2019) E526–E532.

[56] B. Ozturk, C. Parkinson, M. Gonzalez-Miquel, Extraction of polyphenolic antioxidants from orange peel waste using deep eutectic solvents, Sep. Purif. Technol. 206 (2018) 1–13.

[57] G. Garcia, S. Aparicio, R. Ullah, M. Atilhan, Deep eutectic solvents: physicochemical properties and gas separation applications, Energ. Fuel 29 (2015) 2616–2644.

[58] J. Esteban, M. Gonzalez-Miquel, Thermodynamic insights on the viscometric and volumetric properties of binary mixtures of ketals and polyols, J. Mol. Liq. 263 (2018) 125–138.

[59] J. Canosa, A. Rodriguez, M. Iglesias, B. Orge, J. Tojo, Thermodynamic properties of alkanediols+ acetates at 298.15 k, J. Therm. Anal. Calorim. 52 (1998) 915–932.

[60] B. Hawrylak, K. Gracie, R. Palepu, Thermodynamic properties of binary mixtures of butanediols with water, J. Solution Chem. 27 (1998) 17–31.

[61] E. M. Živković, D. M. Bajić, I. R. Radović, S. P. Šerbanović, M. L. Kijevčanin, Volumetric and viscometric behavior of the binary systems ethyl lactate+ 1, 2-propanediol,+ 1, 3-propanediol,+ tetrahydrofuran and+ tetraethylene glycol dimethyl ether. new unifac–visco and asog–visco parameters determination, Fluid Phase Equilib. 373 (2014) 1–19.

[62] M. Moosavi, A. Motahari, A. Omrani, A. A. Rostami, Investigation on some thermophysical properties of poly (ethylene glycol) binary mixtures at different temperatures, J. Chem. Thermodyn. 58 (2013) 340–350.

[63] H. Vogel, The law of the relation between the viscosity of liquids and the temperature, Phys. Z 22 (1921) 645–646.

[64] M. Gonzalez-Miquel, M. Massel, A. DeSilva, J. Palomar, F. Rodriguez, J. F. Brennecke, Excess enthalpy of monoethanolamine+ ionic liquid mixtures: how good are cosmo-rs predictions?, J. Phys. Chem. B 118 (2014) 11512–11522.

[65] P. López-Porfiri, J. F. Brennecke, M. Gonzalez-Miquel, Excess molar enthalpies of deep eutectic solvents (dess) composed of quaternary ammonium salts and glycerol or ethylene glycol, J. Chem. Eng. Data 61 (2016) 4245–4251.

[66] T. Jeliński, P. Cysewski, Application of a computational model of natural deep eutectic solvents utilizing the cosmo-rs approach for screening of solvents with high solubility of rutin, J. Mol. Model. 24 (2018) 180.

[67] B. Ozturk, J. Esteban, M. Gonzalez-Miquel, Deterpenation of citrus essential oils using glycerol-based deep eutectic solvents, J. Chem. Eng. Data 63 (2018) 2384–2393.

[68] B. Ozturk, M. Gonzalez-Miquel, Alkanediol-based deep eutectic solvents for isolation of terpenoids from citrus essential oil: Experimental evaluation and cosmo-rs studies, Sep. Purif. Technol. 227 (2019) 115707.

[69] P. Wongsirichot, M. Gonzalez-Miquel, J. Winterburn, Holistic valorization of rapeseed meal utilizing green solvents extraction and biopolymer production with pseudomonas putida, J. Cleaner Prod. 230 (2019) 420–429.

Appendix A. Supporting information

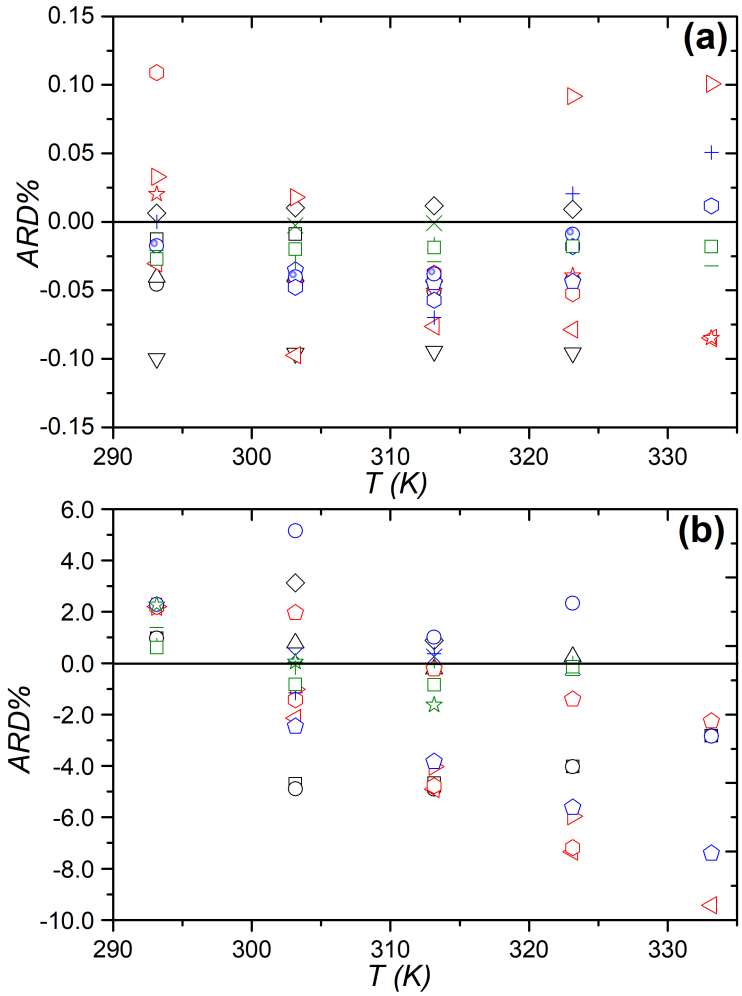

Figure A.1: ***ARD***(%) of the literature date for compared with this work: **(a)** Density comparison with data reported for methanol from Sahin et al. [21] (□), Long et al.[22](○), Gonfa et al.[23](△), Zhang et al.[24](▽), Varfolomeev et al. [25](◇), for ethanol from Smyth et al.[26](◁), Khimenko et al.[27](▷), Fukuchi et al.[32](⬡), Tashima et al. [28](☆), for 1-propanol from Mikhail et al.[29](⬠), Singh al.[30](◫), Westmeier et al.[31](+), Fukuchi et al.[32](⬡) and for 1-butanol from Borun et al.[33](×), Safarov et al.[34](−), Iglesias et al.[35](*j*), Zhu et al.[36](⦶). **(b)** Viscosity comparison with data reported for methanol from Khalilov et al. [37] (□), Ledneva et al.[38](○), Mikhail et al.[39](△), Rauf et al.[40](▽), Saha et al. [41](◇), for ethanol from Misra et al.[42](◁), Tommila et al.[43](▷), Phillips et al.[44](⬡), García et al.[45](⬠), for 1-propanol from Ledneva et al.[38](○), García et al.[45](⬠), Nikam et al.[46](+), Pal et al.[47](×) and for 1-butanol from Chen et al. [48](☆), Knezevic-Stevanonic et al.[49](−), Vzivkovic et al.[61](*j*), Estrada-Baltazar et al.[51](⦶).

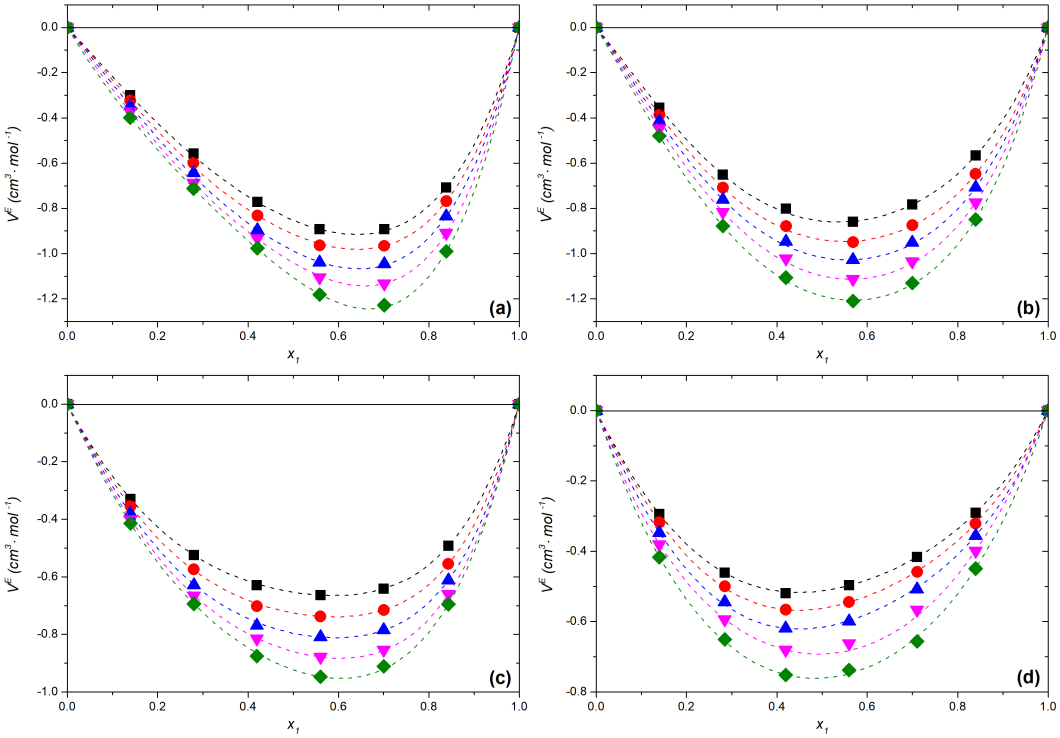

Figure A.2: Temperature effect on the excess molar volume of alcohol + DES-B mixtures. The excess molar volumes (cm^3·mol^{-1}) are in terms of the mole fraction of alcohol for the binary mixtures **(a)** methanol + DES-B, **(b)** ethanol + DES-B, **(c)** 1-propanol + DES-B, **(d)** 1-butanol + DES-B at a pressure of 101.3 kPa and temperatures between 298.15 K and 333.15 K. Temperatures of 293.15 K (■), 303.15 K (●), 313.15 K (▲), 323.15 K (▼) and 333.15 K (◆). The dashed line represents the Redlich-Kister polynomial fitting with parameters reported in Table 7.

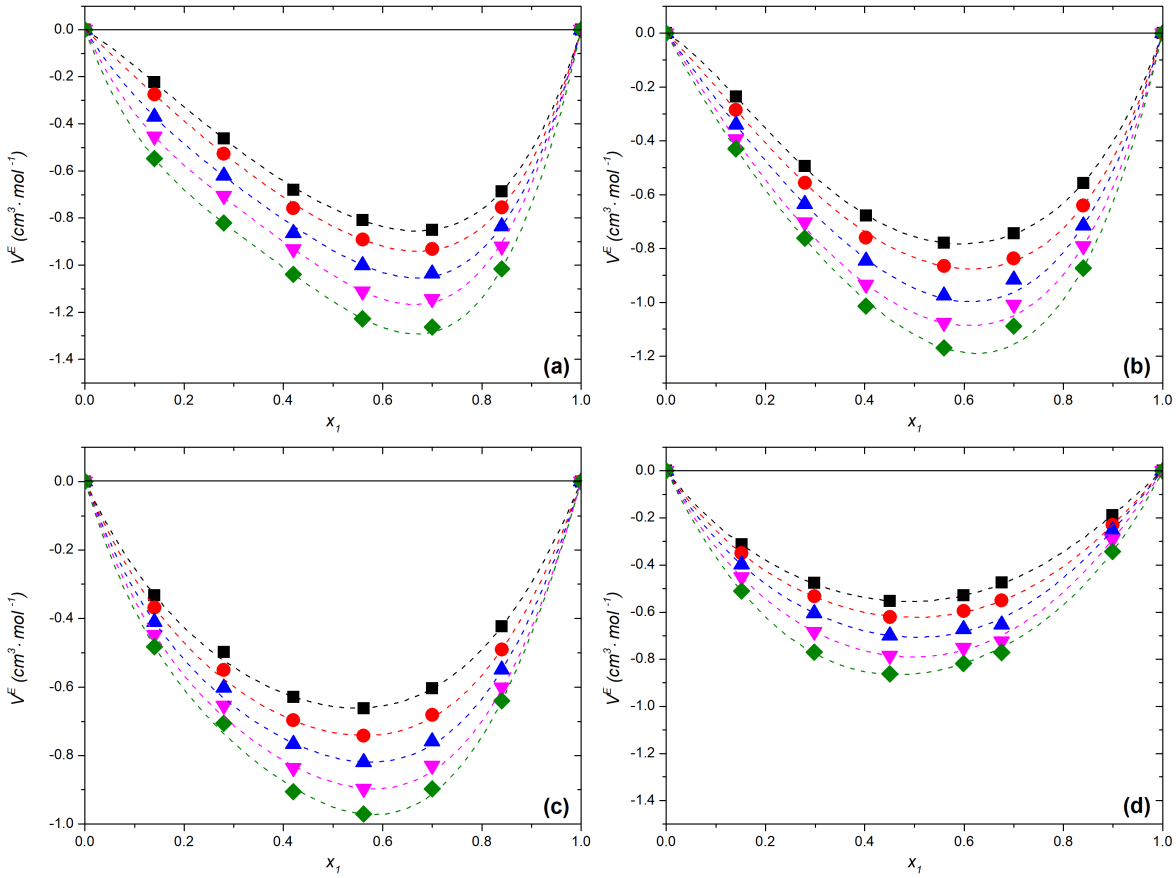

Figure A.3: Temperature effect on the excess molar volume of alcohol + DES-C mixtures. The excess molar volumes (cm^3·mol^{-1}) are in terms of the mole fraction of alcohol for the binary mixtures **(a)** methanol + DES-C, **(b)** ethanol + DES-C, **(c)** 1-propanol + DES-C, **(d)** 1-butanol + DES-C at a pressure of 101.3 kPa and temperatures between 298.15 K and 333.15 K. Temperatures of 293.15 K (■), 303.15 K (●), 313.15 K (▲), 323.15 K (▼) and 333.15 K (◆). The dashed line represents the Redlich-Kister polynomial fitting with parameters reported in Table 7.

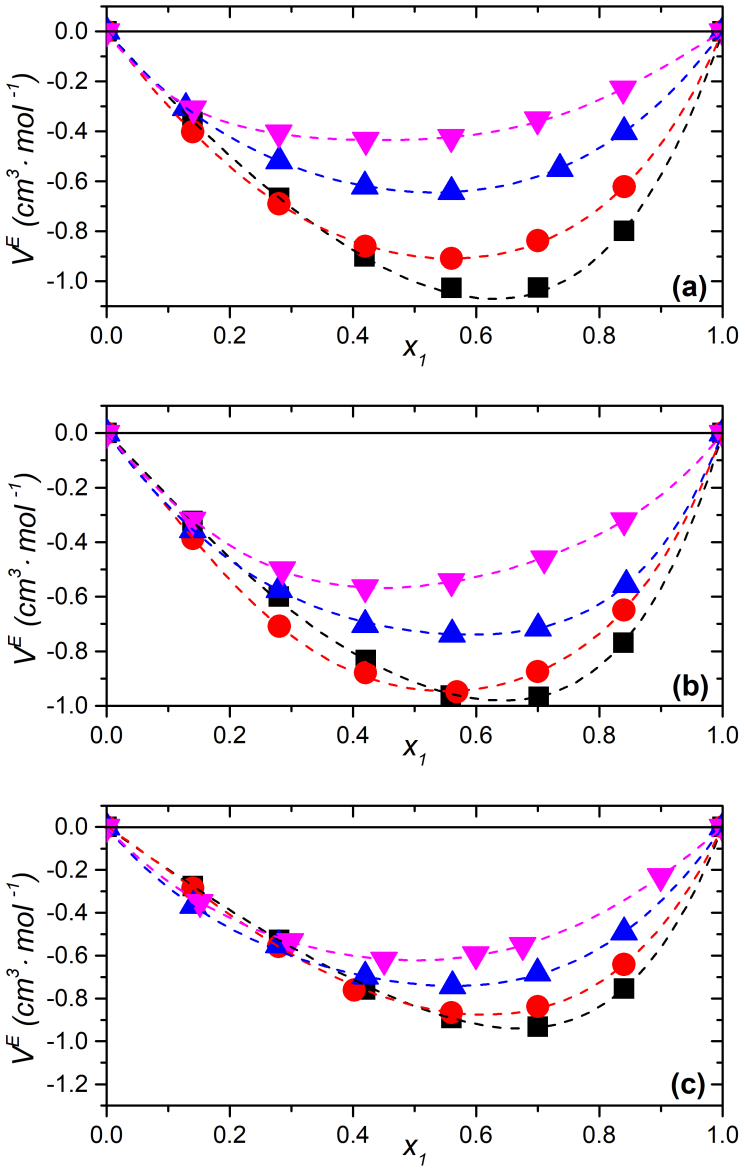

Figure A.4: Alcohol chain effect on the excess molar volume of alcohol + DES. Excess molar volumes ($cm^3 \cdot mol^{-1}$) are in terms of the mole fraction of alcohol for the binary mixtures of **(a)** DES-A, **(b)** DES-B , **(c)** DES-C, at a pressure of 101.3 kPa, temperature of 303.15 K and DES binary system with methanol (■), ethanol (●), 1-propanol (▲), 1-butanol (▼). The dashed line represents the Redlich-Kister polynomial fitting with parameters reported in Table 7.

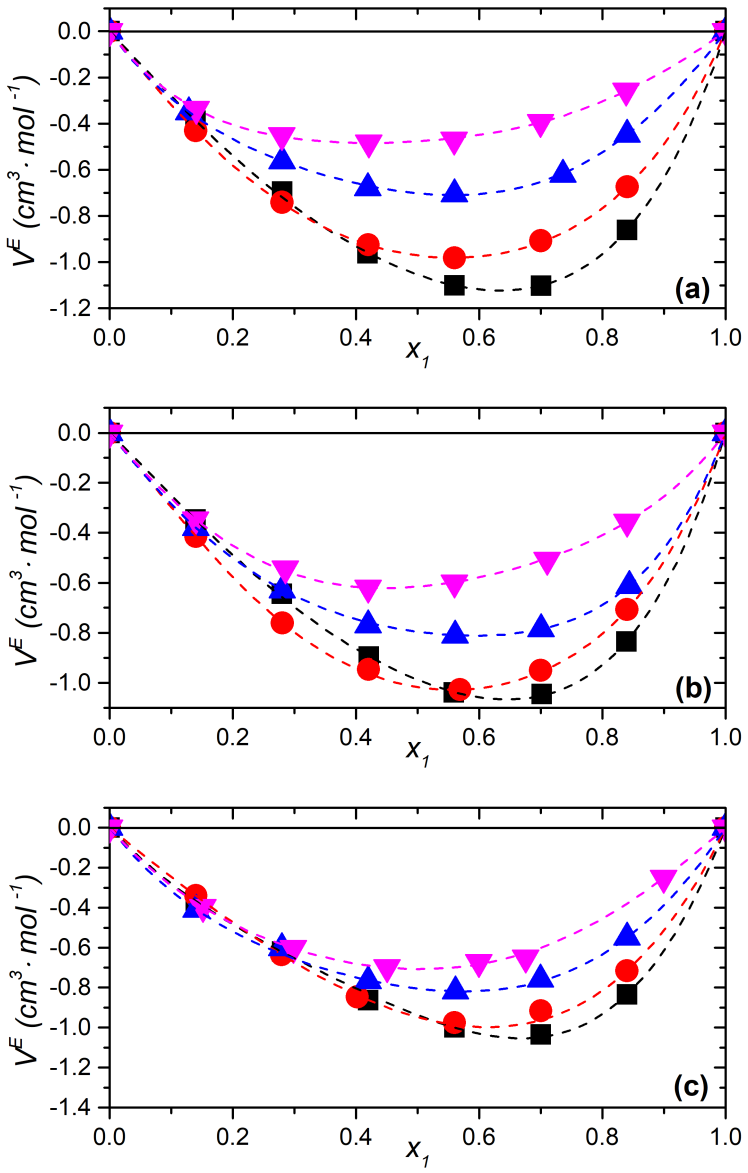

Figure A.5: Alcohol chain effect on the excess molar volume of alcohol + DES. Excess molar volumes ($cm^3 \cdot mol^{-1}$) are in terms of the mole fraction of alcohol for the binary mixtures of **(a)** DES-A, **(b)** DES-B , **(c)** DES-C, at a pressure of 101.3 kPa, temperature of 313.15 K and DES binary system with methanol (■), ethanol (●), 1-propanol (▲), 1-butanol (▼). The dashed line represents the Redlich-Kister polynomial fitting with parameters reported in Table 7.

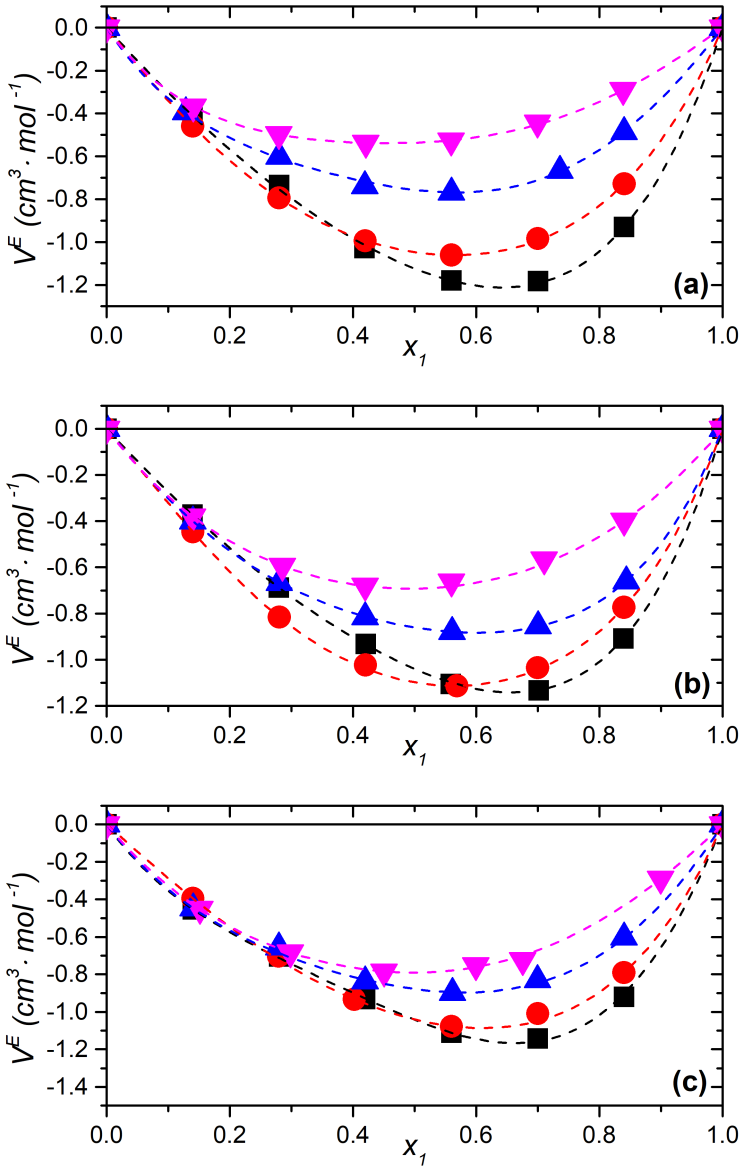

Figure A.6: Alcohol chain effect on the excess molar volume of alcohol + DES. Excess molar volumes ($cm^3 \cdot mol^{-1}$) are in terms of the mole fraction of alcohol for the binary mixtures of **(a)** DES-A, **(b)** DES-B , **(c)** DES-C, at a pressure of 101.3 kPa, temperature of 323.15 K and DES binary system with methanol (■), ethanol (●), 1-propanol (▲), 1-butanol (▼). The dashed line represents the Redlich-Kister polynomial fitting with parameters reported in Table 7.

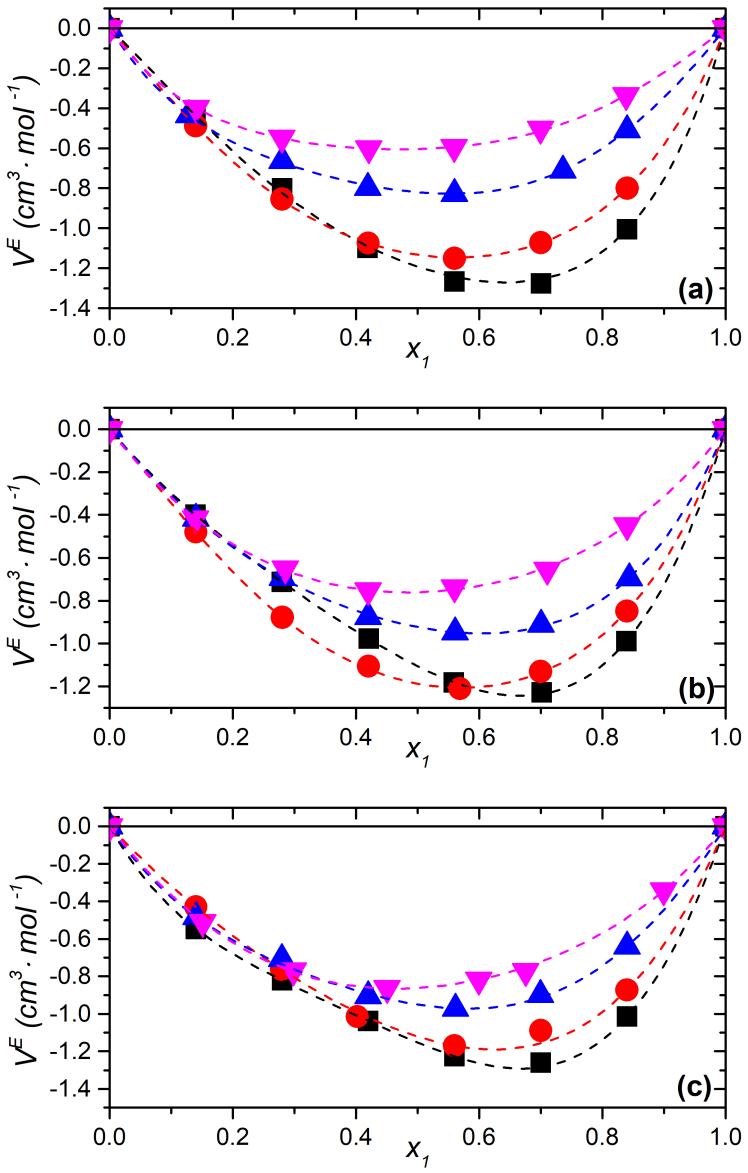

Figure A.7: Alcohol chain effect on the excess molar volume of alcohol + DES. Excess molar volumes ($cm^3 \cdot mol^{-1}$) are in terms of the mole fraction of alcohol for the binary mixtures of **(a)** DES-A, **(b)** DES-B , **(c)** DES-C, at a pressure of 101.3 kPa, temperature of 333.15 K and DES binary system with methanol (■), ethanol (●), 1-propanol (▲), 1-butanol (▼). The dashed line represents the Redlich-Kister polynomial fitting with parameters reported in Table 7.

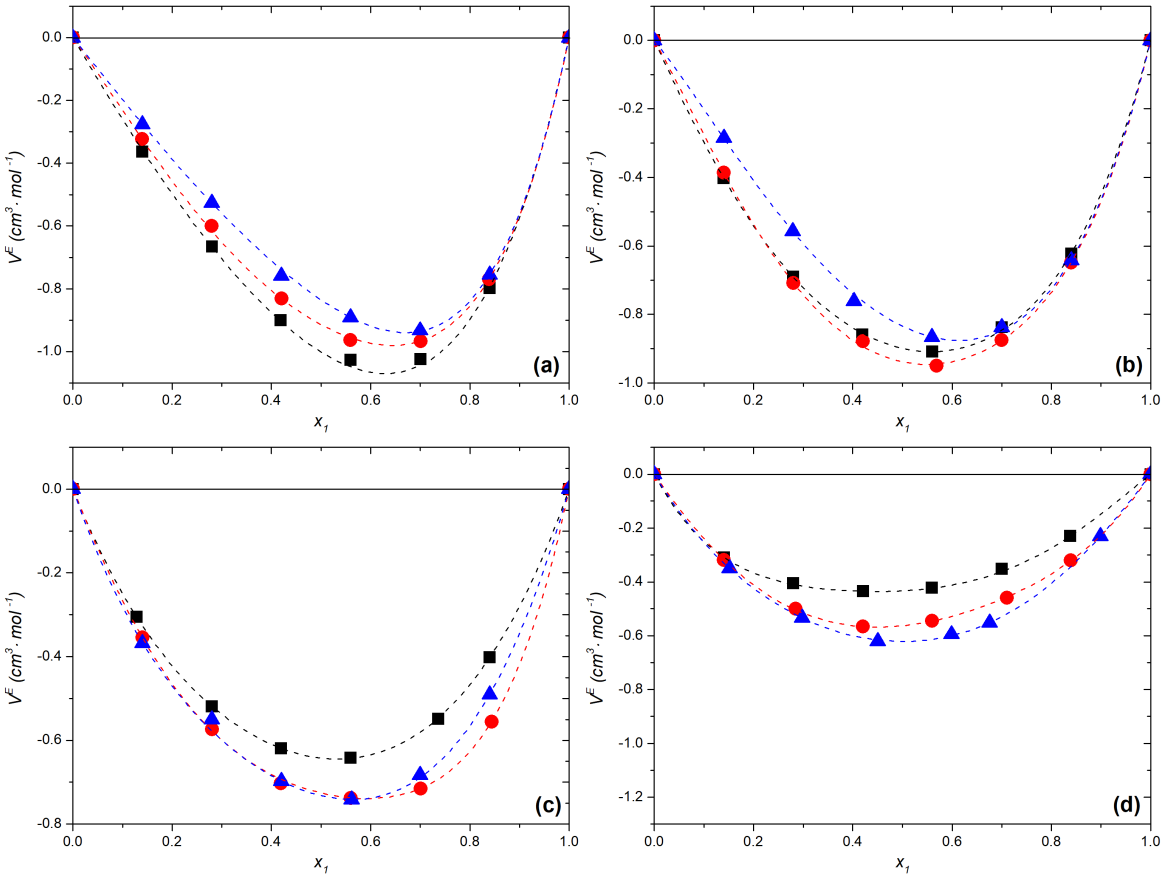

Figure A.8: HBD effect on the excess molar volume of alcohol + DES mixtures. Excess molar volumes ($cm^3 \cdot mol^{-1}$) are in terms of the mole fraction of alcohol for the binary mixtures of DES with **(a)** methanol, **(b)** ethanol , **(c)** 1-propanol, **(d)** 1-butanol at a pressure of 101.3 kPa, temperature of 303.15 K and binary system with DES-A (■), DES-B (●), DES-C (▲). The dashed line represents the Redlich-Kister polynomial fitting with parameters reported in Table 7.

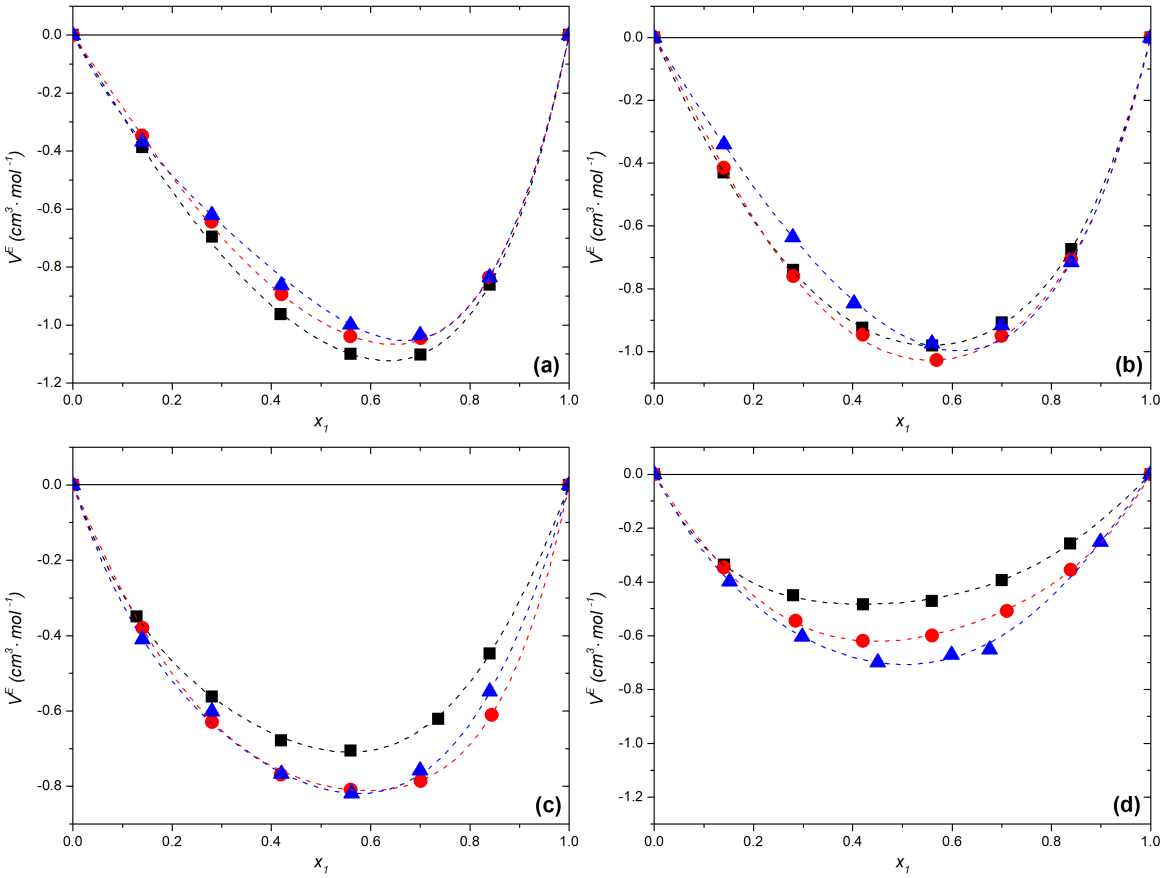

Figure A.9: HBD effect on the excess molar volume of alcohol + DES mixtures. Excess molar volumes ($cm^3 \cdot mol^{-1}$) are in terms of the mole fraction of alcohol for the binary mixtures of DES with **(a)** methanol, **(b)** ethanol , **(c)** 1-propanol, **(d)** 1-butanol at a pressure of 101.3 kPa, temperature of 313.15 K and binary system with DES-A (■), DES-B (●), DES-C (▲). The dashed line represents the Redlich-Kister polynomial fitting with parameters reported in Table 7.

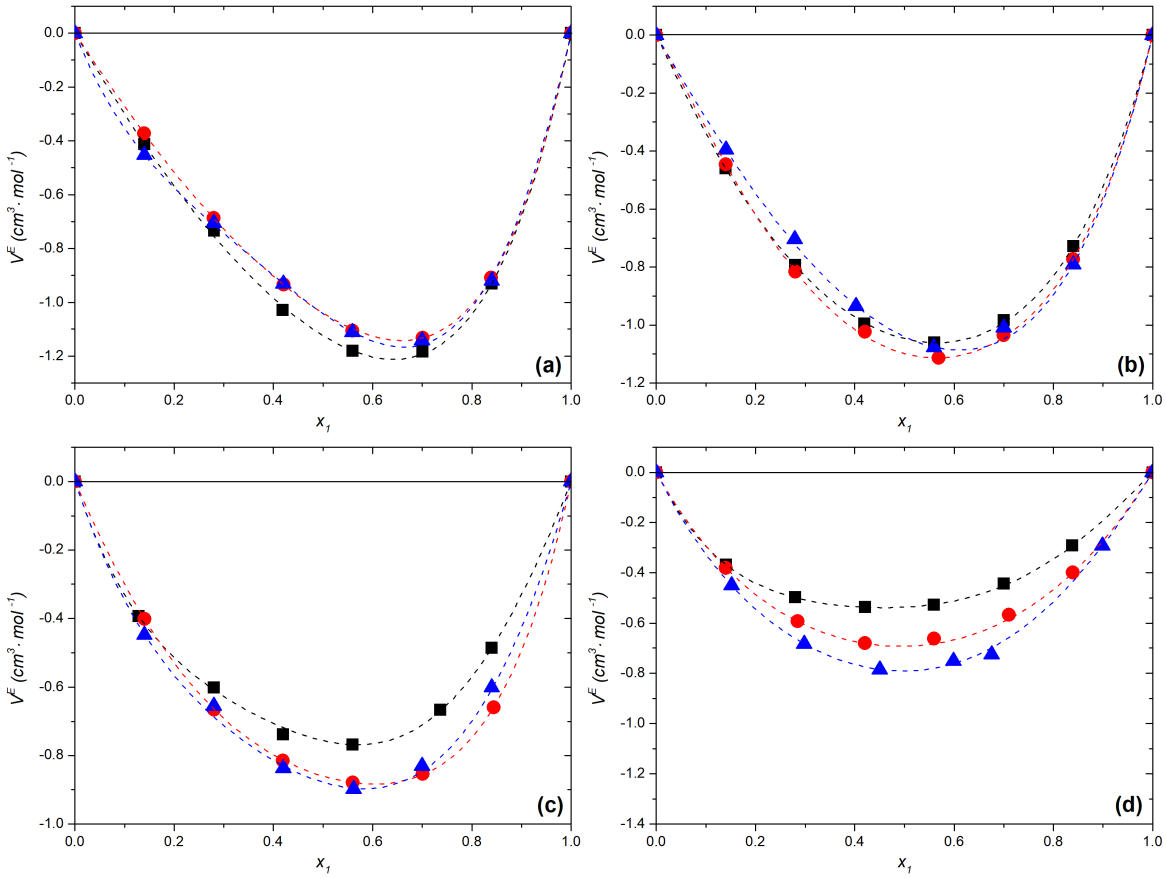

Figure A.10: HBD effect on the excess molar volume of alcohol + DES mixtures. Excess molar volumes ($cm^3 \cdot mol^{-1}$) are in terms of the mole fraction of alcohol for the binary mixtures of DES with **(a)** methanol, **(b)** ethanol , **(c)** 1-propanol, **(d)** 1-butanol at a pressure of 101.3 kPa, temperature of 323.15 K and binary system with DES-A (■), DES-B (●), DES-C (▲). The dashed line represents the Redlich-Kister polynomial fitting with parameters reported in Table 7.

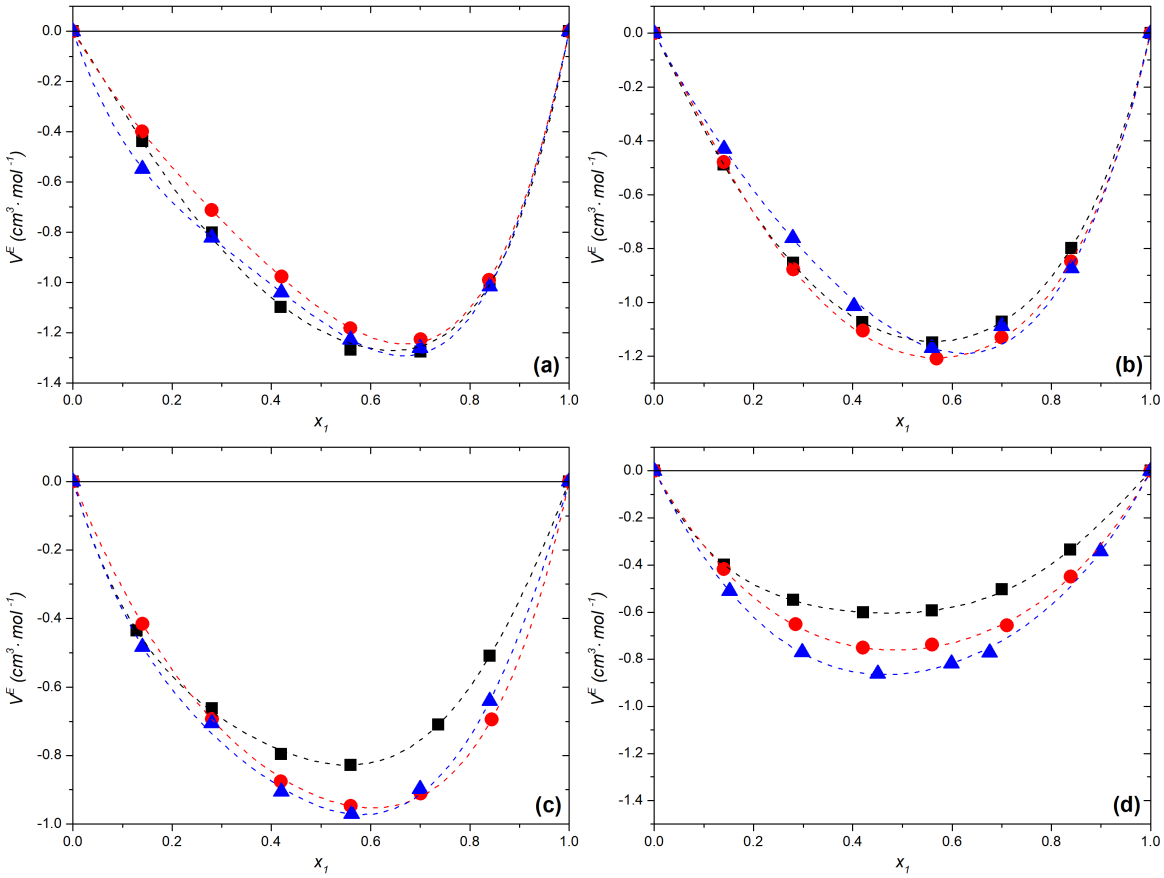

Figure A.11: HBD effect on the excess molar volume of alcohol + DES mixtures. Excess molar volumes ($cm^3 \cdot mol^{-1}$) are terms of the mole fraction of alcohol for the binary mixtures of DES with **(a)** methanol, **(b)** ethanol , **(c)** 1-propanol, **(d)** 1-butanol at a pressure of 101.3 kPa, temperature of 333.15 K and binary system with DES-A (■), DES-B (●), DES-C (▲). The dashed line represents the Redlich-Kister polynomial fitting with parameters reported in Table 7.

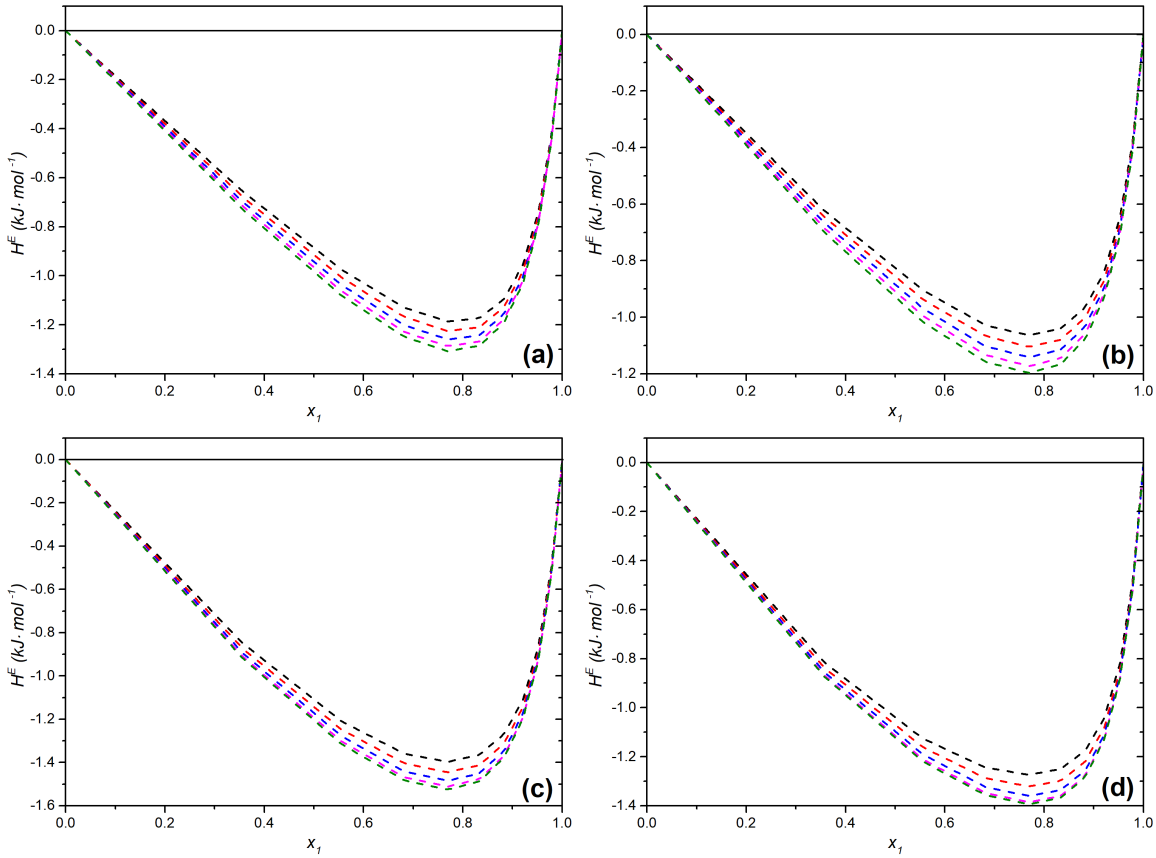

Figure A.12: Temperature effect on the molar excess enthalpy of alcohol + DES-A mixtures predicted with COSMO-RS. The molar excess enthalpies (kJ·mol^{-1}) are in terms of the mole fraction of alcohol for the binary mixtures of **(a)** methanol + DES-B, **(b)** ethanol + DES-B, **(c)** 1-propanol + DES-B, **(d)** 1-butanol + DES-B at a pressure of 101.3 kPa and temperatures between 293.15 K and 333.15 K. The dashed line represents the temperatures of 293.15 K (–), 303.15 K (–), 313.15 K (–), 323.15 K (–), 333.15 K (–).

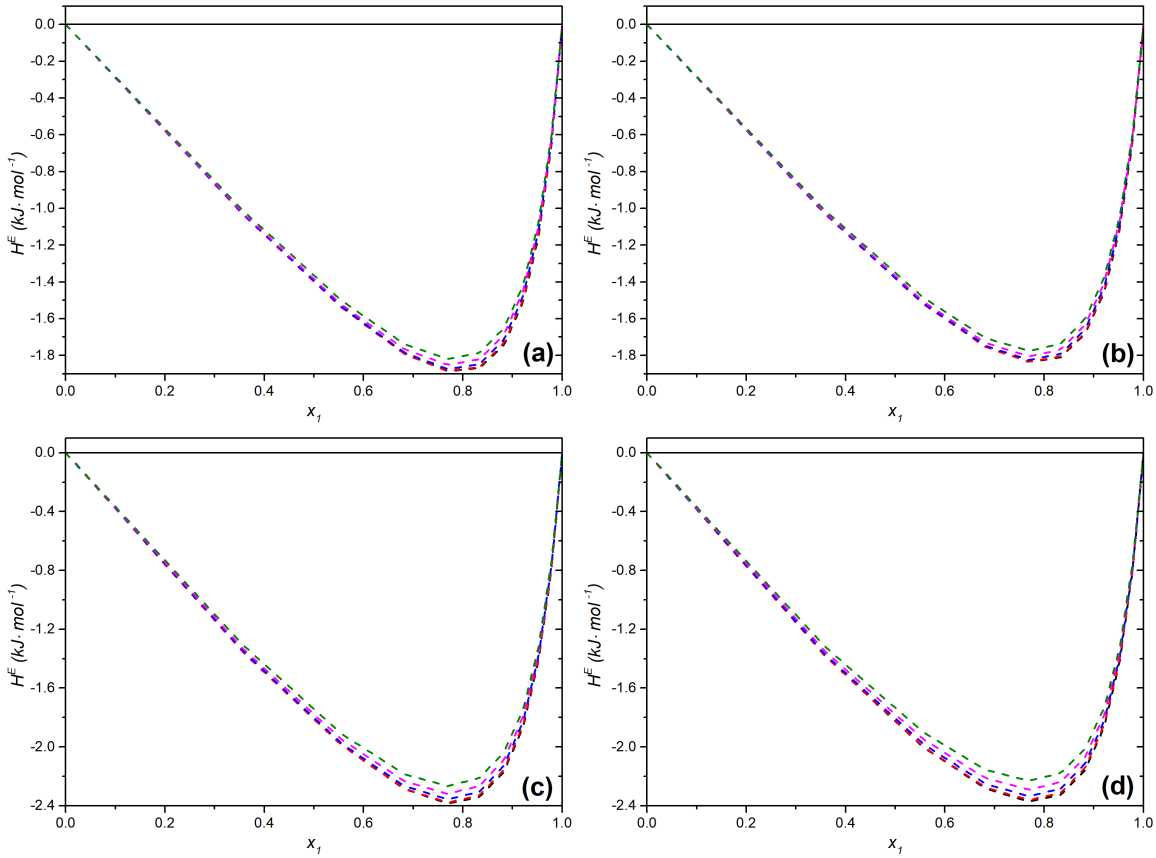

Figure A.13: Temperature effect on the molar excess enthalpy of alcohol + DES-A mixtures predicted with COSMO-RS. The molar excess enthalpies (kJ·mol^{-1}) are in terms of the mole fraction of alcohol for the binary mixtures of **(a)** methanol + DES-C, **(b)** ethanol + DES-C, **(c)** 1-propanol + DES-C, **(d)** 1-butanol + DES-C at a pressure of 101.3 kPa and temperatures between 293.15 K and 333.15 K. The dashed line represents the temperatures of 293.15 K (–), 303.15 K (–), 313.15 K (–), 323.15 K (–), 333.15 K (–)..

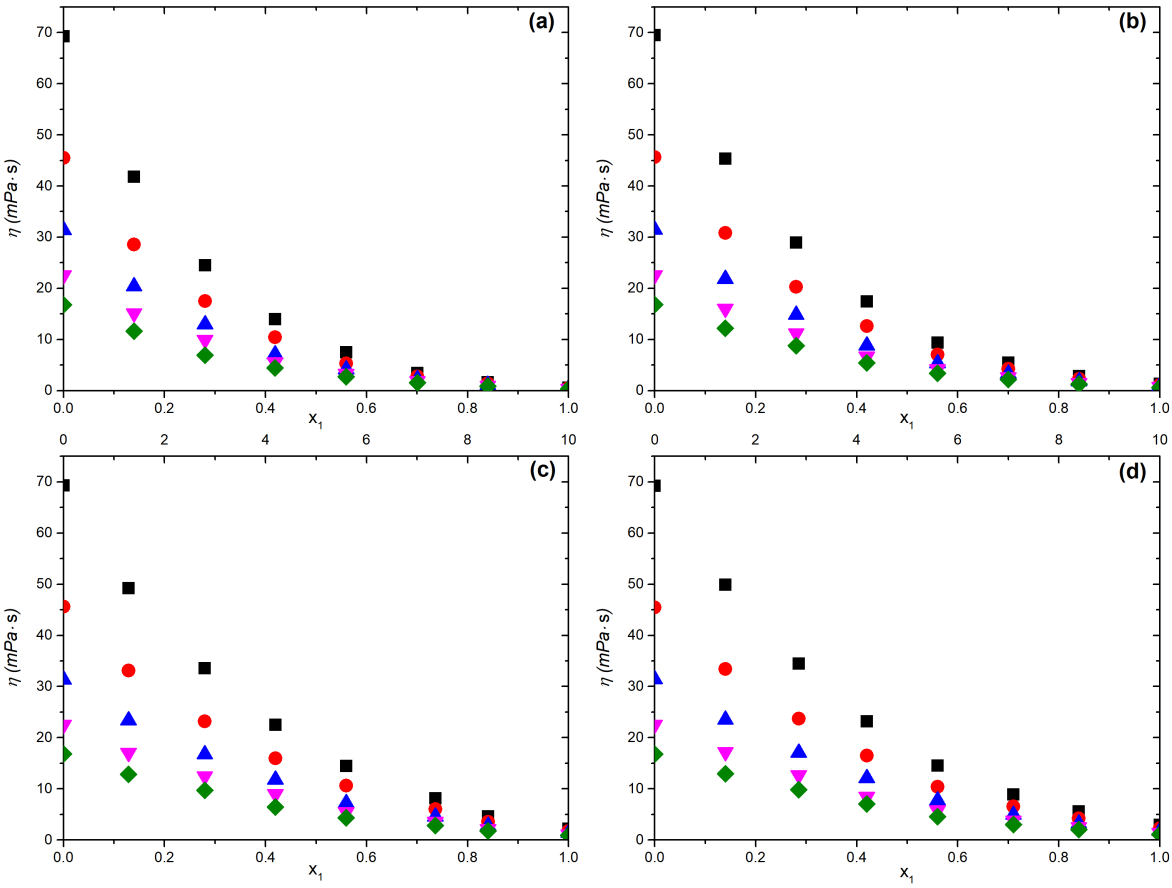

Figure A.14: Dynamic viscosity (mPa·s) in terms of the mole fraction of alcohol for the binary mixtures of **(a)** DES-B1, **(b)** DES-B2, **(c)** DES-B3, **(d)** DES-B4 at a pressure of 101.3 kPa and temperatures between 298.15 K and 333.15 K. Temperatures of 293.15 K (■), 303.15 K (●), 313.15 K (▲), 323.15 K (▼) and 333.15 K (◆).

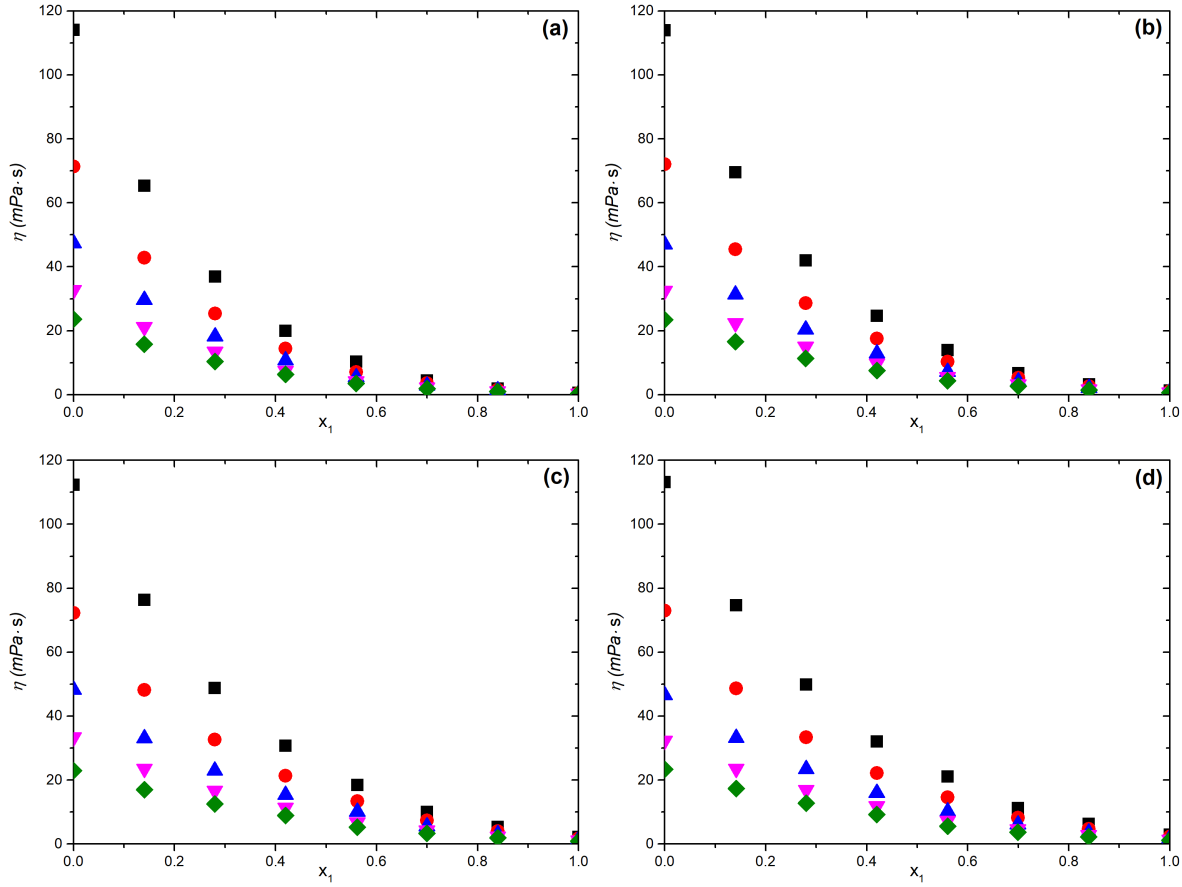

Figure A.15: Dynamic viscosity (mPa·s) in terms of the mole fraction of alcohol for the binary mixtures of **(a)** DES-C1, **(b)** DES-C2, **(c)** DES-C3, **(d)** DES-C4 at a pressure of 101.3 kPa and temperatures between 298.15 K and 333.15 K. Temperatures of 293.15 K (■), 303.15 K (●), 313.15 K (▲), 323.15 K (▼) and 333.15 K (◆).